THE UNIVERSITY OF MELBOURNE
SCHOOL OF CHEMICAL AND BIOMEDICAL ENGINEERING
DEPARTMENT OF CHEMICAL ENGINEERING

# The impact of impurities on the performance of cellulose triacetate membranes for $CO_2$ separation

**HIEP THUAN LU**

**Submitted in total fulfilment of the requirements of the degree of Doctor of Philosophy**

**January – 2018**

# ABSTRACT

Natural gas and coal are the essential energy resources that will continue to occupy over 50% the global electricity market in the coming decades. The natural gas streams normally contain several components that require removal so that the fuel meets pipeline specifications. Membrane separation technology is an outstanding approach for gas processing with advantages in land footprint and energy efficiency. In particular, cellulose triacetate (CTA) membrane have been widely applied in natural gas processing for decades and remain the dominant material on the market share due to their competitive gas separation performance and acceptance by industry. However, the raw natural gas streams also contain several impurities that can negatively affect the performance of the CTA membrane unit. Although several studies on gas separation performance of CTA membrane have been conducted, the impact of impurities on the membrane performance is not fully understood.

Cellulose triacetate membranes also have competitive $CO_2/N_2$ selectivity and are thus a prospective candidate for post-combustion carbon capture. However, studies on the impact of impurities in the flue gas, including liquid water of variable pH, sulphur oxides and nitrogen oxides, on the gas separation performance of CTA membrane are very limited. In this thesis, the impact of solutions of variable pH on CTA membranes was studied by exposing the dense membranes to solutions of pH 3, 7 and 13 solutions for up to 60 days. It was found that the membranes were relatively stable when exposed to water at pH 3 and pH 7 with a 30% increase in $CO_2$ and $N_2$ permeability and no loss in $CO_2/N_2$ selectivity. However, the membrane failed at pH 13 due to hydrolysis of the CTA polymer chains. Similarly, the membrane performance declined significantly when exposed to 0.74 kPa $NO_x$ at 22$^o$C over a 120 day aging period. This was due to the reaction of trace $NO_2$ in the gas mixture with the alcohol functional groups within the membrane structure. Interestingly, the CTA membrane was more selective for $SO_2$ than $CO_2$ and $N_2$ and stable in 0.75 kPa $SO_2$ at 22$^o$C over a 100 day aging period. The results suggest that CTA is a viable membrane material for post-combustion capture if it can form into an ultrathin film to increase permeance.

In natural gas processing, the performance of CTA membranes can also be affected by ethylene glycol, which can be entrained into the membrane separation unit from the upstream dehydration unit. In this thesis, the impact of two common ethylene glycols, monoethylene glycol and triethylene glycol, on the gas separation performance of CTA membranes was investigated. It was found that the glycols initially absorbed into the membrane reducing the permeation of He, $CO_2$ and $CH_4$ by a “pore-blocking” mechanism, but after a period of time, plasticised the membranes and enhanced the transport of $CO_2$ and $CH_4$. This plasticisation effect had less effect on He, which may be due to the lower solubility of He in these glycols which limited the transport of this gas through the swollen membrane structure. Interestingly, the membrane performance recovered when the glycols were removed from the polymer using a methanol wash. The findings highlighted the potential to recover the membrane performance when glycol flooding occurs in industrial plants.

Hydrogen sulfide in the raw natural gas might also affect CTA membrane performance. This impurity is also of concern in pre-combustion carbon capture. To fulfil the gap of knowledge in the literature, this thesis studied the permeability of $H_2S$ across a range of partial pressures (up

to 0.75 kPa) and temperature (22$^{o}$C - 80$^{o}$C). At 0.75 kPa $H_2S$ at 22$^{o}$C, the CTA membrane showed stable $CO_2$ permeability for up to 300 days which confirmed the long-term resistance of this material to the experimental $H_2S$ conditions.

Other impurities that might challenge the performance of CTA membranes in natural gas processing and pre-combustion capture are condensable aromatic hydrocarbons. In this thesis, the performance of CTA membranes at 35$^{o}$C in the presence of toluene and xylene with variable vapour activity was studied. At low $CO_2$ partial pressure (0.75 bar), the permeation of $CO_2$ and $CH_4$ through the CTA membrane declined when adding toluene and xylene up to 0.5 vapour activity. However, the CTA membrane was plasticised when toluene vapour activity increased above 0.5 activity. A similar impact was not clearly observed in the case of high xylene vapour activity. At high $CO_2$ pressure (7.5 bar), the membranes were plasticised by both hydrocarbons at 0.3 vapour activity. This finding demonstrated the co-operative effect of $CO_2$ and condensable hydrocarbons on the CTA membrane. In addition, the sorption and permeability of toluene and xylene through the CTA membrane at vapour activity up to 0.8 at 35$^{o}$C was also recorded.

Overall, the thesis demonstrates that cellulose triacetate membrane is an outstanding material for $CO_2$ separation in natural gas processing, pre- and post-combustion capture with high gas selectivity and resistance to most impurities in these industrial gas streams.

# PREFACE

The result chapters of this thesis have been published elsewhere as following:

**Journal Publications**

**Lu, H.T.**, Kanehashi, S., Scholes, C.A. and Kentish, S.E. (2016). The potential for use of cellulose triacetate membranes in post combustion capture. *International Journal of Greenhouse Gas Control*, 55, 97-104.

**Lu, H.T.**, Kanehashi, S., Scholes, C.A. and Kentish, S.E. (2017). The impact of ethylene glycol and hydrogen sulfide on the performance of cellulose triacetate membranes for $CO_2$ separation. *Journal of Membrane Science*, 539, 432-440.

**Lu, H. T.**; Liu, L.; Kanehashi, S.; Scholes, C. A. and Kentish, S.E. (2018). The Impact of toluene and xylene on the performance of cellulose triacetate membranes for natural gas sweetening. *Journal of Membrane Science*, 555, 362-368.

**Other Publications**

Kanehashi, S., Aguiar, A., **Lu, H..T.**, Chen, G.Q., Kentish, S.E. (2018). Effects of industrial gas impurities on the performance of mixed matrix membranes. *Journal of Membrane Science*, 549, 686-692.

Xie, K., Fu Q., Xu C., **Lu H.**, Zhao Q., Curtain R., Gu D., Webley P.A., and Qiao G.G. (2018) Continuous assembly of a polymer on a metal-organic framework (CAP on MOF): a 30 nm thick polymeric gas separation membrane. *Energy & Environmental Science*, 11, 544-550.

Xie, K., Fu, Q., Kim, J., **Lu, H.**, He, Y., Zhao, Q., Scofield, J., Webley, P.A. and Qiao, G.G. (2017). Increasing both selectivity and permeability of mixed-matrix membranes: Sealing the external surface of porous MOF nanoparticles. *Journal of Membrane Science*, 535, 350-356.

Scholes, C.A., Chen, G.Q., **Lu, H.T.,** Kentish, S.E. (2016). Crosslinked PEG and PEBAX Membranes for Concurrent Permeation of Water and Carbon Dioxide. *Membranes*, 6, 1.

# ACKNOWLEDGEMENTS

The research work in this thesis would not have been possible without the support and contribution from a number of people.

First of all, to my primary supervisor, Prof. Sandra Kentish, thank a million for encouraging and supporting me to apply for this PhD study. Thank you for your heart-warming supervision that has driven me through this challenging but also memorial PhD project. Thank you for spending your time to answer my weekend emails and editing my "poor" manuscript writings. Thank you for your guidance and support not only for my research work but also for my future career planning.

To Dr. Colin Scholes, thank you very much for guidance me through this challenging PhD. Thank you for celebrating the chocolate break that really helped me refreshed from the head-burning research work. Thank you for guiding me to structure the PhD thesis and helping me fixing the manuscript and thesis. Thank you for providing me the job opportunity and support me to go ahead with future career planning.

To Dr. Shinji Kanehashi, thank you for helping me starting the research career in membrane technology. Thank you for be my friend in every single experiment and every challenge issues with the membranes. I wish to say thank for your kindly welcome and guidance during my conference in Japan. Thank you very much for spending most of your precious time in guidance me throughout this PhD.

I would like sincerely thank to Associate Prof. Andrea O'Connor, the chair of my PhD committee, for giving me the valuable guidance and mentorship throughout my PhD study. I also have a special thanks to Dr. Atsushi Morisato for the precious suggestion and support in navigating and enhancing the significance of my PhD project work for industrial applications. A warm thank to Dr. George Chen, Dr. Jinguk Kim, Dr. Liang Liu and Ms. Alita Aguiar for supporting me in setting-up the research plans and the experiment apparatus.

I would like to acknowledge the funding support for this project from The University of Melbourne, Brown Coal Innovation Australia (BCIA), Particulate and Fluid Processing Centre (PFPC) and Peter Cook Centre for Carbon Capture and Storage Research at the University of Melbourne. I would like to gratefully acknowledge the Australian Research Council for funding the specialist gas infrastructure for this project. I also wish to acknowledge the Melbourne School of Engineering – University of Melbourne for awarding me the conference travel scholarships and Riady scholarship to attend the international conferences.

I would like to thank for the support from the Engineering Workshop in setting up the experimental apparatus. A special thank for the Clean Energy research group and Connal's research group for sharing the laboratories during the renovation of my laboratory. To the Diary Processing, Solvent Absorption, Solvent Extraction, Antarctic Remediation and Polymer Science research groups, thank you very much for providing the access to your chemicals and equipment.

To all of my great friends I have made in Membrane team, Solvent team and the Department over my PhD study, thank you for your support and for providing a friendly studying and working environment. I am very grateful for having this opportunity to meet all of you here.

For my parents, Mr. Gia Long Lu and Mrs. Thi Ngoc Hung Tran, thank you for bringing me up, for your daily support and encouragement. Thanks for giving me the opportunity to study and settle in Australia. Thanks for your loves and I am proud to be your son. For my brother, Mr. Hiep Thanh Lu, thanks for your support and be with me in Australia. Thanks for my aunt, Mrs. Diem Gia Tran, for guiding me to adapt quickly into Australia. Thanks aunt and your family for giving me a warm home in Australia.

Finally, I would like to thank my partner, Dr. Wen Li, for your endless love and support, for your understanding and encouragement during my PhD journey. Thanks for staying with me late in office, thanks for spending time to discuss and debate with me about my research work.

# DECLARATION

This is to certify that:

- The thesis includes only my original works towards the Ph.D. except where indicated in the acknowledgements.
- Due acknowledgement has been made in the text to all other materials used.
- The thesis is less than 100,000 words in length, exclusive of tables, figures, bibliographies and appendices.

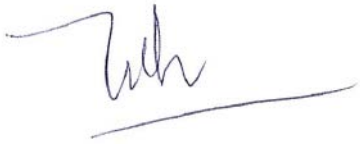

Hiep Thuan Lu

January 2018

# TABLE OF CONTENTS

ABSTRACT ..... I
PREFACE ..... III
ACKNOWLEDGEMENTS ..... IV
DECLARATION ..... VI
TABLE OF CONTENTS ..... VII
LIST OF FIGURES ..... XI
NOMENCLATURE ..... XV
GREEK LETTERS ..... XVI
SUBSCRIPTS ..... XVI
CHAPTER 1. INTRODUCTION ..... 1
CHAPTER 2. LITERATURE REVIEW ..... 4
2.1. INTRODUCTION ..... 4
2.2. GAS SEPARATION BY MEMBRANE TECHNOLOGY ..... 4
2.3. MECHANISM OF PENETRANTS TRANSPORT IN POLYMERIC MEMBRANE ..... 5
2.4. PERMEABILITY AND SELECTIVITY OF GLASSY MEMBRANE ..... 8
2.4.1. Permeability ..... 8
2.4.2. Selectivity ..... 8
2.4.3. Robeson's Upper Bound ..... 9
2.5. SOLUTION – DIFFUSION MODEL ..... 10
2.5.1. Solubility in Glassy Polymers ..... 10
2.5.1.1. Dual-Mode Sorption Model (DMS) ..... 10
2.5.1.2. The Sorption of Vapour ..... 11
2.5.2. Diffusivity in Glassy Polymer ..... 12
2.5.2.1. Fractional Free Volume (FFV) ..... 12
2.5.2.2. Free Volume Dependence of Diffusion ..... 13
2.5.2.3. Measurement of diffusion coefficient ..... 14
2.6. PHYSICAL AGING ..... 15
2.7. MEMBRANE THICKNESS ..... 16
2.8. CELLULSE ACETATE ..... 17
2.8.1. Background ..... 17
2.8.2. Degree of Substitution ..... 17
2.8.3. Pure Gas Transport in Cellulose Triacetate Membrane ..... 19
2.8.4. Mixed Gas Transport in Cellulose Triacetate Membrane ..... 22

2.9. IMPACT OF IMPURITIES ON THE PERFORMANCE OF CELLULOSE TRIACETATE MEMBRANES ..... 23
2.9.1. Impact of Water on Membrane Performance ..... 24
2.9.1.1. Diffusion and Sorption of Water in Cellulose Acetate Membrane ..... 24
2.9.1.2. Infrared Spectroscopy Analysis and State of Water in Cellulose Acetate Membrane ..... 24
2.9.1.3. Impact of Water Vapour on Gas Permeation ..... 25
2.9.1.4. Impact of Solutions of Variable pH on Cellulose Triacetate Membranes ..... 26
2.9.2. Impact of Sulphur Oxides ($SO_x$) on Membrane Performance ..... 27
2.9.3. Impact of Nitrogen Oxides ($NO_x$) on Membrane Performance ..... 27
2.9.4. Impact of Hydrogen Sulfide ($H_2S$) on Membrane Performance ..... 28
2.9.5. Impact of Ethylene Glycols on Membrane Performance ..... 29
2.9.6. Impact of BTEX on Membrane Performance ..... 30
2.10. SCOPE OF THIS THESIS ..... 31
CHAPTER 3. EXPERIMENTAL METHODS ..... 33
3.1. INTRODUCTION ..... 33
3.2. MEMBRANE MATERIALS AND MEMBRANE FABRICATION PROTOCOLS ..... 33
3.2.1. Membrane Materials ..... 33
3.2.2. Experimental Gases ..... 33
3.2.3. Experimental Solvents and Chemicals ..... 34
3.2.4. Dense Membrane Fabrication ..... 35
3.2.5. Thin Film Composite (TFC) Membrane Fabrication ..... 36
3.3. MEMBRANE CHARACTERISATION ..... 37
3.3.1. Membrane Density ..... 37
3.3.2. Membrane Thickness ..... 37
3.3.3. Scanning Electron Microscope (SEM) ..... 38
3.3.4. Wide Angle X-ray Diffraction (WAXD) ..... 38
3.3.5. Differential Scanning Calorimetry (DSC) ..... 38
3.3.6. Thermogravimetric Analysis (TGA) ..... 38
3.4. GAS ANALYSIS ..... 39
3.4.1. Attenuated Total Reflectance (ATR) - Fourier Transform Infrared Spectroscopy (FT-IR) ..... 39
3.4.2. Gas Chromatography (GC) ..... 39
3.5. PENETRANT TRANSPORT PROPERTIES ..... 40
3.5.1. Gas Sorption Analysis ..... 40

3.5.2. Vapour Sorption Analysis ..... 41
3.5.3. Kinetic Sorption Measurement ..... 42
3.5.4. Pure Gas Permeation Measurement ..... 43
3.5.5. Mixed Gas Permeation Measurement ..... 44
3.5.6. Mixed Vapour/Gas Permeation Measurement ..... 44
3.6. PRESSURISED GAS HOLDER FOR MEMBRANE AGING STUDY ..... 45
CHAPTER 4. THE POTENTIAL FOR USE OF CELLULOSE TRIACETATE MEMBRANES IN POST COMBUSTION CAPTURE ..... 47
4.1. INTRODUCTION ..... 47
4.2. EXPERIMENTAL ..... 52
4.2.1. Membrane fabrication ..... 52
4.2.2. Characterisation ..... 52
4.2.3. Gas permeation measurement ..... 53
4.3. RESULTS AND DISCUSSION ..... 54
4.3.1. Impact of water ..... 54
4.3.2. Permeability of $SO_2$ and NO ..... 57
4.3.3. Aging of CTA membrane in $SO_2$ and NO ..... 60
4.4. CONCLUSIONS ..... 63
4.5. ACKNOWLEDGEMENTS ..... 63
CHAPTER 5. THE IMPACT OF ETHYLENE GLYCOL AND HYDROGEN SULFIDE ON THE PERFORMANCE OF CELLULOSE TRIACETATE MEMBRANES IN NATURAL GAS SWEETENING ..... 64
5.1. INTRODUCTION ..... 64
5.2. EXPERIMENTAL ..... 69
5.2.1. Membrane fabrication ..... 69
5.2.2. Gas permeation measurement ..... 69
5.2.3. Static long-term aging of CTA in glycol solutions and $H_2S$ ..... 70
5.3. RESULTS AND DISCUSSION ..... 71
5.3.1. Sorption Uptake of glycol liquids in Cellulose Triacetate ..... 71
5.3.2. Impact of glycol liquids on CTA membrane performance ..... 73
5.3.2.1. The impact of methanol on CTA membrane in glycol extraction step ..... 73
5.3.2.2. The impact of glycols on CTA membrane performance ..... 74
5.3.2.3. The impact of glycols on $CO_2$ permeation through CTA membrane ..... 78
5.3.2.4. The impact of glycols on the glass transition temperature and crystallinity ..... 79
5.3.3. Permeation of hydrogen sulphide on CTA membrane ..... 82

5.3.4. Long-term aging of CTA membrane in $H_2S$ ..... 85
5.4. CONCLUSIONS ..... 87
5.5. ACKNOWLEDGEMENTS ..... 87
CHAPTER 6. THE IMPACT OF TOLUENE AND XYLENE ON THE PERFORMANCE OF CELLULOSE TRIACETATE MEMBRANES FOR NATURAL GAS SWEETENING ..... 88
6.1. INTRODUCTION ..... 88
6.2. EXPERIMENTAL ..... 94
6.2.1. Membrane Fabrication ..... 94
6.2.2. Sorption Measurements ..... 94
6.2.3. Permeability Measurements ..... 95
6.3. RESULTS AND DISCUSSION ..... 95
6.3.1. Solubility of Toluene and Xylene in Cellulose Triacetate ..... 95
6.3.2. Gas and Vapour Sorption Isotherm in Cellulose Triacetate Membranes ..... 96
6.3.3. The Impact of Toluene and Xylene on $CO_2/CH_4$ Separation at Low $CO_2$ Pressure 99
6.3.4. The Impact of Toluene and Xylene on CTA Membranes at Higher $CO_2$ Pressure ..... 101
6.3.5. The Permeabilities of Toluene and Xylene on CTA Membranes ..... 103
6.4. CONCLUSIONS ..... 105
CHAPTER 7. CONCLUSIONS AND FUTURE PERSPECTIVE ..... 106
7.1. CONCLUSIONS ..... 106
7.2. FUTURE PERSPECTIVE ..... 108
CHAPTER 8. REFERENCE ..... 109
APPENDIX A: EXPERIMENTAL METHODS ..... 124
A.1 Membrane Density ..... 124

## LIST OF FIGURES

Figure 1.1 The global market share of primary energy resources [1].....1

Figure 2.1: Sample of flue gas separation by membrane technology, reproduced from [32].....4

Figure 2.2 Hollow fibre membrane module (left) and Spiral wound module (right) [32].....5

Figure 2.3 The diffusion mechanisms for membrane gas separation reproduced from [32, 42]..6

Figure 2.4: The sketch of gas transport through membrane with assumption of linear concentration gradient across membrane thickness.....7

Figure 2.5 The upper bound for $CO_2/CH_4$ and $CO_2/N_2$ gas separation, reproduced from [61] (The white circle represents the current performance of the CTA membrane [12, 40]) .....10

Figure 2.6 The gas sorption by dual-mode sorption model .....11

Figure 2.7 Some typical shapes of vapour sorption isotherms [67, 68].....11

Figure 2.8 The correlations of polymer specific volume versus temperature [87].....13

Figure 2.9 Concentration profile developed in a membrane over time during a dynamic sorption experiment .....15

Figure 2.10 The flowrate of permeate ($Q_p$) versus time in a time lag measurement experiment within a CVVP apparatus.....15

Figure 2.11 Chemical structure of cellulose acetate polymer [12] .....18

Figure 2.12 The permeability coefficient of CTA (DS 2.84) membrane under $CO_2$ pressurisation and depressurisation cycles (the open circles represent the increase in permeability versus experiment time, which was 16 days for the 30 atm $CO_2$ pressure experiment) [40].....20

Figure 2.13 Sorption isotherms for $CO_2$ and $CH_4$ in CTA membranes ( ■ $CO_2$ 35$^o$C and ■ $CH_4$ 35$^o$C [40]; ● $CO_2$ 30$^o$C and ● $CH_4$ 40$^o$C [160]) .....21

Figure 2.14 The permeabilities of $CO_2$ and $CH_4$ in CTA membranes versus partial pressure differential of $CO_2$ with mixed gas (50% $^v/_v$ $CO_2$ in $CH_4$) feed (continuous line) and pure $CO_2$ or $CH_4$ feed (broken line) at 30$^o$C [160] .....22

Figure 2.15 The change of permeate flux at different relative humidity of water in $CO_2/N_2$ separation by cellulose acetate membrane (reprinted from [20]) .....26

Figure 2.16 The potential pH conditions in natural gas and flue gas entrained liquids.....26

Figure 2.17 The permeability of $H_2S$ and $CO_2/H_2S$ selectivity through some polymeric membranes with the slope factor of the upper bound line calculated from (Eq. 2.8) [19, 204-209] .....28

Figure 2.18 The vapour pressure of monoethylene glycol [220] and triethylene glycol [221] at different temperature.....30

Figure 3.1 The scheme of membrane fabrication by solution casting method, adapted from [234].....36

Figure 3.2 The scheme of thin film composite membrane fabrication by a spin coating technique .....37

Figure 3.3 The pattern of locations where the membrane thickness was measured .....38

Figure 3.4 A simplified process flow diagram of the high pressure gas adsorption measuring unit (Belsorp – MicrotracBel Corp., Japan). TIC is temperature indicator controller. .....41

Figure 3.5 A simplified process flow diagram of the vapour sorption analyser (VTI, USA). TIC and MFC are temperature indicator controller and mass flow controller, respectively.....42

Figure 3.6 The setup for the constant volume – variable pressure (CVVP) gas permeation apparatus .....43

Figure 3.7 The mixed gas rig setup for variable volume – constant pressure method (VVCP) .44

Figure 3.8 The mixed vapour/gas permeation rig setup .....45

Figure 3.9 The sketch of pressurised gas holder for membrane aging study.....46

Figure 4.1 (a) Water uptake of a CTA membrane after immersion in water of variable pH at 35◦C for a specified time; (b) Mass loss of a CTA membrane after immersion at pH 13. .....55

Figure 4.2 Gas separation performance of CTA membranes at 10 bar, 35$^{o}$C after immersion in pH (3, 7 and 13) solutions (a) permeability of $CO_2$; (b) permeability of $N_2$; (c)selectivity of $CO_2/N_2$. .....56

Figure 4.3 FT-IR spectra of dried cellulose triacetate membrane before and after aged in different pH solutions for 60 days .....57

Figure 4.4 Gas permeability in CTA thin film composite membranes. (a) permeability of $CO_2$ in 10 v/v% $CO_2$ in $N_2$; (b) permeability of $N_2$ in 10 v/v% $CO_2$ in $N_2$; (c) permeability of SO21000 ppm $SO_2$ in $N_2$.....58

Figure 4.5 $N_2$ permeability in CTA thin film composite membranes with 10 v/v% $CO_2$ in $N_2$ gas feeding and 1000 ppm $SO_2$ in $N_2$ gas feeding .....59

Figure 4.6 Temperature dependence of the $SO_2/N_2$ and $CO_2/N_2$ selectivity in a CTA membrane at zero transmembrane pressure difference.....60

Figure 4.7 Change in permeability of (a) He; (b) $N_2$ and (c) He/$N_2$ selectivity as time progresses for CTA membranes at 35$^{o}$C, 7.5 bar after aging separately in pure $N_2$, 979 ppm NO in balance $N_2$ and 1000 ppm $SO_2$ in balance $N_2$ at 7.5 bar and 22 ± 2$^{o}$C .....62

Figure 5.1 The sorption kinetics of ethylene glycol (MEG) and triethylene glycol (TEG) solutions in a CTA membrane (70µm thickness) at 22$^{o}$C: (a) mass basis and (b) molar basis. The dashed lines are added to guide the eye. .....72

Figure 5.2 Change in permeability of He and $CH_4$ as time progresses relative to the original fresh CTA membranes at 35$^{o}$C and 750 kPa feed pressure: (a) aged in ethylene glycol (MEG) solution at 22$^{o}$C; (b) aged in MEG and washed by methanol for 168 hours at 22$^{o}$C; and (c) He/$CH_4$ selectivity. The dashed lines are added to guide the eye.....75

Figure 5.3 Change in permeability of He and $CH_4$ as time progresses relative to the fresh CTA membranes at 35$^oC$ and 750 kPa feed pressure: (a) aged in triethylene glycol (TEG) solution at 22$^oC$; (b) aged in TEG and washed by methanol for 168 hours at 22$^oC$; and (c) He/$CH_4$ selectivity. The dashed lines are added to guide the eye. .....77

Figure 5.4 Change in permeability of He and $CH_4$ as time progresses relative to the fresh CTA membranes at 35$^oC$, 750 kPa feed pressure after aging in methanol solution.....78

Figure 5.5 The change in glass transition temperature as glycol is sorbed into CTA, measured by dynamic scanning calorimetry (DSC) and calculated from the Fox Equation ($T_g$ of MEG is -118$^oC$ [272]). .....79

Figure 5.6 Wide angle X-Ray Diffraction (WAXD) results for CTA membranes when (a) saturated with glycols; and (b) after washing with methanol; in comparison with a fresh CTA membrane.....81

Figure 5.7 Gas permeability in CTA membranes with a feed gas of 1000ppm $H_2S$ in balance $N_2$ (a) permeability of $H_2S$; (b) permeability of $N_2$; (c) $H_2S/N_2$ gas selectivity. .....83

Figure 5.8 The permeability coefficients of $H_2S$ as a function of temperature at zero partial pressure differential (this study) and 94 kPa (Heilman et al.[211]).....85

Figure 5.9 Change in (a) permeability of He and $CH_4$ and (b) He/$CH_4$ selectivity as time progresses relative to the fresh CTA membranes at 35$^oC$, 750 kPa after aging separately in 1000 ppm $H_2S$ in balance $N_2$ and pure $N_2$ at 750 kPa and 22 ± 2$^oC$. The permeability of He and $CH_4$ in a fresh CTA membrane was 21.6 ± 0.2 barrer and 0.265 ± 0.009 barrer, respectively, giving an He/$CH_4$ gas selectivity at 81 ± 3. The dashed lines are added to guide the eye. .....86

Figure 6.1 The sorption of liquid toluene and xylene into a CTA membrane (62 ± 2μm thickness) at 35$^oC$. The dashed lines are added to guide the eye.....95

Figure 6.2 The sorption isotherms of $CO_2$ and $CH_4$ in CTA at 35$^oC$ .....97

Figure 6.3 The solubility of toluene and xylene in CTA at 35$^oC$: (a) at 0.0 – 0.6 vapour activity; (b) across the full range of vapour activities; (c) as a function of vapour pressure rather than activity.....98

Figure 6.4 The permeability of $CO_2$ and $CH_4$ (a) and $CO_2/CH_4$ selectivity (b) through CTA membranes exposed to toluene at various vapour pressures, for 10% $CO_2/CH_4$ mixed gas feed at 7.5 bar and 35$^oC$.....100

Figure 6.5 The permeability of $CO_2$ and $CH_4$ (a) and $CO_2/CH_4$ selectivity (b) through CTA membrane exposed to xylene at various vapour pressures, for 10% $CO_2/CH_4$ mixed gas feed at 7.5 bar and 35$^oC$.....101

Figure 6.6 The permeability of $CO_2$ through a CTA membrane at 35$^oC$ exposed to (a) toluene and (b) xylene at various vapour pressures, for a 10% $CO_2/CH_4$ mixed gas (0.75 Bar CO2) and for pure $CO_2$ at 7.5 bar. .....103

Figure 6.7 The permeability of (a) toluene and (b) xylene at various vapour pressures and activities, for 10% $CO_2/CH_4$ mixed gas feed and pure $CO_2$ feed at 7.5 bar and 35$^oC$.....104

## LIST OF TABLES

Table 1.1: Composition (mole %) of processing gas streams in some carbon dioxide capture applications .....3

Table 2.1: The kinetic diameter and critical temperature of some common gases in gas separation process .....7

Table 2.2: The front factor value (k) and slope of the upper bound for some common gas pairs in carbon capture [57, 61] .....10

Table 2.3: The comparison in physical properties of cellulose acetate with different degree of acetylation [12, 40, 158, 159] .....19

Table 2.4: The permeability coefficients of cellulose acetate membranes .....19

Table 2.5: The dual-mode sorption parameters for $CH_4$ and $CO_2$ in CTA membranes.....21

Table 2.6: The permeance and selectivity of $CO_2/N_2$ in CTA membrane at 1100kPa [22] .....23

Table 2.7: The main IR spectrum of cellulose triacetate membrane [180, 184, 185].....25

Table 3.1: The specification of cellulose acetate polymer (Product code: LT-35) from Daicel Corporation, reproduced from product specification sheet [233].....33

Table 3.2: Compositions and purities of experimental gases .....34

Table 3.3: List of solvents and chemicals utilised in the thesis .....35

Table 3.4: Operating parameters for micro GC 490 .....40

Table 3.5: The specification of pressurised membrane holder for membrane aging study .....46

Table 4.1: Activation energy for permeation in CTA membrane at zero pressure.....59

Table 4.2: The absorbance ratio between carbonyl functional group and C – O functional group in fresh and aged membranes.....61

Table 5.1: Solubility of glycols in the CTA membrane.....71

Table 5.2: Hildebrand and Hansen solubility parameters of different liquids and CTA [274, 276].....73

Table 5.3: Henry's Law coefficient (MPa) for gases in glycols at 298K .....74

Table 5.4: Density of CTA membranes before and after aging in glycol and methanol. .....76

Table 5.5: The impact of glycols on the change of permeabilities (*P*) of $CH_4$ and $CO_2$ and $CO_2/CH_4$ gas selectivity ($\alpha_{CO2/CH4}$) of CTA membrane at 35$^{o}$C.....79

Table 5.6: The permeability of hydrogen sulphide in cellulose acetate membranes. .....82

Table 5.7: Activation energy for permeation in CTA membrane at zero pressure.....84

Table 6.1: The properties of toluene and xylene and their solubility in CTA membranes.....96

Table 6.2: The dual-mode sorption parameters for $CH_4$ and $CO_2$ in CTA membranes at 35$^{o}$C..... .....97

## NOMENCLATURE

$A$ : Effective membrane area ($cm^2$)
$a$ : vapour activity
$b$ : Langmuir affinity constant ($atm^{-1}$)
$C$ : Concentration of sorbed penetrant ($cm^3$(STP)/$cm^3$ polymer)
$C'$ : Maximum sorption capacity ($cm^3$(STP)/$cm^3$ polymer)
$C_m$ : Concentration of mobile sorbed penetrant ($cm^3$(STP)/$cm^3$ polymer)
$D$ : Diffusion coefficient ($cm^2$/s)
$\overline{D}$ : Average effective diffusion coefficient ($cm^2$/s)
$D_o$ : Infinite dilution Fickian diffusion coefficient ($cm^2$/s)
: Pre-exponential factor of diffusion coefficient in (Eq. 2.25) ($cm^2$/s)
$d$ : Kinetic diameter (Å)
$d$ : Spacing between successive planes in X-ray diffraction (Å)
$DS$ : Degree of acetylation or substitution
$E_D$ : Activation energy of diffusion (kJ/mol)
$E_P$ : Activation energy of permeation (kJ/mol)
$F$ : Immobilisation factor
$f$ : Sorption constant in BET and GAB sorption models
$FFV$ : Fraction free volume
$\Delta H_S$ : Heat of sorption (kJ/mol)
$h$ : Sorption constant in BET and GAB sorption models
$J$ : Flux of penetrant ($cm^3$(STP)/$cm^2$.s)
$k$ : Empirical constant predicted from the Upper Bound in (Eq. 2.7) and (Eq. 2.8) (Barrer)
: Constant characterising membrane – solvent system in kinetic sorption in (Eq. 2.22)
: Reaction rate ($L^2$/$mol^2$.s)
$k_D$ : Henry's law constant ($cm^3$(STP)/$cm^3$ polymer.atm)
$l$ : Thickness of membrane active layer (cm)
$m$ : Sample weight (g)
$m_o$ : Sample initial weight (g)
$m_\infty$ : Sample weight at equilibrium condition (g)
$n$ : Exponential constant characterising the type of diffusion in (Eq. 2.22)
: Slope factor of the Upper Bound in (Eq. 2.7) and (Eq. 2.8)
$P$ : Permeability coefficient (Barrer)
$P_o$ : Pre-exponential factor of permeability coefficient in (Eq. 2.25) (Barrer)
$p$ : Partial pressure (atm)
$p_o$ : Saturated vapour pressure (atm)
$Q$ : Permeance of penetrant (GPU)
$Q_p$ : Permeate flowrate ($cm^3$(STP)/s)
$R$ : Radius of Interaction between components in Hildebrand and Hansen solubility theory ($MPa^{0.5}$)
: Universal gas constant (J/mol.K)
$S$ : Solubility ($cm^3$(STP)/$cm^3$ polymer.atm)
$S_o$ : Pre-exponential factor of solubility in (Eq. 2.25) ($cm^3$(STP)/$cm^3$ polymer.atm)

$T$ : Experimental temperature (K)
$t$ : Experimental time (s)
$T_g$ : Glass transition temperature (K)
$V$ : Polymer specific volume ($cm^3/g$)
: Calibrated volume in pure gas permeation measurement apparatus in (Eq. 3.5) ($cm^3$)
$V_o$ : Volume occupied by polymer chains ($cm^3/g$)
$V_w$ : van der Waals volume ($cm^3/g$)
$W$ : Weight fraction
$w$ : Molar fraction of permeation gas in the polymer as in (Eq. 2.1)
$wt\%$ : mass uptake (%)
$x$ : Molar fraction of gas in the feed stream
$y$ : Molar fraction of gas in the permeate stream

## GREEK LETTERS

$\alpha$ : Ideal gas selectivity
$\alpha'$ : True gas selectivity
$\beta$ : Constant expressing the impact of adsorbed penetrants on the polymer in (Eq. 2.19)
$\chi$ : Flory – Huggins interaction parameter of polymer and penetrant
$\delta$ : Hansen solubility parameter ($MPa^{0.5}$)
$\delta_d$ : Non-polar component in the Hansen solubility parameter ($MPa^{0.5}$)
$\delta_h$ : Hydrogen bonding component in the Hansen solubility parameter ($MPa^{0.5}$)
$\delta_p$ : Polar component in the Hansen solubility parameter ($MPa^{0.5}$)
$\phi_S$ : Volume fraction of penetrant in (Eq. 2.13)
$\phi_P$ : Volume fraction of polymer in (Eq. 2.13)
$\lambda$ : Radiation wavelength (Å)
$\nu$ : Adsorption concentration of adsorbate (g adsorbate/g adsorbent)
$\nu_m$ : Monolayer sorption capacity (g adsorbate/g adsorbent)
$\theta$ : Permeability lag time (s)
: Incidence angle in X-ray diffraction ($^o$)
$\rho$ : Density of solvent or polymer ($g/cm^3$)

## SUBSCRIPTS

1 : Permeate side or downstream
2 : Feed side or upstream
$D$ : Henry's law component
$H$ : Langmuir component
$p$ : polymer
$t$ : At experimental time t

# CHAPTER 1. INTRODUCTION

Global economic expansion and rapid population growth is fuelling a growing demand for energy that is anticipated to increase in the coming decades. Although the demand for renewable energy resources is increasing rapidly, fossil fuels will remain the dominant resource in the global energy market for the foreseeable future (**Figure 1.1**) [1]. Natural gas is a major part of the market, because of its relevant abundance and lower environmental footprint compared to coal and oil. As such global natural gas consumption is anticipated to have an annual growth rate of 1.8% p.a. until 2035, and will overtake coal as the second largest global energy resource [1]. This transition from coal to natural gas is due partly to economics as well as a shift in worldwide energy policies towards sustainable, low-carbon and zero-carbon emission technologies [2, 3].

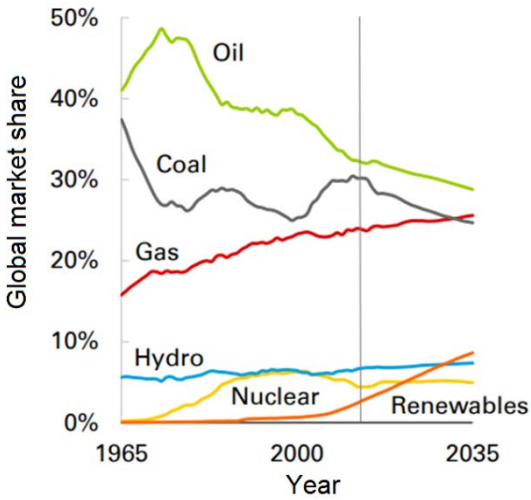


**Figure 1.1** The global market share of primary energy resources [1]

Raw natural gas contains many impurities **(Table 1.1),** which must be removed to meet the pipeline and other transportation specification requirements. In general, the process of removing acid gases and impurities is known as natural gas sweetening. This is a massive chemical engineering industry, with almost all of the annual production of more than 100 trillion standard cubic feet (scf) of natural gas requiring pretreatment [4]. Several separation technologies have been commercialised for the pretreatment of natural gas, of which, membrane separation is a recent approach that has been proven economically viable. Membrane gas separation has been commercial since the mid-1980s, and is implemented in various applications, such as Prism® membranes (Monsanto) for hydrogen separation, as well as Cynara® (Schlumberger) and Separex™ (UOP) for carbon dioxide separation from natural gas [5, 6]. The advantages of membrane technology are its high energy efficiency, high surface area-to-volume ratio, modular nature enabling simple scaling and "chemical free" nature [2]. The advantages of membrane technology make it an attractive technology for the natural gas processing market, and it is projected to increase its share of this market in the future [4].

Cellulose triacetate (CTA) was the first polymer commercialized for removal of the acid gas impurities, hydrogen sulfide ($H_2S$) and carbon dioxide ($CO_2$), and has retained the largest market share since the 1980s [4]. Although several alternative advanced membrane materials have been

developed to achieve greater separation performance compared to CTA membranes, very few of these novel materials have been successfully commercialised, due to reasons relating to poor membrane fabrication ability and unstable separation performance under industrial conditions [4, 7]. As a result, cellulose triacetate is expected to retain its market share in gas separation membranes for natural gas sweetening for decades to come.

The minor components within natural gas, such as water, hydrogen sulfide and carbon dioxide, as well as hydrocarbons (**Table 1.1**) can alter the mechanical properties of the membrane [8] and reduce its ability to selectively separate out acidic gases while retaining methane. The loss in separation performance is through competitive sorption [9-11], plasticization [12-14] antiplasticization, also called pore blocking [12, 15, 16] and chemical degradation [10]. In addition, the acidic gas separation unit is usually integrated with other upstream processes, which may result in more contaminants reaching the membrane unit. The carry-over of ethylene glycol from the upstream natural gas dehydration unit is one such issue, which is often a cause for module replacement [17, 18]. Although $CO_2$ separation from gas mixtures using cellulose acetate membrane has been well studied, there is very limited understanding about the impact of these minor components on the performance of CTA membranes. There are a few studies that have reported the short-term performance of CTA in the presence of impurities, such as hydrogen sulfide, aromatic hydrocarbons and water vapour [11, 12, 19-21]. However, these studies were not sufficient to assess the performance of CTA membranes over the membrane lifetime. In addition, the literature lacks a systematic study on the permeation and sorption properties of these minor components in CTA, which can sequentially limit the opportunity to develop strategies for extending membrane lifetime.

Cellulose triacetate (CTA) membranes also have strong potential for $CO_2$ separation in both pre- and post-combustion capture due to their high $CO_2/N_2$ and $CO_2/H_2$ selectivity [22] and commercial readiness [4]. However, the viability of CTA membranes for this application is not well documented in the literature, in part because of the focus on novel polymeric systems. Post-combustion flue gas also contains impurities, such as sulphur oxides and nitric oxides (**Table 1.1**), which are either emitted from the coal during combustion or carried over from the upstream flue gas purification processes. These impurities will also alter the performance of CTA membranes, and affect the long-term stability of membrane modules in a post-combustion application. In this regard, there is a research gap regarding the impact of impurities in flue gas on the performance of CTA membranes. While coal's contribution to the global energy market is anticipated to decrease over the coming decades, it is still expected to occupy at least 25% of the total global energy resources for the foreseeable future [1]. Furthermore, carbon capture from flue gases produced from other non-power industries will increase in the coming decades, such as cement production, iron and steel production, fertilizer processing and fine chemical fabrication. Hence, CTA membranes may have the potential to assist in meeting emission reduction targets and securing a sustainable development for fossil fuel based industries.

**Table 1.1:** Composition (mole %) of processing gas streams in some carbon dioxide capture applications

| | **Natural gas in U.S. gas wells [4] (Natural gas for sweetening)** | **Mulgrave syngas pilot plant (Victoria) [23] (Pre-combustion)** | **Hazelwood coal-fired power plant (Victoria) [24] (Post-combustion)** | **Munmorah coal-fired power plant (New South Wale) [25] (Post-combustion)** |
|---|---|---|---|---|
| $CO_2$ | 1 – 10 | 13.95 | 13.0 | 8.5 – 12.0 |
| $N_2$ | >4 | 59.96 | 62.0 | 76.0 – 78.0 |
| $CH_4$ | 75 – 90 | 2.52 | - | - |
| $O_2$ | - | - | 3.5 | 6.5-10.0 |
| $H_2O$ | 20 – 1200ppm | 0.11 | 20.5 | 3.0-6.0 |
| $H_2S$ | 4 – 10000ppm | 0.05 | - | - |
| $SO_x$ | - | - | 212 ppm | 190 – 280 ppm |
| $NO_x$ | - | - | 151 ppm | 200 – 300 ppm NO<br><10 ppm $NO_2$ |
| Heavy hydrocarbons ($C_3$+, BTEX…) | 200 – 3000ppm [4, 11] | 0.21 | | |
| pH of saturated liquid | - | | 3.3 – 3.7 | 12.80 (fly ashes) [26] |

The gas transport through cellulose triacetate has been widely studied with several mathematical models developed. One of the most well-known models for ideal gas sorption is the dual-mode sorption (DMS) model that separates the gas sorption into two domains: the Henry's law region and the Langmuir isotherm region [27-29]. However, due to the complicated nature of gas sorption into glassy polymers, the gas transport of condensable penetrants such as water or hydrocarbons requires more complex models such as Brunauer – Emmett – Teller (BET) model [30] or Guggenheim – Andersonde – Boer (GAB) model [31]. These vapors can also alter the diffusion coefficient in the membrane through either plasicisation or antiplasticisation. There is very limited understanding of these minor components in CTA membranes.

Significant criteria in selecting a membrane material for gas separation are the efficiency in gas separation (e.g. $CO_2$ permeability and selectivity), the stable performance and the resistance to impurities in the feed over the lifetime of the membrane module. The introduction has highlighted the importance of cellulose triacetate membranes as viable materials for $CO_2$ separation. However, as will be outlined in **Chapter 2**, the impact of minor components in raw natural gas and flue gas on CTA membrane performance have not been characterized, even though they detrimental to the separation performance and long term viability of the membrane. In particular, the impact of vapour components, as part of the feed gas or sourced from upstream processing units, on CTA membrane performance needs to be fully characterized as this will enable strategies to be developed to increase the lifetime of a module.

# CHAPTER 2. LITERATURE REVIEW

## 2.1. INTRODUCTION

This chapter presents a review of the research literature in the field of membrane gas separation technology for $CO_2$ separation. This includes the utilisation of cellulose acetate based glassy polymers with a focus on the application of cellulose triacetate materials.

The fundamentals of penetrant transport through a membrane is reported, including penetrant sorption, diffusion and permeation. Plasticisation, aging and pore blocking or anti-plasticisation phenomena are also presented and reviewed.

In addition, literature on the impurities in flue gas and natural gas processes and their impacts on $CO_2$ capture processes is also presented. A full critical review for the impact of these impurities on the performance of glassy polymers is also summarised.

Finally, the gaps of knowledge are identified and the scope of this thesis is further defined.

## 2.2. GAS SEPARATION BY MEMBRANE TECHNOLOGY

In membrane separation, the components of a mixture are separated selectively through a barrier, called a membrane (**Figure 2.1**). The driving force for the separation relies on the chemical potential difference (either in the form of a pressure or concentration) of each component on the two sides of the membrane.

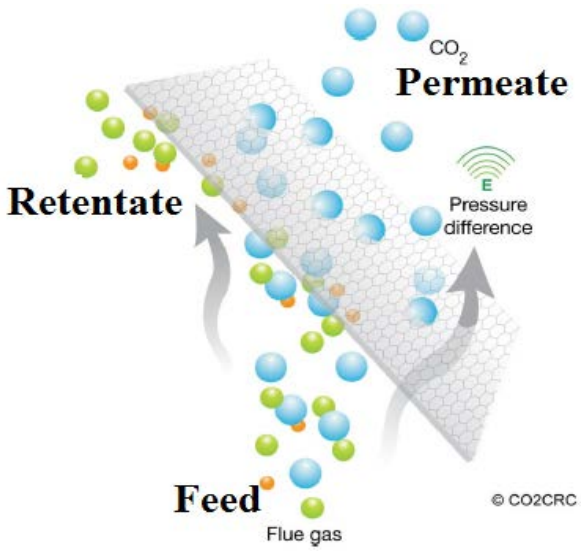


**Figure 2.1**: Sample of flue gas separation by membrane technology, reproduced from [32]

The membrane can be fabricated from inorganic materials or organic materials, with organic membranes favoured in gas separation applications because of their low capital cost, easy fabrication, high pressure and mechanical resistance and capacity to readily change in scale [33]. This thesis will thus focus only on organic polymeric membranes.

For industrial application, the membrane is fabricated into hollow fibre or spiral wound membrane modules (**Figure 2.2**). A hollow fibre membrane is a capillary in which the penetrants are transported through the walls of the fibre. Hollow fibres can take the form of

asymmetric or composite structures. A spiral wound membrane module, on the other hand, is a "wrap" of many flat-sheet membranes and spacers around a central hollow tube. The flat-sheet membrane can be either a homogenous dense polymeric membrane or a thin layer of dense non-porous polymer on a porous support (asymmetric and thin film composite membranes). Depending on the type of membrane morphology and applications, several membrane fabrication technologies have been developed and continuously improved, such as solvent evaporation [34], phase inversion [35], layer by layer [36] or continuous assembly of polymer (CAP) [37].

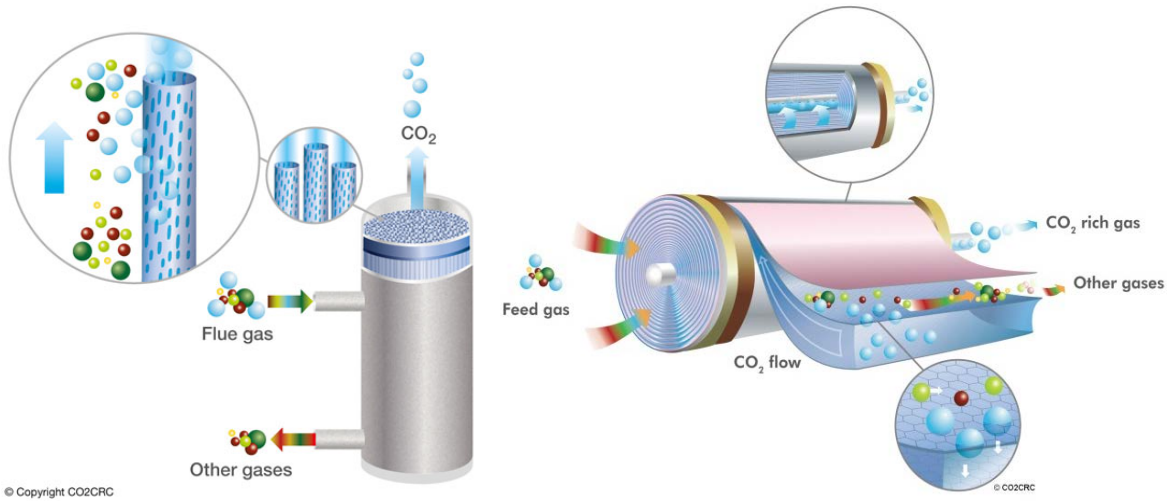


**Figure 2.2** Hollow fibre membrane module (left) and Spiral wound module (right) [32]

Polymeric membrane materials are typically categorised into rubbery and glassy defined by the operating temperature of the membrane relative to the glass transition temperature ($T_g$) of the polymer. A membrane behaves in a "glassy" manner at temperatures lower than $T_g$ where a more rigid polymer structure is present [27, 38]. Alternatively, in the "rubbery" state, the polymer has the potential to obtain thermodynamic equilibrium rapidly with a flexible polymer backbone [5]. Cellulose triacetate has a glass transition temperature that ranges from 185 – 195$^{o}$C, and hence is considered glassy in all major applications [39, 40].

## 2.3. MECHANISM OF PENETRANTS TRANSPORT IN POLYMERIC MEMBRANE

The permeation of gaseous molecules through a membrane can be modelled based on several mechanisms depending of the pore size of the membrane materials [41]. These are Knudsen diffusion, molecular sieving and solution-diffusion (**Figure 2.3**).

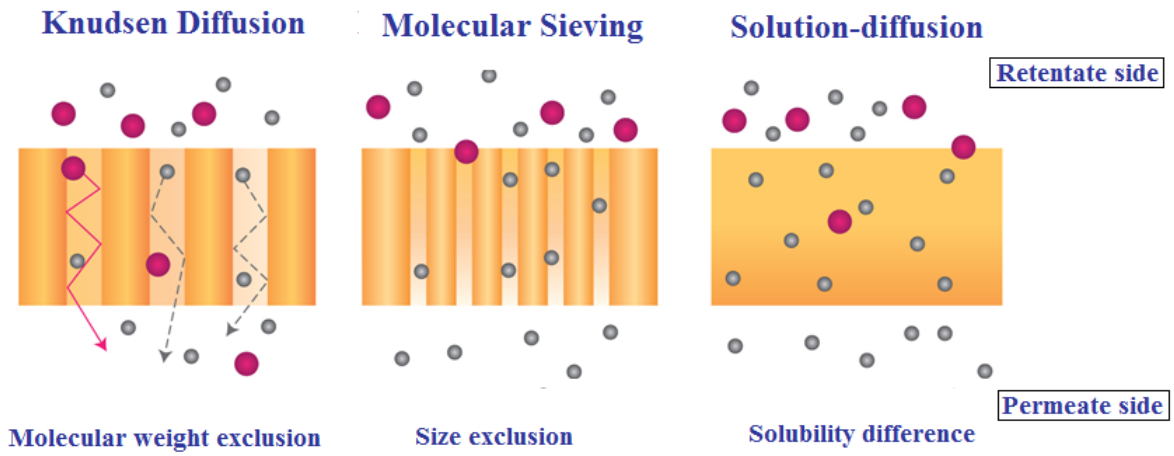


**Figure 2.3** The diffusion mechanisms for membrane gas separation reproduced from [32, 42]

- The *Knudsen diffusion* model applies when the mean pore size ($d_p$) of the membrane is around 20% greater than the mean free path (λ) of gaseous penetrants [43, 44]. The separation is promoted by a pressure driving force and the selectivity for a specified gas is inversely proportional with the molecular weight of transported gases [43, 45]. Hence, this mechanism is not able to separate carbon dioxide from lower molecular weight gases such as nitrogen or methane. In addition, penetrants can absorb on the pore surfaces, which enhances the effective diffusivity. This is called surface diffusion [46].

- The *Molecular sieving* model is dominant when there are similar sizes between gas molecules and the membrane pores. The selectivity is favoured for relative small kinetic diameter molecules. This approach is applied widely in inorganic gas separation membrane or mixed matrix membranes [45]. However, in some cases, penetrants can adsorb on the pore walls and condense when reaching a saturated condition in a process known as capillary condensation. Generally, $CO_2$ can be separated from others processing gases (e.g. $N_2$ and $CH_4$) by molecular sieving due to its smaller kinetic diameter (**Table 2.1**). The challenge, however, is the ability to maintain a relatively narrow pore size distribution during membrane fabrication [42, 46, 47].

- *Solution-diffusion* model is the most common method to explain the transport of penetrants in non-porous polymeric membranes (see **section 2.5**). The penetrants firstly dissolve into the membrane surface on the feed side, diffuse through the bulk of the membrane and finally desorb on the permeate side. Hence, the permeation and selectivity of penetrants depends on both, the solubility and diffusivity of penetrants in the membrane. The penetrant transport is driven by a concentration gradient that can be expressed by Fick's first law at steady state [48]:

$$J = \left(\frac{-D}{1-w}\right)\left(\frac{dC}{dx}\right) = \frac{1}{l}\int_{C_1}^{C_2}\frac{-D}{1-w}dC \qquad \text{(Eq. 2.1)}$$

where $J$ is the gas flux of gas separation; $D$ is the diffusion coefficient of the gas in the polymer; $w$ is molar fraction of gas in the polymer; $l$ is the thickness of the membrane and $C$ is concentration of the gas at any position $x$ across the membrane cross-section as sketched in **Figure 2.4**.

**Table 2.1:** The kinetic diameter and critical temperature of some common gases in gas separation process

| Gas | Kinetic diameter (Å) [49-52] | Critical Temperature(K) [52, 53] |
|---|---|---|
| $CO_2$ | 3.30* | 304.2 |
| $CH_4$ | 3.80 | 190.6 |
| $N_2$ | 3.64 | 126.2 |
| $O_2$ | 3.46 | 154.6 |
| $H_2$ | 2.89 | 33.2 |
| CO | 3.76 | 132.9 |
| $SO_2$ | 3.60 | 430.8 |
| $C_2H_4$ | 3.90 | 282.5 |
| $C_3H_6$ | 4.50 | 365.2 |
| $H_2S$ | 3.60 | 373.2 |
| $H_2O$ | 2.65 | 647.3 |
| NO | 3.20 | 180.0 |
| Toluene | 5.85 | 384 |
| p-xylene | 5.85 | 411 |
| o-xylene | 6.80 | 417 |
| m-xylene | 6.80 | 412 |

* Some authors argue that the diameter for $CO_2$ is underestimated and values in the range of 3.43 – 3.63Å are often preferred [54-56].

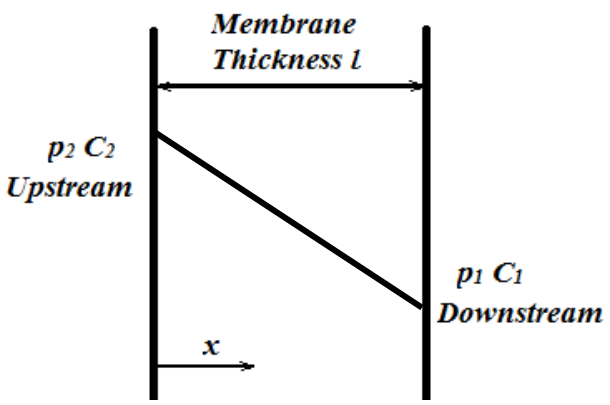


**Figure 2.4**: The sketch of gas transport through membrane with assumption of linear concentration gradient across membrane thickness

## 2.4. PERMEABILITY AND SELECTIVITY OF GLASSY MEMBRANE

### 2.4.1. Permeability

The performance of a membrane is expressed as either the permeability or permeance and its selectivity. The empirical expression for gas permeation flux at steady state assuming a linear concentration across the membrane thickness was introduced by von Wroblewski [57]:

$$J = P\frac{p_2 - p_1}{l} \qquad \text{(Eq. 2.2)}$$

where $p_1$ and $p_2$ are the partial pressures on the two sides of the membrane barrier; $P$ is defined as the permeability coefficient of the membrane. Assuming solution – diffusion mechanism, the consequent derivation from (Eq. 2.1) and (Eq. 2.2) with average effective diffusion coefficient, $\overline{D}$, forms (Eq. 2.3). In the case where the upstream concentration and pressure are much greater than the downstream conditions, (Eq. 2.3) is simplified to the form of (Eq. 2.4).

$$P = \frac{Jl}{p_2 - p_1} = \frac{\int_{C_1}^{C_2} \frac{-D}{1-w} dC}{p_2 - p_1} = \frac{C_2 - C_1}{p_2 - p_1}\overline{D} \qquad \text{(Eq. 2.3)}$$

$$P = \frac{C_2}{p_2}\overline{D} = S.\overline{D} \qquad \text{(Eq. 2.4)}$$

where $S$ is defined as the solubility coefficient of the specified gas in the membrane and defined as the ratio of concentration over partial gas pressure [48]. In this case, the permeability can be defined by both a diffusivity (kinetic term) and solubility (thermodynamic term).

The unit of permeability is usually quoted as barrer. Alternatively, for some commercial membranes where the thickness of the membrane active layer cannot be measured simply (asymmetric or thin film composite membrane), the thickness – normalised flux or permeance, $Q$ or $P/l$, is used and quantified as the Gas Permeation Unit (GPU).

$$1 \text{ barrer} = 10^{-10} \text{ cm}^3\text{(STP).cm/(cm}^2\text{.s.cmHg)}$$

$$1 \text{ GPU} = 10^{-6} \text{ cm}^3\text{(STP)/(cm}^2\text{.s.cmHg)}$$

Permeability through a membrane is commonly measured by either a constant pressure variable volume (CPVV) gas permeation apparatus [19, 23, 58] or a constant volume variable pressure (CVVP) gas rig [59]. In the first method, the feed gas is introduced to the feed side of the membrane and the flowrate of the permeate stream is detected to calculate the permeance or permeability. The permeate stream can also be connected to a gas concentration analyser to determine the composition of the permeate components that is then used to calculated the permeability of each components in a mixed gas feed. In the second method, a pressurised gas at fixed pressure is introduced to the feed side of a membrane with downstream pressure initially set to a full vacuum. The pressure increase on the permeate side is monitored as a function of time to determine the gas flux across the membrane. The detailed description for each method is reported in **Chapter 3**.

### 2.4.2. Selectivity

The "ideal selectivity", $\alpha$, of a membrane is defined by the International Union of Pure and Applied Chemistry (IUPAC) as the ratio of the permeance of two gases (Eq. 2.5) when a

vacuum is applied to the downstream side of the membrane. The "separation factor", $\alpha^*$, is a more practical approach (Eq. 2.6), especially when two or more penetrants are present simultaneously. The "separation factor" is calculated from the mole fractions of penetrants in the feed and permeate, *x* and *y*, respectively. This depends on the composition of the gas feed as well as the inherent membrane performance [48, 60].

Ideal selectivity (for A-B binary system)

$$\alpha_{A/B} = \frac{P_A}{P_B} = \frac{D_A}{D_B}\frac{S_A}{S_B} \qquad \text{(Eq. 2.5)}$$

Separation factor

$$\alpha^*_{A/B} = \frac{y_A x_B}{y_B x_A} \qquad \text{(Eq. 2.6)}$$

### 2.4.3. Robeson's Upper Bound

Membrane separation is restricted by the trade-off between permeability and selectivity in which an increase of membrane permeability generally corresponds with a decrease of selectivity and vice-versa. The behaviour was empirically summarised by Robeson in the well-known Robeson's upper bound [61]. Up to 2008, over 300 gas pairs have been referenced, including $O_2$, $N_2$, $CH_4$, $CO_2$, $H_2$ and He (**Figure 2.5**). By taking account of the activation energy of diffusion as well as the penetrant kinetic diameter, the permeability and selectivity at the Robeson's bond can be predicted theoretically as expressed in (Eq. 2.7) and (Eq. 2.8) [61].

$$P_A = k\alpha^n_{A/B} \qquad \text{(Eq. 2.7)}$$

$$-\frac{1}{n} = \left(\frac{d_B}{d_A}\right)^2 - 1 = \frac{d_A + d_B}{d_A^2}(d_B - d_A) \qquad \text{(Eq. 2.8)}$$

where *n* is the slope factor of the upper bound line; *k* is empirically predicted in **Table 2.2**; $d_A$ and $d_B$ are the kinetic diameters of gas A and B respectively. In general, changing the chemical structure of a glassy polymer may increase the free volume fraction that subsequently enhances the membrane permeability. Conversely, the larger free volume will also reduce the selectivity [62]. The shift in the upper bound between 1991 to 2008 indicates the development of new polymers and new membrane fabrication techniques that are able to improve separation performance.

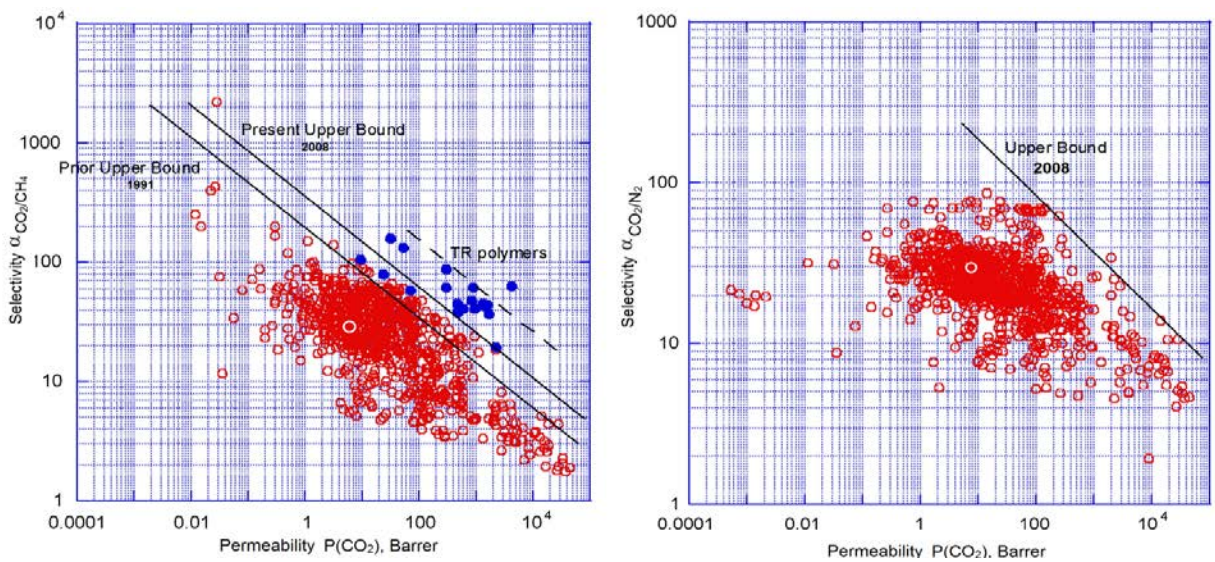

**Figure 2.5** The upper bound for $CO_2/CH_4$ and $CO_2/N_2$ gas separation, reproduced from [61] (The white circle represents the current performance of the CTA membrane [12, 40])

**Table 2.2:** The front factor value (k) and slope of the upper bound for some common gas pairs in carbon capture [57, 61]

| Gas pairs | k (barrer) | n |
|---|---|---|
| $He/CH_4$ | 19,800 | -0.809 |
| $CO_2/N_2$ | 30,967,000 | -2.888 |
| $CO_2/CH_4$ | 5,369,140 | -3.636 |

## 2.5. SOLUTION – DIFFUSION MODEL

The solution – diffusion model has been widely applied to model the gas transportation in a polymeric membrane. Importantly, this approach separates gas behaviour within the polymer to the solubility and diffusivity terms.

### 2.5.1. Solubility in Glassy Polymers

#### 2.5.1.1. Dual-Mode Sorption Model (DMS)

The solubility of gas molecules in glassy polymers has been well-described by the dual-mode sorption model (DMS) [27-29]. This model argues that there are two domains for the sorption of gas molecules into the membrane, identified as the Henry's law region (equilibrium – free – volume region) and the Langmuir isotherm region (excess free volume of the polymer) [5, 29].

The sorption of gas molecules into the equilibrium – free – volume region of the membrane will behave like the dissolution into liquid, which is referred to as Henry's law. The concentration of sorbed gas will be expressed as a linear relationship with the applied pressure (Eq. 2.9) where $C_D$ is the concentration of gas sorbed in the Henry's law region; $k_D$ is Henry's law constant and $p$ is the applied pressure of the penetrant.

$$C_D = k_D p \qquad \text{(Eq. 2.9)}$$

The sorption into the excess free volume region is usually described in the form of a Langmuir sorption isotherm (Eq. 2.10). As the excess free volume is limited, the sorption in this region ($C_H$) will reach a saturation concentration ($C'_H$) when all the voids are filled. The Langmuir affinity constant, $b$, represents the ratio of the equilibrium rate constant of sorption and desorption in the Langmuir region [63] and follows a van't Hoff relationship [64].

$$C_H = \frac{C'_H bp}{1+bp} \qquad \text{(Eq. 2.10)}$$

By combining both sorption regions, the dual-mode sorption model can be expressed in (Eq. 2.11). At low pressure, the Langmuir sorption is dominant and at high gas pressure Henry's law dominates (**Figure 2.6**).

$$C = C_D + C_H = k_D p + \frac{C'_H bp}{1+bp} \qquad \text{(Eq. 2.11)}$$

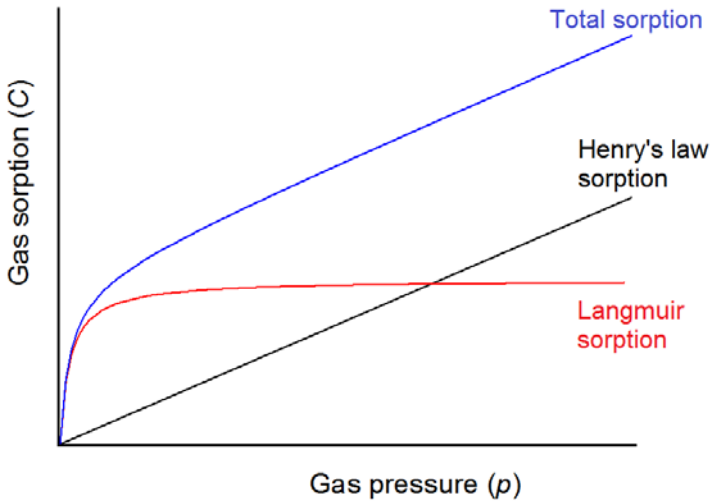


**Figure 2.6** The gas sorption by dual-mode sorption model

Alternatively, Koros [64] extended the dual-mode sorption model for multi-component systems with the assumption that all penetrants behave ideally in the Henry's law region and sorption competition only occurs in Langmuir regions (Eq. 2.12). This approach shows that the sorbed amount of each penetrant is reduced in the multi-component system in comparison with a single component system with the same partial pressure of each component.

$$C_i = C_{D,i} + C_{H,i} = k_{D,i} p_i + \frac{C'_{H,i} b_i p_i}{1+b_i p_i + b_j p_j + \cdots} \quad i,j\ldots \text{ - components} \qquad \text{(Eq. 2.12)}$$

### 2.5.1.2. The Sorption of Vapour

The dual-mode sorption model (**Figure 2.7a**) is commonly applied for ideal gas sorption in glassy polymers [29, 40, 63]. However, the sorption of highly condensable penetrants such as water or hydrocarbons requires a more complex model [65, 66].

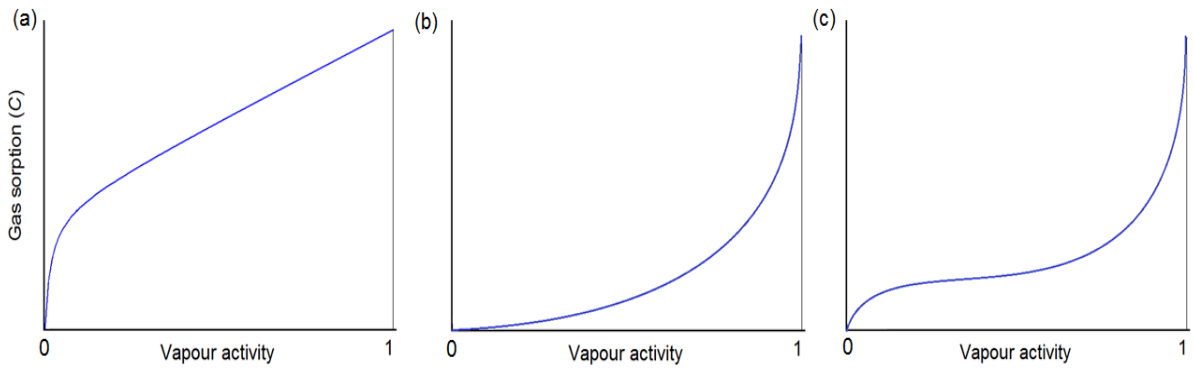


**Figure 2.7** Some typical shapes of vapour sorption isotherms [67, 68]

The Flory – Huggins model can be used for the sorption isotherm shown in **Figure 2.7b**. This model accounts for the free energy of gas mixing with the polymer [5, 69, 70]. The activity of the penetrant in the polymer at equilibrium is expressed in (Eq. 2.13), where $p_i / p_{i,o}$ is the vapour activity; $\Phi_s$ and $\Phi_p$ are volume fractions of penetrant and polymer, respectively; $V_s$ and

$V_p$ are the molar volume of penetrant and polymer, respectively; and $\chi$ is the Flory – Huggins interaction parameter of polymer and the penetrant. Generally, the first term in (Eq. 2.13) corresponds to an entropic contribution while the second term is an enthalpic term [71]. This model has been used for the sorption of hydrocarbons into PDMS membranes [71] and even the sorption of $CO_2$ and $CH_4$ in a cellulose acetate membrane [72]. However, the Flory – Huggins model is not well-suited for membrane – penetrant system with strong interactions [71]. For these systems, several advanced expressions have been developed, such as Flory – Rehner theory [73] and the Engaged species induced clustering (ENSIC) model [74].

$$ln\frac{p_i}{p_{i,0}} = \left[\ln \Phi_s + \left(1 - \frac{V_s}{V_p}\right)\Phi_p\right] + (\chi\Phi_p^2) \qquad \text{(Eq. 2.13)}$$

The sorption isotherm of some vapours into glassy polymer [75-77], is described in **Figure 2.7c**. The popular model for this S-shape isotherm is the Brunauer – Emmett – Teller (BET) model [30] or Guggenheim – Andersonde – Boer (GAB) model [31]. Generally, both models assume that the adsorption of adsorbates on the adsorption sites is multilayered. While the BET model assumes that each adsorbate layer follows Langmuir sorption theory and has no mutual interaction with the alternative layers, the GAB model takes into account the interaction of the first layer with further adsorbed layers. The BET and GAB models can be mathematically expressed by (Eq. 2.14) and (Eq. 2.15), respectively, where $\nu$ is the adsorption concentration of adsorbate (mass of adsorbate per mass of adsorbent); $\nu_m$ is the capacity of monolayer adsorption; $a$ is vapour activity; $h$ and $f$ are sorption constants. The GAB model has been reported to fit better over a larger vapour activity range (0.10 – 0.90) [31] than the BET model (0.05 – 0.45)[30].

BET equation: $$\nu = \frac{\nu_m ha}{(1-a)(1-a+ha)} \qquad \text{(Eq. 2.14)}$$

GAB equation: $$\nu = \frac{\nu_m hfa}{(1-fa)(1-fa+hfa)} \qquad \text{(Eq. 2.15)}$$

However, due to the complicated nature of gas sorption into glassy polymers, the classic models can only be applied effectively to some sorption cases. Recently, some advanced models have been studied and published to fulfil this gaps of knowledge with some significant achievements such as new DMS models [66, 78, 79] or the Non-equilibrium thermodynamics model of glassy polymers (NET-GP) [80-82].

### 2.5.2. Diffusivity in Glassy Polymer

#### 2.5.2.1. Fractional Free Volume (FFV)

"Free volume" represents to the voids within the polymeric membrane in which the penetrant transport occurs. This void fraction or fractional free volume (FFV) can be calculated via (Eq. 2.16), where $V$ is the polymer specific molar volume; $V_o$ is the volume of polymer chains that can be calculated from the van der Waals volume, $V_w$ [83, 84]. $V_w$ can be obtained from the volume of individual functional groups in a monomer as regards to the databases of van Krevelen and Te Nijenhuis [85]. In addition, the FFV can also be experimentally determined by X-ray diffraction or Positron Annihilation Lifetime Spectroscopy (PALS) [12, 27].

$$FFV = \frac{V - V_o}{V} = \frac{V - 1.3V_w}{V} \qquad \text{(Eq. 2.16)}$$

The free volume is related to the glass transition temperature [5, 27, 86] (**Figure 2.8**). A rubbery polymer obtains rapid thermodynamic equilibrium and has high freedom polymer backbone which results in high permeant diffusion [5]. On the other hand, a glassy polymer takes a long time to reach thermodynamic equilibrium due to steric hindrance and this results in non-equilibrium micro-cavities within a rigid polymer structure [27]. It should be noted that the FFV can be influenced by several factors including the concentration of plasticisers, aging history as well as membrane thickness [57].

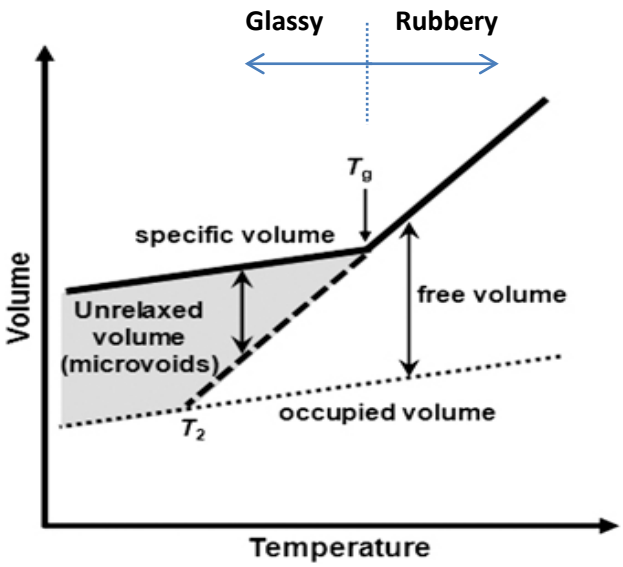


**Figure 2.8** The correlations of polymer specific volume versus temperature [87]

### 2.5.2.2. Free Volume Dependence of Diffusion

Diffusivity in polymeric membrane is the motion of penetrants in response to a chemical potential gradient [27]. Generally, the molecules vibrate and "move" across the membrane via the voids or "free volume" caused by the inefficient packing of polymer chains [88]. A rubbery polymer with rotatable polymer backbones is more favoured for gas transport and leads to higher diffusion. A glassy polymer, inversely, has a more rigid structure due to the steric hindrance between polymer segments which results in low penetrant diffusion [5]. The dependence of diffusivity on FFV of the membrane is commonly expressed via classic free volume theory (Eq. 2.17), where $D$ is the diffusivity or diffusion coefficient; $A$ and $B$ are diffusivity constants [89, 90].

$$D = A \exp\left(\frac{-B}{FFV}\right) \qquad \text{(Eq. 2.17)}$$

However, the above correlation assumes that all voids within the membrane behave equally. In fact, there is a potential for Langmuir voids with "dead ends" within the membrane which will not contribute to the gas transport. Petropoulos took into account this potential by advancing the dual-sorption model with an additional immobilisation factor, $F$, as the ratio of the diffusion coefficient in the Langmuir region (equilibrium voids) to the diffusion coefficient in the Henry's law region (non-equilium voids) (e.g. $D_H/D_D$ or $D_{NE}/D_E$) [91]. This factor is substituted into the typical dual sorption equation (Eq. 2.11) to calculate the concentration of mobile species, $C_m$ as shown in (Eq. 2.18) [92].

$$C_m = k_D p \left[1 + \frac{FK'}{1+\alpha' k_D p}\right] \quad \text{(Eq. 2.18)}$$

with $K' = \frac{C'_H b}{k_D}$ and $\alpha' = \frac{b}{k_D}$

The transport of highly condensable penetrants such as $CO_2$, water or hydrocarbons can also alter the fractional free volume of the membrane. High concentration of penetrants sorbed into the membrane can reduce the interactions between polymer segments resulting in an increase in free volume and thus an increase of gas permeation, a reduction in membrane selectivity and a loss of mechanical strength [93-95]. This effect is defined as "plasticisation". Inversely, the sorption of these penetrants can fill the Langmuir voids and block the pathways of penetrants, which is commonly referred to as "anti-plasticisation" [12, 15, 96]. This often occurs when the penetrants have strong mutual interactions such as water which results in clusters of molecules inside the membrane [94, 97, 98]. In these cases, the diffusion coefficient can be expressed in the form of (Eq. 2.19), where $D_o$ is the Fickian diffusion coefficient at infinite dilution (C → 0); $\beta$ is a constant expressing the impact of adsorbed penetrants on the polymer in which $\beta > 0$ for plasticising and $\beta < 0$ for ant-plasticising penetrant – membrane systems [59, 66, 99].

$$D = D_o \exp(\beta C) \quad \text{(Eq. 2.19)}$$

#### 2.5.2.3. Measurement of diffusion coefficient

The Fickian diffusion coefficient (Eq. 2.1) can be obtained by a dynamic sorption experiment [100] in which the membrane is suspended into the constant penetrant pressure environment. The penetrant will dissolve into the membrane until reaching saturation. Assuming unidimensional diffusion across a flat sheet membrane with thickness *l*, the concentration profile inside the membrane is as shown in **Figure 2.9**.

The diffusion coefficient can be mathematically calculated via (Eq. 2.20), which is derived from Fick's second law [100, 101]. *m* is the mass of the membrane at time *t*; $m_o$ and $m_\infty$ are the initial mass and the mass at equilibrium of the membrane, respectively.

$$\frac{m_0 - m}{m_0 - m_\infty} = 1 - \frac{8}{\pi^2} \sum_{n=0}^{\infty} \frac{1}{(2n+1)^2} \exp\left(-\frac{(2n+1)^2}{l^2} \pi^2 D t\right) \quad \text{(Eq. 2.20)}$$

The Fickian diffusion coefficient can also be determined from a transient permeation experiment in the CVVP gas permeation apparatus aforementioned in **section 2.4.1**. The flux of permeate stream ($Q_p$) is recorded versus experimental time and the diffusion coefficient is calculated via (Eq. 2.21), with $\theta$ is the permeability time lag which is defined as the time for reaching the steady-state concentration profile inside the membrane (referred to **Figure 2.10**) [101].

$$D = \frac{l^2}{6\theta} \quad \text{(Eq. 2.21)}$$

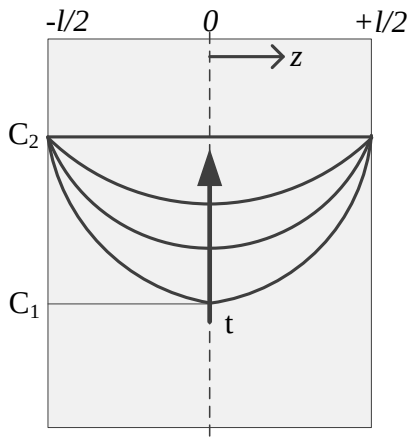


**Figure 2.9** Concentration profile developed in a membrane over time during a dynamic sorption experiment

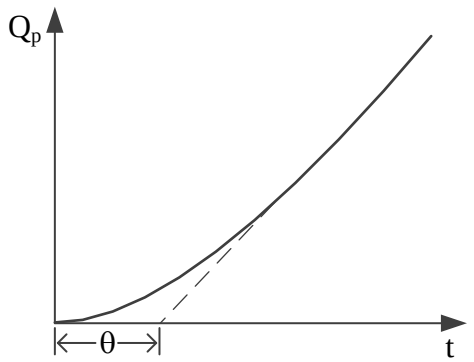


**Figure 2.10** The flowrate of permeate ($Q_p$) versus time in a time lag measurement experiment within a CVVP apparatus

When plasticisation occurs, the sorption behaviour is no longer Fickian [102, 103]. In this case, (Eq. 2.20) can be expressed in a heuristic manner (Eq. 2.22) [104, 105], where $k$ is a constant characterising the membrane – solvent system and $n$ is an exponent characterising the type of diffusion. Ideal Fickian diffusion has $n$ = 0.5 but a range of 0.5 – 0.6 is commonly accepted [106]. For $0.5 < n < 1.0$, the diffusion is anomalous, for example as reported in the sorption of acetone into cellulose acetate film (37.9% acetyl content) [107]. Case – II diffusion with $n$ = 1 is also commonly observed when the penetrant swells the polymer substantially [103, 108]. The mathematical models for non – Fickian diffusions are quite complicated with different approaches reported [103, 108, 109].

$$\frac{m_0 - m_t}{m_0 - m_\infty} = kt^n \qquad \text{(Eq. 2.22)}$$

## 2.6. PHYSICAL AGING

In a glassy polymer, the free volume is in a non-equilibrium state. This means that densification of the polymer matrix towards the equilibrium condition will occur over time [110, 111]. This volume relaxation is generally explained by either the diffusion of free volume to the external surfaces of the polymer [112, 113] or a contraction in the membrane lattice

[114]. This physical aging can result in the alteration of polymer properties such as decreases in polymer creep rate, toughness and increases in membrane density [111, 115, 116].

The effect of physical aging on the performance of gas separation membranes had been studied for several glassy membrane materials. For instance, Lin and Chung [117] studied the permeability, diffusivity and solubility performance of several pure gases on 6FDA – durene polyimide membranes as a function of time. Their results showed that the physical aging led to a decrease in gas permeability and that the smaller kinetic diameter gas was affected less significantly than others. Lin and Chung found that the physical aging reduced both diffusivity and solubility by reducing the free volume pathway for gas diffusion and the adsorption sites for gas sorption [117]. Similar aging behaviour was also observed in poly(methyl methacrylate) (PMMA) [118], bisphenol-A benzophenone-dicarboxylic acid (BPA-BnzDCA) [110, 119] and polymers of intrinsic microporosity (PIMs) [120]. However, the aging of cellulose acetate membranes has not been well characterised.

## 2.7. MEMBRANE THICKNESS

An ultrathin film membrane is more preferred in industrial applications to increase the flux of penetrants (Eq. 2.2). However, several studies have shown that the properties of the membrane are dependent upon the membrane thickness. Huang and Paul [121] classified the membrane thickness into three regimes: a bulk behaviour regime (thickness > 10µm), a thin film regime (~100 nm – 10 µm) and an ultrathin film regime (< 100 nm). In most fundamental studies, the thickness falls into the bulk regime where the membrane performance and properties are independent of this thickness. On the other extreme side, an ultrathin membrane has characteristics that depend significantly upon the membrane thickness [122]. This is related to the so-called “confinement effect” which occurs when the conformation of polymer segments is disturbed by the boundaries of the membrane surfaces [110].

The common membrane thickness in industrial applications is in the thin film regime where the steady state membrane properties do not change significantly with thickness [110]. However, several studies have shown that volume relaxation progresses in a thin membrane faster than a thicker membrane. The resulting density of glassy polymers has been observed to be greater in thin films [123, 124] which corresponds to a lower fractional free volume resulting from more rapid volume relaxation The reduction in free volume results in a loss of diffusion pathways for gas molecules and less Langmuir sorption sites for gas sorption, which will consequently lead to lower gas permeability [42, 110, 119, 125].

To avoid these time dependent effects, some workers anneal fresh membranes at elevated temperature to ensure all membranes start at the same conditions [121]. Others heat the membrane over the $T_g$ and then quench to room temperature [110, 119, 121]. Another approach is to store the fresh annealed membrane for a period to allow volume relaxation to occur [12, 42, 58, 66].

Thin film membranes are more rapidly plasticised than thick films. Scholes et al. showed that the $CO_2$ – induced plasticisation pressure in thin film polysulfone (PSf) membranes was lower than in the thick membrane [126]. A similar behaviour was observed for ultrathin 6FDA-

durene polyimide membranes where it was argued that a decrease in membrane thickness led to a decline in mechanical properties and membrane resistance to plasticisers [127]. Some researchers believe that the accelerated plasticisation that occurs in thin films is due to the differences in free volume distribution, the orientation of polymer segments and the reduction in Langmuir adsorption sites at low FFV [125, 127-129].

## 2.8. CELLULSE ACETATE

### 2.8.1. Background

Cellulose acetate is the first polymer developed for $CO_2$ separation and occupies up to 80% of the commercial membrane market [4, 130]. The first chemical synthesis of cellulose acetate dates back to 1865 when Paul Schützenberger heated cellulose with acetic anhydride at 180$^{o}$C [131]. Several researchers and scientists further developed the cellulose acetate manufacturing process by using other reactants such as acetyl chloride [132], ketene [133], and adding catalysts such as zinc chloride or sulphuric acid [134-136] to increase the reaction efficiency. Currently, cellulose acetate is utilised widely in products such as textiles, cigarette filters [137], and in membranes for hemodialysis, desalination and natural gas sweetening [4]. In gas separation technology, the cellulose acetate based membrane is utilised in Cynara® hollow fibre membrane modules and UOP Separex spiral wound modules [5, 6, 130].

Cellulose acetate polymer production mainly includes two stages: a primary acetylation step to convert hydroxyl functional groups in cellulose into fully esterified cellulose triacetate (CTA) and a secondary hydrolysis step to hydrolyse the CTA to the desirable degree of acetylation [135]. The polymer is then dissolved in a solvent to produce a membrane via solvent – non-solvent phase inversion [35, 138-141]. A significant factor in membrane fabrication is to dry the asymmetric polymer films slowly to prevent the collapse of the microporous support structure [142-145]. Some approaches used to achieve this objective are freeze drying [146] and solvent extraction [147, 148]. The impact of solvent evaporation temperate on the formation of the membrane morphology has also been studied [145].

### 2.8.2. Degree of Substitution

Cellulose acetate polymer is formed from a repeated glycoside monomer (**Figure 2.11**). To characterise cellulose acetate, a critical factor is the degree of acetylation or substitution (DS) that is defined as the average number of acetyl functional groups per monomer unit [40]. For full esterification, the DS number is 3. However, real cellulose triacetate (CTA) materials, also named primary cellulose acetate, have a DS number around 2.9. The DS number for cellulose diacetate (CDA) or secondary cellulose acetate is around 2.45 [40, 135]. The degree of acetylation can also be expressed in term of acetyl value (% content of acetyl or % content of combined acetic acid) with the correlations between these definitions and DS number as stated in (Eq. 2.23) and (Eq. 2.24) [149, 150].

$$DS = \frac{162 \text{ x } (\%\ acetyl)}{4300-(42 \text{ x } \%\ \text{acetyl})} \qquad \text{(Eq. 2.23)}$$

$$DS = \frac{162 \text{ x } (\%\ combined\ acetic\ acid)}{6005-(42 \text{ x } \%\ \text{combined acetic acid})} \qquad \text{(Eq. 2.24)}$$

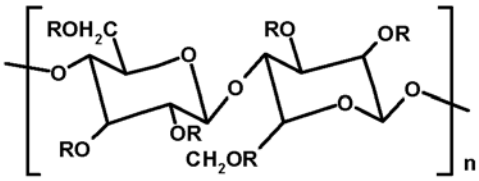


R: $COCH_3$ or H

**Figure 2.11** Chemical structure of cellulose acetate polymer [12]

The DS of cellulose acetate is commonly determined by saponification and back titration of ester functional groups with alkali as given by ASTM D871 – 96 [135, 151]. Other approaches for determining DS is by Nuclear magnetic resonance (NMR) [152, 153] or infrared spectroscopy (IR) [153, 154]. These studies have shown that the essential interactions in a cellulose acetate polymer are hydroxyl – hydroxyl, hydroxyl – acetyl and acetyl – acetyl in which the hydroxyl (–OH) functional group has stronger hydrogen bonding than the acetyl group (–CO–) [153, 155]. As a result, the chain packing of cellulose acetate with a higher DS is less dense than lower DS systems. This also affects the glass transition temperature and the elasticity of high DS cellulose acetate (see **Table 2.3**).

The degree of acetylation also affects the crystallinity of the cellulose acetate polymers. Heat of diffusion and Wide – Angle X-ray scattering (WAXS) studies have shown that the higher DS cellulose acetate has higher crystallinity (**Table 2.3**) [12, 40] due to the higher matrix structure regularity in these materials [156]. Since the crystalline phase is more rigid and well-ordered, gas transport is not favoured through these regions [156, 157]. However, at the same time, the chain mobility in low DS cellulose acetate is more limited than in the high DS polymer due to the increase in the number of hydroxyl functional groups in this polymer [155].

Puleo and Paul's study on pure gas permeability through DS cellulose acetate membranes of different DS showed higher gas permeability in the higher DS membrane [40] (**Table 2.4**). A similar trend was observed in the study of Chen et al. for $CH_4$ permeation through CTA and CDA [12]. However, the water vapour permeability in this study showed an inverse trend with more water permeating through the CDA membrane than the CTA membrane. This was explained by the stronger affinity of CDA (more hydroxyl groups) for water vapour than CTA which consequently increased the sorption of water vapour into the polymer [12].

**Table 2.3:** The comparison in physical properties of cellulose acetate with different degree of acetylation [12, 40, 158, 159]

| Properties | CTA (DS~2.8) | CDA (DS~2.4) | CA (DS~1.8) |
|---|---|---|---|
| Density, g/cm$^3$ | ~1.30 | ~1.33 | ~1.36 |
| Thermal Stability, $^oC$ (Initial degradation temperature) | ~305 | ~300 | - |
| Molecular weight average | 340,000 | 143,000 | 157,000 |
| $T_g$, $^oC$ | ~186 | ~192 | ~210 |
| Crystallinity, % | 52 | 37 | 27 |
| Elastic modulus ($10^5$), MPa | 4.9 | 4.4 | 4.2 |
| Tensile strength ($10^3$), MPa | 14 | 12.7 | 6.6 |

**Table 2.4:** The permeability coefficients of cellulose acetate membranes

| Components | Permeability P, barrer at cellulose acetate with DS | | | Reference |
|---|---|---|---|---|
| | 2.8 – 2.9 | 2.2 – 2.4 | 1.8 | |
| He | 19.6 | 16.0 | 9.34 | [40][a] |
| $N_2$ | 0.23 | 0.15 | 0.057 | |
| $CO_2$ | 6.56 | 4.75 | 1.84 | |
| $CH_4$ | 0.20 | 0.15 | 0.052 | |
| | 0.272 | 0.259 | - | [12][b] |
| Water vapour | 12,000 | 13,000 | - | |

[a] The permeation was determined at 35$^o$C and 1 atm gas pressure

[b] The permeation was determined at 35$^o$C and 0.4 water vapour activity with 7.5 bar $CH_4$ carrier gas

### 2.8.3. Pure Gas Transport in Cellulose Triacetate Membrane

Many studies have been conducted to investigate gas transport through cellulose triacetate (CTA) membranes with a significant focus on $CO_2/CH_4$ separation [12, 40, 72, 160]. Puleo et al. [40] reported the pure gas permeability of $CO_2$ and $CH_4$ at elevated pressures through a CTA membrane (DS 2.84). The study showed that the permeability of $CH_4$ was independent of gas pressure. This behaviour was also observed for the permeabilities of $O_2$ and $N_2$ through CTA hollow fibres in another study [161]. However, the permeability of $CO_2$ through the CTA membrane demonstrated an increasing trend with pressure, which resulted from $CO_2$ – induced plasticisation [40, 72, 160, 162, 163]. The plasticisation pressure for CTA membranes has been recorded in the range 500 kPa to 1200 kPa $CO_2$ depending upon the membrane fabrication

methods and the presence of other components in the gas mixture [40, 72, 161]. The explanation for this behaviour is that the presence of high absorbed $CO_2$ concentrations can increase the segmental motion and disrupt the intramolecular interactions in the membrane [40]. Particularly, the quadrupole moment of $CO_2$ is argued to enhance its solubility by strong dipole interactions with the polar matrix membrane, e.g. acetate and hydroxyl functional groups in cellulose acetate membrane [164, 165]. Puleo et al. also studied the time dependence of $CO_2$ induced plasticisation on the CTA membrane and proved that the plasticisation would approach equilibrium if sufficient time was allowed. In this case, the membrane could approach the original permeability values during the depressurisation process but a much longer time was required for this process (as regards **Figure 2.12**) [40].

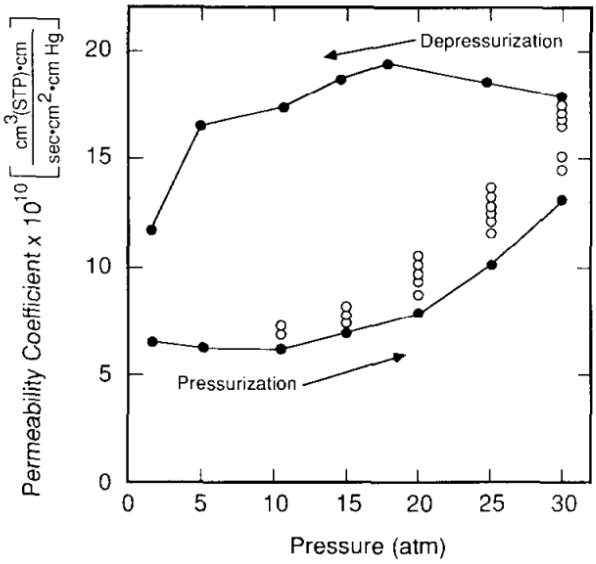


**Figure 2.12** The permeability coefficient of CTA (DS 2.84) membrane under $CO_2$ pressurisation and depressurisation cycles (the open circles represent the increase in permeability versus experiment time, which was 16 days for the 30 atm $CO_2$ pressure experiment) [40]

The most common gas transport model applied to cellulose acetate membranes is the dual-mode sorption model due to the nonlinear concave shape of the sorption curves as shown in **Figure 2.13** [40, 72, 160, 166]. The parameters of this model ($k_D$, $C'_H$ and b, see (Eq. 2.11)) can be calculated via nonlinear regression analysis (parameters provided in **Table 2.5)**. Additionally, the sorption behaviour of the CTA membrane before and after conditioning in high pressure $CO_2$ has been studied [40, 167]. It was found that the $CO_2$ adsorbed into the membrane would redistribute the "free volume" in the Langmuir void regime, and this could not return to the original state quickly when the adsorbed $CO_2$ was evacuated (due to the slow relaxation of the glassy membrane). Hence, a second sorption of $CO_2$ or $CH_4$ into the same membrane would show a significant increase in gas sorption capacity [40, 167]. This suggests that the "exposure history" of the membrane is significant for the gas transport especially in the presence of plasticisers such as $CO_2$. Furthermore, the "immobilisation" model has also been applied in some studies to have a better consistency between sorption and permeability data [72, 166, 168].

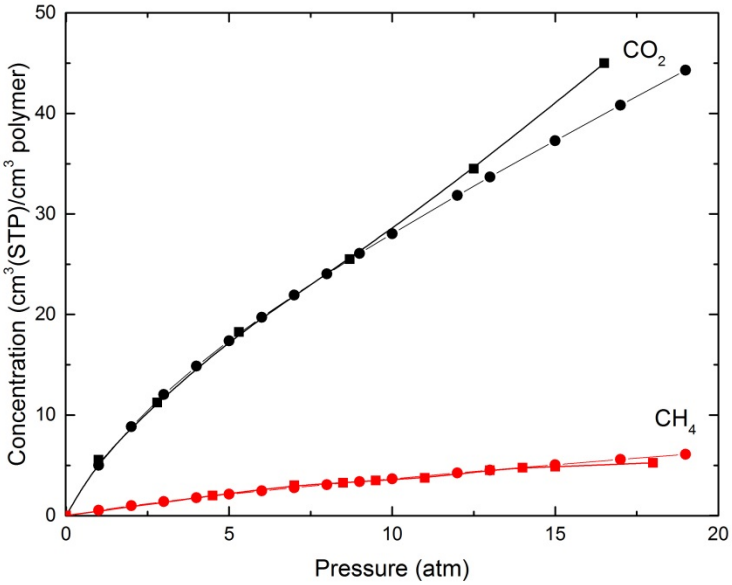


**Figure 2.13** Sorption isotherms for $CO_2$ and $CH_4$ in CTA membranes
( ■ $CO_2$ 35°C and ■ $CH_4$ 35°C [40]; ● $CO_2$ 30°C and ● $CH_4$ 40°C [160])

**Table 2.5:** The dual-mode sorption parameters for $CH_4$ and $CO_2$ in CTA membranes

| Penetrant | $k_D$ ($cm^3$(STP)/$cm^3$.atm) | $C'_H$ ($cm^3$(STP)/$cm^3$) | b ($atm^{-1}$) | Reference |
|---|---|---|---|---|
| $CO_2$, 35°C | 1.647 | 19.63 | 0.291 | [40] |
| $CH_4$, 35°C | 0.184 | 3.15 | 0.134 | |
| $CO_2$, 30°C | 1.60 | 16.8 | 0.253 | [160] |
| $CH_4$, 40°C | 0.237 | 2.13 | 0.156 | |

The impact of temperature on the gas transport in CTA membranes has also been studied [160, 168]. Generally, the permeability coefficient is the product of diffusivity and solubility coefficients (Eq. 2.3), which can be expressed in the form of Arrhenius equations as shown in (Eq. 2.25),

$$P = P_o \exp\left(-\frac{E_P}{RT}\right) = D_o \exp\left(-\frac{E_D}{RT}\right) S_o \exp\left(-\frac{\Delta H_S}{RT}\right) \qquad \text{(Eq. 2.25)}$$

where $P_o$, $D_o$, $S_o$ are pre-exponential factors for permeability, diffusivity and solubility coefficients, respectively; $R$ is universal constant; $T$ is temperature; $E_p$ and $E_D$ are activation energy for permeability and diffusivity, respectively; and $\Delta H_S$ is a heat of sorption [59, 169-171]. The increase of temperature enhances the diffusion of penetrants through the membrane ($E_D > 0$) but diminishes the solubility of these penetrants ($\Delta H_S < 0$). The study of Sada et al. on commercial and cast CTA membranes found that the gas permeation of $CO_2$ and $CH_4$ increased with temperature [160], meaning that the permeation with temperature is diffusion controlled. The activation energies calculated in Sada et al.'s study were +23.9 kJ/mol and +34.8 kJ/mol for $CO_2$ and $CH_4$, respectively. Similar behaviour was also observed in CDA membranes [72,

168] and very similar trends were observed for both asymmetric (0.5 µm) and thick dense membranes (55 – 124 µm) [168].

### 2.8.4. Mixed Gas Transport in Cellulose Triacetate Membrane

The permeation of $CO_2$ and $CH_4$ through a CTA membrane in gas mixtures are lower than in the pure gas due to competitive sorption in the Langmuir void regions [12, 19, 166]. Some studies with $CO_2/CH_4$ mixtures in cellulose acetate [166] and polycarbonate membranes [163] have shown that the gas permeabilities declined when increasing the transmembrane pressure. This is compatible with the multi-component dual sorption model (Eq. 2.12) [64]. However, after a specified partial pressure of $CO_2$, the permeability coefficients of all penetrants increased as the membrane was plasticised by $CO_2$ [160, 161, 163, 166, 172]. Sada et al. showed that the plasticisation of $CO_2$ enhanced the permeability of $CH_4$ but at the same time, the competitive sorption and larger kinetic diameter of $CH_4$ retarded the permeation of $CO_2$ through the membrane (**Figure 2.14**) [160]. As a result, the selectivity of $CO_2/CH_4$ in mixed gas feeds declined when plasticisation occurred.

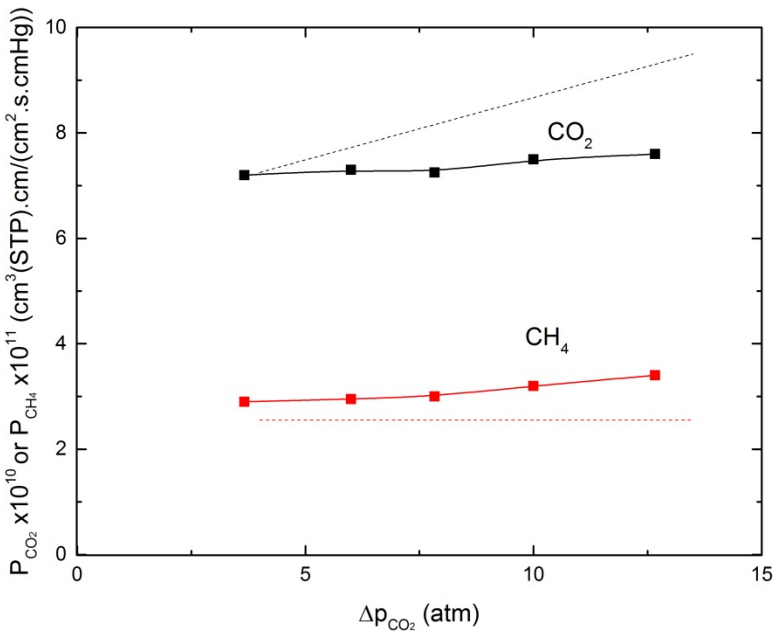


**Figure 2.14** The permeabilities of $CO_2$ and $CH_4$ in CTA membranes versus partial pressure differential of $CO_2$ with mixed gas (50% $^v/_v$ $CO_2$ in $CH_4$) feed (continuous line) and pure $CO_2$ or $CH_4$ feed (broken line) at 30$^o$C [160]

Lee et al. [172] conducted a similar study on the permeation of a $CO_2/CH_4$ mixture (0, 29.4, 69.4 and 100 mol% $CH_4$ in balance $CO_2$) through a asymmetric cellulose acetate membrane. The study observed that the permeance of $CH_4$ was independent of the partial pressure differential ($\Delta p_{CH4}$) in a pure gas feed while the permeance was proportional with the pressure in mixed gas conditions. The increasing rate of $CH_4$ permeability versus $\Delta p_{CH4}$ was more significant when having more $CO_2$ in the feed gas, meaning the membrane was plasticised more significant at higher $CO_2$ concentration. In addition, being similar to the study of Sada et al. [160], the permeance of $CO_2$ in the mixed gas feed was lower than in the pure gas feed and the separation factor of $CO_2/CH_4$ was lower in mixed gas conditions.

The effect of temperature on the permeation of $CO_2/CH_4$ mixtures (60% $CO_2$ in $CH_4$) through cellulose acetate membranes (without DS information) was also studied by Ellig et al. [173]. The study demonstrated an increase of gas permeability with temperature that was similar to that in the pure gas [160]. However, when increasing the temperature, the separation factor for $CO_2/CH_4$ declined significantly, from 28 at 20$^o$C to around 10 at 100$^o$C. This, again, proved that the change of free volume in the membrane with temperature affected the larger molecule (e.g. $CH_4$) more significant than the small molecule (e.g. $CO_2$) [117, 121].

Although applied widely in natural gas processing, academic studies on the CTA membrane for $CO_2/N_2$ separation is limited. In one study on the separation of $CO_2$ and air through a hollow fiber CTA, Sada et al. demonstrated that $N_2$ behaved similarly to $CH_4$ [161] with permeation independent of the transmembrane pressure. The authors also observed plasticisation by $CO_2$ mixtures at 8 atm $CO_2$ differential partial pressure with a 50 mol% $CO_2$/air mixture. In comparison with a pure $CO_2$ feed that plasticised the membrane at around 5 – 6 atm, the pressure dependence of the permeability coefficients was weaker in the mixed gas conditions.

The separation of $CO_2/N_2$ mixtures was also studied by Li et al. [22] using a commercial asymmetric membrane. The conclusions of this study were consistent with that of Sada et al., confirming that continuing the competitive sorption of $CO_2$ and $N_2$ in the mixture could significantly retard the permeance of $CO_2$ (**Table 2.6**). Similarly, Ettouney et al. [174] compared the $CO_2/N_2$ separation performance of a silicon rubber and a cellulose acetate membrane. The authors also observed a drop in $CO_2/N_2$ selectivity when increasing the $CO_2$ concentration, especially at 50% mol $CO_2$ in $N_2$. However, the performance of a cellulose acetate membrane was considered competitive with silicone rubber at low $CO_2$ concentrations.

**Table 2.6:** The permeance and selectivity of $CO_2/N_2$ in CTA membrane at 1100kPa [22]

| Gas mixture | Pure gas (100% $CO_2$ or $N_2$) | 4.72 mol% $CO_2$ in $N_2$ | 50 mol% $CO_2$ in $N_2$ |
|---|---|---|---|
| $N_2$ permeance ($m^3/(s.m^2.kPa)$) | $16 \times 10^{-9}$ | $17 \times 10^{-9}$ | $20 \times 10^{-9}$ |
| $CO_2$ permeance ($m^3/(s.m^2.kPa)$) | $6.3 \times 10^{-7}$ | $4.2 \times 10^{-7}$ | $4.2 \times 10^{-7}$ |
| Selectivity $CO_2$ / $N_2$ | 39.4 | 24.7 | 21.0 |

## 2.9. IMPACT OF IMPURITIES ON THE PERFORMANCE OF CELLULOSE TRIACETATE MEMBRANES

The composition of raw natural gas, syngas and flue gas varies widely depending upon the sources, the production and purification technologies (see **Table 1.1**) [4, 19, 24]. The presences of impurities in gas streams are well-known to alter the separation performance of the membrane materials by either competitive sorption [9-11], plasticisation [12-14], "pore blocking" and anti-plasticisation [12, 15, 16] or by chemical degradation [10]. Even though CTA membranes have been widely applied in industry for decades, there are very limited fundamental studies about the impact of impurities on the CTA membrane.

### 2.9.1. Impact of Water on Membrane Performance

One of the most significant challenges in membrane separation is the presence of water in the processing gas streams. The water content in natural gas is roughly 20 – 1200 ppm and for flue gas from coal-fired power station, 9 – 20 wt% [4, 24, 175]. The presence of water commonly accelerates the corrosive potential of $CO_2$ present and can result in the formation of hydrates in natural gas processing pipelines [176]. In membrane separation processes, water vapour can alter the separation performance of the membrane unit by competitive sorption, plasticisation and anti-plasticisation effects.

#### 2.9.1.1. Diffusion and Sorption of Water in Cellulose Acetate Membrane

Being a popular polymer material used in reserse osmosis, the diffusivity and solubility of water in cellulose triacetate membrane has been well-studied. The water sorption generally depends upon the degree of acetylation, the fabrication method and the history of the membrane samples [177]. The shape of the water sorption isotherm is often simulated via the Flory – Huggins model (as similar as **Figure 2.7b**) [178-180]. However, Gocho et al. observed a deviation of the water sorption isotherm from the traditional Flory – Huggins model at water activity less than 0.2 when studying the water sorption into CA, CDA and CTA membrane [181]. They suggested a modified BET adsorption equation to model this data by assuming two energy levels of water adsorption sites in the membrane corresponding to the hydroxyl and acetoxyl functional groups.

On the other hand, Long and Thompson observed that the diffusion of water in cellulose acetate was initially Fickian but that the diffusion rate declined in the later stages of sorption [100]. Other workers have shown that the water diffusion rate is almost independent of the water activity [100, 182] which is attributed to the combination of water – induced plasticisation (which increases diffusivity) and water clustering (which reduces diffusivity). Furthermore, Rosanbaum and Cotton demonstrated that the water concentration profile across a cellulose acetate membrane at steady state was linear [183] which is consistent with the essential assumptions of the solution – diffusion model [96].

#### 2.9.1.2. Infrared Spectroscopy Analysis and State of Water in Cellulose Acetate Membrane

Fourier transform infrared (FT – IR) spectroscopy analysis is commonly used to characterise organic polymer materials and to probe the impact of penetrants on intramolecular interactions within the membrane [40]. By utilising attenuated total reflectance (ATR) - FTIR analysis, the surface of a cellulose triacetate membrane with 0.5 – 10 μm penetration depth has been characterised (**Table 2.7**) [180, 184, 185]. The sorption of water into the CTA membrane enhances the intensity of the O – H related peaks and can also shift the wavelength of other polar bonds (e.g. C = O and C – O). Toprak et al. (1979) also studied the state of water molecules inside the polymer by comparing the IR spectrum of hydrated CTA with the spectrums of water – ethyl acetate liquid mixtures [180]. They observed that water molecules presented mostly in a monomeric form in the CTA membrane. The spectrums of dimer water and higher clustering forms, in a small proportion, have also been recorded at high water activities [180].

**Table 2.7:** The main IR spectrum of cellulose triacetate membrane [180, 184, 185]

| Wavelength of spectrum ($cm^{-1}$) | Assignment |
|---|---|
| 380 – 800 | Uncertain, mostly HOH libration |
| 1040 – 1050 | C – O stretch |
| 1220 – 1237 | Acetate C – O stretch |
| 1318 – 1319 | C – H deformation |
| 1637 | HOH bend |
| 1735 – 1752 | Acetyl C = O stretch |
| 2880 and 2945 | C – H stretch |
| 3500 | Cellulosic O – H stretch |
| 3000 – 3700 | Water O – H stretch |

#### 2.9.1.3. Impact of Water Vapour on Gas Permeation

Generallty, water is more permeable than other gases such as $CO_2$, $CH_4$ and $N_2$ due to its relatively small kinetic diamter and high critical temperature (**Table 2.1**) [12, 19, 186]. Water vapour can hinder the permeation of other penetrants via competitive sorption orbing into Langmuir void sites in the membrane [165, 187, 188]. The water can also condense forming obstructions that create an additional mass transfer resistance in a process comparable to capillary condensation [12, 19, 94, 97].

This accumulation of water molecules in CTA was demonstrated by Chen et al. [12] through Positron Annihilation Lifetime Spectroscopy (PALS), where under 2.5 kPa water vapour pressure, the average pore diameter declined when increasing the vapour pressure, suggesting that water molecules clustered inside the polymer. Then, when the humidity increased further, the microvoid diameters increased indicative of plasticisation by water. Interestingly, although the permeation of $CO_2$ and $CH_4$ were enhanced by the water – induced plasticisaition effect, the $CO_2/CH_4$ selectivity was not significantly affected [12].

The plasticisation and clustering effects of water vapour on gas separation can occur simultaneously [94]. In a study of the impact of water on cellulose acetate (without specified DS), polysulfone, polyethersulfone and sulfolene modified poly(vinylidene flouride) membranes for $CO_2/CH_4$ separation, Paulson et al. observed the permeate flux increased when introducing the water in feed gas [21]. However, at higher concentrations of water, the flux reduced due to the clustering effect and the condensation of water in the membrane. Similar behaviour was also observed in the study of Funk et al. on $CO_2/N_2$ separation by a cellulose acetate membrane [10]. By increasing the relative humidity of water to over 10%, the flux of permeate declined and even higher relative humidity resulted in a significant drop in gas permeation (see **Figure 2.15**).

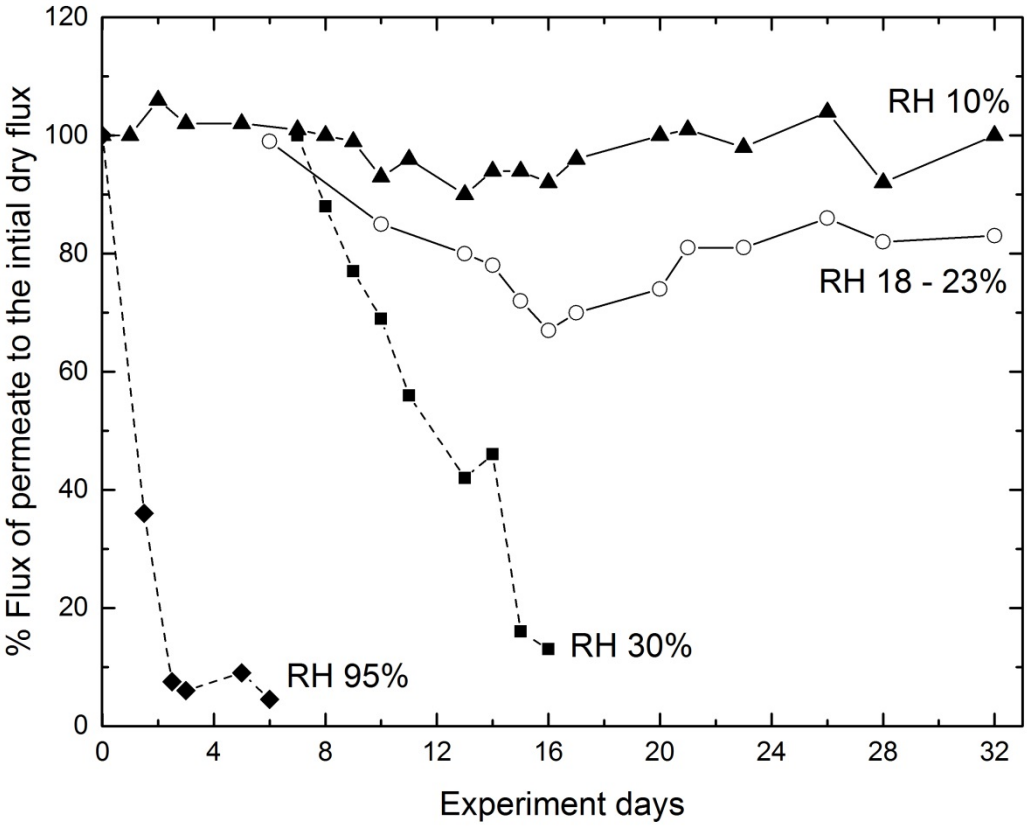


**Figure 2.15** The change of permeate flux at different relative humidity of water in $CO_2/N_2$ separation by cellulose acetate membrane (reprinted from [20])

#### 2.9.1.4. Impact of Solutions of Variable pH on Cellulose Triacetate Membranes

The removal of fly ash and sulfur oxides in post-combustion flue gas treatment processes can also result in the carry-over of liquids of variable pH to the membrane separation unit [24, 26]. The pH of these entrained liquids varies in a wide range depending on the specific treatement process utilised (**Figure 2.16**). For instance, the wet-scrubbing desulfurisation process, which captures the acidic components in the flue gas in lime stone to form gypsum [189], can entrain highly caustic droplets into the feed to the membrane unit. The presence of residual fly ash in the gas stream can also create extremely caustic droplets of up to pH 12.8 in the feed to the downstream unit [26]. Conversely, the membrane unit may come into contact with strong acidic solutions (pH ~ 3.3) overflowing from a direct contact cooler unit upstream [24]. Although the hydrolysis of cellulose acetate is well studied across a broad pH range [190, 191], the impact of these conditions on the gas separation performance of CTA membranes is not well understood.

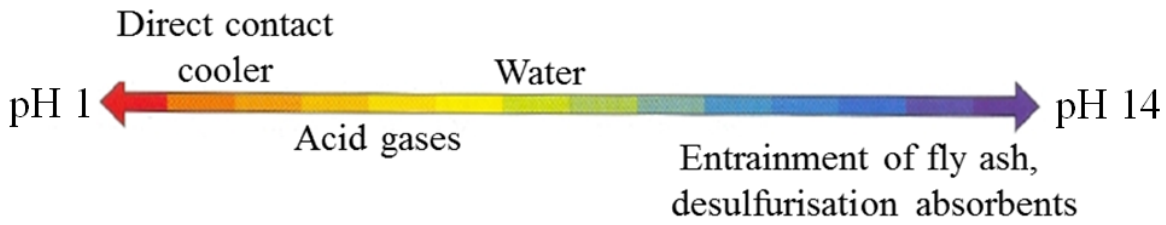


**Figure 2.16** The potential pH conditions in natural gas and flue gas entrained liquids

### 2.9.2. Impact of Sulphur Oxides ($SO_x$) on Membrane Performance

Sulphur oxides ($SO_x$) are a combination of sulphur dioxide ($SO_2$) and sulphur trioxide ($SO_3$) that result from combustion of fuels such as brown coal. The typical concentration of $SO_x$ in post-combustion flue gas is 200 – 5000 ppmv [192, 193] but this can be reduced to 10 – 50 ppmv when desulphurisation treatment processes are applied [192]. The free emission of $SO_x$ into the atmosphere is responsible for environmentally damaging acid rain and so the removal of $SO_x$ from the flue gas is essential for regulatory compliance in some regions.

The main form of sulphur oxide in the flue gas is $SO_2$ and its effect on membrane separation performance has been studied since the 1970s [194]. In general, $SO_2$ is more permeable than other gases such as $CO_2$, $N_2$ and $O_2$ due to its strong condensability [19, 193, 194]. In particular, the $SO_2$ permeability through a CTA membrane was reported by Kuehne et al. [193]. These authors observed increasing $SO_2$ permeability with $SO_2$ partial pressure that could correspond to a $SO_2$ – induced plasticisation effect [193]. However, the partial pressure of $SO_2$ in common flue gas streams is much lower than the conditions in the Kuehne et al. study (e.g. 13 – 93 kPa) so that the plasticisation effect of $SO_2$ in a post-combustion capture membrane unit is expected to be minor [19].

Sulphur trioxide ($SO_3$) is the other component in the flue gas with concentration after desulphurisation around 20 – 30 mg/m$^3$ [195]. Due to its low concentration in the flue gas, extremely high corrosive properties and the fact that it is a liquid at ambient condition, there is very few studies on $SO_3$ reported. To the best knowledge of the author, only one recent report studied the impact of $SO_3$ on the performance of a polyimide membrane [196]. It was found that the presence of $SO_3$ significantly altered the membrane performance in both selectivity and gas transport and the combination of $SO_3$ with water vapour likely decomposed the polymer.

### 2.9.3. Impact of Nitrogen Oxides ($NO_x$) on Membrane Performance

The concentration of nitrogen oxides in a power coal-fired station flue gas is in range of 150 – 300 ppmv nitric oxide (NO) and < 10 ppmv of nitrogen dioxide ($NO_2$). This concentration can be higher depending upon temperature and combustion technologies [24, 25]. A selective catalyst reduction unit is commonly used to convert $NO_x$ into $N_2$ and this can reduce the $NO_x$ concentration by 85 – 98% [192, 197]. The impact of NO on polysulfone and polyimides membranes has recently been reported. This work found that the permeability of NO was less than $CO_2$ and higher than $N_2$ [198]. However, to the best knowledge of the author, there is no study on the impact of NO on CTA membranes. Generally, it is expected that NO will have higher diffusivity through the membrane than $CO_2$ but lower solubility due to its smaller kinetic diameter and lower critical temperature (refer to **Table 2.1**).

In the presence of a minor traces of oxygen, NO will be converted to $NO_2$ with reaction rate, *k*, 6.7 x $10^3$ $L^2.mol^{-2}.s^{-1}$ at 35$^o$C (Eq. 2.26) and (Eq. 2.27) [199]. The reactions of $NO_2$ with cellulosic materials has been a subject of study since the 1940s [200, 201]. It was reported that $NO_2$ can oxidise the primary alcohol (the 6$^{th}$ carbon in the glucose unit) into a carboxylic functional group [200, 201]. However, the impact of $NO_2$ on the gas separation performance of CTA membrane is not currently known.

$$2NO + O_2 \rightarrow 2NO_2 \quad \text{(Eq. 2.26)}$$

$$-\frac{d[NO]}{dt} = +\frac{d[NO_2]}{dt} = 2k[NO]^2[O_2] \quad \text{(Eq. 2.27)}$$

### 2.9.4. Impact of Hydrogen Sulfide ($H_2S$) on Membrane Performance

Hydrogen sulfide ($H_2S$) removal is one of the essential treatments in natural gas and biogas production [19, 202] to meet the pipeline specification (< 4 ppm) and to prevent the risks of toxicity and corrosion [176]. The typical concentration of $H_2S$ in raw natural gas varies from 4 ppm to over 10000 ppm depending on the sources [4]. Several studies on natural gas treatment by membrane technology have observed the co-permeation of $H_2S$ and $CO_2$ with relatively high selectivity over $CH_4$ [19, 20, 203]. The selectivity of $H_2S/CO_2$ varies in a wide range depending on the membrane materials as summarised in **Figure 2.17**. For cellulose acetate membranes, the $H_2S/CO_2$ selectivity is close to unity due to comparable critical temperatures and kinetic diameters (see **Table 2.1**) [19, 204, 205].

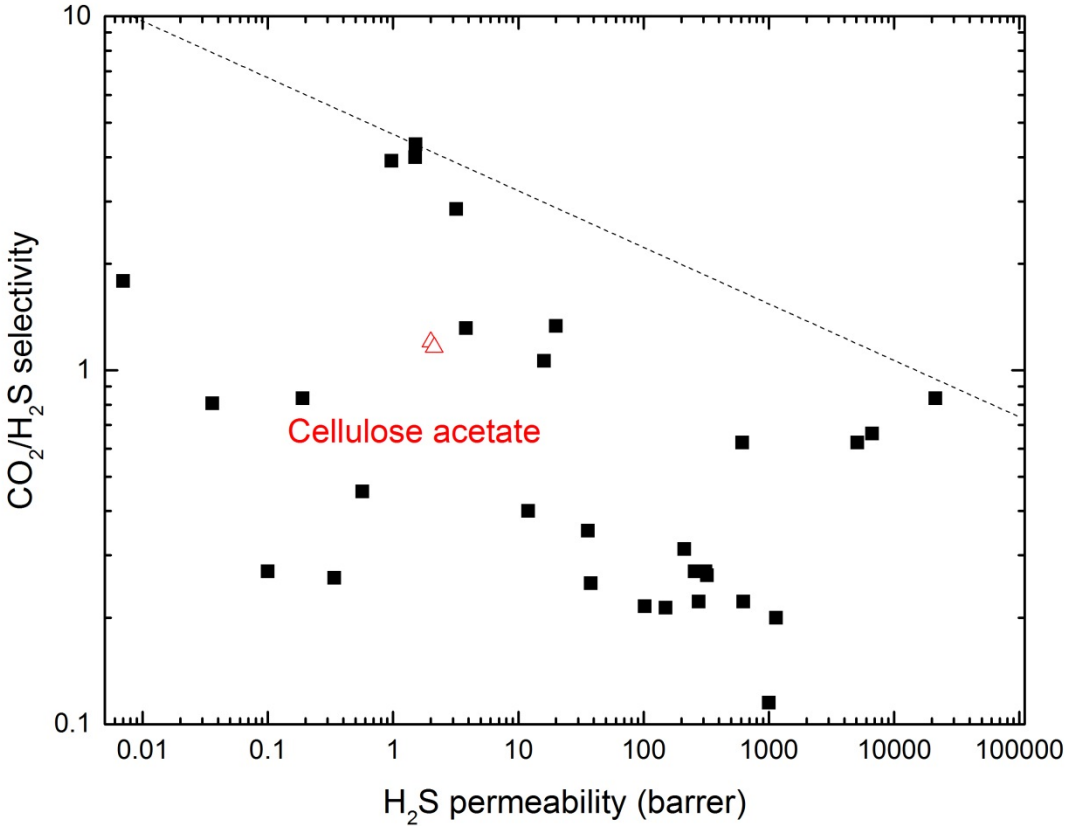


**Figure 2.17** The permeability of $H_2S$ and $CO_2/H_2S$ selectivity through some polymeric membranes with the slope factor of the upper bound line calculated from (Eq. 2.8) [19, 204-209]

Li et al. showed that an asymmetric cellulose acetate membrane (DS not stated) was stable in 69 kPa $H_2S$ at 25°C for 2 weeks without significantly affecting the membrane performance [210]. However, when water vapour was added into the feed gas, the membrane performance dropped over 40%. The loss in permeation is due to the competitive sorption and clustering of water vapour that can hinder the gas transport through the membrane as mentioned earlier in **section 2.9.1.3**. $H_2S$ has also been reported to plasticise cellulose acetate membranes [11, 14,

210]. In addition, the plasticisation effect of a $CO_2$ – $H_2S$ gas mixture has been shown to be more significant than pure $CO_2$ under the same experiment conditions [10].

Although the impact of $H_2S$ on CTA gas separation membrane has been reported widely, there is very limited fundamental studies on the impact of $H_2S$ at different temperatures and pressures. Only, Heilman et al. (1956) have reported the solubility and permeability of $H_2S$ into polymer films including a commercial cellulose acetate (DS not stated) [211]. Furthermore, given the 2 – 5 years lifetime of current membrane units [176], the longer term performance in the presence of $H_2S$ is vital for industry consumers.

### 2.9.5. Impact of Ethylene Glycols on Membrane Performance

Raw natural gas is usually saturated with water vapour which is typically removed in an upstream dehydration unit to prevent hydrate formations and pipeline corrosion [18, 23, 212]. The most common hygroscopic solvents utilised for this purpose are glycols such as monoethylene glycol (MEG), diethylene glycol (DEG) and triethylene glycol (TEG) [20, 213]. Glycol selection is based on several factors, including the dehydrating capacity, vapour pressure, cost and capacity of the glycols to remove other volatile organic compounds (VOCs) [214-216]. TEG is more expensive than other glycols but has higher sorption capacity and lower vapour pressure (**Figure 2.18**), leading to less carryover during the dehydration and glycol regeneration processes [214, 217]. MEG is also injected directly into raw natural gas to prevent hydrate formation. DEG, which is the most toxic glycol, is also utilised in some dehydration plants [17, 18].

Glycol loss is a significant concern in operating the dehydration unit. The carry-over of liquid glycol solution droplets with the processing gas is the dominant cause of loss while vaporisation and mechanical leakage also contribute [18]. This carryover can result in the presence of glycol liquid in the membrane unit, which can alter the permselectivity of the membrane.

Glycols are well-known for their plasticisation properties [218]. The impact of MEG and TEG vapours on $CO_2/CH_4$ separation by a facilitated transport membrane was recently reported, which indicated that the penetrant permeation was enhanced by the presence of glycols [17]. Some other diol-compounds such as polyethylene glycol (PEG) and glycerol have been utilised to increase the wetting behaviour of cellulose acetate membrane in reverse osmosis studies [219]. However, there is no report on the impact of glycols on the gas separation performance of CTA membranes. A systematic study of the impact of glycols is needed to fill the current gap of knowledge

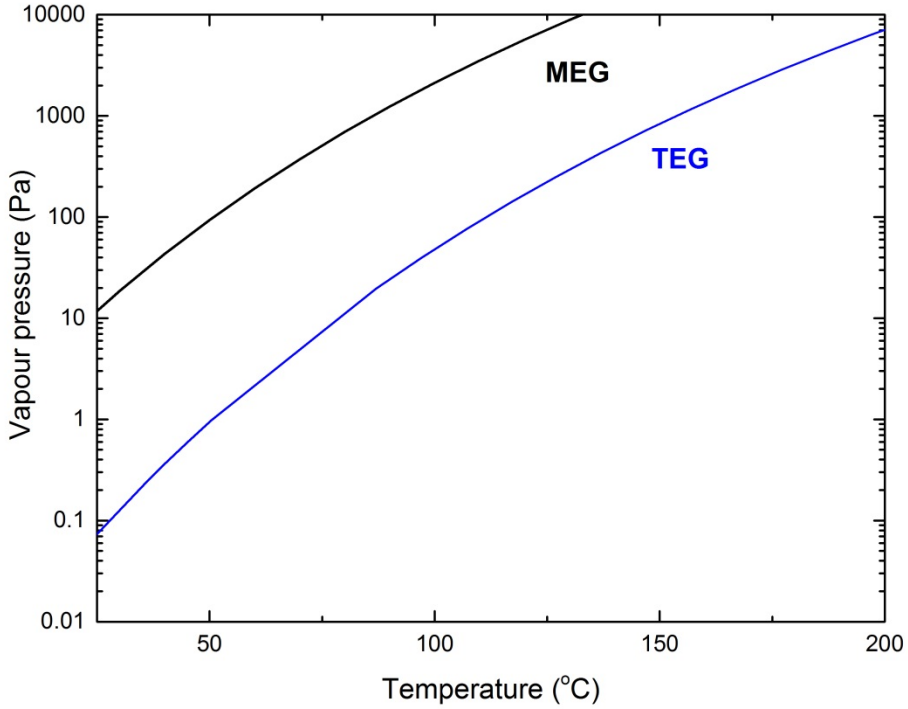


**Figure 2.18** The vapour pressure of monoethylene glycol [220] and triethylene glycol [221] at different temperature

### 2.9.6. Impact of BTEX on Membrane Performance

Benzene, toluene, ethylbenzene and xylene (BTEX) are present in raw natural gas with concentration, commonly in the range of 200 – 3000 ppm [4, 11]. The essential concerns for BTEX in natural gas processing are their freezing potential in processing and their toxicity to environment and health [216]. BTEX and other VOCs are partial absorbed in the dehydration unit and regenerated in the flash tank and glycol stripping column [18, 216]. On the other hand, BTEX is also presented in coal-fired and biomass derived synthesis gases due to side-reactions in the gasifiers [23, 222, 223]. The concentrations of BTEX in syngas varies with the gasification technologies with around 1000 ppm [222] – 2000 ppm [224] recorded on sites at some power plants. The presence of BTEX in syngas is a challenge for pre-combustion capture process and the lifetime of the catalysts.

The presence of BTEX in the membrane separation unit is known to alter the membrane performance. Wind et al. studied the impact of toluene and other hydrocarbons on $CO_2/CH_4$ mixtures separation by 6FDA-DAM:DABA and 6FDA-6FpDA:DABA copolymers and they observed that the $CO_2$ permeability significant declined in the presence of 300 ppm toluene with a moderate reduction in $CO_2/CH_4$ selectivity [225]. A similar result was reported by Omole et al. when they tested the propane-diol mono-esterified cross-linkable polyimide (PDMC) from 50 – 1200 ppm toluene [226]. Toluene also reduced the gas permeation in a carbon hollow fibre membrane [227], matrimid 5218® [9, 226, 228], nanoporous carbon membrane [23] and a perfluorinated membrane [229]. In some cases, the membranes were also plasticised by the toluene and the $CO_2/CH_4$ selectivity significant declined [226, 230].

Although cellulose acetate membranes have been commercialised widely, the impact of BTEX on this membrane material is not well studied and is mostly focused on $H_2/CH_4$ separation.

The presence of toluene (up to 1000ppm) and benzene (up to 3500ppm) in a $H_2/CH_4$ mixture reduced the gas permeation by 10 – 20% for a cellulose acetate membrane but the $H_2/CH_4$ selectivity was enhanced by roughly 10% [11, 231]. Similarly, operating data from Cosmo Oil Refinery (Japan) with 700 – 2000 ppm BTX in a $H_2/CH_4$ mixed gas showed that the permeation rate declined around 20% with a slight increase in $H_2/CH_4$ selectivity [232]. A study on $CO_2/CH_4$ mixed gas separation by a cellulose acetate membrane in the presence of 850ppm BTX at 63 bar showed that the permeation of $CO_2$ and $CH_4$ reduced by 10% without any effect on the $CO_2/CH_4$ selectivity [11].

In comparison with $CO_2$ and $CH_4$, BTEX is expected to have higher solubility and lower diffusivity in the membrane due to their high critical temperature and larger kinetic diameter (refer **Table 2.1**). However, the permeabilities of BTEX are themselves rarely reported in detail. The permeance of toluene was reported to be around 6.4 GPU for a 6FDA-DMB polyimide membrane which was slightly higher than the $CH_4$ permeance in the same study [230]. In another study, BTX were generally found to have lower permeabilities than $CH_4$ [231]. With increasing concern about BTEX emissions, a systematic study on the impact of BTEX on the performance of a CTA membrane and on BTEX permeation is timely.

## 2.10. SCOPE OF THIS THESIS

One of the significant criteria for gas separation by membrane technology is the stable performance and resistance of the membrane material to the feed gas. Although cellulose triacetate membranes have been applied widely in natural gas separation for many decades, there is a lack of systematic investigation of the impact of the minor components in both raw natural gas and flue gas on the membrane performance. The application of CTA membranes in post-combustion capture is not fully characterised despite their high $CO_2/N_2$ selectivity and commercial readiness. Similarly, the impact of glycol solution on gas separation performance is limited, although the carryover of glycols in natural gas processing has been reported [18]. In addition, the impact of $H_2S$ and aromatic hydrocarbons sourced from raw natural gas is not fully understood.

Therefore, the present work aims to address the gap in the knowledge of CTA membrane performance outlined in this chapter by investigating the impact of impurities, resulting from natural gas processing and post-combustion capture, on the separation performance, with a focus on carbon dioxide separation. The body of work presented in this thesis consists of three major experimental systems with the thesis structure set out as follows:

- **Chapter 3** focuses on the experimental methods and techniques developed to investigate the impact of impurities on the $CO_2$ capture by CTA membranes. The membrane characterisation methods and the associated experimental apparatuses are described. The techniques to study the long term impact of impurities on CTA membrane is also presented.
- **Chapter 4** focuses on the impact of both water vapour and liquid water, and importantly the impact of liquid water of different pH on $CO_2$ separation by CTA membrane. In

addition, the impact of $SO_x$ and $NO_x$ on the CTA membrane is investigated. The results provide an assessment of the viability of CTA membranes for post-combustion capture.

- **Chapter 5** investigates the impact of ethylene glycol and high concentration of hydrogen sulfide on CTA membrane performance for $CO_2/CH_4$ separation. The outcome of this work is an understanding of their competitive sorption and plasticization potential which can be quantitatively measured. This brings a deeper understanding of the performance of CTA membranes operating under high $H_2S$ conditions as well as the potential to recover a loss in separation efficiency loss due to glycol exposure by a methanol wash.
- **Chapter 6** studies the impact of aromatic hydrocarbons, toluene and xylene, on the performance of CTA membranes and in particular their ability to induce competitive sorption, plasticization and pore blocking within the membrane structure. This research fills a gap in the understanding of CTA membranes for natural gas processing, as it presents a quantitative study of hydrocarbon vapour effects on the membrane structure. This knowledge is vital for CTA membranes currently being used in natural gas sweetening and will assist in prolonging the life to membrane modules that are exposed to these vapours. There is also application to pre-combustion capture operations which can also contain these hydrocarbons.
- **Chapter** 7 summaries the outcomes of the prior chapters and provides suggestion for prospective future works.

# CHAPTER 3. EXPERIMENTAL METHODS

## 3.1. INTRODUCTION

This chapter details the materials and experimental methods to obtain all the results presented in the thesis. This includes the membrane fabrication protocols for thick dense films as well as thin film composite membranes (TFC). The chapter also includes the methodologies to determine the permeabilities of both pure gas and mixed gases/vapours through the membrane. Furthermore, the design and techniques used to study the long-term impact of impurities is outlined as is the techniques for measuring sorption uptake. All other techniques to obtain the physical, chemical and thermal properties of the membranes are also described.

## 3.2. MEMBRANE MATERIALS AND MEMBRANE FABRICATION PROTOCOLS

### 3.2.1. Membrane Materials

All experiments were conducted on cellulose triacetate, which is kindly supplied by Cellulose Company - Daicel Corporation (Japan) with specifications summarised in **Table 3.1**. To prevent the sorption of moisture, the powdered polymer was stored in desiccators filled with silica gel.

**Table 3.1:** The specification of cellulose acetate polymer (Product code: LT-35) from Daicel Corporation, reproduced from product specification sheet [233]

| | | | |
|---|---|---|---|
| **Appearance** | White powder | **Bulk density (g/cm$^3$)** | 0.25 – 0.52 |
| **Density (g/cm$^3$) at 25$^o$C** | 1.33 – 1.36 | **Melting point ($^o$C)** | 230 – 300 |
| **Glass transition temperature ($^o$C)** | 160 – 180 | **Specific heat (kJ/kg.K)** | 1.34 |
| **Acetylation degree (%)** | 61.6 | **Purity (%)** | > 99 |

### 3.2.2. Experimental Gases

The gases utilised in the thesis were supplied from Coregas Pty Ltd. (Australia) with the excepted of carbon dioxide and nitrogen which were supplied from BOC Gas Ltd. (Australia) and Liquid Nitrogen Services (Australia), respectively. The compositions and purity grades are listed in **Table 3.2**. The compositions of gas mixtures were accredited by the National Association of Testing Authorities (NATA, Australia) with 2% relative measurement uncertainty.

**Table 3.2:** Compositions and purities of experimental gases

| Name/Components | Purity | Supplier |
|---|---|---|
| Air (instrument) | 99.999% | Coregas |
| Argon (Ar) | 99.99% | Coregas |
| Carbon dioxide ($CO_2$) | 99.999% | Coregas |
| | 99.9% | BOC |
| Helium (He) | 99.99%<br>99.999% | Coregas |
| Hydrogen ($H_2$) | 99.999% | Coregas |
| Nitrogen ($N_2$) | 99.999% | Coregas |
| | 99.5% | Liquid Nitrogen Services |
| Oxygen ($O_2$) | 99.9% | Coregas |
| Methane ($CH_4$) | 99.95%<br>99.9995% | Coregas |
| 10% $CO_2$ in Balance $CH_4$ | 99.999% | Coregas |
| 10% $CO_2$ in Balance $N_2$ | 99.999% | Coregas |
| 30% $CO_2$ in Balance $N_2$ | 99.999% | Coregas |
| 90% $CO_2$ in Balance $N_2$ | 99.999% | Coregas |
| 1000ppm $H_2S$ in Balance $N_2$ | 99.999% | Coregas |
| 1000ppm NO in Balance $N_2$ (with minor $NO_2$) | 99.999% | Coregas |
| 1000ppm $SO_2$ in Balance $N_2$ | 99.999% | Coregas |

### 3.2.3. Experimental Solvents and Chemicals

Dichloromethane solvent was utilised to dissolve the CTA polymer powder in the membrane fabrication stage. Others solvents and chemicals were used to study the impact of impurities and to determine the physical properties of the CTA membrane (**Table 3.3**).

**Table 3.3:** List of solvents and chemicals utilised in the thesis

| Name | Chemical structure | Purity | Supplier |
|---|---|---|---|
| Dichloromethane (DCM) | $CH_2Cl_2$ | AR grade, >99.8% | ChemSupply (Australia) |
| Sulfuric acid | $H_2SO_4$ | AR grade, >99.8% | ChemSupply (Australia) |
| Sodium hydroxide | NaOH | ACS grade, >97% | Sigma Aldrich (Australia) |
| Ethylene glycol (MEG) | 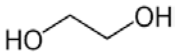 | Anhydrous, 99.8% | Sigma Aldrich (Australia) |
| Triethylene glycol (TEG) | 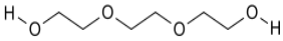 | LR grade, 99% | ChemSupply (Australia) |
| Toluene | 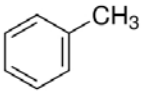 | AR grade, >99.5% | ChemSupply (Australia) |
| Xylenes (mixture of isomers) | 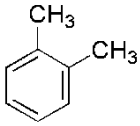 ortho- 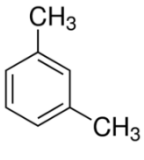 meta- 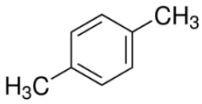 para- | AR grade, >99.0% | ChemSupply (Australia) |
| Methanol | $CH_3OH$ | AR grade, >99.8% | ChemSupply (Australia) |
| *n*-hexane | 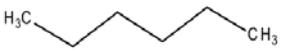 | AR grade, >95% | ChemSupply (Australia) |

### 3.2.4. Dense Membrane Fabrication

Dense CTA membranes were fabricated by a solution casting method (**Figure 3.1**). The cellulose triacetate polymer powder was dissolved in dichloromethane solvent. The solution was filtered to remove any undissolved contaminants before casting into glass petri dishes. The petri dishes were well-covered to control the evaporation rate for forming homogeneous polymer films [12, 42, 59], and to prevent the absorption of moisture. The dried membranes were peeled off after 24 hours of evaporation at ambient conditions (22 ± 2$^{o}$C) and then annealed under vacuum to remove totally the residual solvent. The membrane annealing protocol included 24 hours at 35$^{o}$C and 24 hours at 100$^{o}$C under vacuum. The fabricated membranes were stored in a desiccator filled with silica gel to

minimise the exposure to moisture. The CTA membranes fabricated by this method were in the range of 60 to 200 µm in thickness.

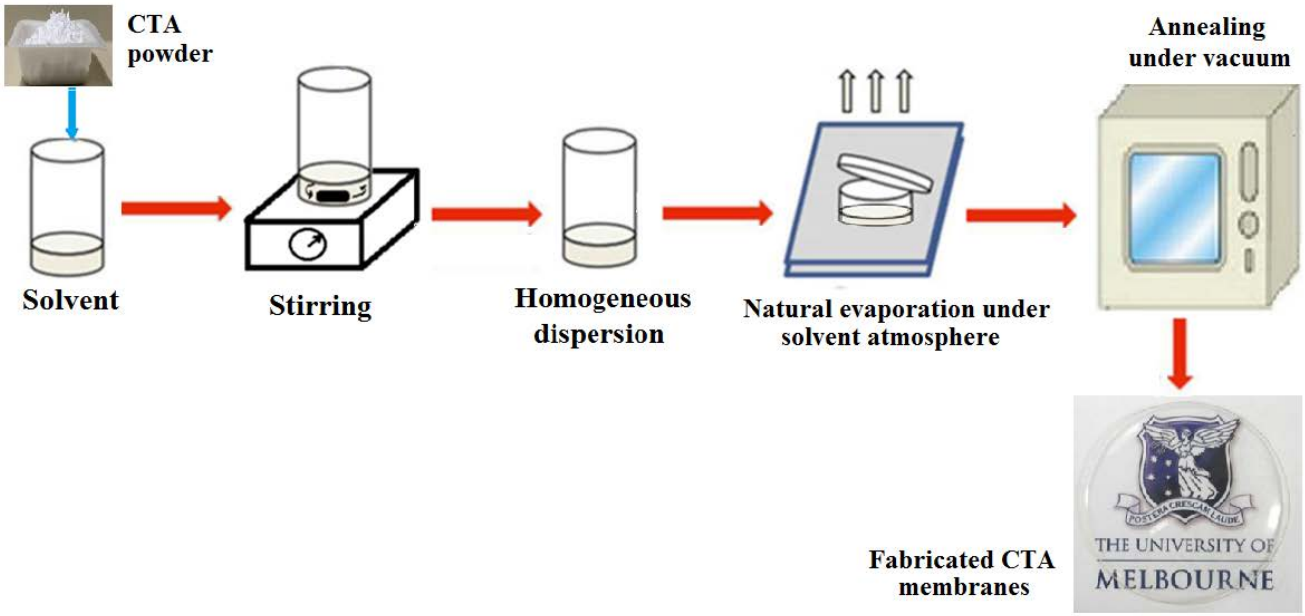


**Figure 3.1** The scheme of membrane fabrication by solution casting method, adapted from [234]

### 3.2.5. Thin Film Composite (TFC) Membrane Fabrication

Thin film composite CTA membranes (3 - 10µm) were fabricated by a spin coating technique, as reported elsewhere in the literature [67, 121]. A hydrophilic polytetrafluoroethylene (PTFE) porous membrane (nominal pore size of 0.2 µm) was selected as the support due to its high stability in organic solvents and to acidic gases. To prevent the casting solution penetrating into the porous structure, the support was pre-wetted with deionised water prior to installation on the spin coater (Laurell WS-400 Lite series, United Kingdom) (**Figure 3.2**). The spinning rate was set at 1500 rpm for 20 seconds. 2 ml of 4 wt% casting (CTA in dichloromethane solvent) was pipetted on the PTFE support. The composite membrane was removed from the spin coater, dried in ambient conditions for 1 hour and then annealed in the vacuum oven with the annealing protocol given in **section 3.2.4**.

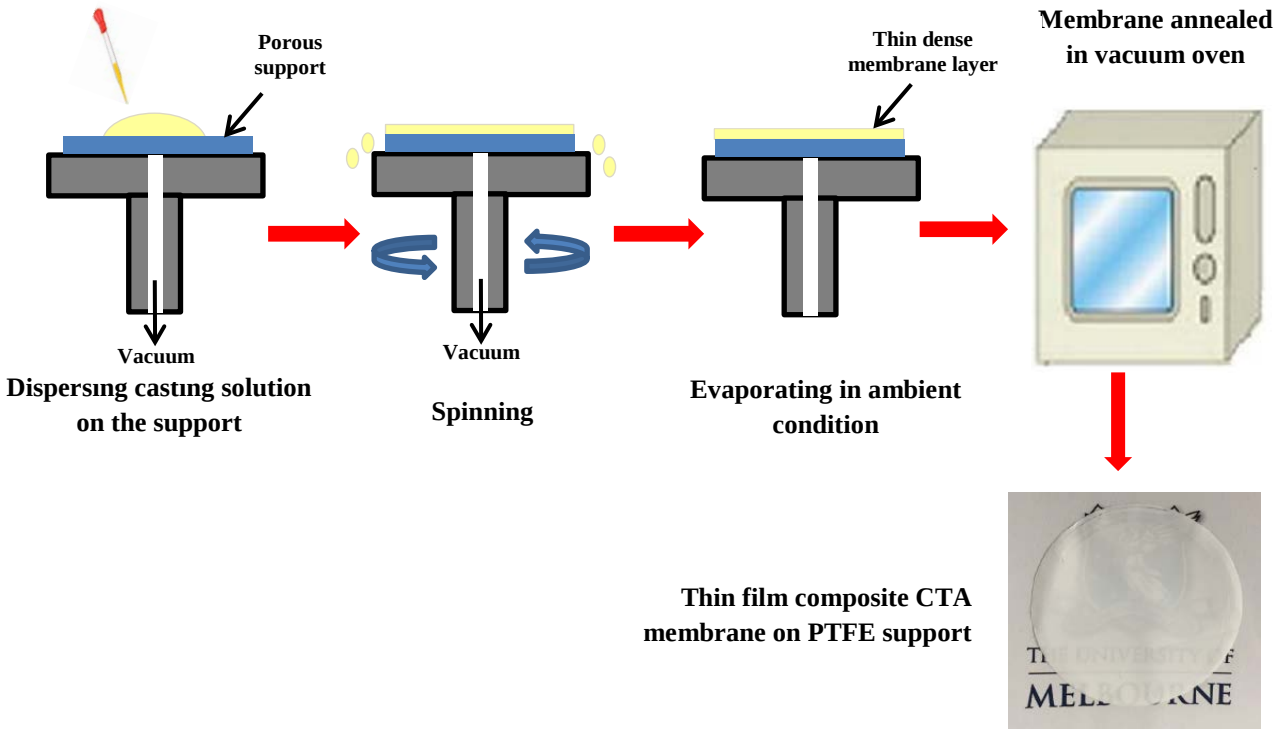


**Figure 3.2** The scheme of thin film composite membrane fabrication by a spin coating technique

## 3.3. MEMBRANE CHARACTERISATION

### 3.3.1. Membrane Density

The membrane density ($\rho_{membrane}$) was determined by the standard buoyancy technique, which relies on the difference in weight between the membrane sample in air ($m_{air}$) and in a reference solvent ($m_{solvent}$) (Eq. 3.1). The mass of membrane was weighed by a Mettler Toledo XS205 DualRange balance (0.01 mg accuracy). The density of a reference solvent ($\rho_{solvent}$) was measured via a calibrated pycnometer at the same conditions with the membrane density measurement experiment. It is noted that the sorption of solvent into the CTA membrane will affect the accuracy of this density measurement. Therefore, the sorption of some common solvents in CTA membrane was studied (see **Appendix A.1 – Membrane density**) and *n*-hexane was selected for the density measurement due to its extremely low solubility in CTA.

$$\rho_{membrane} = \frac{m_{air}}{m_{air} - m_{solvent}} \rho_{solvent} \qquad \text{(Eq. 3.1)}$$

### 3.3.2. Membrane Thickness

A micrometer (Mitutoyo, Japan) was used to measure membrane thickness with accuracy ±1μm. Membrane fabricated by solution casting might experience a slight deviation in thickness due to the flatness of the petri dish and casting platform. Therefore, the membrane thickness was averaged from 25 locations on the membrane effective area (**Figure 3.3**). The effective area is defined as the surface in which the mass transfer occurs and is typically limited by the sealing material (e.g. O-ring) in the gas permeation experiment.

The thickness of thin film composite CTA membranes was measured by Scanning electron microscopy (SEM) as described in **section 3.3.3**.

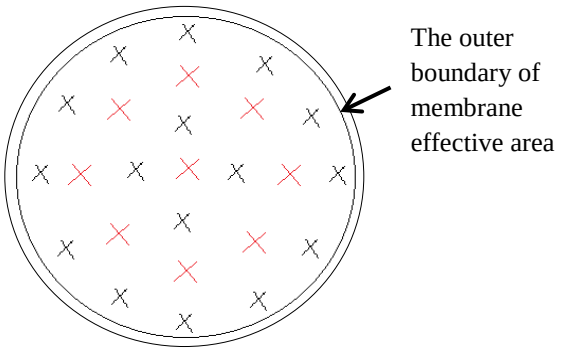


**Figure 3.3** The pattern of locations where the membrane thickness was measured

### 3.3.3. Scanning Electron Microscope (SEM)

Scanning Electron Microscopy (Quanta 200 ESEM FEG – FEI, USA) was used to study the microstructure of the membrane and determine the thickness of the active layer in thin film composite membranes. The membrane samples was frozen and broken in liquid nitrogen prior to gold-coating by a Dynavac Mini Sputter Coater. The coated sample was imaged SEM with magnification varying from 5000x to 15000x.

### 3.3.4. Wide Angle X-ray Diffraction (WAXD)

X-ray diffractometery (D8 Advance Diffractometer – Bruker, Germany) was utilised to study the crystallinity of CTA. CTA membrane is known to be semi-crystalline with well-defined crystalline peaks at around $2\theta = 10^o$ [12, 235, 236] and $17^o$ [237, 238], and a van der Waals amorphous halo at $20 – 21^o$ [236, 237, 239, 240]. In this thesis, WAXD was conducted from $5^o$ to $35^o$ $2\theta$ angles with a Nickel filter and $CuK_\alpha$ radiation source (40kV, 30mA and 1.54 Å wavelength). The scanning rate was $0.02^o$ per 5 seconds.

### 3.3.5. Differential Scanning Calorimetry (DSC)

Differential scanning calorimetry was used to detect the glass transition temperature ($T_g$) of the membrane by determining the deviation in heat flow to the polymer and a reference. A double-furnace DSC 8500 with a high pressure cell from Perkin Elmer (Australia) was used in the study. The operating temperature was varied from $-60^oC$ to $300^oC$ depending upon the experiment. The membrane sample was placed in an aluminium pan and installed into the sample furnace while the empty reference pan was installed into the reference furnace. The furnaces were initially stabilised at the lowest experimental temperature for 10 minutes prior to heating at 20K/min. The furnaces were maintained under ambient pressure dry nitrogen. To determine the $T_g$ of membranes containing glycol, dry nitrogen at 1600 kPa was used to reduce the solvent evaporation during the scan. The $T_g$ was determined as the centre point of the endothermic transition via Pyris™ software.

### 3.3.6. Thermogravimetric Analysis (TGA)

Thermogravimetric analysis (TGA 209 F1 Libra® - Netzsch, Australia) detects the mass change of the membrane sample during a dynamic temperature scan. A membrane sample of ~10 mg was loaded into an alumina sample pan which then was placed into the furnace of the instrument. The measurement was performed from $30 – 500^oC$ under ambient pressure of dry nitrogen and using a 20K/min heating rate.

## 3.4. GAS ANALYSIS

### 3.4.1. Attenuated Total Reflectance (ATR) - Fourier Transform Infrared Spectroscopy (FT-IR)

FT-IR relied on the adsorption and emission from the functional groups when exposed to an infrared beam. In this thesis, a Frontier FT-IR Spectrometer (Perkin Elmer, USA) equipped with a Cyclone$^{TM}$ gas cell was used to quantify the concentration of $SO_2$ and NO during gas permeation. The measurement procedure was based on ISO 19702:2006 [42, 43] in which the wavelength of $SO_2$ and NO are observed in range of 1410 – 1290 $cm^{-1}$ and 2000 – 1775 $cm^{-1}$, respectively. The FT-IR was calibrated against $SO_2$ and NO gas mixtures (1000ppm in $N_2$) across a range of pressures to generate the calibration curves. Prior to each experiment, a background scan was conducted with 1 bar helium (99.999% purity).

Similarly, FT-IR equipped with an ATR accessory can identify the functional groups in a membrane based on the internal reflection of the infrared beam. The membrane was scanned across a full wave number range 700 – 4000 $cm^{-1}$. Two different instruments were used in the thesis, a Frontier FT-IR Spectrometer (Perkin Elmer, USA) and a FTS 7000 FTIR Spectrometer (Varian, USA).

### 3.4.2. Gas Chromatography (GC)

Gas chromatography was also used to analyse the gas/vapour composition. Gas chromatography relies on the strength of the interaction between the gas components with a stationary phase which then affects the retention time of the components inside this phase. This stationary phase is usually composed of a packed bed of size selective resins within a capillary column. Different kinds of detectors are available to detect the components exiting the column and the signals are used to identify and quantify the gas compositions.

Two different micro GC 490 analysers (Agilent technologies, Australia) were used to determine the composition of the gas stream. Depending on the gases (e.g. $CO_2$, $N_2$, $CH_4$, $H_2S$ or BTEX), different columns and operating parameters were applied as regards **Table 3.4**. The GC was operated in the static mode with sample time in the range of 5 – 45 seconds. Helium grade 5 (99.999%) were used as the carrier gas.

The GC was calibrated with standard gas mixtures to generate the calibration curves (peak area versus gas composition) for each gas component. In the case of toluene and xylene, the helium gas was bubbled through a chamber containing the relevant liquid to carry the vapour to the GC. By varying the temperature of the chamber and assuming that the exit stream was saturated with hydrocarbon [23, 229], the calibration curves of toluene and xylene (peak area versus hydrocarbon saturated pressure) were generated. Stainless steel balls were added into the chamber to enhance the mass transfer rate and the exit piping was covered with heating tape to prevent the condensation of vapour.

**Table 3.4:** Operating parameters for micro GC 490

| Column name | MS5A (Molsieve 5Å) | PPU (poraPLOT U) | CB-Sil 5CB |
|---|---|---|---|
| Length (m) | 10 | 10 | 6 |
| Injector temperature ($^oC$) | 50 | 110 | 110 |
| Injection time (ms) | 40 | 40 | 40 |
| Column temperature ($^oC$) | 80 | 80 | 100 |
| Initial pressure (kPa) | 138 | 150 | 150 |
| Run time (s) | 120 | 90 | 150 |
| Gas detected | $N_2$, $CH_4$ | $CH_4$, $CO_2$, $H_2S$, $N_2$ & $O_2$ (co-eluted) | BTEX (e.g. Toluene, Xylene) |

## 3.5. PENETRANT TRANSPORT PROPERTIES

### 3.5.1. Gas Sorption Analysis

Gas sorption isotherms were measured via a high pressure gas adsorption measuring unit (Belsorp – MicrotracBel Corp., Japan) which is based on a gravimetric approach. The diagram of the analyser is shown in **Figure 3.4**. A membrane sample ( ≥ 600 mg) was installed into the sample chamber and the stability of the micro balance was checked and tared after installing the sample. The adsorption unit was then leak tested at the experimental temperature for up to 100 bar absolute helium gas, which is assumed to have extremely low sorption in the polymer [241, 242]. Afterward, the unit was evacuated overnight before increasing the gas pressure ($N_2$, $CH_4$, $CO_2$) in increments from 50 kPa to 40 bar absolute. Equilibrium at each pressure step was set at 0.2 µg per 120 minutes.

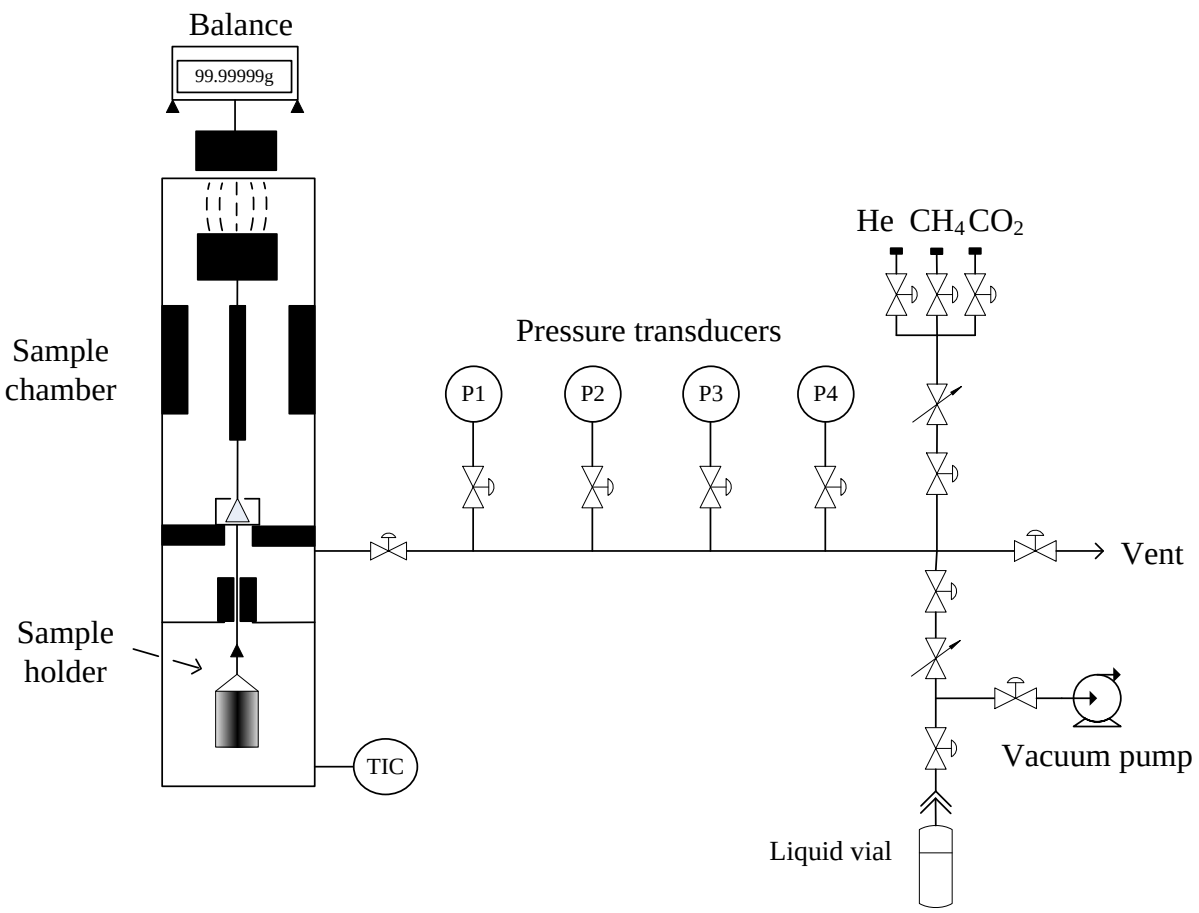


**Figure 3.4** A simplified process flow diagram of the high pressure gas adsorption measuring unit (Belsorp – MicrotracBel Corp., Japan). TIC is temperature indicator controller.

The sorbed mass is affected by the buoyancy created from the pressurised experimental gases. Therefore, a buoyancy correction is essential to obtain the actual adsorption amount. The correction method is summarised in (Eq. 3.2) where the fluid density is measured by the balance continuously with the weight change.

Adsorption amount = Weight change + exclusion volume x Fluid density

Exclusion volume = Decoupling mechanism and hook volume + sample basket volume + Sample volume (Eq. 3.2)

### 3.5.2. Vapour Sorption Analysis

The sorption of toluene and xylene into the CTA membrane was studied on an alternate gravimetric sorption analyser, GHP – FS with a Cahn D-200 balance (VTI Scientific Instruments, USA). The analyser was operated in a the flow-mode where the helium or nitrogen at 1 bar absolute pressure was used as a sweep gas to carry the hydrocarbon vapours from a solvent chamber through the sample chamber. The impact of nitrogen and helium on the sorption result were negligible due to the inert nature and low operating pressure. The vapour activities were controlled by mixing dry and saturated sweep gas streams. The diagram of the analyser is shown in **Figure 3.5.** Prior to each experiment, the whole system was flushed with dry sweep gas to remove all the vapour and air. A drying step was then operated by dry sweep gas at 1 bar absolute pressure and experimental temperature (e.g. 35$^{o}$C) overnight to remove all residues absorbed in the membrane.

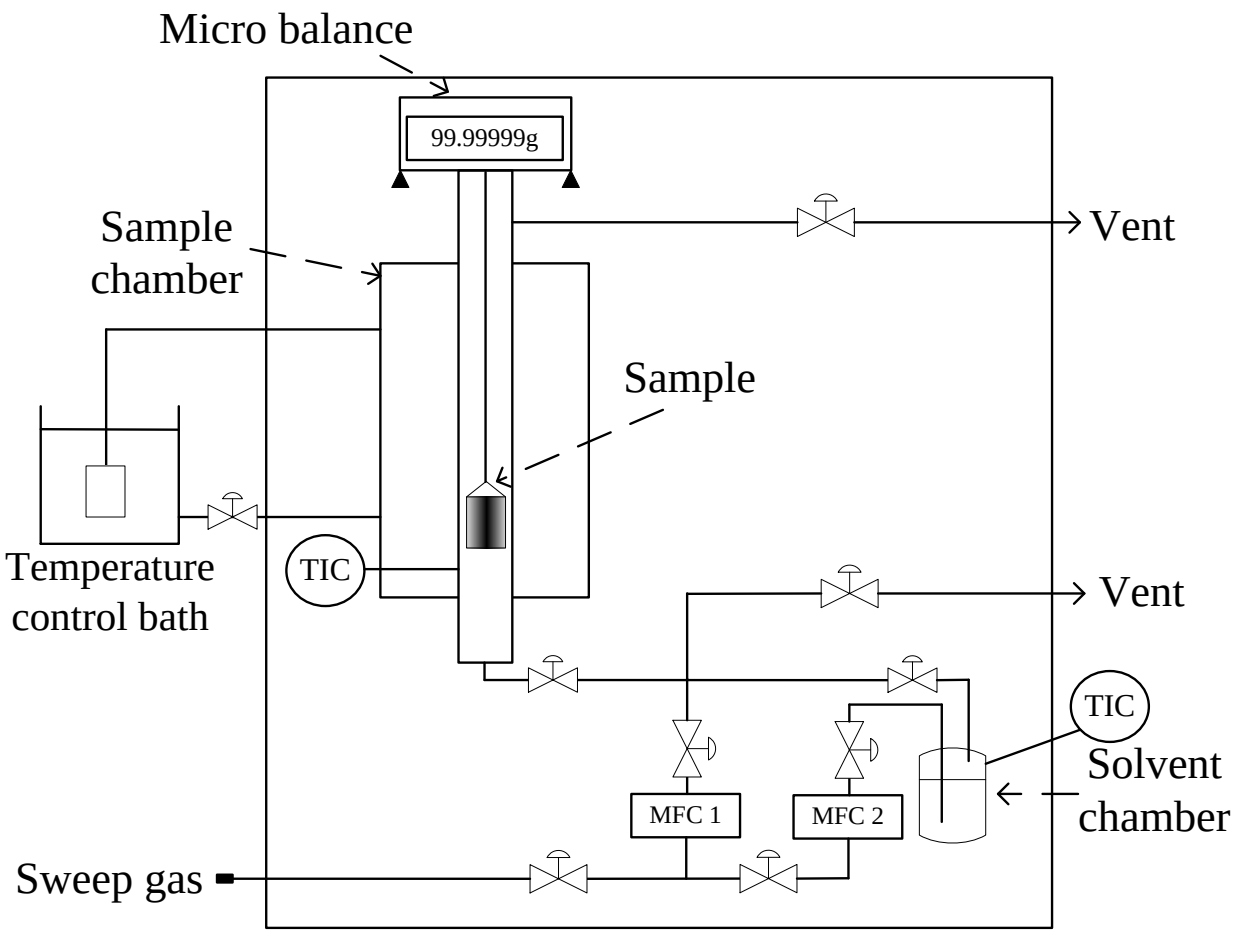


**Figure 3.5** A simplified process flow diagram of the vapour sorption analyser (VTI, USA). TIC and MFC are temperature indicator controller and mass flow controller, respectively.

### 3.5.3. Kinetic Sorption Measurement

The sorption kinetics of liquid penetrants into the CTA membrane was obtained by immersing the membrane into the relevant liquid. The membrane was initially dried overnight in vacuum to remove totally any absorbed water. The membrane was then immersed into the solution. The solution container was well-sealed and placed inside a fan forced oven to regulate the sorption temperature. After a specified immersion time, the membrane was removed from the solution, liquid droplets on the membrane surfaces were removed with a tissue and the membrane was weighed on an analytical balance XS205 (0.01 mg accuracy, Mettler Toledo - Australia) to record the mass of solvent uptake.

In this thesis, the sorption was considered at equilibrium conditions when the mass change was less than 0.1% over a 24-hour timespan. The solvent uptake is calculated via (Eq. 3.3), where $m_o$ and $m_\infty$ are the mass of membrane originally and at equilibrium, respectively. However, when the chemistry of the membrane was altered by the solvent, $m_o$ was replaced by the dried mass of the membrane after the solvent was removed by vacuum or solvent extraction ($m_{\infty,\,\text{dried}}$ (Eq. 3.4)).

$$\textit{Solvent uptake (\%)} = \frac{m_\infty - m_o}{m_o} x 100 \qquad \text{(Eq. 3.3)}$$

$$Solvent\ uptake\ (\%) = \frac{m_{\infty} - m_{\infty,dried}}{m_{\infty,dried}} x 100 \qquad \text{(Eq. 3.4)}$$

### 3.5.4. Pure Gas Permeation Measurement

The permeation of pure gas through the CTA membrane was measured via a constant volume – variable pressure (CVVP) gas permeation apparatus as reported in the literature [12, 42, 59, 90]. The process flow diagram for the single gas rig is shown in **Figure 3.6**. The membrane was installed into the membrane holder which was housed in a fan forced oven to control the experiment temperature. The whole system was evacuated overnight to remove all gases inside the pipelines and the membrane. The maximum vacuum pressure is limited to $10^{-4}$ mbar. Before measuring the gas permeation, both feed and permeate sides of the gas rig were disconnected from the vacuum pump and the leakage rate recorded by recording the pressure in the permeate versus time. The pressure in the permeate was recorded by a Baratron® pressure transducer (MKS, USA) with measurement range of 1.33 Pa – 2.66 kPa. Afterward, the pure gas of desired pressure was fed into the gas rig and the gas permeability was calculated via (Eq. 3.5).

$$P = \frac{273.2 \text{ x } 10^{10}}{760} \frac{l\,V}{AT\frac{(p \text{ x } 76)}{14.7}} \left[\frac{dp}{dt} - \left(\frac{dp}{dt}\right)_{leakage}\right] \qquad \text{(Eq. 3.5)}$$

where $P$ is the gas permeability (Barrer or $10^{-10}$ $cm^3(STP).cm.cm^{-2}.s^{-1}.cmHg^{-1}$); $V$ is the calibrated volume of downstream ($cm^3$); $l$ is the membrane thickness (cm); $A$ is the effective area of the film ($cm^2$); $T$ is the experimental temperature (K); $p$ is the absolute pressure of feed gas (psia); $(dp/dt)$ and $(dp/dt)_{leakage}$ are the change in pressure with time of the permeate in gas permeation and leakage tests, respectively (mmHg/s).

The volume of the permeate side includes the volume of pipelines and the cylinder. This volume was calibrated by measuring the permeability of oxygen through a commercial Styrex polystyrene film (Mitsubishi Plastics, Japan) at 30°C and 1 atm feed pressure, which is well-known to be 2.27 barrer [67].

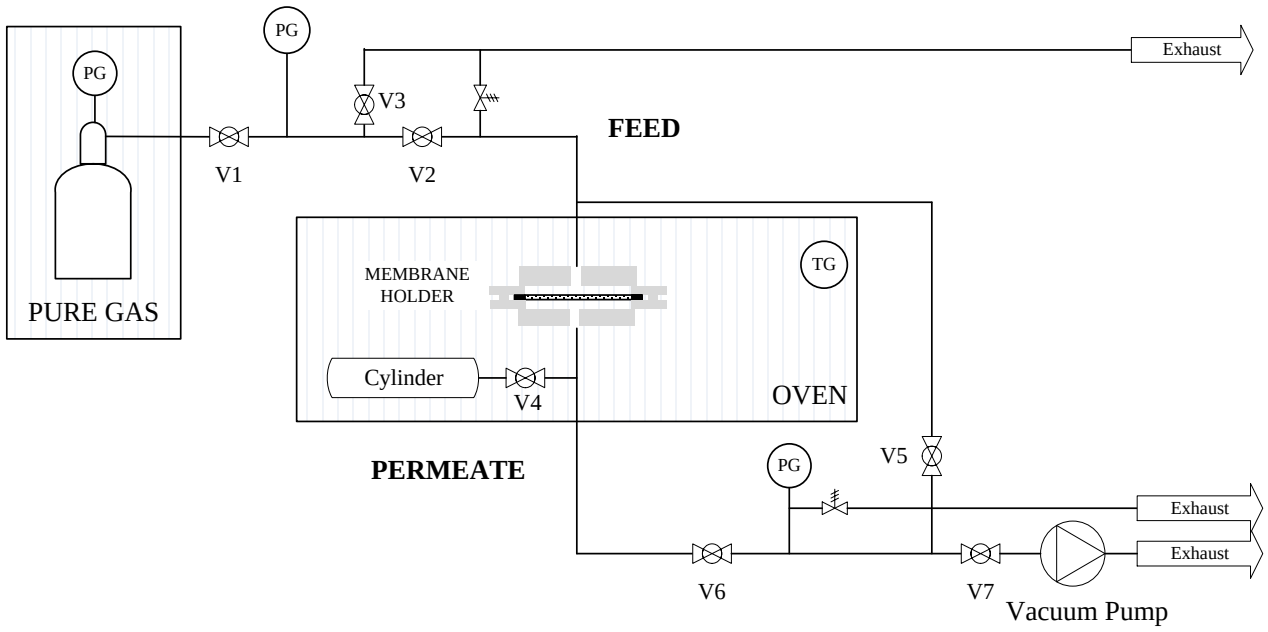


**Figure 3.6** The setup for the constant volume – variable pressure (CVVP) gas permeation apparatus

### 3.5.5. Mixed Gas Permeation Measurement

A variable volume – constant pressure (VVCP) mixed gas permeation apparatus was used to measure the permeation of gas mixtures through the membrane (**Figure 3.7**). The membrane was installed in the membrane holder and mounted into the fan forced oven. The mixed gas was fed into the feed side of the holder with feed pressure of 100 – 1000 kPa absolute and the temperature was controlled in range 20 – 80°C. A helium sweep gas at 101 kPa absolute pressure was introduced to the permeate side of the membrane holder and carried the permeate to the concentration analyser (GC and/or FTIR). To enhance gas mixing, stainless steel wool packing was filled into both sides of the membrane [67].

The gas permeability was evaluated from (Eq. 3.6) where $J_i$ is the flux of penetrant i, $cm^3(STP).cm^{-1}$; $l$ is the membrane thickness, cm; $p_{i,feed}$, $p_{i,permeate}$ are partial pressures of penetrant i in feed and permeate sides, respectively; $Q_p$ is the total flowrate of permeate side recorded from the flow meter, $cm^3(STP).s^{-1}$; $x_i$ is the composition of the penetrant i in the permeate stream obtained from GC or FTIR analysis; and $A$ is the effective area of the membrane, $cm^2$.

$$P_i = \frac{J_i\, l}{p_{i,feed} - p_{i,permeate}} = \frac{Q_p x_i}{A} \frac{l}{p_{i,feed} - p_{i,permeate}} \qquad \text{(Eq. 3.6)}$$

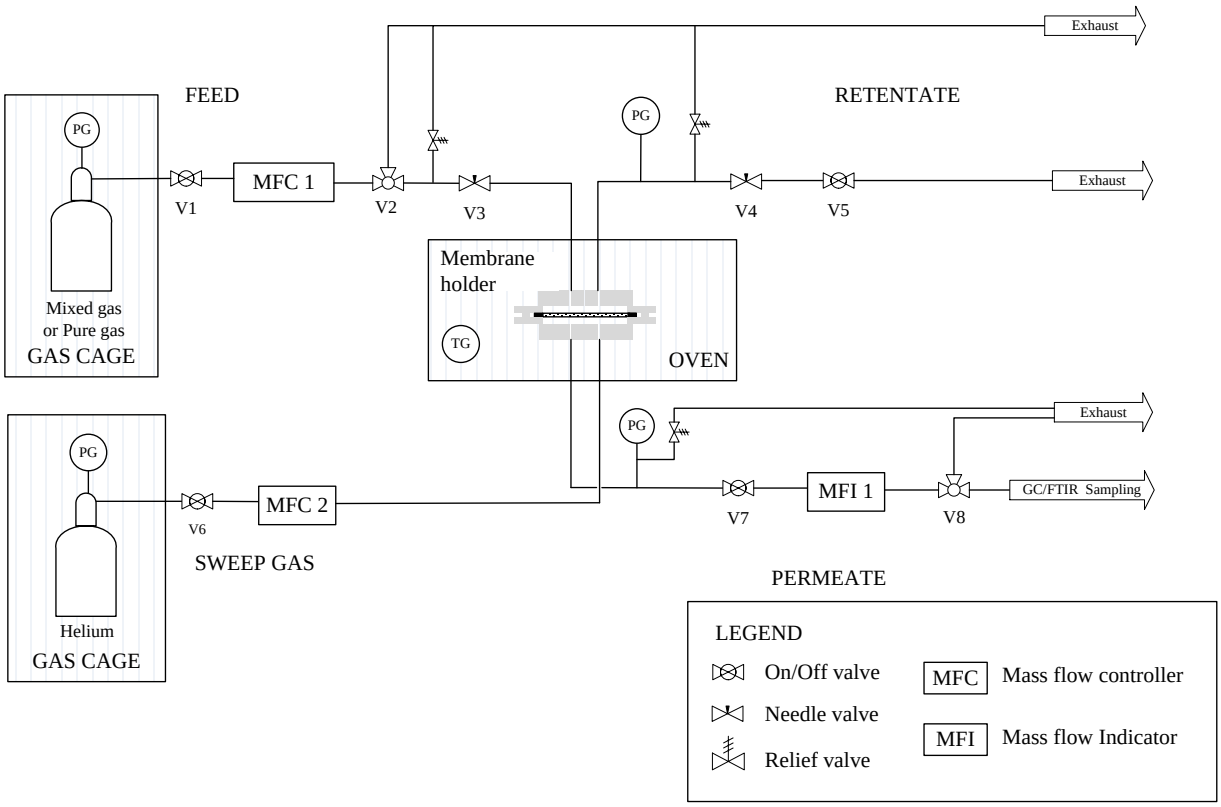


**Figure 3.7** The mixed gas rig setup for variable volume – constant pressure method (VVCP)

### 3.5.6. Mixed Vapour/Gas Permeation Measurement

The mixed vapour/gas permeation apparatus was modified from the typical mixed gas rig by adding a bubbling system to generate the solvent vapour (**Figure 3.8**). The vapour was introduced into the gas stream via a bubbling arrangement similar to the design in the gravimetric sorption analyser

(**section 3.5.2**) and our previous publications [23, 42, 229]. The dry feed gas was bubbled through the first chamber containing the penetrant liquid carry the vapour (e.g. toluene or xylene) to the second chamber where any entrained liquid was released prior to entering the membrane holder. The vapour activity was controlled via a temperature control bath with temperature range adjustable from -10$^{o}$C to 50$^{o}$C. The piping after the hydrocarbon chambers was covered with heating tape to prevent condensation. In addition, stainless steel balls were added into the first hydrocarbon chamber to enhance the bubbling effect. The permeability of each penetrant was analysed by the micro GC 490 analyser (Agilent technologies, Australia) and quantified via (Eq. 3.6).

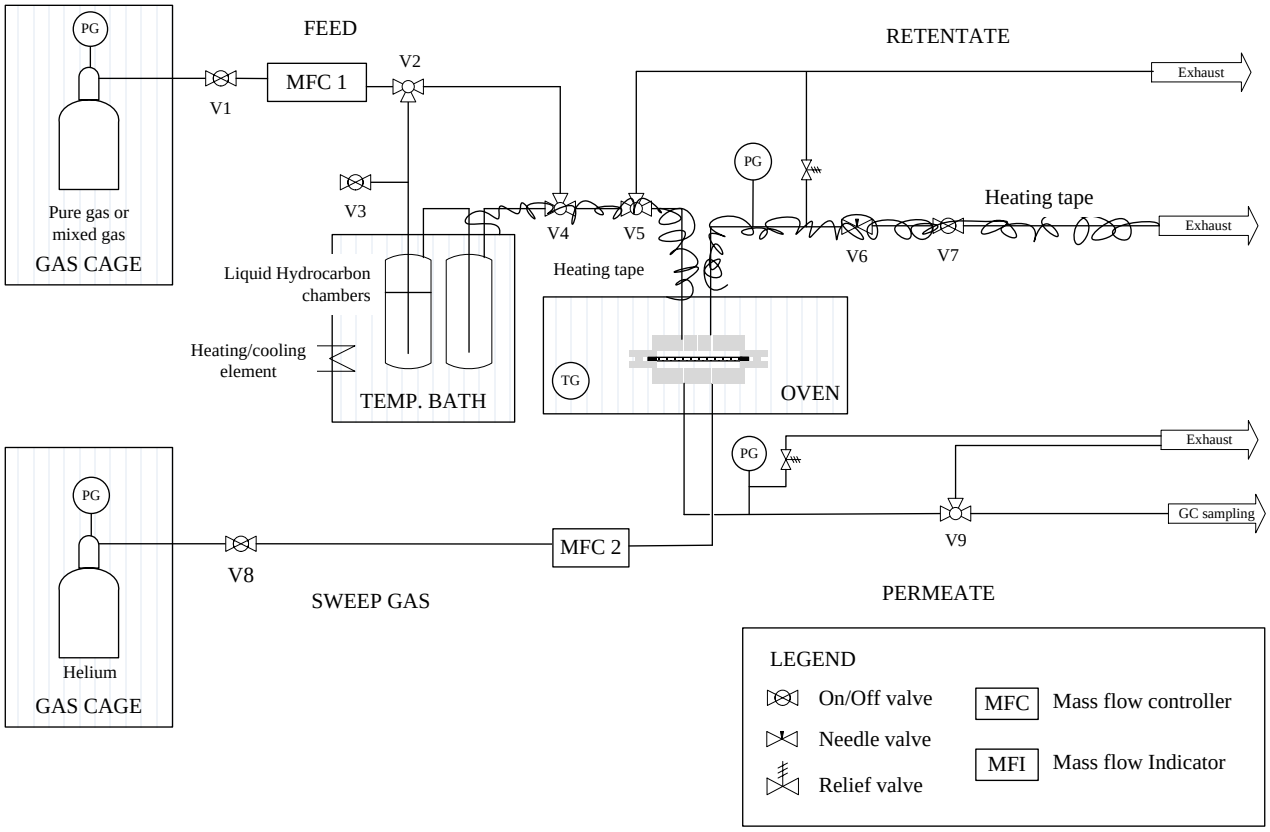


**Figure 3.8** The mixed vapour/gas permeation rig setup

## 3.6. PRESSURISED GAS HOLDER FOR MEMBRANE AGING STUDY

One of the points of interest in this thesis is the long-term aging of CTA membranes in pressurised gas. The membrane aging holder was designed with specifications summarised in **Table 3.5** and **Figure 3.9** The membranes were stored in the holder with 7.5 bar absolute pressure of a gas mixture (1000ppm $H_2S$, $SO_2$, NO in balance $N_2$) for up to 300 days. The holders were kept inside an operating fume hood to reduce the impact of toxic gases in case of gas leakage. After the scheduled period of time, the holder was evacuated slowly inside the fume hood for 5 minutes before opened to remove the membrane for gas testing.

**Table 3.5:** The specification of pressurised membrane holder for membrane aging study

| Specifications | | Design – dimension | |
|---|---|---|---|
| Material | | Stainless steel | |
| Absolute operating pressure (bar) | | 10 | |
| Operation temperature ($^{o}$C) | | 20 – 100 | |
| Operating gases | | $H_2S/SO_2/NO/N_2/O_2/CO_2$ (dry state) | |
| **Vessel Body** | | | |
| Shape | Vertical cylinder | Outer diameter (mm) | 80 ± 0.25 |
| Outer height (mm) | 100 ± 0.50 | Thickness (mm) | 10 (all sides) |
| **Flange** | | | |
| Outer diameter (mm) | 100 ± 0.50 | Inner diameter (mm) | 60 ± 0.25 |
| Thickness (mm) | 10 | O-ring | Kalrez® |
| Bolts (mm) | 6 x OD13 | | 69.44 x 3.00 |
| **Lid** | | | |
| Diameter (mm) | 100 ± 0.50 | Bolts (mm) | 6 x OD13 |
| Tubing holes (mm) | 2 x OD11 | | |

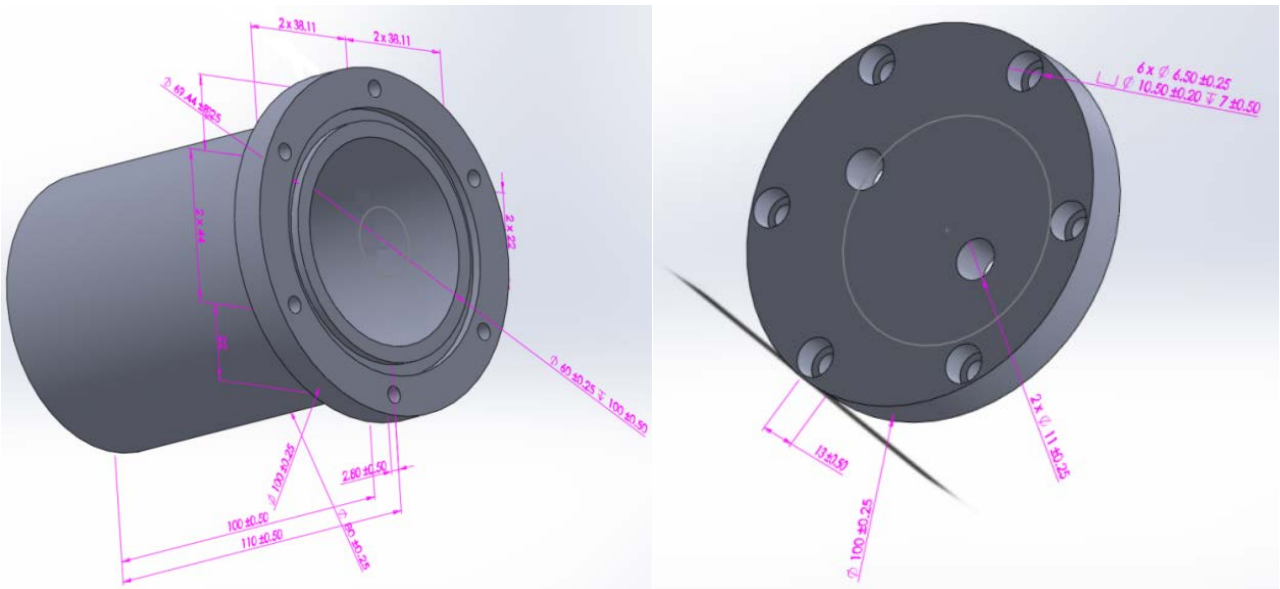


**Figure 3.9** The sketch of pressurised gas holder for membrane aging study

# CHAPTER 4. THE POTENTIAL FOR USE OF CELLULOSE TRIACETATE MEMBRANES IN POST COMBUSTION CAPTURE

## 4.1. INTRODUCTION

Carbon dioxide ($CO_2$) emissions are the leading cause for anthropogenic global warming, [243-246], with the major source being the combustion of fossil fuels. Carbon Capture and Storage (CCS) is one potential pathway for achieving $CO_2$ emission reduction targets, securing a sustainable energy industry while taking advantage of vital resources. Membrane gas separation is one technology proposed for the carbon capture step that combines high energy efficiency with high surface area-to-volume ratios and is 'chemical free' [2].

Membrane gas separation is already commercialised for carbon capture, in natural gas sweetening for the removal of $H_2S$ and $CO_2$. Cellulose triacetate (CTA) membranes have the greatest industry acceptance for this application, making up to 80% of this membrane market [5, 6]. CCS from coal-fired power station flue gas is another proposed strategy, known as post-combustion capture, where membrane gas separation has potential. While CTA membranes prepared by the phase inversion technique do not have the ideal permeability for post combustion capture, their high $CO_2/N_2$ selectivity, commercial readiness and proven industrial resilience means that they could have strong potential. Thin film composite CTA membranes have been prepared by other workers [247-249] and emerging membrane fabrication technologies such as layer by layer [36] and continuous assembly of polymers (CAP) [37] approaches could allow the thickness of the active layer to be reduced further, which would result in adequate permeance to meet gas flux requirements. Alternatively, the use of porous additives within the active layer to form a mixed matrix structure could also improve the permeability of the structure, without compromising the selectivity [58].

However, flue streams normally contain moisture (100ppm – 20 wt% [175, 212]) which is known to alter the separation performance of many membrane materials [42, 176, 250]. Chen et al. showed that the presence of water vapour at low partial pressures reduced the permeability of $CO_2$ and $CH_4$ through dense CTA membranes due to competitive sorption and "anti-plasticisation" behaviour [12]. Conversely, higher water vapour pressures plasticised or swelled the membrane resulting in an increase in gas permeability and a decline of gas selectivity [12, 21]. Upstream processing can also result in liquid water occasionally reaching the membrane unit, as droplets. In a post-combustion application, highly alkaline water may result from entrained fly ashes or the caustic slurry used in desulfurisation [26, 189]. Conversely, acidic water may overflow from a direct contact cooler if desulfurisation is not employed [24, 26]. As one of the earliest polymer used in membrane applications for both gas separation and water treatment, the hydrolysis of the cellulose acetate polymer in liquid water has been well studied across a range of pH conditions [180, 191, 251]. The overall hydrolysis rate constant, k, can be expressed as:

$$k = k_{H+}[H^+] + k_{OH-}[OH^-] + k_{H2O} \qquad \text{(Eq. 4.1)}$$

where the quantities in brackets are the ion activities. At ambient temperature, this results in a hydrolysis rate of around 5.4 x $10^{-10}$ $s^{-1}$ at pH 3, 1.4 x $10^{-10}$ at pH 7 and 0.0014 $s^{-1}$ at pH 13.

However, the impact of this hydrolysis on the gas separation performance of the membrane is less well understood.

Post-combustion flue gas typically contains 200-5000 ppmv $SO_x$ when it exits the combustion chamber[192, 193]. If flue gas desulphurisation is used, this reduces the $SO_x$ content to between 10 and 50 ppmv [192]. This is mainly in the form of $SO_2$, with some $SO_3$ also present. Many polymeric membranes are selective for $SO_2$ relative to other major gases, because of the strong condensability of $SO_2$ [19, 194, 252, 253]. The permeability of $SO_2$ within a composite CTA membrane has been reported by Kuehne and Friedlander, who focused on the impact of $SO_2$ pressure and membrane fabrication technique [193]. However, the impact of $SO_2$ on a CTA membrane at different temperatures was not considered, which is important given the range of temperatures that can be present in flue gas. Further, the long term effects of $SO_2$ on CTA membrane performance have not been established.

The concentration of nitrogen oxides in power station flue gas is in the range of 150-300 ppmv, with nitric oxide (NO) the major component and <10 ppmv nitrogen dioxide ($NO_2$), with some variation dependant on combustion technologies [24]. Again, these levels can be reduced through the use of selective catalytic reduction (SCR), which can remove 85 to 98% of these pollutants [192, 254], but this is not always in place. To the best of the authors' knowledge, there is no reported information on the impact of NO on a CTA membrane, though the effect on another class of polymeric membranes, polyimides, is reported [255]. It is expected that NO will have higher diffusivity than $CO_2$ because of smaller kinetic diameter, but the solubility of NO will be lower than $CO_2$, based on critical temperature behaviour [57]. An understanding of the impact of NO on CTA membranes is of vital importance if they are to be applied to post-combustion capture.

In this investigation, the gas transport performance of CTA membranes in single gas and mixed gas feeds of $CO_2$, $N_2$ and impurities ($H_2O$, $SO_2$ and NO) are reported. In addition, the impact of these impurities on the CTA membrane over 60 – 120 day periods is reported. This information will assist in evaluating the potential for CTA membranes to be used in this emerging industrial application.

The chapter was published in International Journal of Greenhouse Gas Control, detailed as below:

Lu, H.T., Kanehashi, S.; Scholes, C. A.; Kentish, S. E., The potential for use of cellulose triacetate membranes in post combustion capture. International Journal of Greenhouse Gas Control, 2016. 55: p. 97-104.

# Declaration for a thesis with publication

THE UNIVERSITY OF MELBOURNE

PhD and MPhil students may include a primary research publication in their thesis in lieu of a chapter if:

- The student contributed greater than 50% of the content in the publication and is the "primary author", ie. the student was responsible primarily for the planning, execution and preparation of the work for publication
- It has been peer-reviewed and accepted for publication
- The student has approval to include the publication in their thesis from their Advisory Committee
- It is a primary publication that reports on original research conducted by the student during their enrolment
- The initial draft of the work was written by the student and any subsequent editing in response to co-authors and editors reviews was performed by the student
- The publication is not subject to any obligations or contractual agreements with a third party that would constrain its inclusion in the thesis

Students must submit this form, along with *Co-author authorisation forms* completed by each co-author, when the thesis is submitted to the Thesis Examination System: *https://tes.app.unimelb.edu.au/*. If you are including multiple publications in your thesis you will need to complete a separate form for each publication. Further information on this policy is available at: *gradresearch.unimelb.edu.au/preparing-my-thesis/thesis-with-publication*

## A. PUBLICATION DETAILS *(to be completed by the student)*

| | | |
|---|---|---|
| Full title | The potential for use of cellulose triacetate membranes in postcombustion capture | |
| Authors | Hiep Thuan Lu, Shinji Kanehashi, Colin Scholes, Sandra Kentish | |
| Student's contribution (%) | 70 | |
| Journal or book name | International Journal of Greenhouse Gas Control | |
| Volume/page numbers | 55 (2016) 97-104 | |
| Status | ☐ Accepted and In press ☒ Published | Date accepted/ published 2 Nov 2016 |

## B. STUDENT'S DECLARATION

I declare that the publication above meets the requirements to be included in the thesis

| Student's name | Student's signature | Date *(dd/mm/yy)* |
|---|---|---|
| Hiep Thuan Lu | | 09/01/18 |

## C. PRINCIPAL SUPERVISOR'S DECLARATION

I declare that:

- the information above is accurate
- The advisory committee has met and agreed to the inclusion of this publication in the student's thesis
- All of the co-authors of the publication have reviewed the above information and have agreed to its veracity
- 'Co-Author Authorisation' forms for each co-author are attached.

| Supervisor's name | Supervisor's signature | Date *(dd/mm/yy)* |
|---|---|---|
| Sandra Kentish | | 09/01/18 |

THE UNIVERSITY OF MELBOURNE

# Co-author authorisation form

All co-authors must complete this form. By signing below co-authors agree to the listed publication being included in the student's thesis and that the student contributed greater than 50% of the content of the publication and is the "primary author" ie. the student was responsible primarily for the planning, execution and preparation of the work for publication.

In cases where all members of a large consortium are listed as authors of a publication, only those that actively collaborated with the student on material contained within the thesis should complete this form. This form is to be used in conjunction with the *Declaration for a thesis with publication form*.

Students must submit this form, along with the *Declaration for thesis with publication form*, when the thesis is submitted to the Thesis Examination System: *https://tes.app.unimelb.edu.au/*

Further information on this policy and the requirements is available at:
*gradresearch.unimelb.edu.au/preparing-my-thesis/thesis-with-publication*

| **A. PUBLICATION DETAILS** *(to be completed by the student)* | | |
|---|---|---|
| Full title | The potential for use of cellulose triacetate membranes in postcombustion capture | |
| Authors | Hiep Thuan Lu, Shinji Kanehashi, Colin Scholes, Sandra Kentish | |
| Student's contribution (%) | 70 | |
| Journal or book name | International Journal of Greenhouse Gas Control | |
| Volume/page numbers | 55 (2016) 97-104 | |
| Status | ☐ Accepted and In-press ☒ Published | Date accepted/published 2 Nov 2016 |

**B. CO-AUTHOR'S DECLARATION** *(to be completed by the collaborator)*

I authorise the inclusion of this publication in the student's thesis and certify that:

- the declaration made by the student on the *Declaration for a thesis with publication form* correctly reflects the extent of the student's contribution to this work;
- the student contributed greater than 50% of the content of the publication and is the "primary author" ie. the student was responsible primarily for the planning, execution and preparation of the work for publication.

| Co-author's name | Co-author's signature | Date *(dd/mm/yy)* |
|---|---|---|
| Colin Scholes | | 09/01/18 |

THE UNIVERSITY OF MELBOURNE

# Co-author authorisation form

All co-authors must complete this form. By signing below co-authors agree to the listed publication being included in the student's thesis and that the student contributed greater than 50% of the content of the publication and is the "primary author" ie. the student was responsible primarily for the planning, execution and preparation of the work for publication.

In cases where all members of a large consortium are listed as authors of a publication, only those that actively collaborated with the student on material contained within the thesis should complete this form. This form is to be used in conjunction with the *Declaration for a thesis with publication form*.

Students must submit this form, along with the *Declaration for thesis with publication form*, when the thesis is submitted to the Thesis Examination System: *https://tes.app.unimelb.edu.au/*

Further information on this policy and the requirements is available at:
*gradresearch.unimelb.edu.au/preparing-my-thesis/thesis-with-publication*

## A. PUBLICATION DETAILS *(to be completed by the student)*

| | | |
|---|---|---|
| Full title | The potential for use of cellulose triacetate membranes in postcombustion capture | |
| Authors | Hiep Thuan Lu, Shinji Kanehashi, Colin Scholes, Sandra Kentish | |
| Student's contribution (%) | 70 | |
| Journal or book name | International Journal of Greenhouse Gas Control | |
| Volume/page numbers | 55 (2016) 97-104 | |
| Status | ☐ Accepted and In-press ☒ Published | Date accepted/published 2 Nov 2016 |

## B. CO-AUTHOR'S DECLARATION *(to be completed by the collaborator)*

I authorise the inclusion of this publication in the student's thesis and certify that:

- the declaration made by the student on the *Declaration for a thesis with publication form* correctly reflects the extent of the student's contribution to this work;
- the student contributed greater than 50% of the content of the publication and is the "primary author" ie. the student was responsible primarily for the planning, execution and preparation of the work for publication.

| Co-author's name | Co-author's signature | Date *(dd/mm/yy)* |
|---|---|---|
| Shinji Kanehashi | Kanehashi | 09/01/18 |

## 4.2. EXPERIMENTAL

### 4.2.1. Membrane fabrication

The basic chemical structure of CTA is shown in **Figure 2.11**. The CTA polymer utilised in the study was supplied by Cellulose Company – Daicel Corporation, Japan with an acetylation degree of 61.6%. Prior to membrane fabrication, the polymer powder was dried overnight under vacuum at 100$^{o}$C to remove the moisture. At least two membranes were tested in each experiment to confirm the reproducibility.

Dense membranes were fabricated using dicholoromethane (ChemSupply, Australia) as the solvent. The solution (1 wt%) was filtered and cast into glass petri dishes that were kept covered for 24 hours for solvent evaporation. The thickness of each membrane was measured with a micrometer and found to be in the range of 60–80 µm.

A thin film CTA membrane was also fabricated by spin coating to measure the permeability of $SO_2$ and NO [37, 121]. A 4 wt% CTA in dichloromethane solution was spin coated onto a hydrophilic polytetrafluoroethylene (PTFE) membrane filter of 0.2 µm nominal pore size (Omnipore$^{TM}$, Merck Millipore, Australia). The spinning rate was set at 1500 rpm for 20 s and the substrate was pre-wetted by deionised water to reduce the pore penetration of polymer and solvent [37]. The thickness of the thin film composite CTA was measured by Scanning Electron Microscopy (FEI Quanta 200 ESEM FEG). The membrane was gold-coated by a Dynavac Mini Sputter Coater prior to imaging. The thin film thickness was found to be in the range of 3 to 6 µm.

All membranes were dried under vacuum at 35$^{o}$C for 24 hours and then 100$^{o}$C for a further 24 hours. The fabricated membranes were kept in a desiccator to minimise the exposure to moisture. The membranes were stored for 14 days prior to permeability measurements. Densification due to loss of free volume (physical aging) is greatest for any glassy membrane during these first two weeks and hence the delay ensured that this densification did not over power any other more subtle changes in membrane permeability. Further, in engineering practice, at least 14 days would be needed to trans-port and install the membrane module after fabrication, hence the performance in this initial period is less relevant.

### 4.2.2. Characterisation

The sorption kinetics of the membrane was determined by immersing the membrane samples into solutions at 35$^{o}$C. Solutions of pH 3.0, 7.0 and 13.0 were prepared from sulphuric acid (Chem-supply, Australia), purified water (Millipore Elix) and sodium hydroxide (Sigma Aldrich, Australia). After a specified immersion time, the membrane was removed from the solution, excess liquid droplets on the membrane surfaces removed by wiping with a tissue and weighed on an analytical balance XS205 (Mettler Toledo Australia) with maximum error of 0.06% [256]. The mass change per unit time allowed the diffusion coefficient ($D$) to be determined from (Eq. 4.2) [100].

$$\frac{m_0-m}{m_0-m_\infty} = 1 - \frac{8}{\pi^2}\sum_{n=0}^{\infty}\frac{1}{(2n+1)^2}\exp\left(-\frac{(2n+1)^2}{l^2}\pi^2 Dt\right) \qquad \text{(Eq. 4.2)}$$

where $m$ is the mass at time $t$ , $m_o$ the initial mass, $m_\infty$ the mass at equilibrium and $l$ the thickness of the membrane. At least five membranes, from more than one fabrication batch, were used to determine the diffusion coefficient using Eq. 4.2.

The total water uptake was also obtained by determining the mass of the CTA membrane when equilibrium sorption had been achieved. The membrane was removed from the solutions at equilibrium and again wiped free of surface liquid before weighing equilibrium mass ($m_\infty$). As the CTA membrane could be hydrolysed by the pH solutions [191] causing the mass of polymer to change, the total uptake was calculated via Eq. 4.3 where the dried membrane mass ($m_{\infty,dried}$) was obtained by drying the wet membrane under vacuum.

$$\text{Water uptake (\%)} = \frac{m_\infty - m_{\infty,\text{dried}}}{m_{\infty,\text{dried}}} \text{x } 100 \qquad \text{(Eq. 4.3)}$$

The impact of pH solutions on gas separation performance was also determined by immersion of the dense membranes in pH solutions for periods of up to 60 days. After immersion, the membranes were well-dried by vacuum at ambient temperature (22$^o$C) overnight before permeation testing.

The impact of toxic gases was similarly determined by placing dense membranes into a sealed chamber at ambient temperature (22 ± 2$^o$C). The chamber was evacuated and then filled with a gas mixture (pure $N_2$, 1000 ppm $SO_2$ or 979 ppm NO (988 ppm $NO_x$) in balance $N_2$, Coregas Australia) to a pressure of 7.5 bar. The pressure in the chamber was monitored to ensure that leakage did not occur. After a period of up to 100 days, a vacuum was applied for 5 minutes to remove the toxic gases before the chamber was opened and the membranes removed for permeation testing.

Changes in membrane structure were determined using Fourier Transform Infrared Spectroscopy (FT-IR, Perkin Elmer Frontier) fitted with an attenuated total reflectance (ATR) attachment.

### 4.2.3. Gas permeation measurement

The gas permeability (*P*) of individual gases ($CO_2$ (99.5% purity), $N_2$, He (99.99% purity), $CH_4$ (99.9% purity, Coregas Australia) through the dense CTA membranes was measured by a constant volume - variable pressure (CVVP) gas permeation apparatus operating at 35$^o$C and 7.5 and 10 bar transmembrane pressure difference as reported in our previous studies [59]. These pressures are higher than that expected in a flue gas environment but were chosen to ensure accuracy in the use of a CVVP approach. The membrane was installed into the membrane cell and placed under vacuum overnight before the gas permeation measurement.

A constant pressure variable volume (CPVV) method was used to test gas permeability of both dense and thin film composite membranes in gas mixtures across a temperature range of 22 – 80$^o$C again as reported in previous studies [23, 42]. The mixed gas (10% $CO_2$ in balance $N_2$, 1000 ppm $SO_2$ in $N_2$, or 979 ppm NO, 9 ppm $NO_2$ in $N_2$, Coregas Australia) was introduced into the feed side of the permeation cell at a feed pressure of 100 – 900 kPa gauge (stage cut less than 0.3%). These pressures are typical of those that might be experienced in a post-combustion environment. A helium sweep gas at 1 bar absolute pressure flowed across the permeate side of the permeation cell at a flowrate of 35 ml/min and was fed directly to the concentration analyser.

The concentrations of $SO_2$ and NO in the sweep gas were measured through Fourier transform infrared spectroscopy (FT-IR), as set out in ISO 19702:2006 [257, 258], in the wave number range of 1410 – 1290 cm$^{-1}$ and 2000 – 1775 cm$^{-1}$, respectively (Perkin Elmer Frontier FT-IR). The concentration of $CO_2$ and $N_2$ was determined by gas chromatography with an infrared detector (490 micro GC Agilent technologies, Australia). The FT-IR was calibrated against $SO_2$ and NO gas mixtures at a range of pressures to generate the calibration curves while the calibration curves for the GC were generated by calibration against four standard compositions of $CO_2$–$N_2$ gas mixtures.

The ratio of gas permeability of two gas species (i and j) is defined as the ideal gas selectivity ($\alpha_{ij}$) (Eq. 4.4).

$$\alpha_{ij} = P_i/P_j \qquad \text{(Eq. 4.4)}$$

## 4.3. RESULTS AND DISCUSSION

### 4.3.1. Impact of water

The water uptake at pH 3 and pH 7 was comparable to that previously published [12]. After an initial uptake over 2 hours, these values were stable over the experimental period (**Figure 4.1a**). It should be noted that this uptake period of two hours would be reduced to few seconds for a thinner active layer of say 50 nm, as would be used in an industrial application. The diffusion coefficient determined for water in these membranes was calculated from Equation 2 as 3.8 ± 0.4 x $10^{-8}$ $cm^2/s$ at both pH values, already consistent with literature results, 4.6 x $10^{-8}$ $cm^2/s$ [100].

Conversely, the water uptake of the membrane at pH 13 increases dramatically over time. This is consistent with the significant hydrolysis of CTA under alkali conditions [40, 191]. A significant reduction in the membrane dry mass was also observed for this membrane (**Figure 4.1b**), which reflects the dissolution of cellulosic polymers into the aqueous phase [259].

In general, the permeability of CTA membrane was enhanced after exposure to pH 3 and pH 7 solutions due to water-induced plasticisation, while the $CO_2/N_2$ selectivity changed little (**Figure 4.2**). The changes were roughly 6 % greater at pH 3 than at pH 7, which could be due to the stronger plasticisation impact of the hydronium ions in the acidic solution. Cellulose acetate polymer chains are known to become more flexible in strongly polar solvents [155]. Results in mixed gas conditions were comparable.

Membranes aged at pH 13, however, showed a significant and rapid decline in permeability, which is attributed to the hydrolysis of the CTA membrane in alkaline solution. The hydrolysis reactions converted the acetyl functional groups in the polymer matrix into hydroxyl functional groups [191, 260] that could be verified by FT-IR study (**Figure 4.3**). This significantly reduced the fractional free volume due to the strong intermolecular hydrogen bonding of these hydroxyl groups [191, 260].

Remarkably, the mass loss due to hydrolysis of the CTA membrane at pH 13 occurred continuously over 6 days (**Figure 4.1**), while the permeabilities of $CO_2$ and $N_2$ declined by 97% after just after few hours of immersion (**Figure 4.2**). This phenomenon suggests that the hydrolysis of the CTA membrane occurred initially on the membrane surfaces, converting these surfaces into impermeable regions. The solvated hydroxide ions then diffused through these hydrophilic surface regions and continued to hydrolyse the bulk of the CTA matrix.

As the permeability $CO_2$ and $N_2$ for the pH 13 case rapidly approached the detection limits of the gas permeation measurement methodologies, the $CO_2/N_2$ selectivity could not be determined with any precision and so is not reported in **Figure 4.2c**.

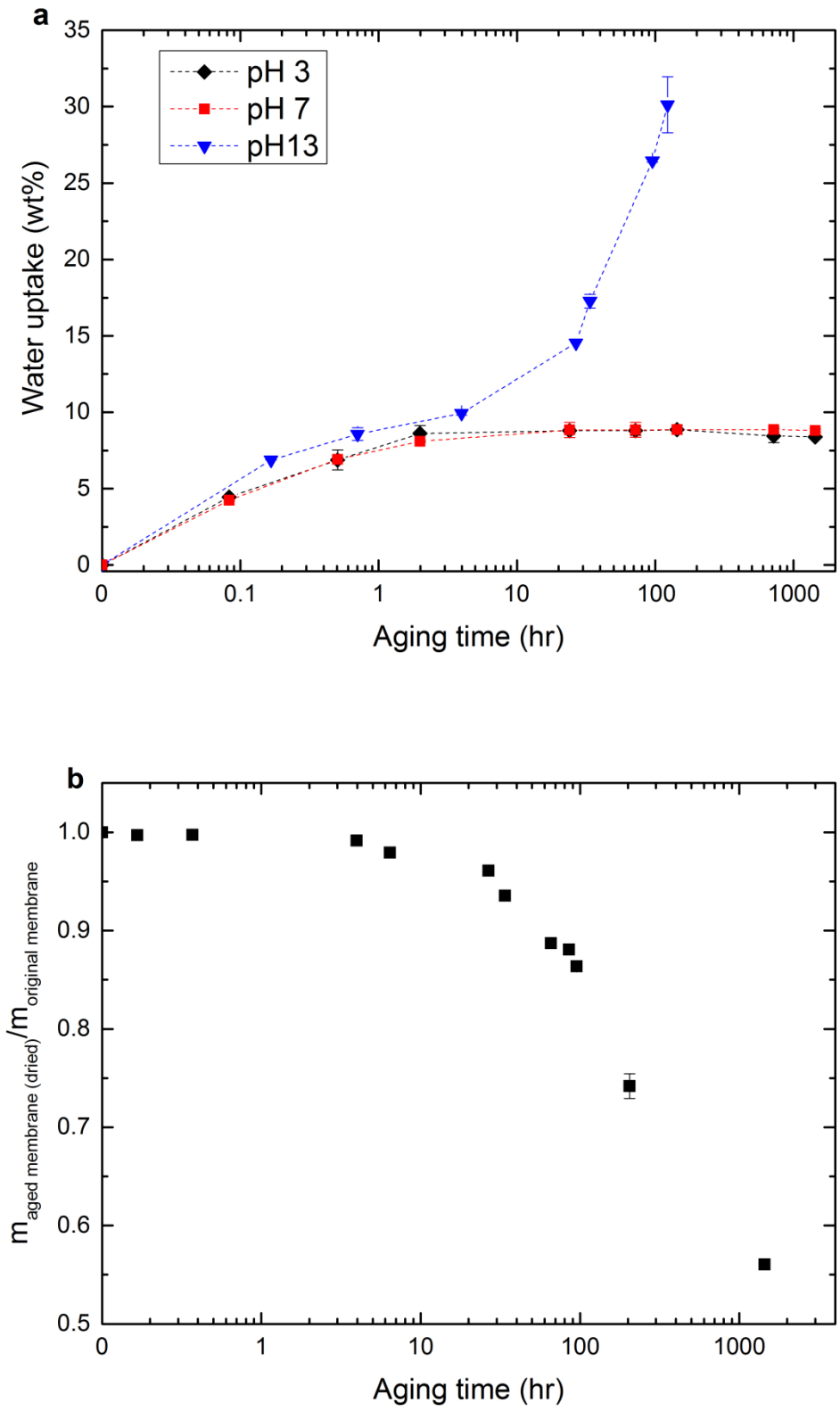


**Figure 4.1** (a) Water uptake of a CTA membrane after immersion in water of variable pH at 35◦C for a specified time; (b) Mass loss of a CTA membrane after immersion at pH 13.

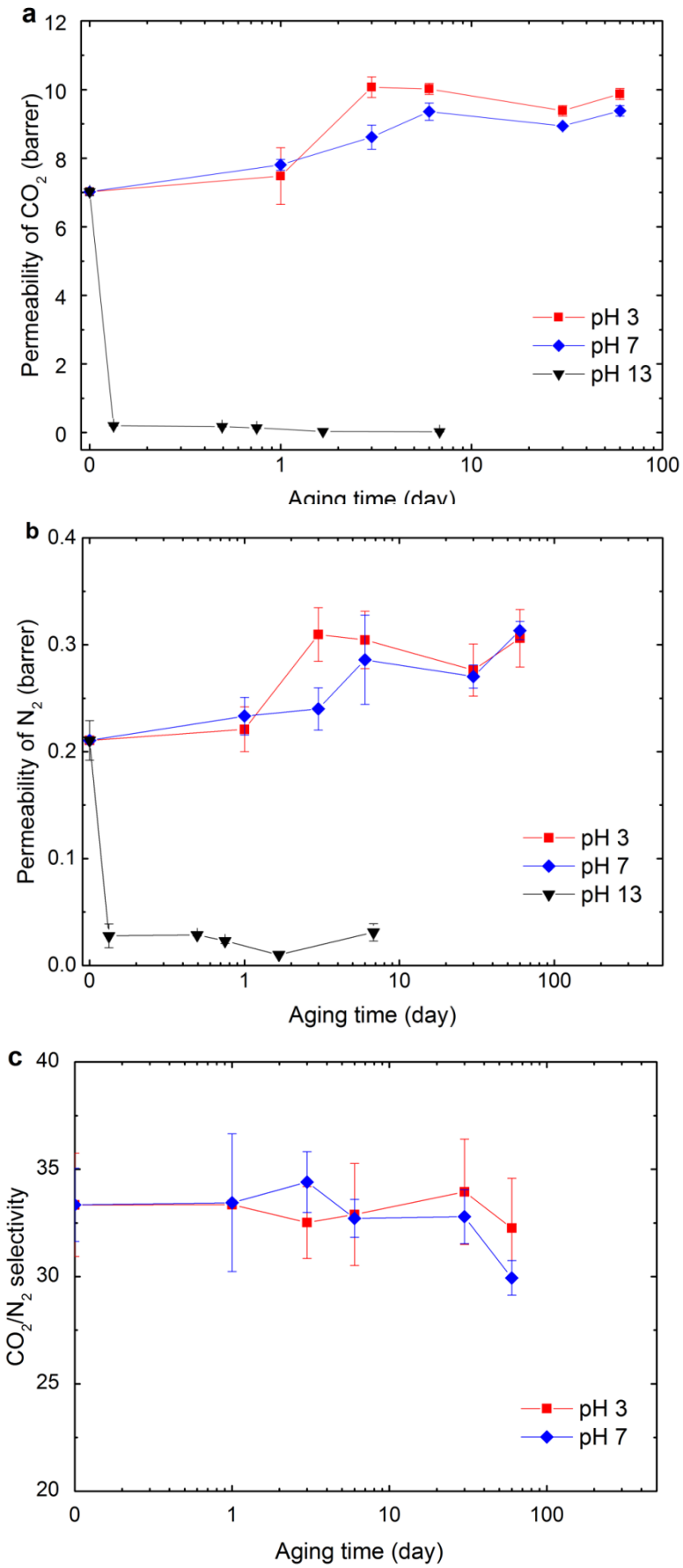


**Figure 4.2** Gas separation performance of CTA membranes at 10 bar, 35°C after immersion in pH (3, 7 and 13) solutions (a) permeability of $CO_2$; (b) permeability of $N_2$; (c)selectivity of $CO_2/N_2$.

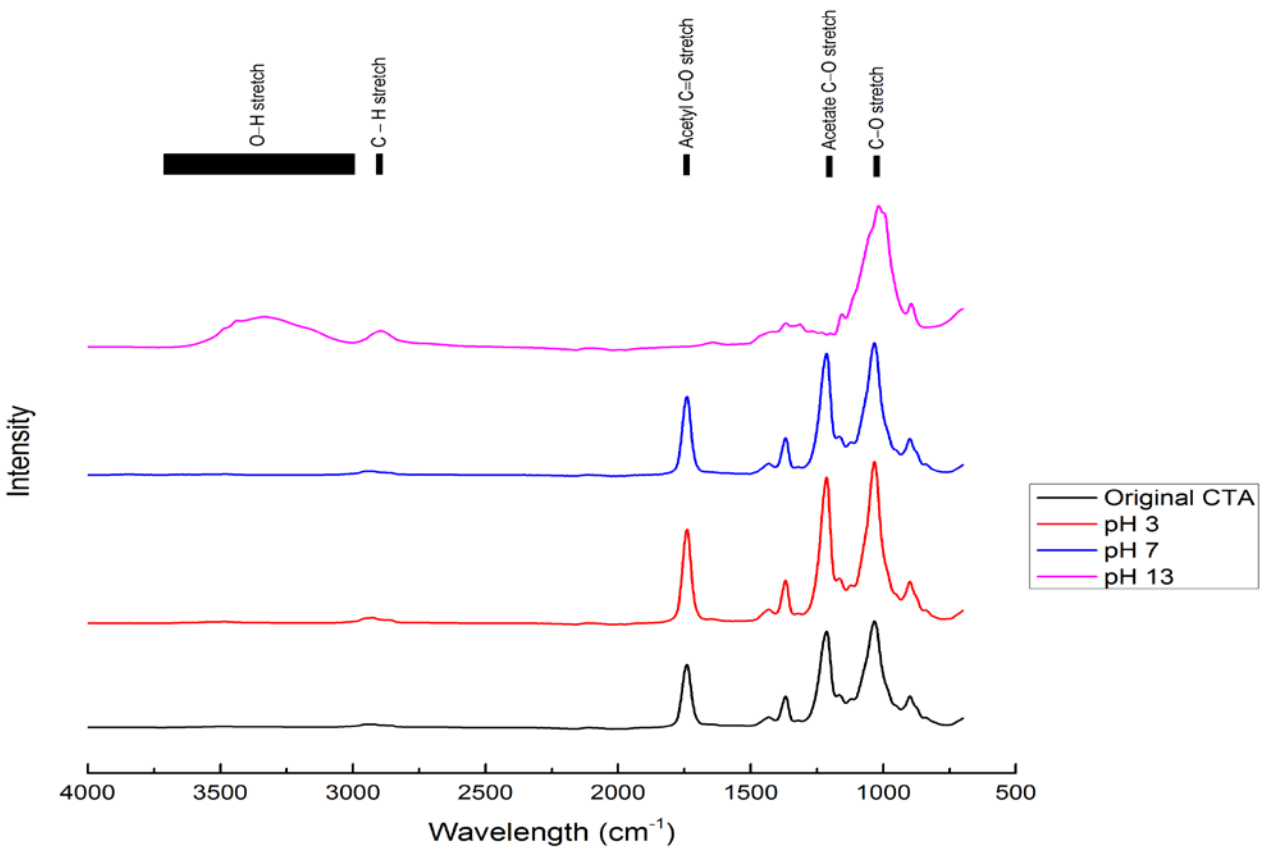


**Figure 4.3** FT-IR spectra of dried cellulose triacetate membrane before and after aged in different pH solutions for 60 days

### 4.3.2. Permeability of $SO_2$ and NO

The permeability of $CO_2$, $N_2$ and $SO_2$ through thin film composite CTA membranes was studied at different feed pressures (**Figure 4.4**). All membranes were tested 2 weeks after fabrication to reduce the effects of physical aging. The use of asymmetric membranes here was necessary to ensure the permeability of $SO_2$ could be detected, given the low partial pressure supplied.

For the temperature range 22 – 50$^o$C, the permeabilities of $N_2$, $CO_2$ and $SO_2$ were independent of the feed gas pressure within error. It should be noted that while **Figure 4.4b** provides the $N_2$ permeability in the $CO_2$-$N_2$ mixture, the data for the $N_2$-$SO_2$ mixture is highly comparable (**Figure 4.5**). At 80$^o$C, the permeability of $CO_2$ and $SO_2$ both initially decrease with pressure as the Langmuir microvoid regions typical of glassy polymers become saturated [117, 187, 261]. However within the error margins, plasticization is not clearly observed. Conversely, there is a slight increase in $N_2$ permeability in both $CO_2$-$N_2$ (**Figure 4.4b**) and $N_2$-$SO_2$ (**Figure 4.5**) mixtures across the entire partial pressure range, which might be indicative of plasticisation affecting the $N_2$ diffusivity. For $CO_2$, the literature reports that plasticisation occurs at 1200 kPa at 24$^o$C for dense films [166] and 500 – 800 kPa for thin films at 50 – 53$^o$C [168, 262]. Given, the plasticisation pressure should increase with temperature for a glassy membrane [59] a significantly higher $CO_2$ partial pressure than tested in this study should be required to observe $CO_2$ plasticisation. Conversely, Kuehne et al. [193] observe a continuous increase in permeability across an $SO_2$ partial pressure range of 13 – 93 kPa for dense membranes, consistent with the plasticisation pressure having been exceeded at these pressures.

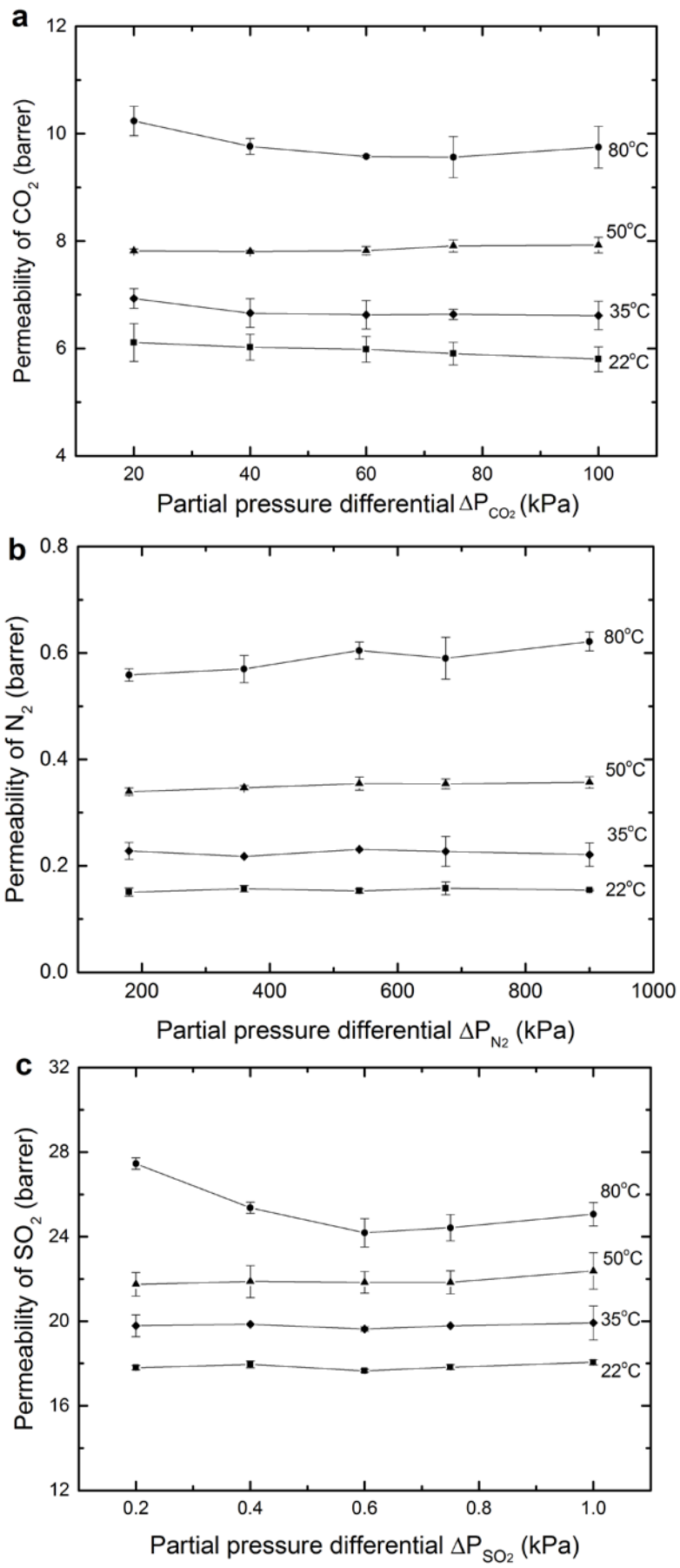


**Figure 4.4** Gas permeability in CTA thin film composite membranes. (a) permeability of $CO_2$ in 10 v/v% $CO_2$ in $N_2$; (b) permeability of $N_2$ in 10 v/v% $CO_2$ in $N_2$; (c) permeability of SO21000 ppm $SO_2$ in $N_2$.

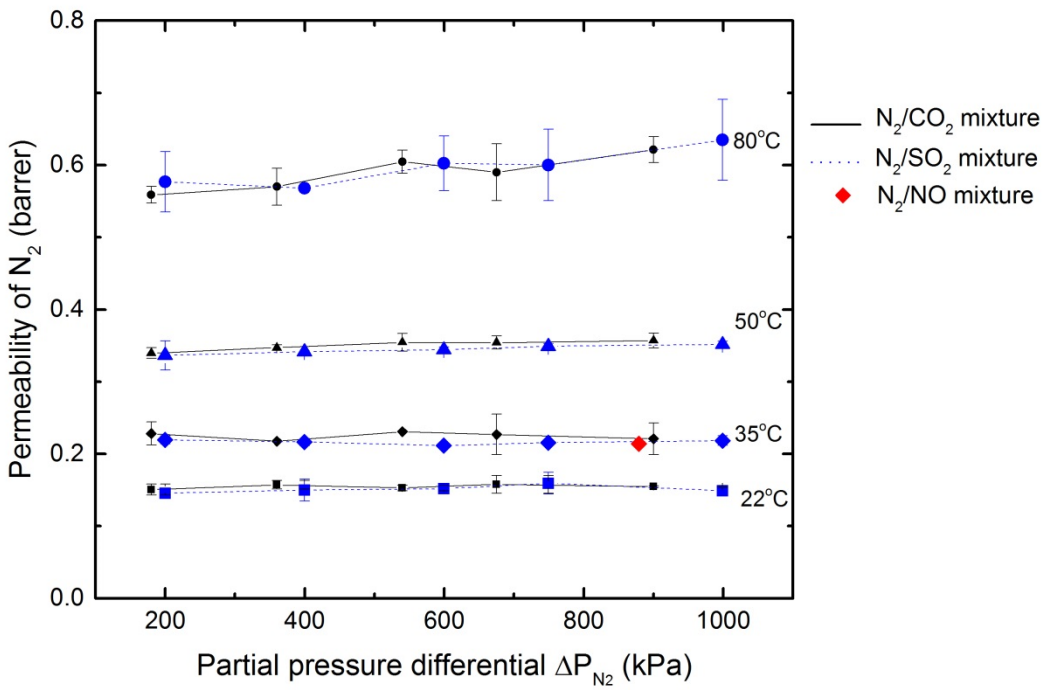


**Figure 4.5** $N_2$ permeability in CTA thin film composite membranes with 10 v/v% $CO_2$ in $N_2$ gas feeding and 1000 ppm $SO_2$ in $N_2$ gas feeding

The activation energy for permeation was determined at a total pressure differential of zero pressure to avoid any impact of plasticisation (**Table 4.1**). Increasing temperature enhances the diffusion of penetrants through membrane ($E_D > 0$) but diminishes the solubility of gas species in polymer ($\Delta H_S < 0$). The positive values of $E_P$ in this study showed that the permeation of gas penetrants is diffusion controlled.

**Table 4.1:** Activation energy for permeation in CTA membrane at zero pressure

| | $CH_4$* | $N_2$ | $CO_2$ | $SO_2$ | NO |
|---|---|---|---|---|---|
| Kinetic diameter (Å) [51] | 3.80 | 3.64 | 3.30** | 3.60 | 3.20 |
| Critical temperature (K) [263] | 190.6 | 126.2 | 304.2 | 430.8 | 180.0 |
| Activation energy for permeation, $E_p$ (kJ/mol) | 18.6 ± 0.2 | 18.8 ± 2 | 8.5 ± 0.7 | 7.3 ± 0.7 | |

* The permeability of methane was also measured by single gas permeation through a dense membrane to provide a comparison between different penetrants

** Many authors believe this diameter to be an underestimate of the diameter relevant to diffusion, with alternate values of 3.43 to 3.63 Å often preferred [54-56].

For species with relatively low critical temperatures ($CH_4$, $N_2$) the activation energy for permeation declines with the decrease of kinetic diameter of the penetrant species. This result is similar to other

studies in both CTA [160] and other glassy polymers [117, 264]. However, the activation energies for permeation of $SO_2$ and $CO_2$ are smaller, reflecting the high critical temperature of these penetrants that results in a large absolute value of heat of sorption and thus reduces the final activation energy for permeation [171].

$CO_2/N_2$ and $SO_2/N_2$ selectivities decreased with increasing temperature, consisted with diffusion controlled permeation (**Figure 4.6**). Importantly, the selectivity was constant with respect to partial pressure, even for $SO_2/N_2$, indicating that $SO_2$ plasticization was not significant enough to alter this parameter.

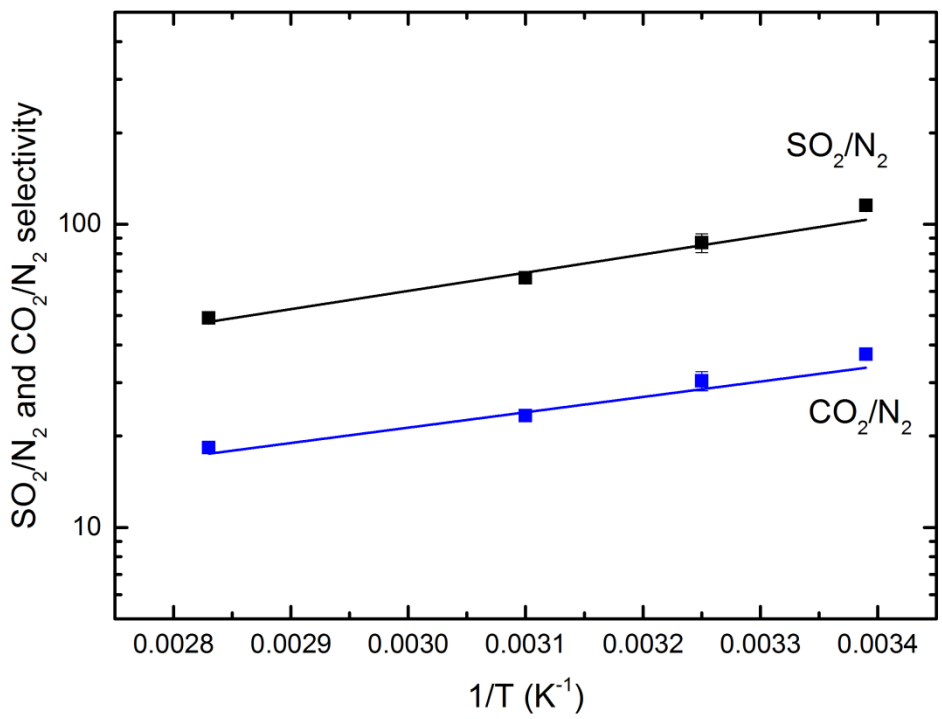


**Figure 4.6** Temperature dependence of the $SO_2/N_2$ and $CO_2/N_2$ selectivity in a CTA membrane at zero transmembrane pressure difference

We also attempted to record the NO permeability. However, the concentration of NO in the sweep gas was under the detection limit, even for a membrane of 3μm active layer thickness and a reduced sweep gas flowrate. This indicates that the permeability of NO at 35$^{o}$C is below 4 Barrer.

### 4.3.3. Aging of CTA membrane in $SO_2$ and NO

The CTA membranes were aged separately in pure $N_2$, 1000 ppm $SO_2$ and 979 ppm NO (988 ppm $NO_x$) to study the long term impact of these impurities on membrane performance. After a specified aging period (up to 120 days), the single gas permeation of He and $N_2$ was determined. The permeability of helium through the fresh CTA membranes at 7.5 bar and 35$^{o}$C was recorded as 21.8 ± 0.8 Barrer, which is comparable with the literature [40].The permeability and selectivity of the aged membranes was expressed as the ratio to the permeability and selectivity of the original fresh membrane to eliminate the variability between membrane samples (**Figure 4.7**).

Generally, the polymer chains of a glassy polymer are in a non-equilibrium state when a membrane is formed and so membrane densification or aging will occur over time [121]. As the excess free volume of the membrane is reduced, gas permeability declines, as observed in this study (**Figure 4.7**) [117, 121, 265]. The decline in permeability is less in helium than in nitrogen, which is due to its smaller kinetic diameter [117, 121]. This results in an increasing ($He/N_2$) selectivity as reported in **Figure 4.7c**.

This aging process was not affected by a partial pressure of 0.75 kPa $SO_2$ (**Figure 4.7**). Although $SO_2$ plasticisation was possibly observed at 80$^o$C in the previous permeation experiment (**Figure 4.4b**), this effect was not sufficient at 22$^o$C to alter the membrane aging process within experimental error. As the membranes used here are significantly thicker than the ones used for **Figure 4.4b**, this result is not unexpected.

Conversely, aging in the presence of 0.74 kPa $NO_x$ was significantly faster despite the relatively low critical temperature of NO. This could be caused by the presence of small quantities of $NO_2$ in the gas, both due to impurities in the original NO - $N_2$ gas mixture (1% $NO_2$ in total $NO_x$) and possibly due to oxidation of residual NO with ambient oxygen [199] at the end of the aging process. It is well-known that $NO_2$ can oxidise the primary alcohol of cellulosic materials into a carboxyl moiety [200, 201]. To determine if this has occurred, an additional FT-IR - Attenuated total reflectance (ATR) experiment was conducted on the aged membrane. The results indeed showed evidence of an increased ratio of carboxyl groups relative to alcohol groups (**Table 4.2**) for this membrane. The hydrogen bonding capacity of the carboxyl functional group is stronger than that of a primary alcohol and this could enhance the polymer interchain interactions, increasing chain packing and reducing the transport of gas penetrants.

**Table 4.2**: The absorbance ratio between carbonyl functional group and C – O functional group in fresh and aged membranes

| | **Original CTA** | **CTA aged 120 days in $N_2$** | **CTA aged 120 days in $NO/N_2$ mixture** |
|---|---|---|---|
| $\frac{\text{Max absorbance (C=O)}}{\text{Max absorbance (C − O)}}$ | 0.715 ± 0.08 | 0.712 ± 0.002 | 0.750 ± 0.02 |

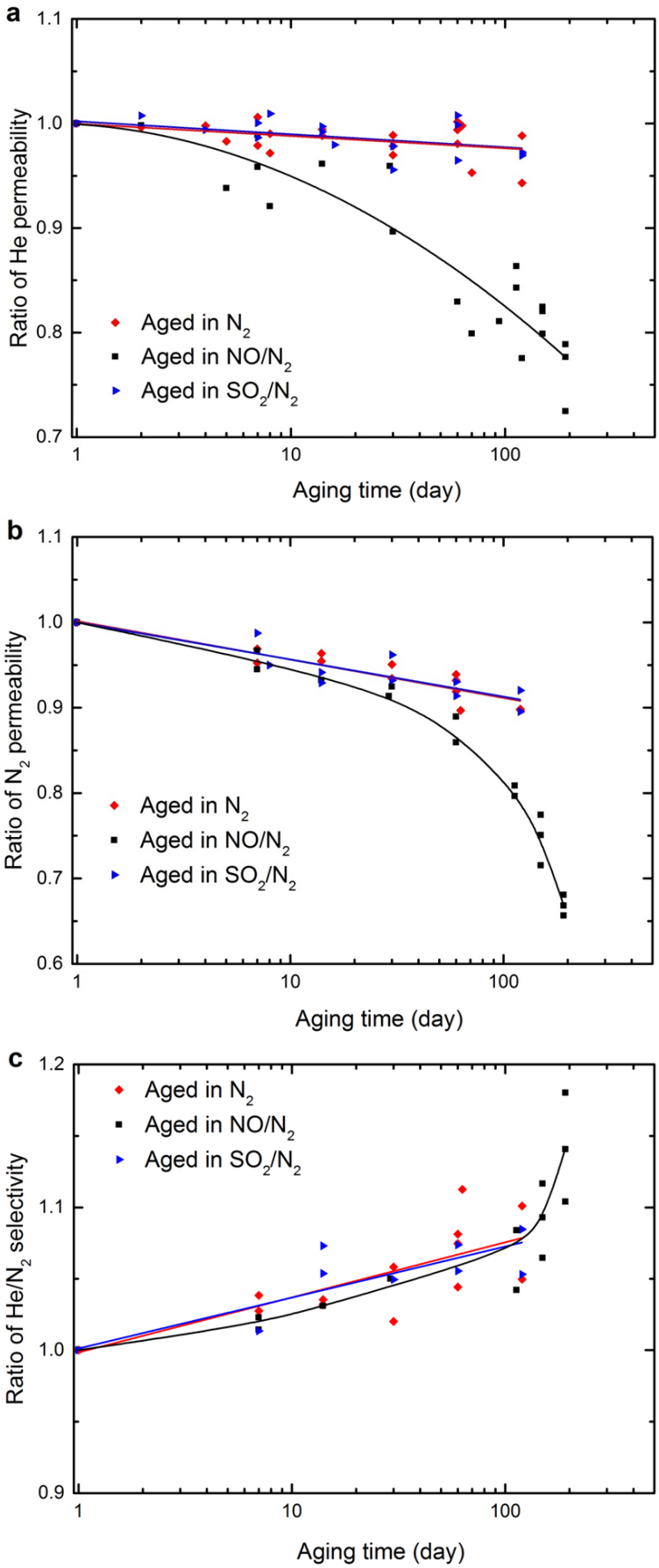


**Figure 4.7** Change in permeability of (a) He; (b) $N_2$ and (c) He/$N_2$ selectivity as time progresses for CTA membranes at 35$^o$C, 7.5 bar after aging separately in pure $N_2$, 979 ppm NO in balance $N_2$ and 1000 ppm $SO_2$ in balance $N_2$ at 7.5 bar and 22 ± 2$^o$C

## 4.4. CONCLUSIONS

This work has shown that cellulose triacetate membranes are relatively stable when exposed to liquid water at at pH 3 or pH 7, with a 30% increase in permeability and no loss of selectivity after immersion for 6 days, after which the performance stabilised. Conversely, caustic solutions (pH 13) hydrolysed and dissolved the membrane significantly over time. The CTA membranes also showed stable performance upon exposure to 0.75 kPa $SO_2$ for up to 100 days, with the membranes aging at the same rate as when exposed to inert nitrogen. Conversely, exposure of 0.74 kPa of NOx resulted in a significantly greater loss of permeability. This loss in permeability was attributed to reaction of the alcohol moieties in the cellulose acetate structure with trace quantities of $NO_2$ in the gas mixture.

$SO_2$ permeated through a CTA membrane more readily than $CO_2$ and $N_2$ with a permeability at 35$^o$C of 20 Barrer. There was some evidence of plasticisation in the $N_2$ permeability data for both $SO_2$ and $CO_2$ mixtures at 80$^o$C in short term permeability testing, but no membrane plasticisation was observed after a 120 days aging period at 22$^o$C and 0.75 kPa $SO_2$. The permeability of NO was below detection limits indicating a permeability of below 4 Barrer.

It should be noted that the aging studies were conducted hereon relatively thick membranes (60–80 m). In industrial practice, a membrane with a much thinner dense layer (<1 µm) would be used. It is likely that the effects observed here would occur more rapidly in this thinner structure, as it is well known that both plasticisation [255] and loss of free volume [121] occurs more rapidly in thinner glassy systems. However, the magnitude of the effect should be unchanged.

The results suggest that CTA membranes could be applied in post combustion capture operations if a sufficiently thin film composite membrane could be prepared. Both water and $SO_2$ could be tolerated in the flue gas stream under most common operating conditions. However, the control and removal of $NO_2$ down to very low levels is essential to maintain the membrane performance in the long term. The resulting $CO_2$ permeate from the gas separation process will be enriched with $SO_2$ but depleted in NO. The increased $SO_2$ concentration may cause concern with downstream corrosion of piping and this may also need careful consideration.

## 4.5. ACKNOWLEDGEMENTS

The authors would like to acknowledge the funding support for this research project from The University of Melbourne, Particulate and Fluid Processing Centre (PFPC), Brown Coal Innovation Australia (BCIA) and the Peter Cook Centre for Carbon Capture and Storage Research at the University of Melbourne. The specialist gas infrastructure was funded by the Australian Research Council (LE120100141) and by the Australian Government Education Investment fund and this support is also gratefully acknowledged.

# CHAPTER 5. THE IMPACT OF ETHYLENE GLYCOL AND HYDROGEN SULFIDE ON THE PERFORMANCE OF CELLULOSE TRIACETATE MEMBRANES IN NATURAL GAS SWEETENING

## 5.1. INTRODUCTION

Natural gas is a primary energy resource that will occupy over 25% of the global electricity market in the next decades, as well as acting as a transport fuel and direct heating resource [266]. The composition of raw natural gas varies widely but typically contains impurities such as nitrogen ($N_2$), carbon dioxide ($CO_2$), water ($H_2O$) and hydrogen sulphide ($H_2S$) that require removal to meet pipeline specifications. Membrane separation has been used for many decades for acid gas removal, known as natural gas sweetening, with advantages in energy efficiency, land footprint and a lack of chemical consumption [2]. Although many new membrane materials have been developed, cellulose triacetate (CTA) membranes still retain the bulk of this separation market because of their high $CO_2$ – methane ($CH_4$) selectivity, commercial readiness and acceptance as a low risk option by the industry [5, 6].

Raw natural gas is usually saturated with water which is generally removed upstream of the membrane unit to avoid pipeline corrosion and hydrate formation [18, 20, 23, 212]. Glycols such as monoethylene glycol (MEG), diethylene glycol (DEG) and triethylene glycol (TEG) are the most common solvents utilised for this purpose [20, 213]. Due to the extremely low vapour pressure of glycols (28Pa for monoethylene glycol [220] and <1Pa for triethylene glycol [221] at 35$^{o}$C), carryover of these solvents in the vapor state is usually limited. However, carryover of entrained glycol droplets can occur [20]. This is a significant issue, because glycol is known to plasticise polymers [218], and the entrainment of the glycol solution into the membrane unit can thus alter the permselectivity of the membrane [267]. A study on the effect of MEG and TEG vapours on $CO_2/CH_4$ separation across a facilitated transport membrane has been reported [17]. However, to the best knowledge of the authors, there is no study on the effect of glycol solutions on the gas separation performance of CTA membranes.

Hydrogen sulfide is a common species in natural gas with concentration varying from 4 – 10000 ppm [20] that will enter the membrane unit with the natural gas. Many studies on $CO_2$ removal from natural gas by cellulose acetate membranes have observed the co-permeation of $H_2S$ with $CO_2$ in the membrane unit [10, 20, 268]. Li et al (1987) reports the performance of cellulose acetate membranes in the presence of $H_2S$ – $H_2O$ mixtures [210]. However, the impact of temperature on $H_2S$ permeation through the CTA membrane has not been well studied. Heilman et al. [211] reported the permeability and sorption of $H_2S$ into several polymer films including a cellulose acetate film manufactured by Polaroid but the results presented were limited. Data on the long term effect of $H_2S$ on CTA gas separation performance is also limited.

In this investigation, the effect of two standard glycols, MEG and TEG, on the gas separation of CTA membranes over a 2000 hour period is investigated. The permeation of $H_2S$ through CTA

membrane at different partial pressures (0.2 – 0.75 kPa) and temperatures (22 – 80$^{o}$C) is also reported, as is the long term impact of $H_2S$ on the membrane performance over a 7200 hour period.

The chapter was published in Journal of Membrane Science, detailed as below:

Lu, H.T., Kanehashi, S., Scholes, C.A. and Kentish, S.E. (2017). The impact of ethylene glycol and hydrogen sulfide on the performance of cellulose triacetate membranes for $CO_2$ separation. *Journal of Membrane Science*, 539, 432-440.

THE UNIVERSITY OF MELBOURNE

# Declaration for a thesis with publication

PhD and MPhil students may include a primary research publication in their thesis in lieu of a chapter if:

- The student contributed greater than 50% of the content in the publication and is the "primary author", ie. the student was responsible primarily for the planning, execution and preparation of the work for publication
- It has been peer-reviewed and accepted for publication
- The student has approval to include the publication in their thesis from their Advisory Committee
- It is a primary publication that reports on original research conducted by the student during their enrolment
- The initial draft of the work was written by the student and any subsequent editing in response to co-authors and editors reviews was performed by the student
- The publication is not subject to any obligations or contractual agreements with a third party that would constrain its inclusion in the thesis

Students must submit this form, along with *Co-author authorisation forms* completed by each co-author, when the thesis is submitted to the Thesis Examination System: *https://tes.app.unimelb.edu.au/*. If you are including multiple publications in your thesis you will need to complete a separate form for each publication. Further information on this policy is available at: *gradresearch.unimelb.edu.au/preparing-my-thesis/thesis-with-publication*

## A. PUBLICATION DETAILS *(to be completed by the student)*

| | | |
|---|---|---|
| Full title | The impact of ethylene glycol and hydrogen sulphide on the performance of cellulose triacetate membranes in natural gas sweetening | |
| Authors | Hiep Thuan Lu, Shinji Kanehashi, Colin Scholes, Sandra Kentish | |
| Student's contribution (%) | 70 | |
| Journal or book name | Journal of Membrane Science | |
| Volume/page numbers | 539 (2017) 432-440 | |
| Status | ☐ Accepted and In press ☒ Published | Date accepted/ published 8 June 2017 |

## B. STUDENT'S DECLARATION

I declare that the publication above meets the requirements to be included in the thesis

| Student's name | Student's signature | Date *(dd/mm/yy)* |
|---|---|---|
| Hiep Thuan Lu | | 09/01/18 |

## C. PRINCIPAL SUPERVISOR'S DECLARATION

I declare that:

- the information above is accurate
- The advisory committee has met and agreed to the inclusion of this publication in the student's thesis
- All of the co-authors of the publication have reviewed the above information and have agreed to its veracity
- 'Co-Author Authorisation' forms for each co-author are attached.

| Supervisor's name | Supervisor's signature | Date *(dd/mm/yy)* |
|---|---|---|
| Sandra Kentish | | 09/01/18 |

THE UNIVERSITY OF MELBOURNE

# Co-author authorisation form

All co-authors must complete this form. By signing below co-authors agree to the listed publication being included in the student's thesis and that the student contributed greater than 50% of the content of the publication and is the "primary author" ie. the student was responsible primarily for the planning, execution and preparation of the work for publication.

In cases where all members of a large consortium are listed as authors of a publication, only those that actively collaborated with the student on material contained within the thesis should complete this form. This form is to be used in conjunction with the *Declaration for a thesis with publication form*.

Students must submit this form, along with the *Declaration for thesis with publication form*, when the thesis is submitted to the Thesis Examination System: *https://tes.app.unimelb.edu.au/*

Further information on this policy and the requirements is available at:
*gradresearch.unimelb.edu.au/preparing-my-thesis/thesis-with-publication*

| **A. PUBLICATION DETAILS** *(to be completed by the student)* | | |
|---|---|---|
| Full title | The impact of ethylene glycol and hydrogen sulphide on the performance of cellulose triacetate membranes in natural gas sweetening | |
| Authors | Hiep Thuan Lu, Shinji Kanehashi, Colin Scholes, Sandra Kentish | |
| Student's contribution (%) | 70 | |
| Journal or book name | Journal of Membrane Science | |
| Volume/page numbers | 539 (2017) 432-440 | |
| Status | ☐ Accepted and In-press ☒ Published | Date accepted/published 8 June 2017 |

**B. CO-AUTHOR'S DECLARATION** *(to be completed by the collaborator)*

I authorise the inclusion of this publication in the student's thesis and certify that:

- the declaration made by the student on the *Declaration for a thesis with publication form* correctly reflects the extent of the student's contribution to this work;
- the student contributed greater than 50% of the content of the publication and is the "primary author" ie. the student was responsible primarily for the planning, execution and preparation of the work for publication.

| Co-author's name | Co-author's signature | Date *(dd/mm/yy)* |
|---|---|---|
| Colin Scholes | | 09/01/18 |

THE UNIVERSITY OF MELBOURNE

# Co-author authorisation form

All co-authors must complete this form. By signing below co-authors agree to the listed publication being included in the student's thesis and that the student contributed greater than 50% of the content of the publication and is the "primary author" ie. the student was responsible primarily for the planning, execution and preparation of the work for publication.

In cases where all members of a large consortium are listed as authors of a publication, only those that actively collaborated with the student on material contained within the thesis should complete this form. This form is to be used in conjunction with the *Declaration for a thesis with publication form*.

Students must submit this form, along with the *Declaration for thesis with publication form*, when the thesis is submitted to the Thesis Examination System: *https://tes.app.unimelb.edu.au/*

Further information on this policy and the requirements is available at:
*gradresearch.unimelb.edu.au/preparing-my-thesis/thesis-with-publication*

## A. PUBLICATION DETAILS *(to be completed by the student)*

| | | |
|---|---|---|
| Full title | The impact of ethylene glycol and hydrogen sulphide on the performance of cellulose triacetate membranes in natural gas sweetening | |
| Authors | Hiep Thuan Lu, Shinji Kanehashi, Colin Scholes, Sandra Kentish | |
| Student's contribution (%) | 70 | |
| Journal or book name | Journal of Membrane Science | |
| Volume/page numbers | 539 (2017) 432-440 | |
| Status | ☐ Accepted and In-press ☒ Published | Date accepted/published 8 June 2017 |

## B. CO-AUTHOR'S DECLARATION *(to be completed by the collaborator)*

I authorise the inclusion of this publication in the student's thesis and certify that:

- the declaration made by the student on the *Declaration for a thesis with publication form* correctly reflects the extent of the student's contribution to this work;
- the student contributed greater than 50% of the content of the publication and is the "primary author" ie. the student was responsible primarily for the planning, execution and preparation of the work for publication.

| Co-author's name | Co-author's signature | Date *(dd/mm/yy)* |
|---|---|---|
| Shinji Kanehashi | SKanehashi | 09/01/18 |

## 5.2. EXPERIMENTAL

### 5.2.1. Membrane fabrication

The polymer utilised in the investigation was a commercial cellulose triacetate powder supplied by Cellulose Company – Daicel Corporation, Japan. The degree of substitution of acetyl groups on the polymer is 2.85, corresponding to a degree of acetylation of 61.6%.

Dense CTA membranes were fabricated by a solvent casting method. The polymer powder was dried under vacuum at 100$^{o}$C overnight prior to membrane fabrication. The dried powder was then dissolved in dicholoromethane (ChemSupply, Australia) to form a 1 wt % solution. The solution was filtered to remove any impurities before casting into glass petri-dishes. The petri-dishes were kept covered for 24 hours for solvent evaporation. Afterward, the membranes were dried under vacuum at 35$^{o}$C for 24 hours and 100$^{o}$C for another 24 hours and the final membranes stored in a desiccator to prevent exposure to moisture. The membranes were stored for two weeks before utilisation in permeability measurements, to allow the initial rapid loss of permeability due to physical aging to occur. The thickness of each membrane was measured with a micrometer to be in the range of 65 to 75 µm. At least two membranes were tested for each experimental condition to confirm the reproducibility.

The membrane density ($\rho$) was determined by the buoyancy technique using a XS205 DualRange balance (Mettler Toledo, Australia) with maximum 0.06% error. The density was based on the difference in weight of membrane samples in air ($m_{\text{air}}$) and in n-hexane ($m_{\text{hexane}}$) at room condition (22 ± 1$^{o}$C) (Eq. 5.1). The density ($\rho_{\text{hexane}}$) of *n*-hexane (Chem-supply, Australia, 95%) was 0.655 g/ml as measured by a calibrated pycnometer.

$$\rho = \frac{m_{\text{air}}}{m_{\text{air}} - m_{\text{hexane}}} \rho_{\text{hexane}} \qquad \text{(Eq. 5.1)}$$

### 5.2.2. Gas permeation measurement

A variable volume constant pressure (VVCP) gas permeation apparatus was utilised to measure the permeability of gas mixtures through CTA membranes across the pressure range from 100 to 900 kPa gauge and temperature range from 22 to 80$^{o}$C. The gas permeation set-up has been reported in previous studies [23, 42, 269]. The $H_2S$ mixed gas (1000ppm $H_2S$ in balance $N_2$, Coregas Australia) was fed into the feed side of the permeation cell with stage cut less than 0.2%. A sweep gas of absolute helium (99.99% purity, Coregas Australia) at 1 atm absolute pressure flowed across the permeate side of the membrane cell at 35 ml/min and was directed to a gas chromatograph (490 micro GC, Agilent technologies Australia) for concentration analysis. The GC was calibrated against pure $N_2$ and a mixure of 1000 ppm $H_2S$ in $N_2$ to generate the calibration curve.

For measuring the permeability of individual gases (He (99.99% purity, Coregas Australia), $CH_4$ (99.9% purity, Coregas Australia) and $CO_2$ (99.5% purity, BOC Australia), a constant volume - variable pressure (CVVP) gas permeation apparatus was used. The gas permeation rig was operated at 35$^{o}$C and the setup was also as reported in previous studies [59, 269]. The membrane with an effective area of 10.75 cm$^2$ was installed into the permeation cell and placed under a vacuum overnight prior to the gas permeation measurement. The gas permeation coefficient, *P* (Barrer or $10^{-10}$ cm$^3$(STP).cm/cm$^2$.s.cmHg), was determined from the slope of the pressure versus time curve, under steady state conditions.

### 5.2.3. Static long-term aging of CTA in glycol solutions and $H_2S$

The long term impact of ethylene glycol (MEG, 99.8% purity - anhydrous, Sigma Aldrich Inc., America) and triethylene glycol (TEG, 99% purity – 0.1% water, Chemsupply, Australia) on the CTA membranes was determined by immersing the membranes into pure glycol solutions, separately at ambient conditions (22 ± 2$^o$C) for up to 2000 h (80 days). The solutions were stored in glass containers and kept inside a desiccator to prevent exposure to moisture. The water content of the glycol solutions was regularly determined by a volumetric Karl Fischer titrator (915 KF Ti-Touch, Metrohm AG Switzerland) to ensure the glycol concentration remained above 99.0%, which is similar to the concentration of lean glycol in industrial dehydrators [18]. Membrane samples were removed regularly to test the sorption uptake and the pure gas permeability in a "wet" state.

To determine the sorption uptake, the membrane was removed from the solution and excess liquid droplets on the membrane surfaces removed by wiping with a tissue. The membranes were then weighed to record the mass uptake ($m_t$). The total glycol uptake was calculated via Eq 5.2 where $m_o$ is the original mass of the membrane and $m_\infty$ the value at equilibrium sorption.

$$Glycol\ uptake\ (\%) = \frac{m_\infty - m_o}{m_o} \text{ x } 100 \qquad \text{(Eq. 5.2)}$$

Some "wet" membrane samples were also immersed in methanol (MeOH, 99.8% purity – 0.1% water, Chemsupply Australia) for 168 hours (1 week) to extract the glycol from the membrane structure. The washed membranes were removed from the MeOH solution and dried by vacuum overnight before testing the gas permeation in this "dry" state. To confirm the extraction efficiency of MeOH, thermogravimetric analysis was conducted (TGA 209 F1 Libra®, Netzsch Australia).

Fresh CTA membranes were also aged in pure methanol at ambient conditions for up to 550 hours. The wet membranes were removed from the solution and dried in vacuum overnight to evaporate all methanol before testing.

Similarly, the long-term impact of $H_2S$ on the performance of CTA membranes was conducted by placing dense membranes in a sealed chamber at room temperature (22 ± 2$^o$C). The chamber was evacuated and then filled with the experimental gases (1000ppm $H_2S$ in balance $N_2$ or pure $N_2$) to 750 kPa absolute pressure. After a specified aging period of up to 7200 hours (300 days), the membranes were removed and the permeability recorded. The chamber was evacuated for around 5 minutes to remove the toxic gases before opening and removing the membranes.

Differential scanning calorimetry (DSC) was used to determine the glass transition temperature ($T_g$) of original and "wet" state CTA using a differential scanning calorimeter DSC 8500 with a DSC high pressure cell addendum (Perkin Elmer, Australia). The heating rate was 20$^o$C/min, from 22$^o$C to 250$^o$C, under 1600 kPa nitrogen pressure to prevent glycol evaporation. The $T_g$ was determined by the centre point of the endothermic transition. The result for MEG was compared to the Fox equation for ideal mixtures (Eq. 5.3) [270, 271].

$$\frac{1}{T_g} = \frac{w_1}{T_{g1}} + \frac{w_1}{T_{g2}} \qquad \text{(Eq. 5.3)}$$

where $w_1$, $T_{g1}$, $w_2$, $T_{g2}$ are the weight fraction and glass transition temperature in Kelvin of CTA and glycol, respectively. The Tg of pure CTA was taken as 190 ± 5$^o$C [272] while that of MEG was -118$^o$C [106]. It was not possible to find the glass transition temperature for pure TEG.

Wide angle X-ray diffraction (WAXD) analysis was conducted to study the impact of glycols on the crystallinity of the CTA polymer. A D8 Advance Diffractometer (Bruker, Germany) was used to analyse the membranes over a 2θ range from $5^o$ to $35^o$ at a rate of $0.02^o$ every 5 seconds with a Ni-filtered $CuK_\alpha$ radiation source, 30mA and 40kV. Bragg's equation was applied to calculate the mean distance, *d*-spacing, between polymer chains (Eq. 5.4),

$$\lambda = 2d \sin\theta \qquad \text{(Eq. 5.4)}$$

Where $\lambda$ is the radiation wavelength (1.54 Å) and $\theta$ is the incident angle.

## 5.3. RESULTS AND DISCUSSION

### 5.3.1. Sorption Uptake of glycol liquids in Cellulose Triacetate

The sorption uptake of both MEG and TEG (**Figure 5.1)** shows a sigmoidal shape which indicates that while the glycols initially swell the CTA membrane by Fickian diffusion, polymer relaxation or plasticisation occurs as the solute concentration increases [8, 93, 106, 273]. The transition from Fickian diffusion to non-Fickian polymer relaxation occurs at roughly 30 hours of exposure of these 70µm membranes to the solution. It should be noted that the transition time would be of the order of seconds for commercial membranes where the active layer is of the order of a hundred nanometers in thickness.

The equilibrium solubilities of the two penetrants are summarised in **Table 5.1.** The solubility of the glycols is greater for TEG than MEG by mass (**Figure 5.1**). However, comparison on a molar basis indicates that the CTA membrane accommodates similar amounts of both glycols.

**Table 5.1:** Solubility of glycols in the CTA membrane

| Liquids | | MEG | TEG |
|---|---|---|---|
| Molecular Weight (g/mol) | | 62.1 | 150.2 |
| Solubility | wt % | 18.8 ± 0.4 | 37.7 ± 0.7 |
| | mol/100g polymer | 0.30 ± 0.006 | 0.25 ± 0.005 |

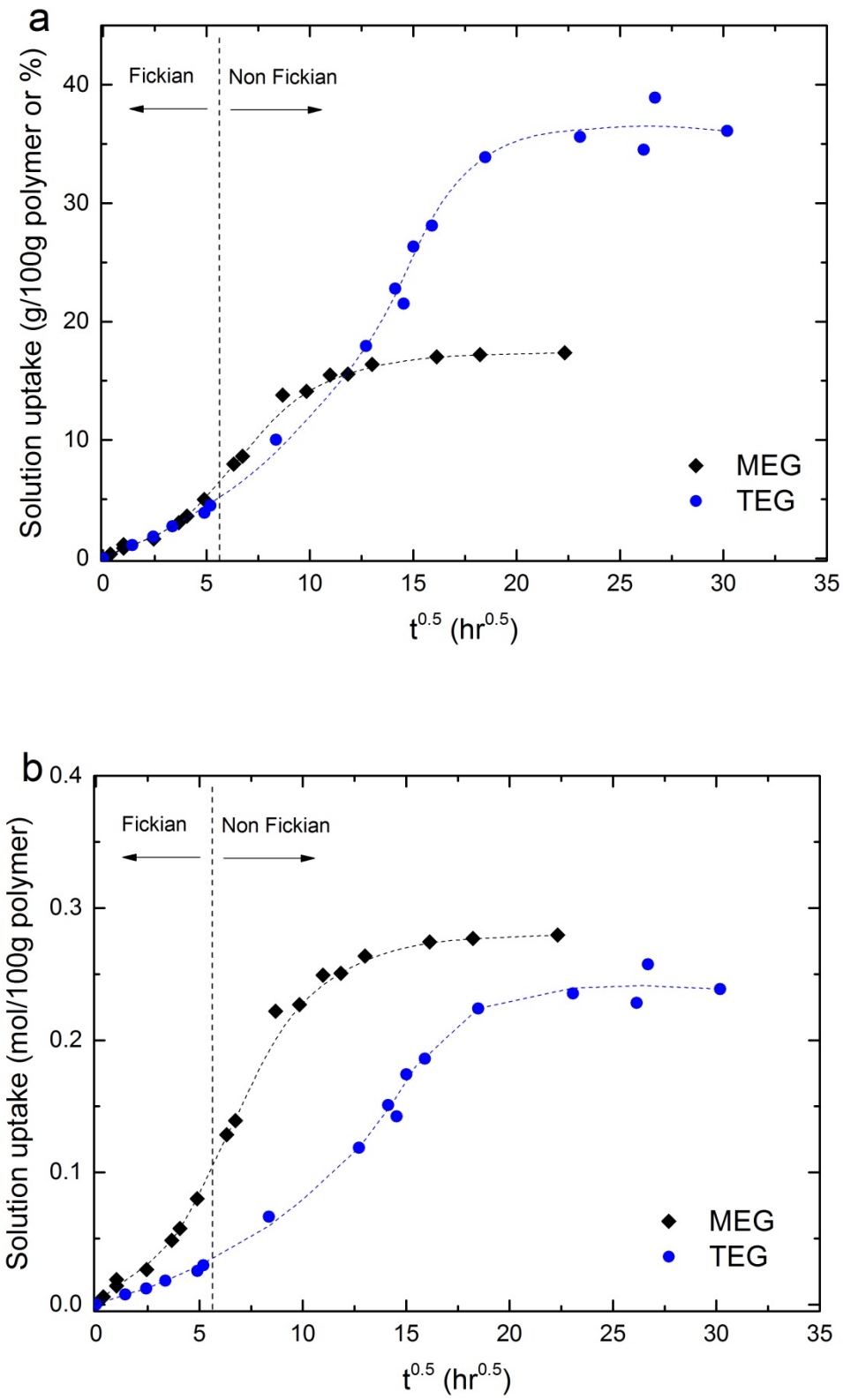


**Figure 5.1** The sorption kinetics of ethylene glycol (MEG) and triethylene glycol (TEG) solutions in a CTA membrane (70µm thickness) at 22$^{o}$C: (a) mass basis and (b) molar basis. The dashed lines are added to guide the eye.

### 5.3.2. Impact of glycol liquids on CTA membrane performance

#### 5.3.2.1. The impact of methanol on CTA membrane in glycol extraction step

The impact of these glycols on CTA membrane performance was determined by testing the permeation of pure He and $CH_4$ through the original fresh membranes, the "wet" membranes (after absorbing glycols for a specified time) and the "dry" membranes (after removal of the glycols). As the saturation partial pressures of the glycols are relatively low (11 Pa for MEG and <1 Pa for TEG at 20°C [17, 18]), the removal of the glycols from "wet" CTA membranes was not possible by simple drying, but was instead conducted by solvent exchange with methanol prior to drying. Thermogravimetric analysis for the "dry" CTA confirmed that both glycols and methanol were removed totally by this solvent exchange.

The selection of methanol as a glycol solvent was based on Hildebrand and Hansen solubility theory, which suggests that effective solubilisation is favoured between components having least heat of sorption per unit volume [274, 275]. The approach defines three solubility parameters, a hydrogen bonding component ($\delta_h$), a polar interaction component ($\delta_p$) and a nonpolar interaction component ($\delta_d$). The Hansen solubility parameter is the square root of the sum of squares of these components [274, 276] with similar values indicating good mutual solubility. Specifically, the mutual solubility of components is strongest when the radius of interaction between the Hansen solubility parameters is smallest [274] (**Table 5.2**). As a result, the solubility of methanol – glycol mixtures system is more favoured than methanol – CTA or glycol – CTA mixtures. A solubility envelope for CTA polymer was constructed by Klein et al. (1975) based on Hansen's approach [277] and the liquids utilised in this study are outside the boundary. This further indicates that there will be no dissolution of the CTA polymer into the solutions during the sorption and aging experiments.

**Table 5.2:** Hildebrand and Hansen solubility parameters of different liquids and CTA [274, 276]

| Components | MEG | MeOH | TEG | CTA |
|---|---|---|---|---|
| Hydrogen bonding components ($\delta_h$), $MPa^{0.5}$ | 26.0 | 22.3 | 18.6 | 11.0 |
| Polar interaction components ($\delta_p$), $MPa^{0.5}$ | 11.0 | 12.3 | 12.5 | 12.7 |
| Nonpolar interaction components ($\delta_d$), $MPa^{0.5}$ | 17.0 | 15.1 | 16.0 | 18.6 |
| Hansen solubility parameter* ($\delta$), $MPa^{0.5}$ | 33.7 | 29.6 | 27.5 | 25.1 |
| Radius of interaction** between components and CTA ($R_{component - CTA}$), $MPa^{0.5}$ | 15.4 | 13.3 | 9.2 | 0 |
| Radius of interaction** between components and methanol ($R_{component - methanol}$), $MPa^{0.5}$ | 5.5 | 0 | 4.1 | 13.3 |

* Hansen solubility parameter $\delta = \sqrt{{\delta_h}^2 + {\delta_p}^2 + {\delta_d}^2}$, $MPa^{0.5}$

** Radius of interaction: $R_{ij} = \sqrt{({}^i\delta_h - {}^j\delta_h)^2 + ({}^i\delta_p - {}^j\delta_p)^2 + 4({}^i\delta_d - {}^j\delta_d)^2}$, $MPa^{0.5}$

#### 5.3.2.2. The impact of glycols on CTA membrane performance

The impact of contact with MEG on the permeability of He and $CH_4$ through the CTA membrane is shown in **Figure 5.2**. Over the first 30 hours, the "wet" membranes showed a significant decline in both helium and methane permeability (**Figure 5.3a**). This decline is too great to be caused by physical aging alone (see Section 3.4). Rather, it suggests that the absorbed MEG reduces either the diffusivity and solubility of penetrants through the membrane matrix [12]. As helium is not strongly adsorbed to any polymer, it is unlikely that the decline in He permeability results from competitive sorption. This suggests that the decline in this permeability occurs through a 'pore blocking' mechanism [12, 96], where MEG molecules occupy the free volume and block pathways through the polymer structure, causing a loss of diffusivity. This phenomenon is often referred to as "anti-plasticisation" [15]. Conversely, the loss in $CH_4$ permeability could occur through either competitive sorption or pore blocking, or a combination of both.

A dramatic increase in $CH_4$ permeation occurs at the 30 hour mark, which is a time roughly comparable to that observed earlier for the onset of polymer relaxation (**Figure 5.1)**. However, no comparable impact is observed in He permeability. Polymer relaxation will impact the larger molecule ($CH_4$) significantly more than He, as larger free volume elements are created [54, 160]. It is also likely that $CH_4$ can more readily penetrate the glycol-rich regions that form in the membrane, as it has significantly greater solubility in MEG than Helium (see **Table 5.3**). Therefore, the MEG continues to obstruct the diffusion of He in the "wet" membrane, resulting in a continuous decline of He permeability (**Figure 5.2a)**. Consequently, the He/$CH_4$ gas selectivity also drops significantly once polymer relaxation commences (**Figure 5.2c)**.

**Table 5.3:** Henry's Law coefficient (MPa) for gases in glycols at 298K

| | **$CO_2$** | **$CH_4$** | **He** |
|---|---|---|---|
| MEG | 78.5[a][278] | 968.6[a][278]<br>656.3[279, 280] | 6775[279] |
| TEG | 11.95[281]<br>10.5[b] | 179.2[281]<br>177[b] | 1410[b] |

[a]Data is at 303K

[b]Calculated using the Glycol package within Aspen HYSYS V8.6 at 1 Bar total pressure.

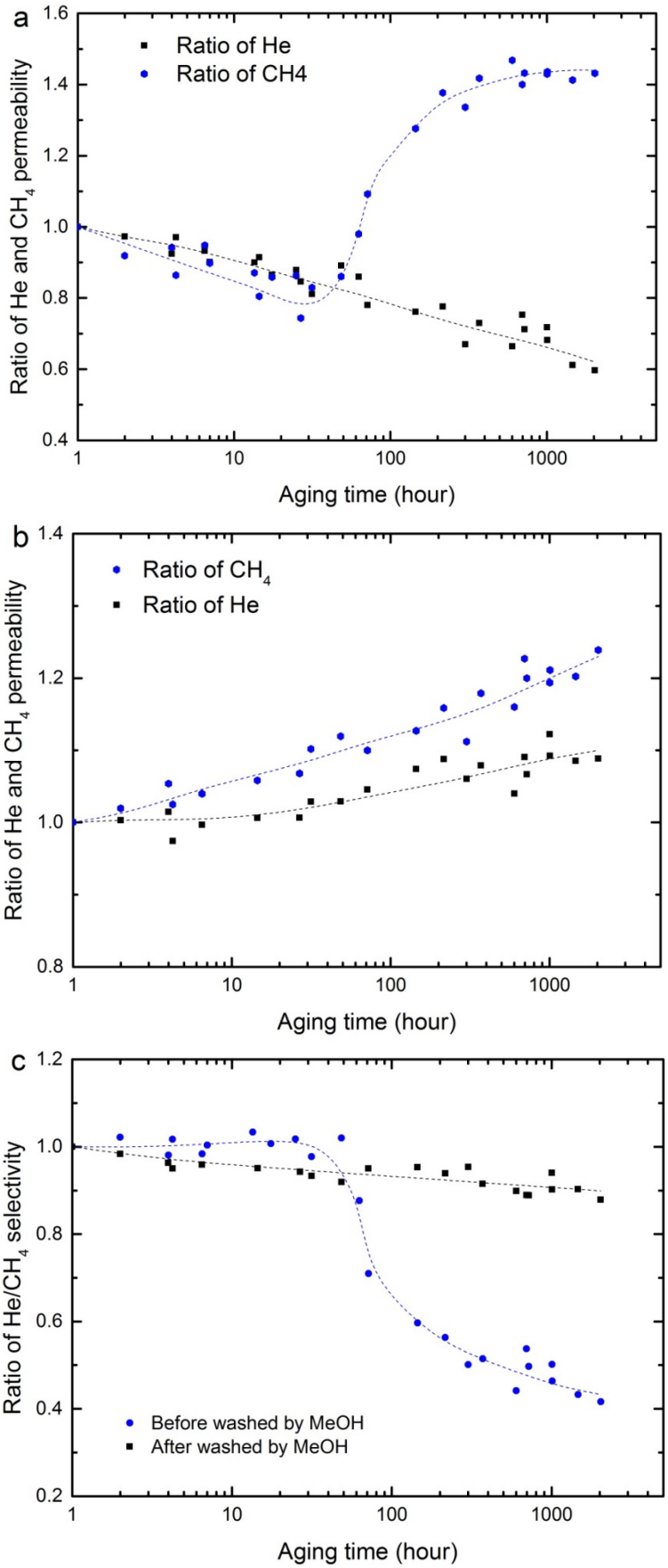


**Figure 5.2** Change in permeability of He and $CH_4$ as time progresses relative to the original fresh CTA membranes at 35°C and 750 kPa feed pressure: (a) aged in ethylene glycol (MEG) solution at 22°C; (b) aged in MEG and washed by methanol for 168 hours at 22°C; and (c) He/$CH_4$ selectivity. The dashed lines are added to guide the eye.

After extracting MEG from the CTA membrane with methanol, both He and $CH_4$ show a small, but significant increase in permeability with time (**Figure 5.2b**). The increase is greater for the larger $CH_4$ than for He, again suggesting that it is caused by a net increase in free volume. This implies that even after the complete removal of the glycol, the polymer structure is not fully recovered from the effects of polymer relaxation. This result is also supported by a decrease in the density of the "dry" membranes after aging in glycols in comparison with fresh CTA (**Table 5.4**).

**Table 5.4:** Density of CTA membranes before and after aging in glycol and methanol.

| Glycols | Density (g/ml) | | |
|---|---|---|---|
| | **"Dry" CTA membranes after aging in glycols for 2000 hours** | **"Dry" CTA membranes after aging in methanol for 550 hours** | **Original CTA membranes** |
| MEG | 1.277 ± 0.008 | 1.297 ± 0.003 | 1.299 ± 0.001 |
| TEG | 1.270 ± 0.010 | | |

Control membranes aged in methanol alone did not show the same increase in permeability with time (**Figure 5.4**). Methanol has been reported to plasticise CTA in a pervaporation study [282], but the effect is minimal here, relative to the greater impact of the glycol exposure.

The impact of TEG on the CTA membrane was also studied as shown in **Figure 5.3**. The trends in performance are identical, with the magnitude significantly greater. This reflects the higher solubility of TEG in CTA (**Table 5.1**) and in turn, the higher solubility of $CH_4$ in TEG (**Table 5.3**).

It is notable that the permeability enhancement after removal of the glycols with methanol is quite similar, at around 10% over the aging period. The plasticising effect of TEG on the CTA membrane is likely stronger than MEG given the lower Hansen radius of interaction for the TEG – CTA pair (**Table 5.2**). However, there are fewer moles of TEG absorbed per unit of CTA membrane and the solution uptake is slower (**Table 5.1b**), meaning that the effective plasticising molar concentration is lower at any given time during the aging process. All these aspects result in the similar plasticisation effect of TEG and MEG on the CTA membrane.

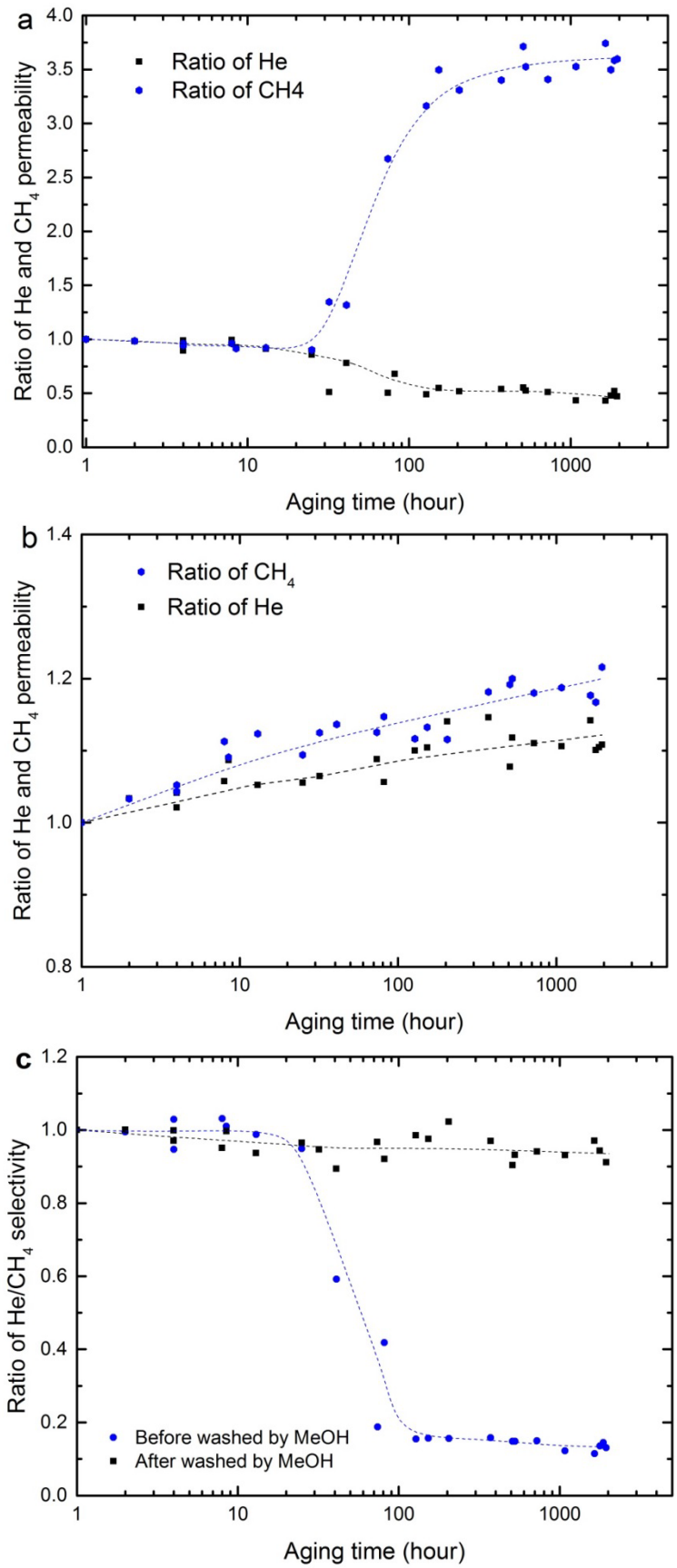


**Figure 5.3** Change in permeability of He and $CH_4$ as time progresses relative to the fresh CTA membranes at 35$^o$C and 750 kPa feed pressure: (a) aged in triethylene glycol (TEG) solution at 22$^o$C; (b) aged in TEG and washed by methanol for 168 hours at 22$^o$C; and (c) He/$CH_4$ selectivity. The dashed lines are added to guide the eye.

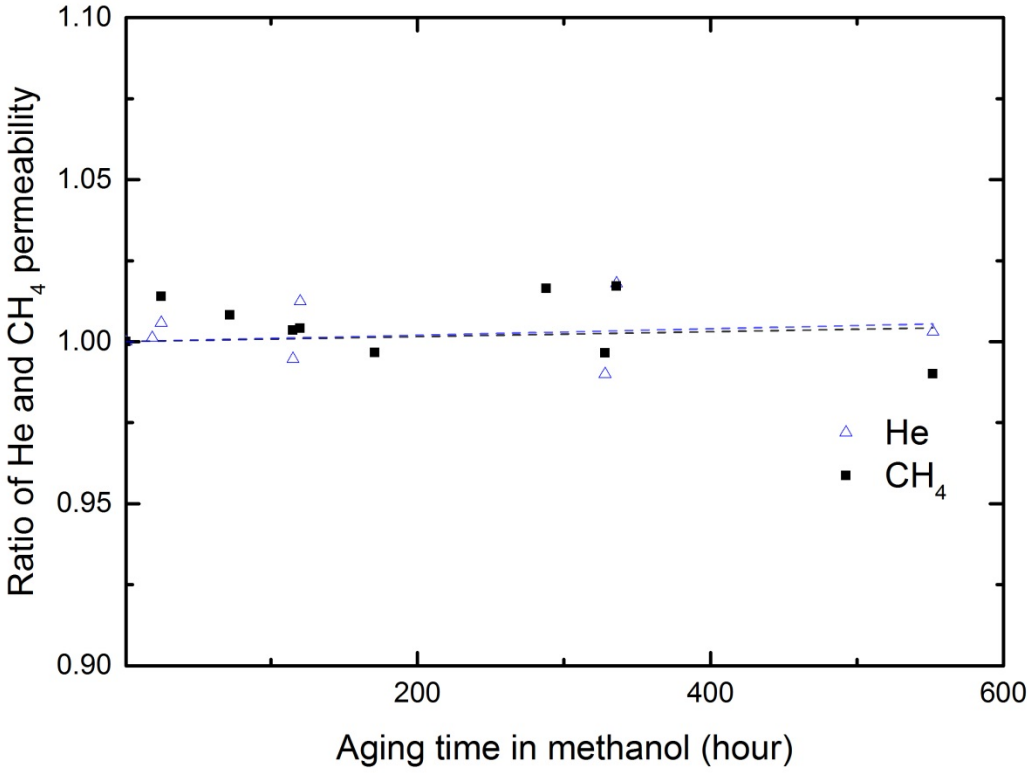


**Figure 5.4** Change in permeability of He and $CH_4$ as time progresses relative to the fresh CTA membranes at 35°C, 750 kPa feed pressure after aging in methanol solution

### 5.3.2.3. The impact of glycols on $CO_2$ permeation through CTA membrane

The impacts of MEG and TEG on the permeation of $CO_2$ were also studied by testing the permeability of $CO_2$ with 200 kPa feed pressure (**Table 5.5**). The feed pressure was selected to prevent $CO_2$ – induced plasticisation which can occur between 500 – 1200 kPa $CO_2$ pressure depending upon the degree of acetylation, membrane thickness and testing temperature [72, 166, 168]. In general, the impact of glycols on $CO_2$ permeation is similar to the impact on $CH_4$. The absorption of glycols into membranes enhanced the permeability of $CO_2$ and the impact was more significant in membranes aged in TEG. In addition, the $CO_2$ permeability through the "dry" membranes was also enhanced due to the residual plasticisation arising from the glycol absorption.

The permeability ratio for $CO_2$ in both the "wet" and "dry" membranes was lower than that of $CH_4$. This reflects the smaller kinetic diameter of $CO_2$ [54], which means that its diffusivity is less affected by polymer relaxation. Further, while $CO_2$ has a stronger affinity for glycol than $CH_4$ (see **Table 5.3**), the ratio of the Henry's Law coefficients suggests a solubility selectivity for $CO_2/CH_4$ in pure glycol of around 12. This selectivity ratio is lower than that observed for pure CTA (28 ± 1), suggesting that movement through glycol rich regions of the membrane is less $CO_2$ selective than in the dry polymer. Consequently, the selectivity of $CO_2/CH_4$ declines slightly in the 'wet' polymer.

**Table 5.5:** The impact of glycols on the change of permeabilities (*P*) of $CH_4$ and $CO_2$ and $CO_2/CH_4$ gas selectivity ($\alpha_{CO_2/CH_4}$) of CTA membrane at 35°C.

| | | Ratio of $P(CO_2)^*$ | Ratio of $P(CH_4)^*$ | Ratio of $\alpha_{CO_2/CH_4}$ |
|---|---|---|---|---|
| "Wet" CTA** | Aged in MEG | 1.34 ± 0.04 | 1.44 ± 0.02 | 0.93 ± 0.03 |
| | Aged in TEG | 2.88 ± 0.1 | 3.61 ± 0.04 | 0.80 ± 0.03 |
| "Dry" CTA | Aged in MEG | 1.19 ± 0.01 | 1.21 ± 0.04 | 0.98 ± 0.04 |
| | Aged in TEG | 1.18 ± 0.04 | 1.20 ± 0.02 | 0.99 ± 0.04 |

* Permeability relative to the fresh CTA membrane i.e. $P(CO_2)$ = 7.20 ± 0.2 barrer, $P(CH_4)$ = 0.254 ± 0.007 barrer and $\alpha_{CO2/CH4}$ = 28 ± 1. The permeation pressures were 200 kPa absolute for pure $CO_2$ and 750 kPa absolute for pure $CH_4$.

** The aging times for CTA membranes in MEG was 1440 hours in comparison with 2000 hours in case of TEG

### 5.3.2.4. The impact of glycols on the glass transition temperature and crystallinity

The dramatic changes in solubility and permeability that occur after 30 hours of immersion of the membranes in glycol are clearly caused by polymer relaxation of some type. Such changes are also often related to a fall in the glass transition temperature as the composition of the membrane material changes, so that this dramatic shift also correlates to a transition from a glassy to a rubbery state. However, DSC measurements of the glycol-swollen membranes suggest that the transition to a rubbery state does not occur under the conditions shown here, as this temperature does not fall to the experimental temperature (22 - 35°C) (**Figure 5.5**).

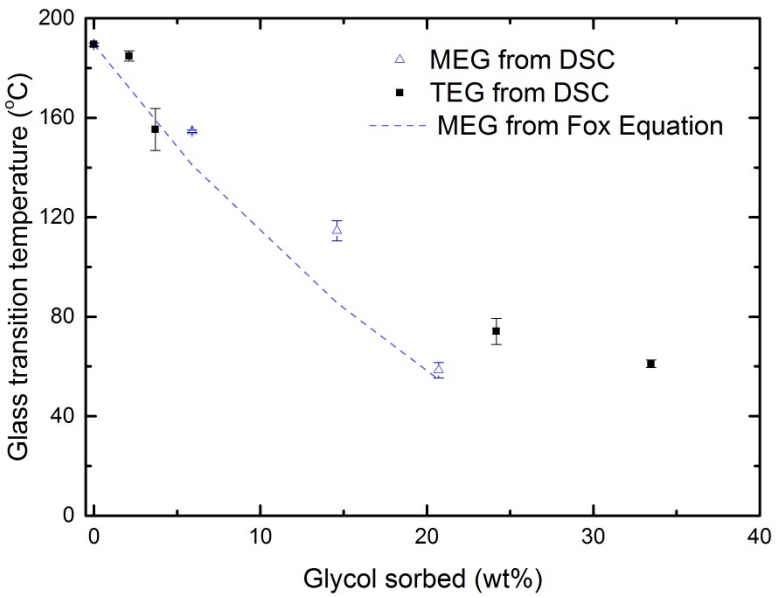


**Figure 5.5** The change in glass transition temperature as glycol is sorbed into CTA, measured by dynamic scanning calorimetry (DSC) and calculated from the Fox Equation ($T_g$ of MEG is -118°C [272]).

It is well known that the CTA polymer can contain areas of crystallinity. WAXD analysis was consistent with these reports with two typical semi-crystalline peaks observed at $2\theta \sim 10^{o}$ [12, 235, 236] and $17^{o}$ [237, 238], and a van der Waals amorphous halo at $20 - 21^{o}$ [236, 237, 239, 240] in the fresh CTA membrane (**Figure 5.6**). By using an X-ray diffraction deconvolution method [283], the crystallinity index of this membrane was calculated to be 56 ± 5% which is compatible with the literature [40]. However, exposure of this membrane to liquid MEG and TEG resulted in an increase in the relative intensity of the amorphous peak in comparison with the crystalline peaks of the WAXD scan. The crystallinity index dropped to 47 ± 3% when aged in MEG and 32 ± 6% when aged in TEG. This increase in the amorphous nature of the "wet" membrane arises from the polymer relaxation described above. The greater decrease in crystallinity caused by TEG is also consistent with the stronger affinity of TEG to CTA than MEG (as regards **Table 5.2**).

After removal of the glycols by methanol, the relative intensity of the amorphous peak reduced again and the crystallinity index recovered to 53 ± 1% and 50 ± 3% for membranes aged in MEG and TEG, respectively. Again, the lower crystallinity of "dry" membranes in comparison with fresh CTA confirmed the partial recovery of the polymer as concluded in section 5.3.2.2.

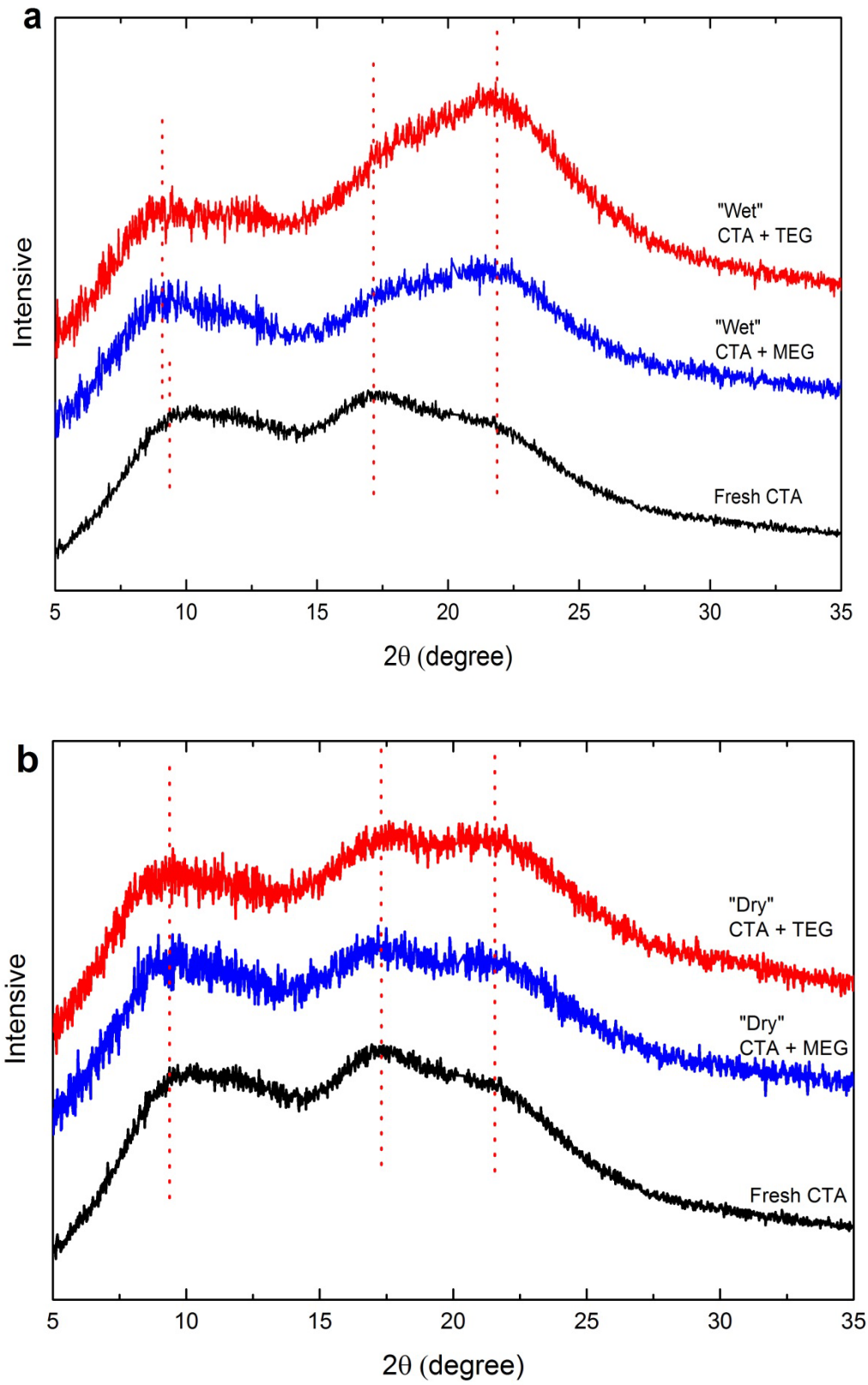


**Figure 5.6** Wide angle X-Ray Diffraction (WAXD) results for CTA membranes when (a) saturated with glycols; and (b) after washing with methanol; in comparison with a fresh CTA membrane.

### 5.3.3. Permeation of hydrogen sulphide on CTA membrane

The permeability of $H_2S$ and $N_2$ through the CTA membranes was studied at different feed pressures (**Figure 5.7**). For the temperature range 22 – 80°C, the permeability of $H_2S$ was independent of the feed gas pressure within the error margins, and was between 4.7 and 10.2 Barrer, rising with temperature. The $H_2S$ permeability coefficient measured in this investigation is higher than reported in the literature (summarised in **Table 5.6**). The deviation may due to the difference in degree of acetyl substitution (DS). A lower degree of acetyl substitution results in less free volume within the membrane matrix and thus a lower diffusivity [40]. However, it also probably reflects the lower $H_2S$ partial pressures applied in this study. At these lower partial pressures the Langmuir component of the sorption isotherm is more dominant, resulting in higher solubility [96, 176]. There was no evidence of $H_2S$ plasticization of the CTA membrane, as indicated in **Figure 5.7a**. To the best knowledge of the authors, only one study has observed plasticisation of CTA by $H_2S$, and this was at a much higher partial pressure of 69 kPa [13, 14, 210].

**Table 5.6:** The permeability of hydrogen sulphide in cellulose acetate membranes.

| Polymer | Feed gas conditions | Partial pressure (kPa) | Temperature (°C) | $P_{H2S}$ (Barrer) | Reference |
|---|---|---|---|---|---|
| CTA (DS 2.9) | 1000 ppm $H_2S$ in balance $N_2$ | 0.1 – 0.8 | 22 | 4.7 ± 0.2 | This study |
| | | | 35 | 5.9 ± 0.1 | |
| | | | 50 | 8.1 ± 0.1 | |
| | | | 80 | 10.2 ± 0.1 | |
| CA film (DS not stated) | $H_2S$ 99.9% purity | 94 | 0 | 1.3 | [211] |
| | | 94 | 15 | 2.0 | |
| | | 23 – 94 | 30 | 3.3 ± 0.2 | |
| | | 98 | 45 | 4.5 | |
| | | 93 | 60 | 6.1 | |
| Cellulose diacetate (DS 2.45) | $H_2S/CO_2/CH_4$ (6/29/65) | 60 | 35 | 2.1 | [205] |
| Asymetric CA (DS not stated) | $H_2S/CO_2/CH_4$ | 68.9 | 25 | 4.17 | [10] |

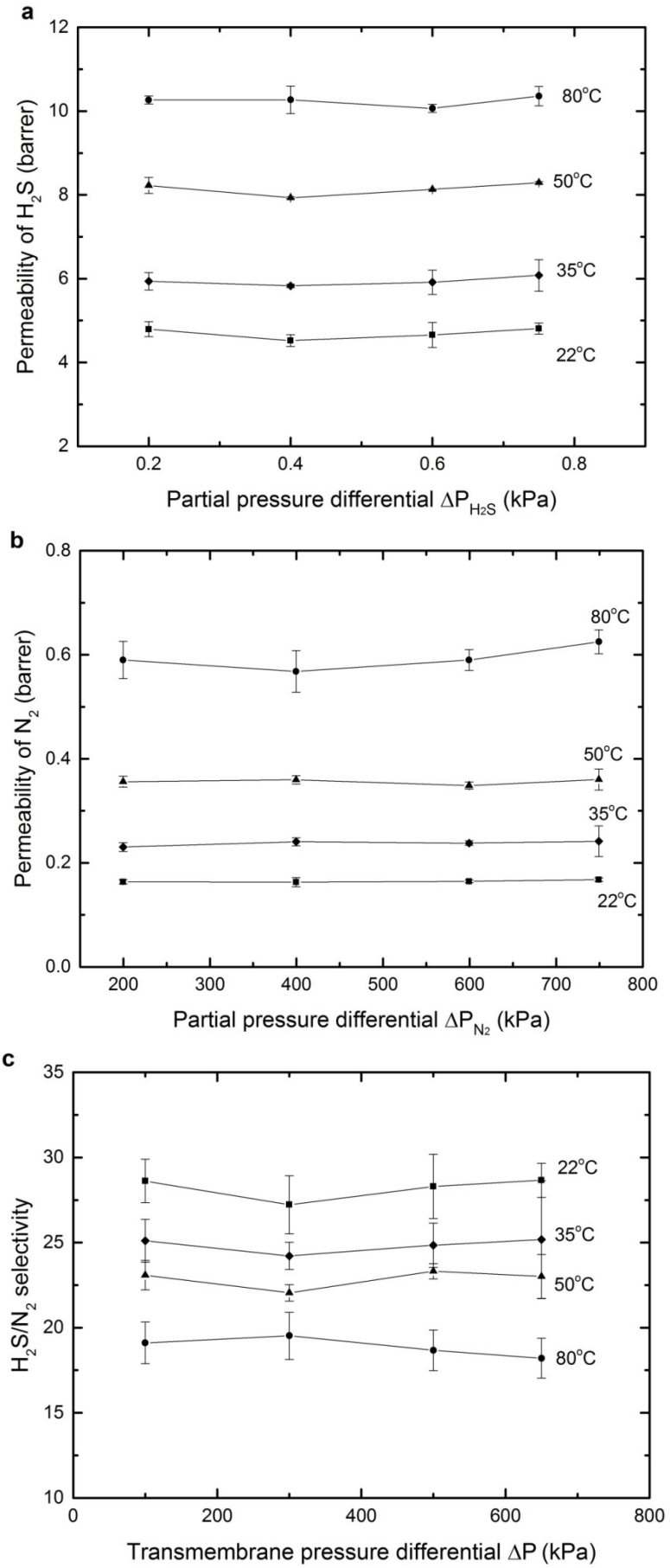


**Figure 5.7** Gas permeability in CTA membranes with a feed gas of 1000ppm $H_2S$ in balance $N_2$ (a) permeability of $H_2S$; (b) permeability of $N_2$; (c) $H_2S/N_2$ gas selectivity.

The permeability of nitrogen was also independent of feed pressure, indicative of standard behaviour for this inert gas (**Figure 5.7b**). The $H_2S/N_2$ gas selectivity (**Figure 5.7c**) showed the favourable permeation of $H_2S$ in the membrane over $N_2$. Similar phenomena has been observed when introducing $H_2S$ – $N_2$ gases through other glassy polymers, such as polysulfone and cyclic perfluoroether [204]. This is due to the higher critical temperature of $H_2S$ which results in greater solubility.

The permeability coefficients of $H_2S$ and $N_2$ at a zero partial pressure differential ($\Delta p_i \rightarrow 0$ kPa) were extrapolated from the data presented in **Figure 5.7**. This enables the activation energy for permeation ($E_P$) to be determined (**Table 5.7)**. The positive values of $E_P$ for all gas species in this investigation suggest that diffusivity is dominant over solubility [117]. Furthermore, the activation energy is higher for the gas species with lower critical temperature (lower gas sorption), again reflecting a lower heat of sorption [48, 57].

**Table 5.7:** Activation energy for permeation in CTA membrane at zero pressure.

| | **$CH_4$*** | **$N_2$** | **$CO_2$*** | **$H_2S$** | **$SO_2$*** |
|---|---|---|---|---|---|
| Kinetic diameter (Å) [51] | 3.80 | 3.64 | 3.30** | 3.60 | 3.60 |
| Critical temperature (K) [263] | 190.6 | 126.2 | 304.2 | 373.2 | 430.8 |
| Activation energy for permeation, $E_p$ (kJ/mol) | 18.6 ± 0.2 | 18.7 ± 2 | 8.5 ± 0.7 | 10.1 ± 0.7 | 7.3 ± 0.7 |

* The permeability of methane and carbon dioxide were reported in a previous study [269]

** Some recent studies argue that the kinetic diameter of $CO_2$ relevant to diffusion could be larger at 3.43 – 3.63 Å [54, 121, 265]

Heilman et al. reported an activation energy for $H_2S$ permeation of 19 kJ/mol [211] when operating with a feed pressure of 94 kPa in comparison with 10.1 kJ/mol calculated in this study (**Figure 5.8**). Again, the deviation may be due to differences in both degree of acetylation and operating pressures.

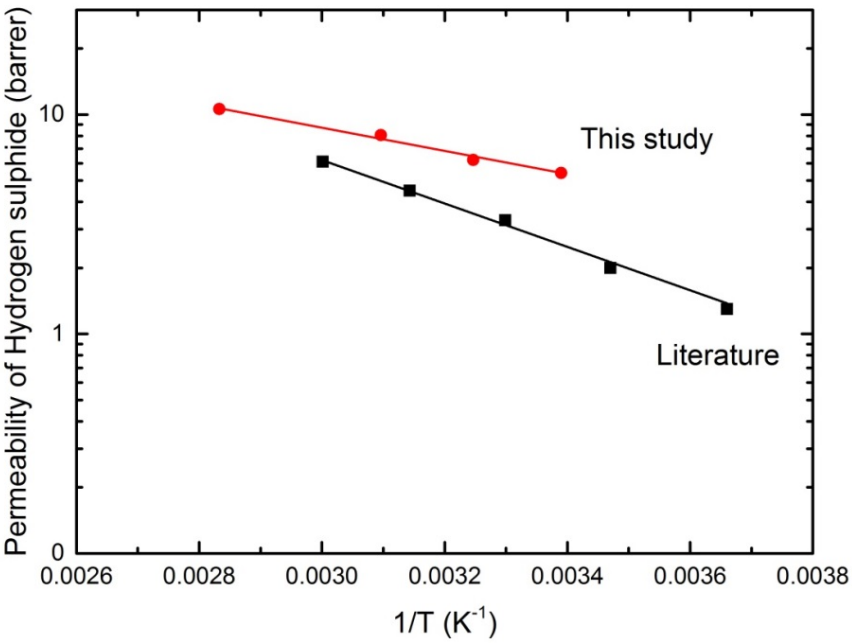


**Figure 5.8** The permeability coefficients of $H_2S$ as a function of temperature at zero partial pressure differential (this study) and 94 kPa (Heilman et al.[211])

### 5.3.4. Long-term aging of CTA membrane in $H_2S$

The long-term impact of $H_2S$ on CTA membranes was studied by aging the membranes separately in 1000 ppm $H_2S$ in balance $N_2$ and in pure $N_2$. After a specified aging period up to 7200 hours, the membranes were tested for the permeation of pure He and $CH_4$ at 35$^o$C and 750 kPa absolute feed pressure. To reduce the variability between membrane samples, the change of permeability and selectivity of the aged membranes as time progresses is expressed as the ratio of permeability and He/$CH_4$ selectivity of the aged membranes to the original fresh membrane (**Figure 5.9**).

Gas permeability generally falls with time due to the densification of membrane matrix as observed in **Figure 5.9a** and in other studies [117, 121, 265, 269]. As observed in section 5.3.2.2, the changes in free volume impact most the penetrant of larger kinetic diameter ($CH_4$) [117, 121, 269]. Consequently, the He/$CH_4$ selectivity is enhanced during aging as indicated in **Figure 5.9b**.

**Figure 5.9** showed that the aging process of CTA membranes was not affected by the presence of 0.75 kPa partial pressure of $H_2S$. This is consistent with the $H_2S$ permeability result in **Figure 5.7,** where no plasticisation is observed for these partial pressures of $H_2S$ on the CTA membranes at the same pressure and temperature. The partial pressure of $H_2S$ in a natural gas sweetening process is typically 0.02 – 3 kPa (assuming 30 bar operating pressure) [20], which is much lower than the plasticisation pressure for $H_2S$, observed to be up to 69 kPa in the presence of $CO_2$ [14, 210]. This result is confirmed by the present work.

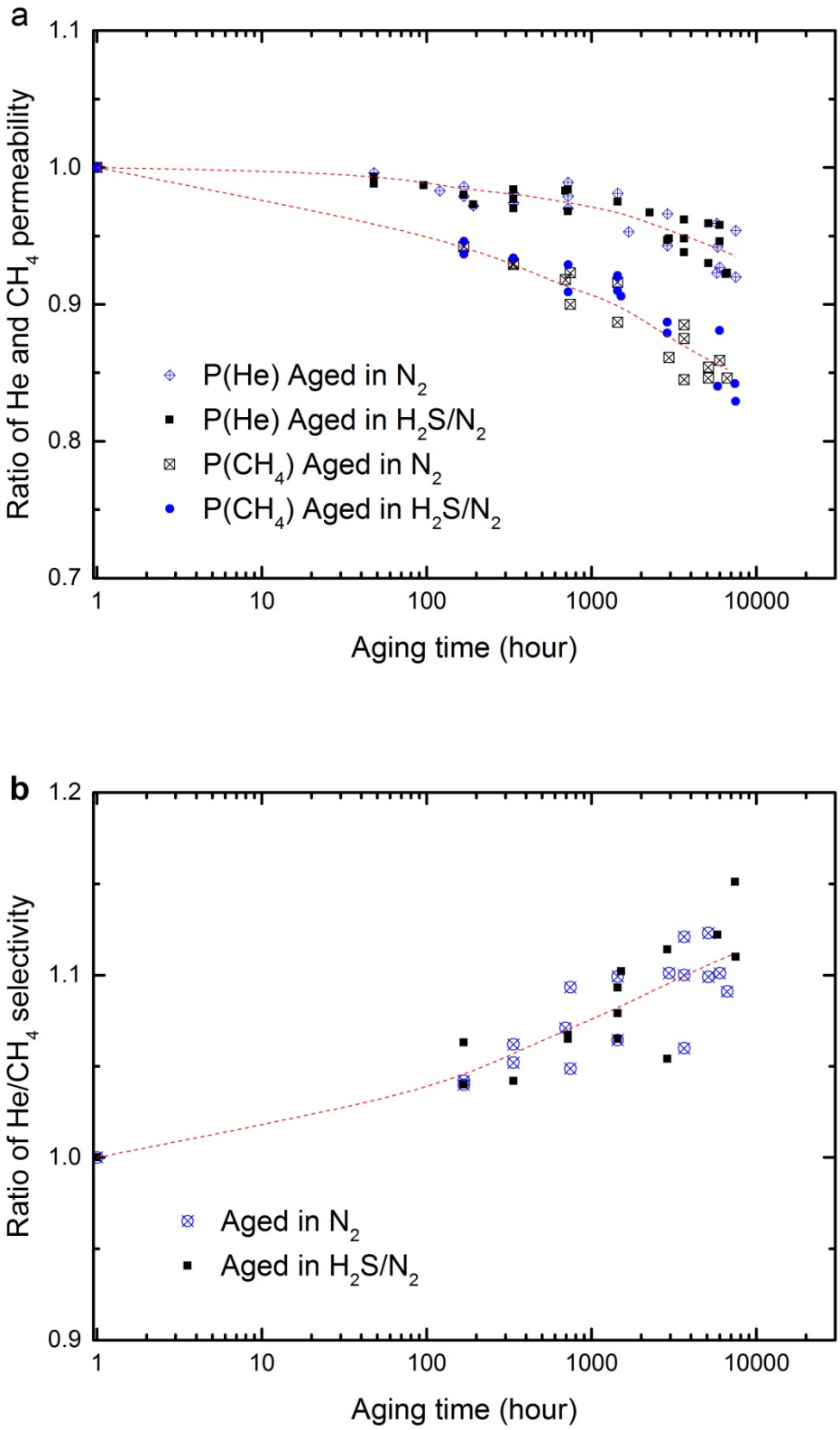


**Figure 5.9** Change in (a) permeability of He and $CH_4$ and (b) He/$CH_4$ selectivity as time progresses relative to the fresh CTA membranes at 35°C, 750 kPa after aging separately in 1000 ppm $H_2S$ in balance $N_2$ and pure $N_2$ at 750 kPa and 22 ± 2°C. The permeability of He and $CH_4$ in a fresh CTA membrane was 21.6 ± 0.2 barrer and 0.265 ± 0.009 barrer, respectively, giving an He/$CH_4$ gas selectivity at 81 ± 3. The dashed lines are added to guide the eye.

## 5.4. CONCLUSIONS

The impact of glycols on dense CTA membranes has been studied for up to 2000 hours. The absorption of ethylene glycol and triethylene glycol into the CTA membrane enhanced the permeation of $CH_4$ and $CO_2$ through the wet membranes but resulted in a gradual decline in the permeation of He. This reflected relaxation of the polymer structure. In particular, WAXD analysis confirmed that a significant loss of crystallinity occurred during exposure to these glycols, providing more accessible free volume in the structure. Methane and $CO_2$ were able to move through the glycol-rich regions within the swollen membrane, whereas these regions blocked the movement of He. It should be noted that the changes in free volume observed here, while similar in magnitude, are expected to occur much faster in the thinner active layers (<1 µm) used in industrial membrane systems [121, 126].

Importantly, the use of a methanol wash was able to reverse these effects, with only small residual swelling observed after removal of the glycol. The use of such a methanol wash may be an important mitigation strategy when glycol overflow into the membrane unit occurs in industrial practice. However, it would require careful application to prevent a collapse of the structure of the porous support layer of the membrane during methanol removal due to surface tension effects.

This study has also shown that cellulose triacetate membranes are stable upon exposure to 0.75 kPa $H_2S$ for up to 7200 hours. No plasticisation was observed after aging the membranes at 0.75 kPa $H_2S$ and 22$^{o}$C for 7200 hours. However, it should be noted that in many applications of CTA in natural gas sweetening, the $H_2S$ partial pressures are considerably higher than studied here and the onset of plasticisation cannot be discounted in such scenarios.

## 5.5. ACKNOWLEDGEMENTS

The authors would like to acknowledge the funding support for this research project from The University of Melbourne, Particulate and Fluid Processing Centre (PFPC), the Peter Cook Centre for Carbon Capture and Storage Research at the University of Melbourne and Brown Coal Innovation Australia (BCIA). The X-ray diffraction analysis was performed within the Materials Characterisation and Fabrication Platform (MCFP) at the University of Melbourne and the Victorian Node of the Australian National Fabrication Facility (ANFF). The specialist gas infrastructure was funded by the Australian Research Council (LE120100141) and by the Australian Government Education Investment fund and this support is also gratefully acknowledged.

# CHAPTER 6. THE IMPACT OF TOLUENE AND XYLENE ON THE PERFORMANCE OF CELLULOSE TRIACETATE MEMBRANES FOR NATURAL GAS SWEETENING

## 6.1. INTRODUCTION

Natural gas will become the second largest energy resource globally within the next few decades [284, 285]. Raw natural gas contains condensable hydrocarbons, acid gases and impurities that require pre-treatment to meet consumer specifications and for pipeline transport. A range of separation technologies have been commercialised for natural gas processing, with membrane gas separation commercially proven for natural gas sweetening (acidic gas removal). Cellulose triacetate (CTA) membranes are the market leaders for gas sweetening membranes, because of their low cost, durability and competitive gas separation performance [5, 6].

Condensable aromatic hydrocarbons, known as BTEX (Benzene, Toluene, Ethylbenzene and Xylene) are present in raw natural gas at concentrations ranging from 200 to 3000 ppm, dependent on the natural gas source [4, 11]. The presence of these hydrocarbons presents significant challenges. Firstly, they are toxic and thus not readily vented with the waste acid gases. Secondly, they can freeze during cryogenic separation [216]. The presence of BTEX in natural gas can also alter the gas separation performance of polymeric membranes, by competing for sorption sites with the acid gases, by blocking the gas transport pathways through the polymeric matrix or by plasticising the polymeric matrix [286]. Toluene has been shown to reduce the $CO_2$ permeability and $CO_2/CH_4$ selectivity in polyimides [9, 225, 226, 228] and amorphous perfluoropolymers [229] Polyimide membranes have also been reported to be plasticised by toluene, resulting in a significant decline in $CO_2/CH_4$ selectivity [226, 230].

Studies of the impact of BTEX on cellulose acetate based membranes are limited and focus mainly on $H_2/CH_4$ separation [11, 231, 287]. Wensley and King show that the presence of toluene (up to 2.5 kPa) or benzene (up to 8.8 kPa) reduces $H_2$ and $CH_4$ permeabilities by 10 – 15% but the $H_2/CH_4$ selectivity is increased by 10% [11, 231]. Cellulose acetate membranes used in the Cosmo Oil Refinery (Japan) for hydrogen separation were stable over a three year operating period in 1.8 – 5.2 kPa BTX but the gas permeability declined around 20% in the presence of the BTX [287].

The kinetic diameter and critical temperature of $H_2$ (2.89 Å and 33.2 K [51]) is much smaller than $CO_2$ (3.3 Å and 304.2 K [51]) and hence the impact of BTEX on $CO_2/CH_4$ separation may be quite different. Schell et al. [11] report a 10% decrease in $CO_2$ and $CH_4$ permeability in cellulose acetate membranes in the presence of 5.4 kPa BTX within a 6% $CO_2$ balance $CH_4$ gas mixture. The permeability of BTEX through cellulose acetate membranes is generally reported to be lower than methane [231] but no numerical data has been reported. To the best knowledge of the authors, there are no reports of plasticisation of cellulose acetate membranes by BTEX.

Given the significance of these aromatic hydrocarbons and the lack of literature, we present in this work a detailed study of the effect of toluene and xylene on the separation of $CO_2$ and $CH_4$ when using CTA membranes. The hydrocarbons are exposed to the CTA membrane over a range of vapor pressures representative of the BTEX concentrations that are experienced in natural gas processing. The solubility and permeability of toluene and xylene within the membranes are also reported.

The chapter was published in Journal of Membrane Science, detailed as below:

Lu, H. T.; Liu, L.; Kanehashi, S.; Scholes, C. A. and Kentish, S.E. (2018). The Impact of toluene and xylene on the performance of cellulose triacetate membranes for natural gas sweetening. Journal of Membrane Science, 555, 362-368.

THE UNIVERSITY OF MELBOURNE

# Declaration for a thesis with publication

PhD and MPhil students may include a primary research publication in their thesis in lieu of a chapter if:

- The student contributed greater than 50% of the content in the publication and is the "primary author", ie. the student was responsible primarily for the planning, execution and preparation of the work for publication
- It has been peer-reviewed and accepted for publication
- The student has approval to include the publication in their thesis from their Advisory Committee
- It is a primary publication that reports on original research conducted by the student during their enrolment
- The initial draft of the work was written by the student and any subsequent editing in response to co-authors and editors reviews was performed by the student
- The publication is not subject to any obligations or contractual agreements with a third party that would constrain its inclusion in the thesis

Students must submit this form, along with *Co-author authorisation forms* completed by each co-author, when the thesis is submitted to the Thesis Examination System: *https://tes.app.unimelb.edu.au/*. If you are including multiple publications in your thesis you will need to complete a separate form for each publication. Further information on this policy is available at: *gradresearch.unimelb.edu.au/preparing-my-thesis/thesis-with-publication*

## A. PUBLICATION DETAILS *(to be completed by the student)*

| | | |
|---|---|---|
| Full title | The Impact of toluene and xylene on the performance of cellulose triacetate membranes for natural gas sweetening | |
| Authors | Hiep Thuan Lu, Liang Liu, Shinji Kanehashi, Colin Scholes, Sandra Kentish | |
| Student's contribution (%) | 65 | |
| Journal or book name | Journal of Membrane Science | |
| Volume/page numbers | 555 (2018) 362-368 | |
| Status | ☐ Accepted and In press ☒ Published | Date accepted/ published 18 Mar 2018 |

## B. STUDENT'S DECLARATION

I declare that the publication above meets the requirements to be included in the thesis

| Student's name | Student's signature | Date *(dd/mm/yy)* |
|---|---|---|
| Hiep Thuan Lu | | 10/05/2018 |

## C. PRINCIPAL SUPERVISOR'S DECLARATION

I declare that:

- the information above is accurate
- The advisory committee has met and agreed to the inclusion of this publication in the student's thesis
- All of the co-authors of the publication have reviewed the above information and have agreed to its veracity
- 'Co-Author Authorisation' forms for each co-author are attached.

| Supervisor's name | Supervisor's signature | Date *(dd/mm/yy)* |
|---|---|---|
| Sandra Kentish | | 10/05/18 |

THE UNIVERSITY OF MELBOURNE

# Co-author authorisation form

All co-authors must complete this form. By signing below co-authors agree to the listed publication being included in the student's thesis and that the student contributed greater than 50% of the content of the publication and is the "primary author" ie. the student was responsible primarily for the planning, execution and preparation of the work for publication.

In cases where all members of a large consortium are listed as authors of a publication, only those that actively collaborated with the student on material contained within the thesis should complete this form. This form is to be used in conjunction with the *Declaration for a thesis with publication form*.

Students must submit this form, along with the *Declaration for thesis with publication form*, when the thesis is submitted to the Thesis Examination System: *https://tes.app.unimelb.edu.au/*

Further information on this policy and the requirements is available at:
*gradresearch.unimelb.edu.au/preparing-my-thesis/thesis-with-publication*

## A. PUBLICATION DETAILS *(to be completed by the student)*

| | | |
|---|---|---|
| Full title | The Impact of toluene and xylene on the performance of cellulose triacetate membranes for natural gas sweetening | |
| Authors | Hiep Thuan Lu, Liang Liu, Shinji Kanehashi, Colin Scholes, Sandra Kentish | |
| Student's contribution (%) | 65 | |
| Journal or book name | Journal of Membrane Science | |
| Volume/page numbers | 555 (2018) 362-368 | |
| Status | ☐ Accepted and In-press ☒ Published | Date accepted/published 18 Mar 2018 |

## B. CO-AUTHOR'S DECLARATION *(to be completed by the collaborator)*

I authorise the inclusion of this publication in the student's thesis and certify that:

- the declaration made by the student on the *Declaration for a thesis with publication form* correctly reflects the extent of the student's contribution to this work;
- the student contributed greater than 50% of the content of the publication and is the "primary author" ie. the student was responsible primarily for the planning, execution and preparation of the work for publication.

| Co-author's name | Co-author's signature | Date *(dd/mm/yy)* |
|---|---|---|
| Colin Scholes | | 10/05/2018 |

THE UNIVERSITY OF MELBOURNE

# Co-author authorisation form

All co-authors must complete this form. By signing below co-authors agree to the listed publication being included in the student's thesis and that the student contributed greater than 50% of the content of the publication and is the "primary author" ie. the student was responsible primarily for the planning, execution and preparation of the work for publication.

In cases where all members of a large consortium are listed as authors of a publication, only those that actively collaborated with the student on material contained within the thesis should complete this form. This form is to be used in conjunction with the *Declaration for a thesis with publication form*.

Students must submit this form, along with the *Declaration for thesis with publication form*, when the thesis is submitted to the Thesis Examination System: *https://tes.app.unimelb.edu.au/*

Further information on this policy and the requirements is available at:
*gradresearch.unimelb.edu.au/preparing-my-thesis/thesis-with-publication*

## A. PUBLICATION DETAILS *(to be completed by the student)*

| | | |
|---|---|---|
| Full title | The Impact of toluene and xylene on the performance of cellulose triacetate membranes for natural gas sweetening | |
| Authors | Hiep Thuan Lu, Liang Liu, Shinji Kanehashi, Colin Scholes, Sandra Kentish | |
| Student's contribution (%) | 65 | |
| Journal or book name | Journal of Membrane Science | |
| Volume/page numbers | 555 (2018) 362-368 | |
| Status | ☐ Accepted and In-press ☒ Published | Date accepted/published 18 Mar 2018 |

## B. CO-AUTHOR'S DECLARATION *(to be completed by the collaborator)*

I authorise the inclusion of this publication in the student's thesis and certify that:

- the declaration made by the student on the *Declaration for a thesis with publication form* correctly reflects the extent of the student's contribution to this work;
- the student contributed greater than 50% of the content of the publication and is the "primary author" ie. the student was responsible primarily for the planning, execution and preparation of the work for publication.

| Co-author's name | Co-author's signature | Date *(dd/mm/yy)* |
|---|---|---|
| Liang Liu | Liang Liu | 10/05/2018 |

THE UNIVERSITY OF MELBOURNE

# Co-author authorisation form

All co-authors must complete this form. By signing below co-authors agree to the listed publication being included in the student's thesis and that the student contributed greater than 50% of the content of the publication and is the "primary author" ie. the student was responsible primarily for the planning, execution and preparation of the work for publication.

In cases where all members of a large consortium are listed as authors of a publication, only those that actively collaborated with the student on material contained within the thesis should complete this form. This form is to be used in conjunction with the *Declaration for a thesis with publication form*.

Students must submit this form, along with the *Declaration for thesis with publication form*, when the thesis is submitted to the Thesis Examination System: *https://tes.app.unimelb.edu.au/*

Further information on this policy and the requirements is available at:
*gradresearch.unimelb.edu.au/preparing-my-thesis/thesis-with-publication*

## A. PUBLICATION DETAILS *(to be completed by the student)*

| | | |
|---|---|---|
| Full title | The Impact of toluene and xylene on the performance of cellulose triacetate membranes for natural gas sweetening | |
| Authors | Hiep Thuan Lu, Liang Liu, Shinji Kanehashi, Colin Scholes, Sandra Kentish | |
| Student's contribution (%) | 65 | |
| Journal or book name | Journal of Membrane Science | |
| Volume/page numbers | 555 (2018) 362-368 | |
| Status | ☐ Accepted and In-press ☒ Published | Date accepted/published 18 Mar 2018 |

## B. CO-AUTHOR'S DECLARATION *(to be completed by the collaborator)*

I authorise the inclusion of this publication in the student's thesis and certify that:

- the declaration made by the student on the *Declaration for a thesis with publication form* correctly reflects the extent of the student's contribution to this work;
- the student contributed greater than 50% of the content of the publication and is the "primary author" ie. the student was responsible primarily for the planning, execution and preparation of the work for publication.

| Co-author's name | Co-author's signature | Date *(dd/mm/yy)* |
|---|---|---|
| Shinji Kanehashi | Kanehashi | 10/05/2018 |

## 6.2. EXPERIMENTAL

### 6.2.1. Membrane Fabrication

The cellulose triacetate (CTA) polymer utilised in this study was kindly supplied by Cellulose Company – Daicel Corporation (Japan) with 61.6% degree of substitution. Dense membrane fabrication followed a typical solvent casting method as described in **section 3.2.4**. A 1 wt% solution was prepared by dissolving the dried CTA powder into dichloromethane (ChemSupply, Australia). The solution was filtered and cast into glass petri dishes, which were then kept covered for solvent evaporation. After 24 hours, the membranes were peeled from the petri dishes and annealed in a vacuum oven for 24 hours at 35$^{o}$C and another 24 hours at 100$^{o}$C. The annealed CTA membranes were kept in a desiccator for 14 days prior to utilisation in sorption and permeation studies to minimise the impact of the initial physical aging of the glassy membranes [110, 119]. The membrane density and crystallinity were 1.297 ± 0.003 (g/cm$^3$) and 56 ± 5 (%) respectively [288].

Thin film composite (TFC) membranes were also fabricated by a spin coating method that is also well described in the literature [37, 121, 269]. A 4 wt% CTA in dichloromethane solution was coated onto a porous hydrophilic polytetrafluoroethylene (PTFE) membrane with 0.2 µm nominal pore size (Omnipore$^{TM}$, Merck Millipore, Australia). The PTFE support was initially wetted by water to minimise the penetration of solution into the pores [37]. The spinning rate was 1500 rpm in 20 s. The membrane thickness was determined by Scanning Electron Microscopy (FEI Quanta 200 ESEM FEG).and was in the range of 10 – 15 µm.

### 6.2.2. Sorption Measurements

The sorption of toluene (>99.5% purity, ChemSupply, Australia) and xylene (>99.0% purity, ChemSupply Australia) in CTA was studied by immersing dense membrane samples into the hydrocarbon liquid at 35$^{o}$C. The mass of the dried membrane ($m_o$) was initially weighed by a XS205 DualRange balance (Mettler Toledo, Australia) with maximum 0.02% error. After immersing into the hydrocarbon solution for a specified time ($t$), the membrane was removed, the excess liquid droplets were wiped from the membrane surfaces and the mass uptake ($m_t$) recorded by weighing. The membrane was determined to be at equilibrium ($m_\infty$) when the mass change was less than 0.1 wt% over a 24 hour timespan. At least two membranes were tested in each experiment to confirm the reproducibility. The sorption kinetics is described here by a simple heuristic equation (Eq. 2.22) [104, 105]. In addition, the hydrocarbon uptake was calculated via (Eq. 6.1).

$$\text{Hydrocarbon uptake (\%)} = \frac{m_t - m_o}{m_o} \text{ x } 100 \qquad \text{(Eq. 6.1)}$$

A gravimetric sorption analyser, GHP – FS, equipped with a Cahn D-200 microbalance (VTI Scientific Instruments, USA) as described previously [242], was utilised to determine the solubility of toluene and xylene vapour. Equilibrium at each vapour pressure increment was determined as a mass change of less than 0.003 wt% over 15 minutes (toluene) and 90 minutes (xylene), respectively.

The solubility of $CO_2$ and $CH_4$ in CTA was determined using a high pressure gravimetric sorption analyser (Belsorp, MicrotracBel Corporation, Japan). The membrane sample was installed into the sample chamber and the chamber was evacuated overnight. The experiment gas was then fed into the chamber with incremental increases in gas pressure from 50 kPa to 38000 kPa absolute pressure.

Sorption equilibrium at each pressure increment was determined as a mass change of less than 0.2 µg over two hours, following which the mass of swollen membrane was recorded.

### 6.2.3. Permeability Measurements

The permeabilities of gas mixtures were measured by a variable volume constant pressure (VVCP) gas permeation apparatus. The hydrocarbon vapour was introduced into the feed gas via a bubbling arrangement, as reported previously [23, 42, 229]. Either 10% $CO_2$ in balance $CH_4$ mixed gas (99.999% purity, Coregas, Australia) or pure $CO_2$ (99.9% purity, BOC, Australia) at 7.5 bar was introduced to the bubbler to carry the hydrocarbon vapour to the feed side of the membrane holder. The permeate stream was swept by helium (99.99% purity, Coregas, Australia) at 1 bar absolute pressure to a gas chromatograph equipped with thermal conductivity detectors (490 micro GC, Agilent technologies, Australia) for concentration analysis. The hydrocarbon activity was regulated by changing the temperature of the bubbler [23]. The GC was calibrated against five different partial pressures of toluene and xylene by passing helium directly through the bubbler and to the GC. The xylene utilised in this study was composed of 75 mol% of the *o*- and *m*-xylene isomers as determined by the gas chromatography trace. In addition, the GC was also calibrated against pure $CO_2$, pure $CH_4$ (99.95% purity, Coregas, Australia) and the 10% $CO_2$ in balance $CH_4$ gas mixture.

## 6.3. RESULTS AND DISCUSSION

### 6.3.1. Solubility of Toluene and Xylene in Cellulose Triacetate

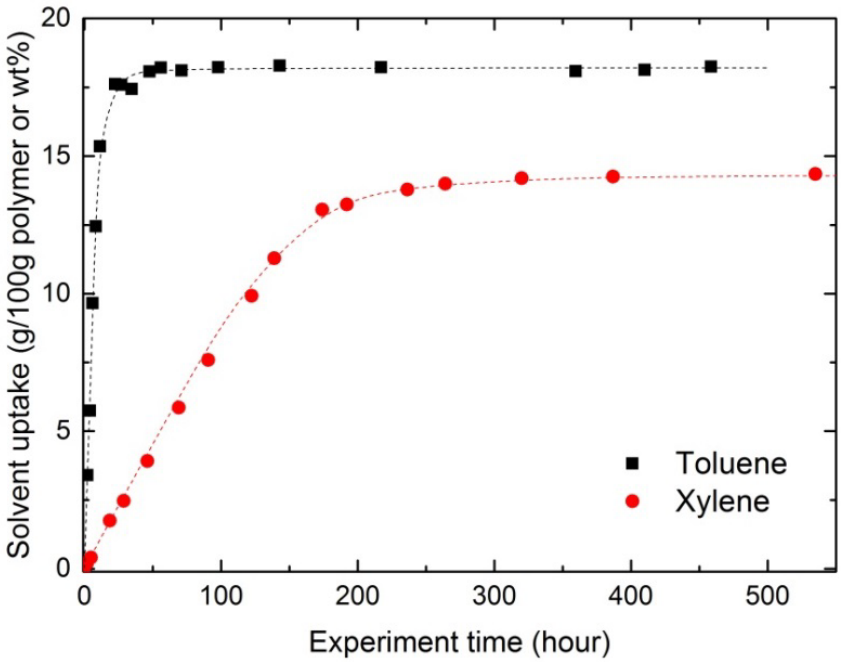


**Figure 6.1** The sorption of liquid toluene and xylene into a CTA membrane (62 ± 2µm thickness) at 35°C. The dashed lines are added to guide the eye.

Both xylene and toluene absorb initially into CTA in a manner that is linear with time (**Figure 6.1**). The calculated exponent *n* (Eq. 2.22) for toluene and xylene during this initial period was 0.99 ± 0.04 and 0.98 ± 0.03, respectively. This is referred to as Case II diffusion [103, 108, 289] and occurs when a region of non-Fickian swelling moves through the polymer as a function of time. Such behaviour has been reported in several hydrocarbon – glassy polymers system such as toluene

– poly(vinyl chloride) [290], toluene - polystyrene [291] and dichloromethane – cellulose acetate [292].

The sorption rate of toluene is greater than xylene at the same CTA membrane thickness (**Figure 6.1**) because of the smaller kinetic diameter of toluene (**Table 6.1)**. This is also evident from the greater value of the k constant calculated from (Eq. 2.22) for toluene (0.00143 ± 0.0004 $s^{-1}$) versus xylene (0.000127 ± 0.00002 $s^{-1}$). On a molar basis, the equilibrium solubility of xylene is slightly greater than toluene (**Table 6.1**), due to its higher critical temperature. [274-276].

**Table 6.1:** The properties of toluene and xylene and their solubility in CTA membranes

| | | **Toluene** | **Xylene** | **$CH_4$** | **$CO_2$** |
|---|---|---|---|---|---|
| Molecular Weight (g/mol) | | 92.14 | 106.16 | 16.04 | 44.01 |
| Kinetic diameter (Å) [49-52] | | 5.85 | 5.85 (*p*-xylene) 6.80 (*o*- & *m*-xylene) | 3.80 | 3.30 |
| Critical temperature (K) [52, 53] | | 384 | 411 – 417 | 191 | 304 |
| Solubility | wt %[1] | 19.0 ± 0.6 | 14.1 ± 0.2 | | |
| | mol/100g polymer[1] | 0.207 ± 0.006 | 0.133 ± 0.002 | | |
| | ($cm^3$(STP)/$cm^3$ polymer.bar)[2] | 620 | 663 | 0.39 | 5.3 |

[1] Solubility of liquid toluene and xylene (1.0 vapor activity) at 35°C
[2] Solubility of gases recorded at 35°C and 5.4 kPa for toluene, 1.6 kPa for xylene (0.8 vapor activity), at 6.75 Bar for methane and 0.75 Bar for carbon dioxide.

### 6.3.2. Gas and Vapour Sorption Isotherm in Cellulose Triacetate Membranes

The gas sorption isotherms of $CO_2$ and $CH_4$ in CTA are plotted in **Figure 6.2**, and correspond well with the data of Puleo, Paul and Kelley [40]. The nonlinear concave shapes of the isotherms are described well by the dual-mode sorption model (Eq. 2.11) [27-29, 40, 160]. The parameters fitted to Eq. 2.11 are summarised in **Table 6.2**. The deviations in these parameters for methane compared with previous work [40] are due to inaccuracies in the data fitting approach at these low concentrations.

**Table 6.2:** The dual-mode sorption parameters for $CH_4$ and $CO_2$ in CTA membranes at 35°C

| Penetrant | $k_D$ ($cm^3$(STP)/$cm^3$.atm) | $C'_H$ ($cm^3$(STP)/$cm^3$) | b ($atm^{-1}$) | Reference |
|---|---|---|---|---|
| $CO_2$ | 1.75 ± 0.06 | 20 ± 3 | 0.21 ± 0.05 | This study |
| $CH_4$ | 0.12 ± 0.02 | 8 ± 2 | 0.042 ± 0.008 | |
| $CO_2$ | 1.647 | 19.63 | 0.291 | [40] |
| $CH_4$ | 0.184* | 3.15 | 0.134 | |

* The study of Puleo, Paul and Kelley quoted a $k_D$ value of 1.84 [40] but the authors believe this to be a typographical error, as the data calculated from this value do not match with results presented in the paper.

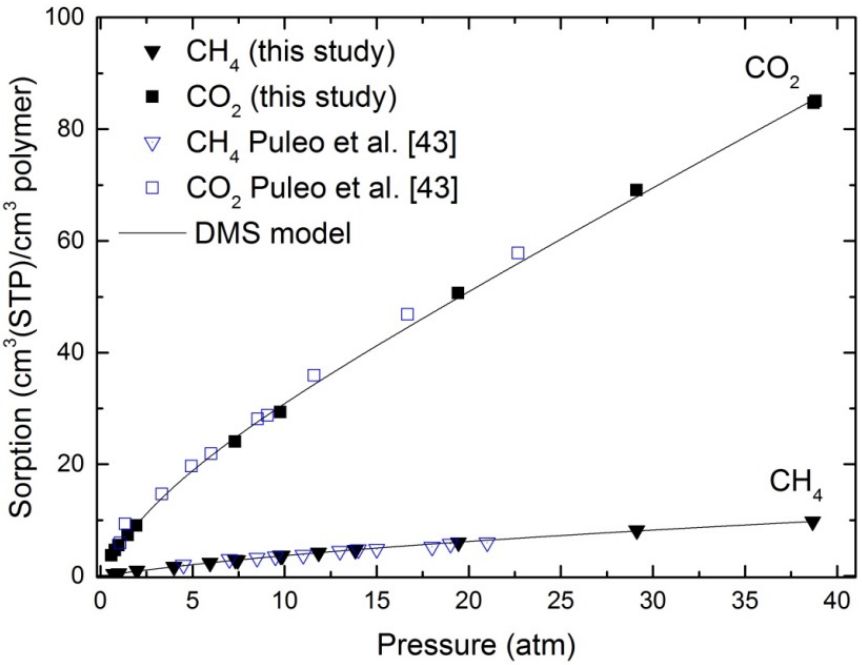


**Figure 6.2** The sorption isotherms of $CO_2$ and $CH_4$ in CTA at 35°C

The vapour sorption isotherms of toluene and xylene in CTA membranes are provided in **Figure 6.3.** The isotherms are S-shaped [75-77], which has also been observed for the sorption of methanol, acetone, dimethyl carbonate and methyl acetate into CTA [77]. Specifically, dual mode sorption is observed at low vapour activity (**Figure 6.3a**), which reflects the sorption of hydrocarbons into the macrovoids of the polymer matrix [229]. At vapour activity greater than 0.5, there is a rapid increase in sorption (**Figure 6.3b**) which is associated with swelling and plasticisation of the polymer [77, 79]. The sorption of toluene is stronger than xylene at the same vapour activity due to the difference in partial pressure of toluene in comparison with xylene at the specified activity. However, when plotted as a function of the vapour pressure, the sorption of xylene and toluene is identical for a vapour pressure up to 0.65 kPa (**Figure 6.3c**). The polymer is plasticised by xylene at this vapour pressure while toluene plasticised the membranes at 3.4 kPa.

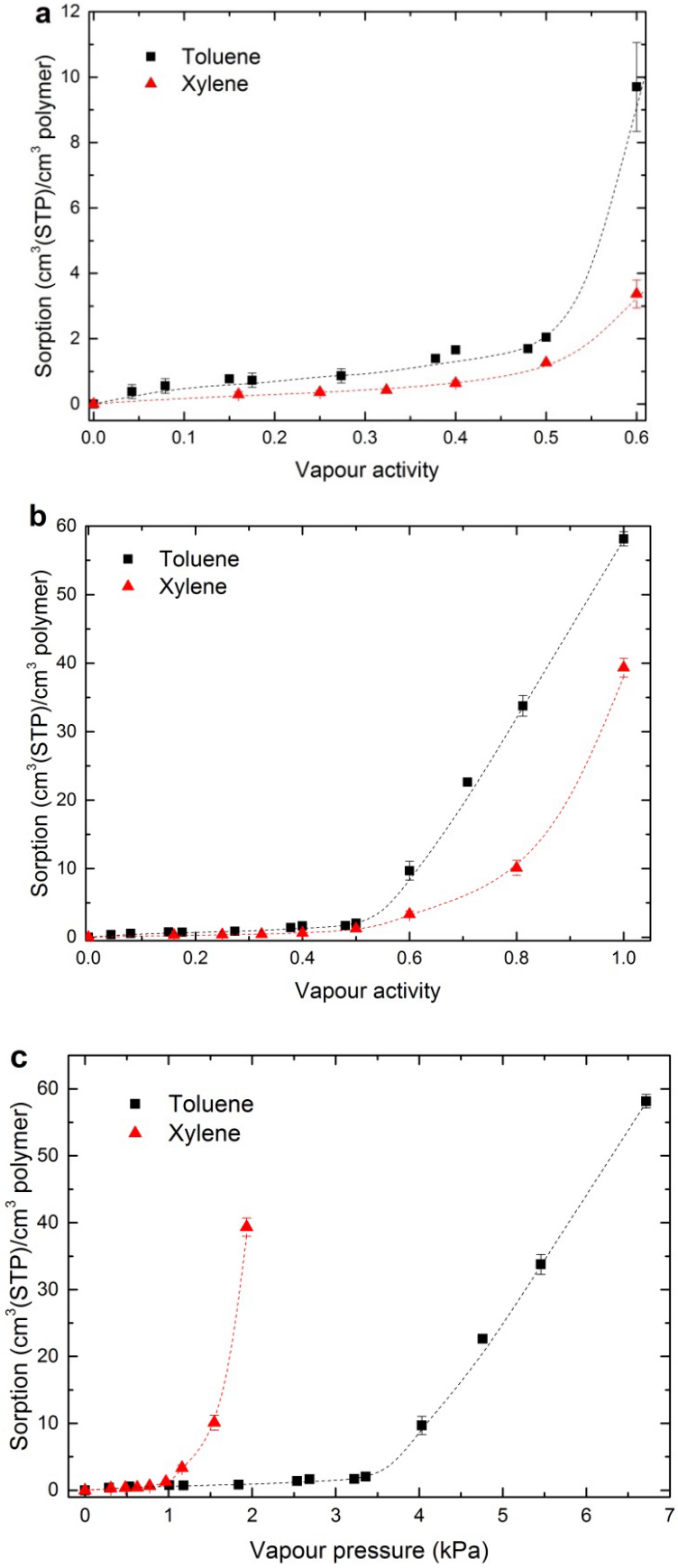


**Figure 6.3** The solubility of toluene and xylene in CTA at 35°C: (a) at 0.0 – 0.6 vapour activity; (b) across the full range of vapour activities; (c) as a function of vapour pressure rather than activity.

### 6.3.3. The Impact of Toluene and Xylene on $CO_2/CH_4$ Separation at Low $CO_2$ Pressure

The impact of toluene vapour on the permeability of CTA in a mixture of 10% $CO_2$ in methane is shown in **Figure 6.4**. The permeability of $CO_2$ and $CH_4$ fell by 10% and 12%, respectively, as toluene partial pressure increased to 3.5 kPa (0.5 vapour activity). This is consistent with the literature where a decline in $CO_2$ permeability of 10% was also observed when the toluene vapour pressure was varied in the range of 0.3 – 2.5 kPa [11, 231]. The decline in gas permeability may be partly attributed to "pore blocking" [12, 96], also known as "anti-plasticisation" [15, 16, 286]. This is where hydrocarbons molecules fill the free volume and block the penetrant transport pathways in the polymer. The fall in permeability may also relate to the competitive sorption of toluene, displacing $CO_2$ and $CH_4$ from sorption sites. Conversely, once the vapour pressure exceeds 3.5 kPa, there is a rapid increase in permeability. This corresponds to toluene-induced plasticisation, consistent with the sorption isotherm (**Figure 6.3b**). Interestingly, the presence of toluene vapour has no effect on the selectivity of $CO_2/CH_4$ in CTA membrane, which is consistent with previous literature reports [11].

The impact of xylene on $CO_2/CH_4$ separation in CTA membrane is provided in **Figure 6.5**. Similar to toluene, the presence of xylene in the feed gas reduced the permeability of $CO_2$ and $CH_4$ slightly, with a decrease of 12 to 14% in gas permeability at 1.0 kPa xylene partial pressure (0.5 vapour activity). However, at higher xylene vapour pressures, up to 1.6 kPa (0.8 activity), the $CO_2$ and $CH_4$ permeabilities remains unchanged with plasticisation not clearly evident. This probably reflects the much smaller increase in solubility for the xylene penetrant at 0.8 activity relative to toluene (see **Figure 6.3a)**.

As a comparison, the negative impacts of aromatic hydrocarbons on polyimide membranes are much more significant, with a decline of 90% in gas permeabilities reported in the literature [286] and a 30 – 50% drop in $CO_2/CH_4$ selectivity [4, 230]. The resistance of cellulose triacetate membrane to hydrocarbon contaminants, relative to other polymeric membranes, is attributed to the chemical structure of the polymer and the different solubility of the hydrocarbons within the membrane film.

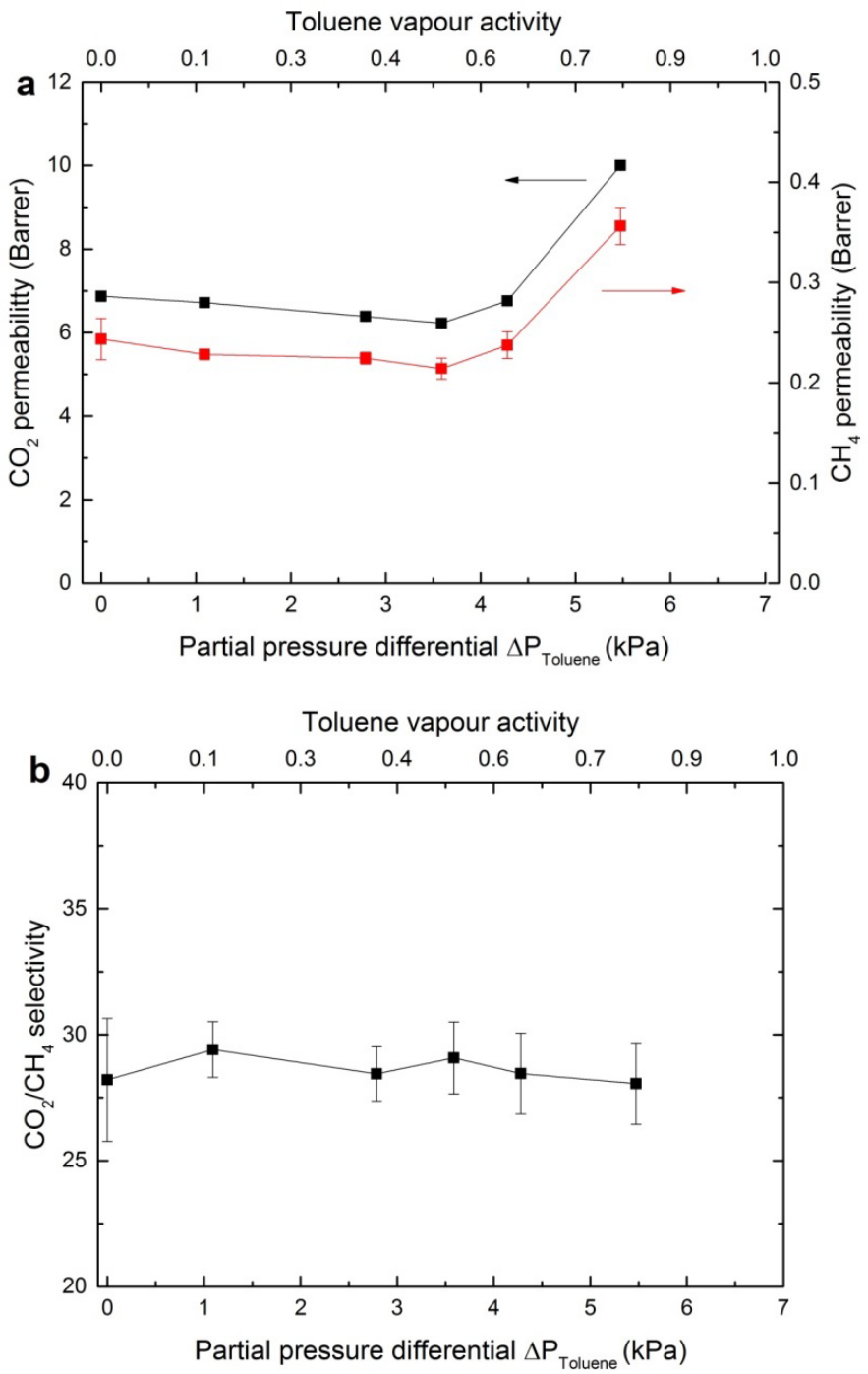


**Figure 6.4** The permeability of $CO_2$ and $CH_4$ (a) and $CO_2/CH_4$ selectivity (b) through CTA membranes exposed to toluene at various vapour pressures, for 10% $CO_2/CH_4$ mixed gas feed at 7.5 bar and 35$^{o}$C

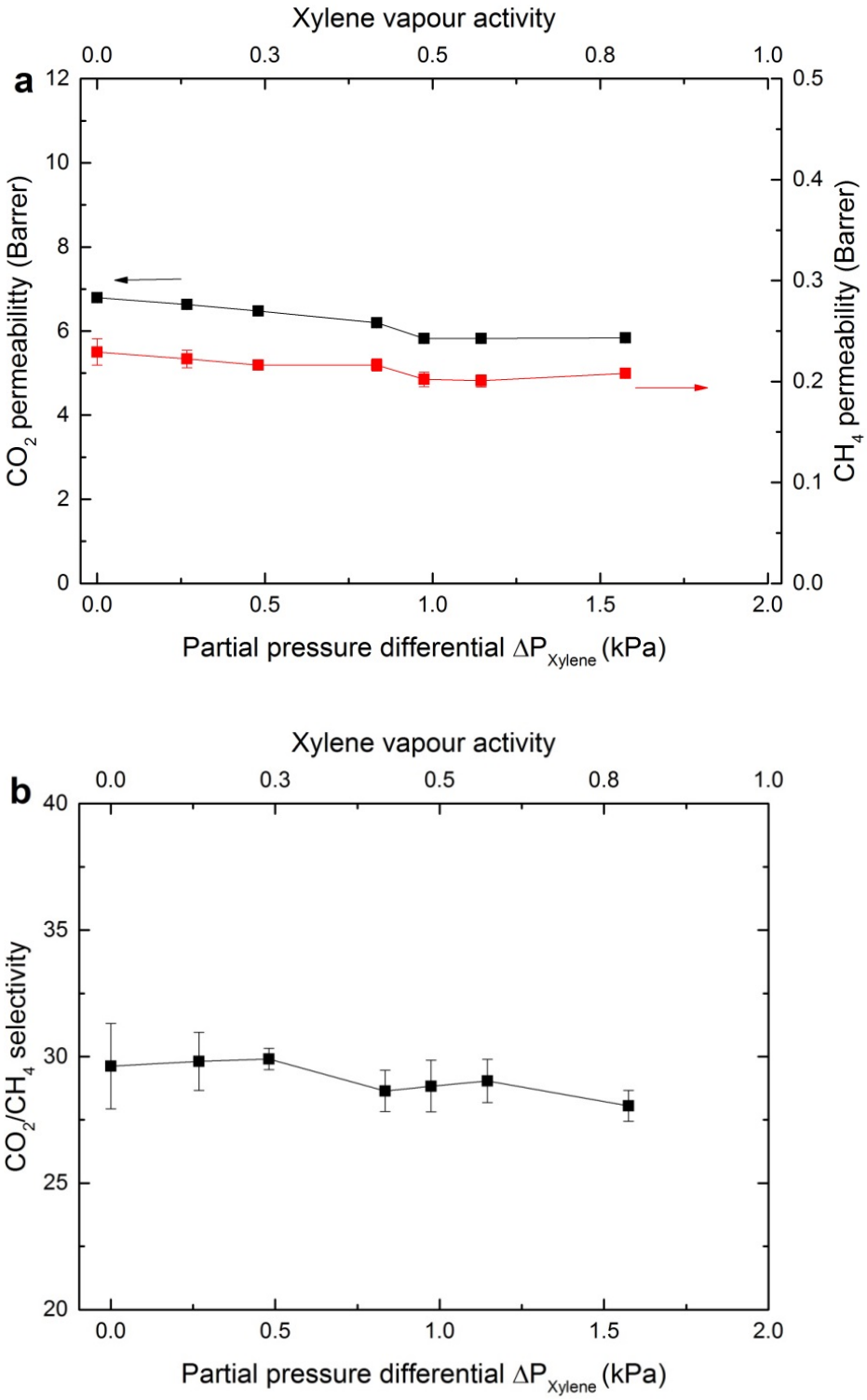


**Figure 6.5** The permeability of $CO_2$ and $CH_4$ (a) and $CO_2/CH_4$ selectivity (b) through CTA membrane exposed to xylene at various vapour pressures, for 10% $CO_2/CH_4$ mixed gas feed at 7.5 bar and 35$^{o}$C

### 6.3.4. The Impact of Toluene and Xylene on CTA Membranes at Higher $CO_2$ Pressure

The partial pressure of $CO_2$ in the raw natural gas can be over 7 bar depending on the source [4], so the impact of toluene and xylene on CTA membranes at 7.5 bar pure $CO_2$ pure was also studied. As shown in **Figure 6.6**, the higher $CO_2$ pressure results in a slightly higher permeability in the absence

of any aromatic hydrocarbon. This permeability was maintained for up to 18 days of exposure to the pure $CO_2$ at 7.5 Bar feed pressure.

The $CO_2$ permeability is otherwise similar at low partial pressures of either xylene or toluene. However, plasticisation clearly occurs at a lower partial pressure of xylene or toluene, when the $CO_2$ partial pressure is higher. At the higher $CO_2$ pressure, plasticisation first occurred at a vapour activity of 0.3 (partial pressure of 0.58 kPa for xylene and 2.0 kPa for toluene), versus 0.5 with low $CO_2$ partial pressure. In this case, the $CO_2$ and the aromatic hydrocarbon act cooperatively to lower the glass transition temperature, so that a transition to a swollen rubbery state now occurs at a lower temperature for a given vapour pressure.

Such changes in the glass transition temperature are often described by the Fox Equation (Eq. 6.2) [270]:

$$\frac{1}{T_g} = \frac{w_1}{T_{g1}} + \frac{w_2}{T_{g2}} \qquad \text{(Eq. 6.2)}$$

where $T_g$ is the glass transition temperature in Kelvin and $w$ the mass fraction of each component in a mixture of species 1 and 2. However, in the present case, this simple model (extended to three species) is unable to successfully predict the experimental data. Assuming glass transition temperatures of 190$^o$C for CTA [39], -156 $^o$C for toluene [293] and -78 $^o$C for $CO_2$ [294], would suggest that a glass transition temperature of 178$^o$C for the polymer at 0.75 Bar $CO_2$ and 0.5 toluene activity, falling to 160$^o$C for 7.5 Bar $CO_2$ and 0.3 toluene activity. These temperatures are clearly well above that of the experimental temperature of 35 $^o$C.

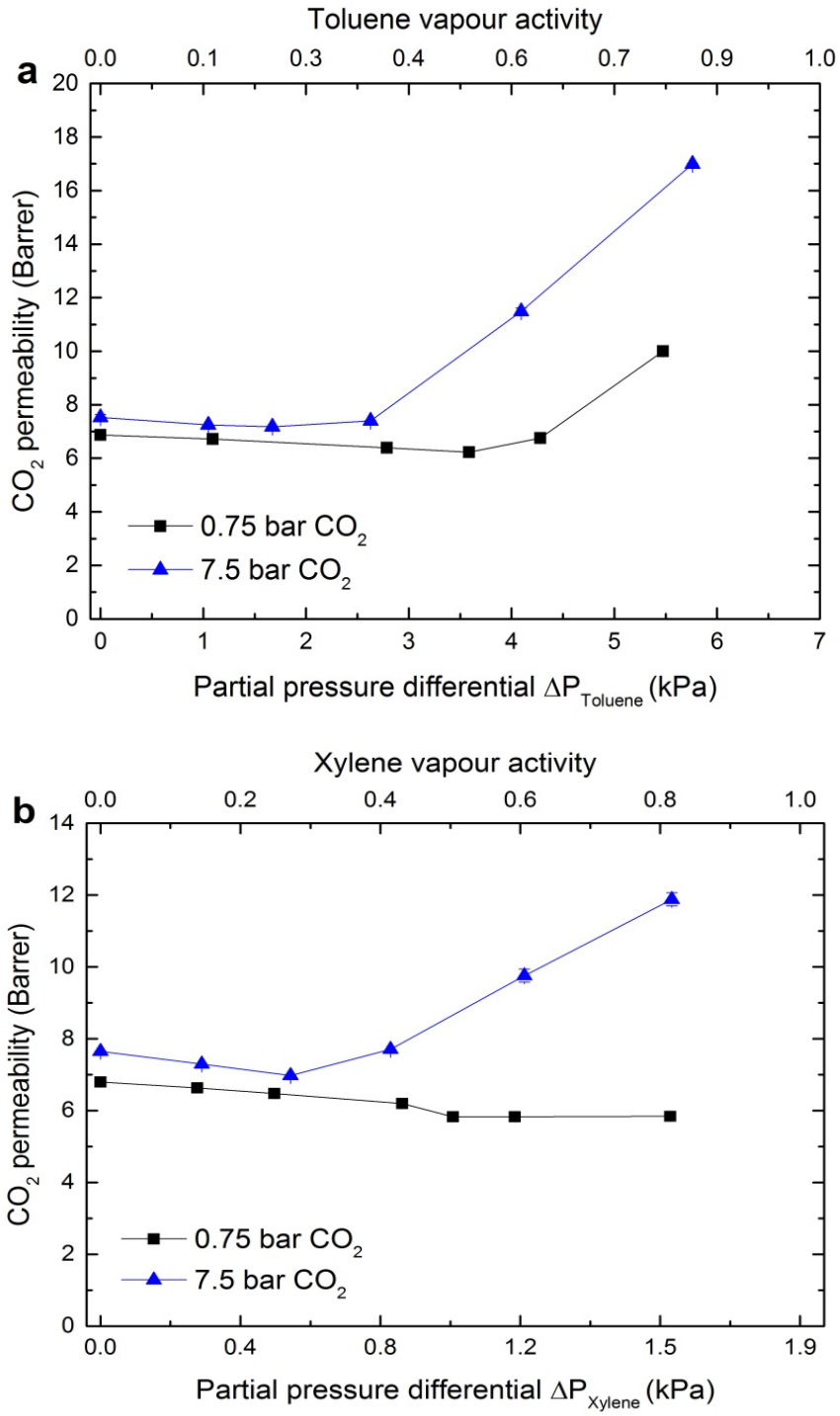


**Figure 6.6** The permeability of $CO_2$ through a CTA membrane at 35°C exposed to (a) toluene and (b) xylene at various vapour pressures, for a 10% $CO_2/CH_4$ mixed gas (0.75 Bar CO2) and for pure $CO_2$ at 7.5 bar.

### 6.3.5. The Permeabilities of Toluene and Xylene on CTA Membranes

The permeabilities of toluene and xylene through the CTA membranes at two different $CO_2$ pressures are summarised in **Figure 6.7**. The changes in toluene permeability with vapour pressure are similar to the trends for $CO_2$, where permeability declined with vapour pressure initially and turned upward when the membranes were plasticised (**Figure 6.6)**. In addition, at high toluene vapour pressure, the higher $CO_2$ pressure also enhanced the permeation of toluene through the

plasticised membranes. These changes are less evident in the xylene data, where the permeability is constant at all conditions within the error margins.

The permeability of toluene, xylene and methane at the same experiment conditions is in the order P(Toluene) > P(xylene) ≈ P($CH_4$) (refer to **Figure 6.4a**, **Figure 6.5a** and **Figure 6.7**). This can be explained by the solution – diffusion mechanism of penetrant transport through the dense membrane. The solubility of xylene and toluene are significantly greater than $CH_4$ due to the higher critical temperatures of aromatic hydrocarbons (**Table 6.1**). However, the larger kinetic diameters results in reduced diffusion of xylene and toluene through the membranes compared with $CH_4$.

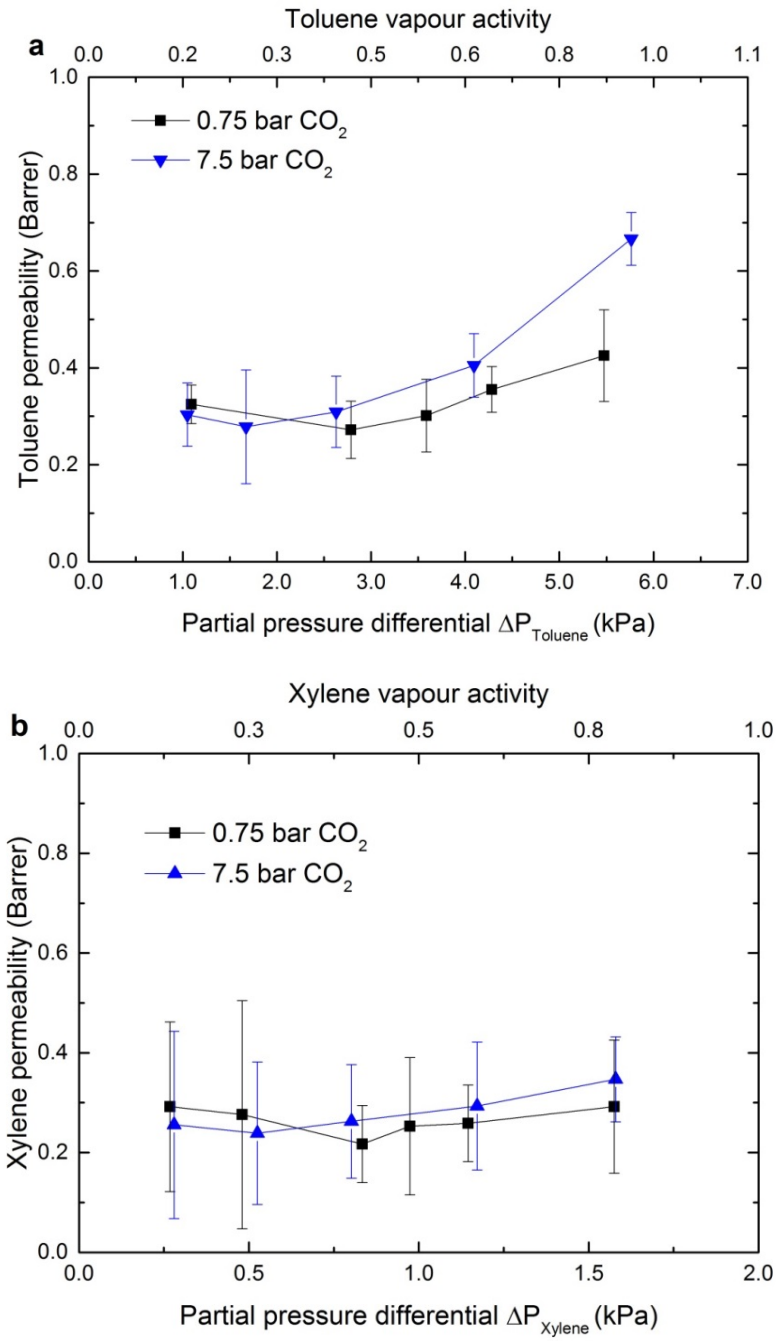


**Figure 6.7** The permeability of (a) toluene and (b) xylene at various vapour pressures and activities, for 10% $CO_2/CH_4$ mixed gas feed and pure $CO_2$ feed at 7.5 bar and 35°C

## 6.4. CONCLUSIONS

The impact of toluene and xylene on dense CTA membranes was investigated. The sorption kinetics of liquid toluene and xylene showed type II behaviour, indicative of significant plasticisation of the structure. The presence of toluene or xylene at low vapour pressure reduced the permeation of $CO_2$ and $CH_4$ through the membrane. At higher vapour pressures, plasticisation occurred, resulting in a dramatic increase in permeability. For low $CO_2$ partial pressures (0.75 Bar), the plasticisation occurred at 0.5 vapour activity, consistent with solubility measurements. However, in the presence of a higher $CO_2$ pressure (7.5 bar), plasticisation occurred at a low vapour activity of 0.3. This shift reflects a lowering of the glass transition temperature in the presence of both penetrants. However, the use of the Fox Equation, a simple additive model, was unable to predict this transition. The permeability of toluene and xylene itself through the CTA membranes was also determined.

# CHAPTER 7. CONCLUSIONS AND FUTURE PERSPECTIVE

## 7.1. CONCLUSIONS

Natural gas and coal will remain the dominant global energy resources over the coming decades. Gas processing is a significant industry required to improve the quality of natural gases to meet the pipeline specifications while carbon capture is an approach that has potential to enable fossil fuel dominated industries to reduce their carbon footprint and secure a sustainable low carbon global energy industry. Membrane separation by cellulose triacetate membranes is a viable technology for these purposes with commercial readiness and high $CO_2/CH_4$ and $CO_2/N_2$ selectivity. However, industry feed streams contain a wide number of minor components that alter the CTA membrane performance. Although several past studies have been conducted on CTA membranes, the systematic study on impact of impurities on the performance of CTA is limited. Therefore, this thesis focuses on the short-term and long-term performance of CTA membranes in the presence of these impurities and characterises the transport properties of these impurities through the membrane.

❖ **<u>The potential for use of CTA membrane in post combustion carbon capture</u>**

While CTA membrane have high $CO_2/N_2$ selectivity, commercial readiness and proven industrial resilience, their application for post combustion capture has not been considered by other workers. In this thesis, the potential for use of CTA membranes in post-combustion capture has been investigated, with new information provided on their ability to withstand the presence of flue gas impurities. The dense CTA membranes showed stable performance when exposed to liquid water (pH 7) or acid solution (pH 3) for 6 days, with a 30% increase in $CO_2$ and $N_2$ permeabilities and no loss in $CO_2/N_2$ selectivity. The membrane also demonstrated resistance to 0.75 kPa $SO_2$ at 22$^{o}$C for up to 100 days with a minor decline in gas permeability due to the membrane aging commonly observed in all glassy polymers. However, the membranes were unstable when exposed to caustic solution at pH 13 or 0.74 kPa $NO_{x.}$ This suggests that industrial application of these membranes would require the removal of these impurities to very low levels to maintain performance.

Current commercial CTA membranes are fabricated by phase inversion and this leads to relatively thick active layers that would provide insufficient flux for post combustion processes. However, as the use of thin film composite CTA membranes [247-249] or other emerging membrane fabrication technologies [36, 37] could reduce the thickness of the active layer to provide adequate gas permeance in the near future. This thesis provides the significant fundamental support for extending the application and market of CTA membranes into post combustion processes.

❖ **<u>The impact of ethylene glycol on CTA membrane performance</u>**

The thesis also systematically investigated the gas separation performance of CTA membranes exposed to ethylene glycol and triethylene glycol for up to 2000 hours and suggested a potential solution to recover the membrane performance after such exposures. The glycols absorbed into

the CTA membrane enhanced the permeation of $CO_2$ and $CH_4$ but significantly reduced the permeability of He. Wide Angle X-ray Diffraction study demonstrated that the membrane was plasticised by the glycols with a significant loss of crystallinity. A significant increase in helium permeability was not observed, which was attributed to the low solubility of this gas in the glycol phase. Importantly, the thesis showed that the performance of a CTA membrane contaminated with ethylene glycols could be potentially reversed by a methanol wash. Only minor residual swelling remained in the membranes after this washing step.

While the entrainment of glycol droplets to the membrane unit is a significant issue in natural gas processing, there is very limited understanding about what fundamentally occurs inside the membrane. The solutions used in industry mainly focus on improving the design and operation of the glycol contactor [18]. The findings in this thesis not only provide new fundamental knowledge of the impact of glycols on CTA gas separation but also present a novel approach to reuse damaged membrane modules after glycol exposure and hence provide savings to the industry.

❖ **<u>The impact of hydrogen sulfide on CTA membrane performance</u>**

The thesis also provided the fundamental knowledge on the short-term and long-term impact of hydrogen sulfide on the performance of CTA membranes. For $H_2S$ partial pressure up to 0.75 kPa, CTA membranes have a strong resistance to 0.75 kPa $H_2S$ at 22$^oC$ for up to 7200 hours without any plasticisation phenomena observed. The permeability of $H_2S$ through CTA membrane at elevated pressure (up to 0.75 kPa) and temperature (22 – 80$^oC$) were also studied. This findings provide understanding of the impact of $H_2S$ on CTA performance. The gas permeation data will be essential in the development of more sophisticated models of $H_2S$ transport in the future.

❖ **<u>The impact of BTEX on CTA membrane performance</u>**

Other significant impurities in natural gas processing are BTEX (benzene, toluene, ethylbenzene and xylene). The sorption kinetics of liquid toluene and xylene into CTA were evaluated for the first time and shown to demonstrate type II sorption behaviour. Vapour sorption data for these hydrocarbons at 35$^oC$ showed that both hydrocarbons plasticised the membrane at 0.5 vapour activity. A low vapour pressure of toluene and xylene reduced the permeability of $CO_2$ and $CH_4$ while the membranes were plasticised at higher vapour pressures. Interestingly, both toluene and xylene plasticised the CTA membrane at a vapour activity 0.5 when at 0.75 bar $CO_2$ partial pressure; but the plasticisation pressure shifted to 0.3 vapour activity at 7.5 bar $CO_2$ pressure. This indicates that the plasticisation effects of the two penetrants are not simply additive and that sophisticated models will be needed to describe the performance. The permeabilities of toluene and xylene through CTA membrane at up to 0.8 vapour activity and 35$^oC$ were also determined.

While CTA occupies around 80% the membrane market for natural gas separation, knowledge of the impact of BTEX on CTA membrane performance was extremely limited prior to this thesis. Hence, this study of BTEX is of significant value for scientists and engineers in process simulation and equipment design.

In summary, this thesis demonstrates that cellulose triacetate is an outstanding material for carbon dioxide gas separation in industrial applications, with high gas selectivity and strong resistance to

minor components and impurities in the industrial feed gas streams. The thesis demonstrates the potential to extend the CTA membrane market for applying in post-combustion $CO_2$ capture process if a sufficiently thin active layer membrane could be prepared. The thesis also demonstrated a potential strategy to recover the membrane after ethylene glycol exposure. However, careful washing protocols must be applied to prevent the collapse of the support layer. In addition, this thesis builds on existing database of $SO_2$, $H_2S$ and BTEX permeability and solubility in CTA which provides clearer insight of as to the transport properties of the impurities through the membrane. The challenge for simulating the transport properties of these impurities is utilising and developed the advanced and multi-parameters models that will be considered for future study project.

## 7.2. FUTURE PERSPECTIVE

To retain and increase the dominance of cellulose triacetate in the acidic gas removal membrane market, for natural gas processing and other industrial applications, the following recommendations are made for future researchers to consider:

- The concentration of impurities in industrial gas streams varies by location, dependent on the gas being treated and processing technologies. In this thesis, typical gas concentrations of industrial practice were used. However, in many applications such as natural gas processing in remote areas, the concentration of $H_2S$ is considerably higher. Therefore, the impact of higher concentrations of $H_2S$ on CTA as well as fluctuating concentrations are essential to extend the application of the CTA membranes in industrial applications.
- The impact of toluene and xylene on CTA membrane performance was investigated in this thesis. It would be useful to develop a mathematical model to transform these fundamental findings into a form that could be extended to other situations. However, the sorption and permeability data such as the dual mode approach collected in the thesis cannot be simulated by simple fundamental models. It would be valuable for further researchers to investigate multi-parameters models that account for non-ideal effects to better simulate the performance of CTA membranes in the presence of BTEX.
- In the thesis, the impact of each impurity was studied in isolation. However, in practice, these impurities occur in combination, and the combined impact of impurities is likely to deviate from the simple sum of each individual impurity. Hence, the study of gas stream containing a mixture of impurities is also a valuable approach for further research work. Studies over extended time frames under challenging conditions would assist better in characterizing CTA performance degradation.

To conclude, the study of CTA membranes for gas separation, with a focus on $CO_2$ separation, was successfully investigated here in relation to performance under exposure from water, glycol and BTEX vapour as well as hydrogen sulfide, sulphur oxides and nitric oxides. The ability of the CTA membrane to retain its separation performance under most of these conditions investigated clearly demonstrates why this membrane material remains the choice of industry.

# CHAPTER 8. REFERENCE


1. British Petroleum, *BP Energy Outlook 2016 edition.* Outlook to 2035, 2016.
2. Wang, M., Lawal A., Stephenson P., Sidders J., and Ramshaw C., *Post-combustion $CO_2$ capture with chemical absorption: A state-of-the-art review.* Chemical Engineering Research and Design, 2011. **89**(9): p. 1609-1624.
3. Chen, W., Yin X., and Zhang H., *Towards low carbon development in China: a comparison of national and global models.* Climatic change, 2016. **136**(1): p. 95-108.
4. Baker, R.W. and Lokhandwala K., *Natural Gas Processing with Membranes: An Overview.* Industrial & Engineering Chemistry Research, 2008. **47**(7): p. 2109-2121.
5. W., B.R., *Membrane Technology and Applications*. 2 ed. 2004, California, U.S.: John Wiley & Sons Ltd.
6. Henis, J.M.S. and Tripodi M.K., *A Novel Approach to Gas Separation Using Composite Hollow Fiber Membranes.* Separation Science and Technology, 1980. **15**: p. 1059.
7. Kanehashi, S., Aguiar A., Lu H.T., Chen G.Q., and Kentish S.E., *Effects of industrial gas impurities on the performance of mixed matrix membranes.* Journal of Membrane Science, 2017.
8. Wessling, M., Huisman I., Boomgaard T.v.d., and Smolders C.A., *Dilation kinetics of glassy, aromatic polyimides induced by carbon dioxide sorption.* Journal of Polymer Science Part B: Polymer Physics, 1995. **33**(9): p. 1371-1384.
9. Vu, D.Q., Koros W.J., and Miller S.J., *Effect of condensable impurity in $CO_2/CH_4$ gas feeds on performance of mixed matrix membranes using carbon molecular sieves.* Journal of Membrane Science, 2003. **221**(1): p. 233-239.
10. Funk, E., Kulkarni S., and Swamikannu A. *Effect of impurities on cellulose acetate membrane performance*. in *Recent Adv. in Separation Tech. AIChE Symposium Series*. 1986.
11. Schell, W.J., Wensley C.G., Chen M.S.K., Venugopal K.G., Miller B.D., and Stuart J.A., *Recent advances in cellulosic membranes for gas separation and pervaporation.* Gas Separation & Purification, 1989. **3**(4): p. 162-169.
12. Chen, G.Q., Kanehashi S., Doherty C.M., Hill A.J., and Kentish S.E., *Water vapor permeation through cellulose acetate membranes and its impact upon membrane separation performance for natural gas purification.* Journal of Membrane Science, 2015. **487**(0): p. 249-255.
13. Sridhar, S., Smitha B., and Aminabhavi T.M., *Separation of Carbon Dioxide from Natural Gas Mixtures through Polymeric Membranes—A Review.* Separation & Purification Reviews, 2007. **36**(2): p. 113-174.
14. Bhide, B.D. and Stern S.A., *Membrane processes for the removal of acid gases from natural gas. II. Effects of operating conditions, economic parameters, and membrane properties.* Journal of Membrane Science, 1993. **81**(3): p. 239-252.
15. Lee, J.S., Chandra P., Burgess S.K., Kriegel R., and Koros W.J., *An advanced gas/vapor permeation system for barrier materials: Design and applications to poly(ethylene terephthalate).* Journal of Polymer Science Part B: Polymer Physics, 2012. **50**(17): p. 1262-1270.
16. Maeda, Y. and Paul D., *Effect of antiplasticization on gas sorption and transport. I. Polysulfone.* Journal of Polymer Science Part B: Polymer Physics, 1987. **25**(5): p. 957-980.
17. Washim Uddin, M. and Hägg M.-B., *Effect of monoethylene glycol and triethylene glycol contamination on CO2/CH4 separation of a facilitated transport membrane for natural gas sweetening.* Journal of Membrane Science, 2012. **423–424**(0): p. 150-158.

18. Kohl, A.L. and Nielsen R.B., *Chapter 11 - Absorption of Water Vapor by Dehydrating Solutions*, in *Gas Purification (Fifth Edition)*. 1997, Gulf Professional Publishing: Houston. p. 946-1021.
19. Scholes, C.A., Kentish S.E., and Stevens G.W., *Effects of Minor Components in Carbon Dioxide Capture Using Polymeric Gas Separation Membranes.* Separation & Purification Reviews, 2009. **38**(1): p. 1-44.
20. Lokhandwala, K.A., Baker R.W., and Amo K.D., *Sour gas treatment process*. 1995, Membrane Technology and Research, Inc., Menlo Park, California.
21. Paulson, G.T., Clinch A.B., and McCandless F., *The effects of water vapor on the separation of methane and carbon dioxide by gas permeation through polymeric membranes.* Journal of Membrane Science, 1983. **14**(2): p. 129-137.
22. Li, K., Acharya D.R., and Hughes R., *Performance of a cellulose acetate permeator with permeability-influenced feed.* AIChE Journal, 1990. **36**(10): p. 1610-1612.
23. Anderson, C.J., Tao W., Scholes C.A., Stevens G.W., and Kentish S.E., *The performance of carbon membranes in the presence of condensable and non-condensable impurities.* Journal of Membrane Science, 2011. **378**(1–2): p. 117-127.
24. Mumford, K.A., Smith K.H., Anderson C.J., Shen S., Tao W., Suryaputradinata Y.A., Qader A., Hooper B., Innocenzi R.A., and Kentish S.E., *Post-combustion capture of $CO_2$: results from the solvent absorption capture plant at Hazelwood power station using potassium carbonate solvent.* Energy & Fuels, 2011. **26**(1): p. 138-146.
25. CSIRO Advanced Coal Technology. *Assessing Post-Combustion Capture for Coal-fired Power Stations in Asia-Pacific Partnership Countries*. 2012 [cited 2015 16 Feb]; Available from: http://www.canadiancleanpowercoalition.com/files/9713/5303/7000/AS31-204_AssessingPost-CombustionCaptureReport.pdf.
26. Aitken, R., Campbell D., and Bell L., *Properties of Australian fly ashes relevant to their agronomic utilization.* Soil Research, 1984. **22**(4): p. 443-453.
27. Paul, D.R. and Yampol'skii Y.P., *Polymeric gas separation membranes*. 1993: CRC Press.
28. Barrer, R.M., Barrie J.A., and Slater J., *Sorption and diffusion in ethyl cellulose. Part III. Comparison between ethyl cellulose and rubber.* Journal of Polymer Science, 1958. **27**(115): p. 177-197.
29. Vieth, W.R. and Amini M.A., *Generalized dual sorption theory*, in *Permeability of Plastic Films and Coatings*. 1974, Springer. p. 49-61.
30. Brunauer, S., Emmett P.H., and Teller E., *Adsorption of gases in multimolecular layers.* Journal of the American chemical society, 1938. **60**(2): p. 309-319.
31. Anderson, R.B., *Modifications of the Brunauer, Emmett and Teller equation1*. Journal of the American Chemical Society, 1946. **68**(4): p. 686-691.
32. CO2CRC. *Carbon capture and storage facilities*. Images and Videos 2012 [cited 2017 31/03]; Available from: http://old.co2crc.com.au/imagelibrary3/general.php.
33. Tanh Jeazet, H.B., Staudt C., and Janiak C., *Metal-organic frameworks in mixed-matrix membranes for gas separation.* Dalton Transactions, 2012. **41**(46): p. 14003-14027.
34. Ladewig, B. and Al-Shaeli M.N.Z., *Fundamentals of Membrane Bioreactors: Materials, Systems and Membrane Fouling*. 2016: Springer.
35. Sidney, L. and Srinivasa S., *High flow porous membranes for separating water from saline solutions*. 1964, University of California: USA.
36. Sullivan, D.M. and Bruening M.L., *Ultrathin, Gas-Selective Polyimide Membranes Prepared from Multilayer Polyelectrolyte Films.* Chemistry of Materials, 2003. **15**(1): p. 281-287.
37. Fu, Q., Kim J., Gurr P.A., Scofield J.M.P., Kentish S.E., and Qiao G.G., *A novel cross-linked nano-coating for carbon dioxide capture.* Energy & Environmental Science, 2016. **9**(2): p. 434-440.

38. Matteucci, S., Yampolskii Y., Freeman B.D., and Pinnau I., *Transport of Gases and Vapors in Glassy and Rubbery Polymers*, in *Materials Science of Membranes for Gas and Vapor Separation*. 2006, John Wiley & Sons, Ltd. p. 1-47.
39. Kamide, K. and Saito M., *Thermal Analysis of Cellulose Acetate Solids with Total Degrees of Substitution of 0.49, 1.75, 2.46, and 2.92.* Polym J, 1985. **17**(8): p. 919-928.
40. Puleo, A.C., Paul D.R., and Kelley S.S., *The effect of degree of acetylation on gas sorption and transport behavior in cellulose acetate.* Journal of Membrane Science, 1989. **47**(3): p. 301-332.
41. H.Strathmann, *Introduction to Membrane Science and Technology*. 2011: Wiley-VCH. ch. 4.3.
42. Chen, G.Q., Scholes C.A., Qiao G.G., and Kentish S.E., *Water vapor permeation in polyimide membranes.* Journal of Membrane Science, 2011. **379**: p. 479-487.
43. Koros, W.J. and Fleming G.K., *Membrane-based gasseparation.* Journal of MembraneScience, 1993. **83**: p. 1-80.
44. Wijmans, J.G. and Baker R.W., *The solution-diffusion model: a review.* Journal ofMembrane Science, 1995. **107**: p. 1-21.
45. Jeazet, H.B.T., Staudt C., and Janiak C., *Metal-organic frameworks in mixed-matrix membranes for gas separation.* Dalton Transactions, 2012. **41**(46): p. 14003-14027.
46. Paul, D.R., *1.04 - Fundamentals of Transport Phenomena in Polymer Membranes*, in *Comprehensive Membrane Science and Engineering*. 2010, Elsevier: Oxford. p. 75-90.
47. Fuertes, A.B. and Centeno T.A., *Preparation of supported asymmetric carbon molecular sieve membranes.* Journal of Membrane Science, 1998. **144**(1–2): p. 105-111.
48. Ghosal, K. and Freeman B.D., *Gas separation using polymer membranes: an overview.* Polymers for Advanced Technologies, 1994. **5**(11): p. 673-697.
49. Breck, D.W., *Zeolite molecular sieves: structure, chemistry, and use*. 1973: New York, Wiley [1973, c1974].
50. Yi, H., Deng H., Tang X., Yu Q., Zhou X., and Liu H., *Adsorption equilibrium and kinetics for $SO_2$, NO, $CO_2$ on zeolites FAU and LTA.* Journal of hazardous materials, 2012. **203**: p. 111-117.
51. Robeson, L.M., Freeman B.D., Paul D.R., and Rowe B.W., *An empirical correlation of gas permeability and permselectivity in polymers and its theoretical basis.* Journal of Membrane Science, 2009. **341**(1–2): p. 178-185.
52. Baertsch, C.D., Funke H.H., Falconer J.L., and Noble R.D., *Permeation of Aromatic Hydrocarbon Vapors through Silicalite−Zeolite Membranes.* The Journal of Physical Chemistry, 1996. **100**(18): p. 7676-7679.
53. *Lange's handbook of chemistry*. Knovel. 1973: Binghamton, N.Y. : Knovel.
54. Robeson, L.M., Smith Z.P., Freeman B.D., and Paul D.R., *Contributions of diffusion and solubility selectivity to the upper bound analysis for glassy gas separation membranes.* Journal of Membrane Science, 2014. **453**: p. 71-83.
55. Dal-Cin, M.M., Kumar A., and Layton L., *Revisiting the experimental and theoretical upper bounds of light pure gas selectivity-permeability for polymeric membranes.* Journal of Membrane Science, 2008. **323**(2): p. 299-308.
56. Shieh, J.J. and Chung T.S., *Gas permeability, diffusivity, and solubility of poly(4-vinylpyridine) film.* Journal of Polymer Science, Part B: Polymer Physics, 1999. **37**(20): p. 2851-2861.
57. Yampolskii, Y., Pinnau I., and Freeman B.D., *Materials science of membranes for gas and vapor separation*. 2006: Wiley Online Library.
58. Kanehashi, S., Chen G.Q., Scholes C.A., Ozcelik B., Hua C., Ciddor L., Southon P.D., D'Alessandro D.M., and Kentish S.E., *Enhancing gas permeability in mixed matrix membranes through tuning the nanoparticle properties.* Journal of Membrane Science, 2015. **482**: p. 49-55.

59. Duthie, X., Kentish S., Powell C., Nagai K., Qiao G., and Stevens G., *Operating temperature effects on the plasticization of polyimide gas separation membranes.* Journal of Membrane Science, 2007. **294**(1–2): p. 40-49.
60. Coker, D., Freeman B., and Fleming G., *Modeling multicomponent gas separation using hollow‐fiber membrane contactors.* AIChE Journal, 1998. **44**(6): p. 1289-1302.
61. Robeson, L.M., *The upper bound revisited.* Journal of Membrane Science, 2008. **320**(1–2): p. 390-400.
62. Alexander Stern, S., *Polymers for gas separations: the next decade.* Journal of Membrane Science, 1994. **94**(1): p. 1-65.
63. Vieth, W.R., Tam P.M., and Michaels A.S., *Dual sorption mechanisms in glassy polystyrene.* Journal of Colloid and Interface Science, 1966. **22**(4): p. 360-370.
64. Koros, W.J., *Model for sorption of mixed gases in glassy polymers.* Journal of Polymer Science: Polymer Physics Edition, 1980. **18**(5): p. 981-992.
65. Lim, L.-T., Britt I.J., and Tung M.A., *Sorption and transport of water vapor in nylon 6,6 film.* Journal of Applied Polymer Science, 1999. **71**(2): p. 197-206.
66. Chen, G.Q., Scholes C.A., Doherty C.M., Hill A.J., Qiao G.G., and Kentish S.E., *Modeling of the sorption and transport properties of water vapor in polyimide membranes.* Journal of Membrane Science, 2012. **409–410**: p. 96-104.
67. Chen, G.Q., *Water vapour permeation through glassy polyimide membranes and its impact upon carbon dioxide capture operations*, in *Department of Chemical and Biomolecular Engineering*. 2012, University of Melbourne: Melbourne, Australia.
68. ALOthman, Z.A., *A review: fundamental aspects of silicate mesoporous materials.* Materials, 2012. **5**(12): p. 2874-2902.
69. Flory, P.J., *Thermodynamics of High Polymer Solutions.* The Journal of Chemical Physics, 1942. **10**(1): p. 51-61.
70. Huggins, M.L., *Thermodynamic properties of solutions of long-chain compounds.* Annals of the New York Academy of Sciences, 1942. **43**(1): p. 1-32.
71. Favre, E., Clement R., Nguyen Q.T., Schaetzel P., and Neel J., *Sorption of organic solvents into dense silicone membranes. Part 2.-Development of a new approach based on a clustering hypothesis for associated solvents.* Journal of the Chemical Society, Faraday Transactions, 1993. **89**(24): p. 4347-4353.
72. Donohue, M.D., *Permeation behavior of carbon dioxide-methane mixtures in cellulose acetate membranes.* Journal of Membrane Science, 1989. **42**(3): p. 197-214.
73. Flory, P.J. and Jr. J.R., *Statistical Mechanics of Cross‐Linked Polymer Networks I. Rubberlike Elasticity.* The Journal of Chemical Physics, 1943. **11**(11): p. 512-520.
74. Favre, E., Nguyen Q.T., Clément R., and Néel J., *The engaged species induced clustering (ENSIC) model: a unified mechanistic approach of sorption phenomena in polymers.* Journal of Membrane Science, 1996. **117**(1): p. 227-236.
75. Jonquières, A. and Fane A., *Modified BET models for modeling water vapor sorption in hydrophilic glassy polymers and systems deviating strongly from ideality.* Journal of Applied Polymer Science, 1998. **67**(8): p. 1415-1430.
76. Timmermann, E., Chirife J., and Iglesias H., *Water sorption isotherms of foods and foodstuffs: BET or GAB parameters?* Journal of food engineering, 2001. **48**(1): p. 19-31.
77. Vopička, O., Pilnáček K., Číhal P., and Friess K., *Sorption of methanol, dimethyl carbonate, methyl acetate, and acetone vapors in CTA and PTMSP: General findings from the GAB Analysis.* Journal of Polymer Science Part B: Polymer Physics, 2016. **54**(5): p. 561-569.
78. Feng, H., *Modeling of vapor sorption in glassy polymers using a new dual mode sorption model based on multilayer sorption theory.* Polymer, 2007. **48**(10): p. 2988-3002.
79. Berens, A.R., *Transport of organic vapors and liquids in poly(vinyl chloride).* Makromolekulare Chemie. Macromolecular Symposia, 1989. **29**(1): p. 95-108.

80. Fleming, G.K. and Koros W.J., *Carbon dioxide conditioning effects on sorption and volume dilation behavior for bisphenol A-polycarbonate.* Macromolecules, 1990. **23**(5): p. 1353-1360.
81. Sarti, G.C., Gostoli C., and Masoni S., *Diffusion of alcohols and relaxation in poly(methyl methacrylate): effect of thermal history.* Journal of Membrane Science, 1983. **15**(2): p. 181-192.
82. De Angelis, M.G. and Sarti G.C., *Solubility of gases and liquids in glassy polymers.* Annual review of chemical and biomolecular engineering, 2011. **2**: p. 97-120.
83. Bondi, A., *van der Waals Volumes and Radii.* The Journal of Physical Chemistry, 1964. **68**(3): p. 441-451.
84. Yang, H., Xu Z., Fan M., Gupta R., Slimane R.B., Bland A.E., and Wright I., *Progress in carbon dioxide separation and capture: A review.* Journal of Environmental Sciences, 2008. **20**(1): p. 14-27.
85. Van Krevelen, D.W. and Te Nijenhuis K., *Chapter 4 - Volumetric Properties,* in *Properties of Polymers (Fourth Edition).* 2009, Elsevier: Amsterdam. p. 71-108.
86. Aaron, D. and Tsouris C., *Separation of $CO_2$ from flue fas: a review. Separation.* Science and Technology, 2005. **40**: p. 321-348.
87. Yoshimizu, H., Ohta S., Asano T., Suzuki T., and Tsujita Y., *Temperature dependence of the mean size of polyphenyleneoxide microvoids, as studied by Xe sorption and 129Xe NMR chemical shift analyses.* Polym J, 2012. **44**(8): p. 821-826.
88. Müller-Plathe, F., *Permeation of polymers — a computational approach.* Acta Polymerica, 1994. **45**(4): p. 259-293.
89. Lee, W., *Selection of barrier materials from molecular structure.* Polymer Engineering & Science, 1980. **20**(1): p. 65-69.
90. Kanehashi, S., Nakagawa T., Nagai K., Duthie X., Kentish S., and Stevens G., *Effects of carbon dioxide-induced plasticization on the gas transport properties of glassy polyimide membranes.* Journal of Membrane Science, 2007. **298**(1): p. 147-155.
91. Petropoulos, J., *Plasticization effects on the gas permeability and permselectivity of polymer membranes.* Journal of Membrane Science, 1992. **75**(1): p. 47-59.
92. Paul, D.R. and Koros W.J., *Effect of partially immobilizing sorption on permeability and the diffusion time lag.* Journal of Polymer Science: Polymer Physics Edition, 1976. **14**(4): p. 675-685.
93. Immergut, E.H. and Mark H.F., *Principles of Plasticization,* in *Plasticization and Plasticizer Processes.* 1965, AMERICAN CHEMICAL SOCIETY. p. 1-26.
94. Paul, D.R., *Water vapor sorption and diffusion in glassy polymers.* Macromolecular Symposia, 1999. **138**(1): p. 13-20.
95. Kesting, R.E. and Fritzsche A., *Polymeric gas separation membranes.* 1993: Wiley New York.
96. Wijmans, J. and Baker R., *The solution-diffusion model: a review.* Journal of Membrane Science, 1995. **107**(1): p. 1-21.
97. Barrie, J.A. and Platt B., *The diffusion and clustering of water vapour in polymers.* Polymer, 1963. **4**: p. 303-313.
98. Starkweather, H.W., *Clustering of water in polymers.* Journal of Polymer Science Part B: Polymer Letters, 1963. **1**(3): p. 133-138.
99. Sato, S., Suzuki M., Kanehashi S., and Nagai K., *Permeability, diffusivity, and solubility of benzene vapor and water vapor in high free volume silicon- or fluorine-containing polymer membranes.* Journal of Membrane Science, 2010. **360**(1–2): p. 352-362.
100. Long, F.A. and Thompson L.J., *Diffusion of water vapor in polymers.* Journal of Polymer Science, 1955. **15**(80): p. 413-426.
101. Crank, J., *The mathematics of diffusion.* 1979: Oxford university press.

102. Satterfield, M.B. and Benziger J.B., *Non-Fickian Water Vapor Sorption Dynamics by Nafion Membranes.* The Journal of Physical Chemistry B, 2008. **112**(12): p. 3693-3704.
103. Guidotti, P. and Pelesko J.A., *Transient instability in case II diffusion.* Journal of Polymer Science Part B: Polymer Physics, 1998. **36**(16): p. 2941-2947.
104. Chiou, J., Barlow J.W., and Paul D.R., *Plasticization of glassy polymers by $CO_2$.* Journal of Applied Polymer Science, 1985. **30**(6): p. 2633-2642.
105. Franson, N.M. and Peppas N.A., *Influence of copolymer composition on non-fickian water transport through glassy copolymers.* Journal of Applied Polymer Science, 1983. **28**(4): p. 1299-1310.
106. Harogoppad, S.B. and Aminabhavi T.M., *Diffusion and sorption of organic liquids through polymer membranes. 5. Neoprene, styrene-butadiene-rubber, ethylene-propylene-diene terpolymer, and natural rubber versus hydrocarbons (C8-C16).* Macromolecules, 1991. **24**(9): p. 2598-2605.
107. Mandelkern, L. and Long F.A., *Rate of sorption of organic vapors by films of cellulose acetate.* Journal of Polymer Science, 1951. **6**(4): p. 457-469.
108. Thomas, N.L. and Windle A.H., *A theory of case II diffusion.* Polymer, 1982. **23**(4): p. 529-542.
109. Astaluta, G. and Sarti G.C., *A class of mathematical models for sorption of swelling solvents in glassy polymers.* Polymer Engineering & Science, 1978. **18**(5): p. 388-395.
110. McCaig, M.S. and Paul D.R., *Effect of film thickness on the changes in gas permeability of a glassy polyarylate due to physical aging Part I. Experimental observations.* Polymer, 2000. **41**(2): p. 629-637.
111. Struik, L.C.E., *Physical aging in amorphous glassy polymers.* Annals of the New York Academy of Sciences, 1976. **279**(1): p. 78-85.
112. Nagai, K. and Nakagawa T., *Effects of aging on the gas permeability and solubility in poly(1-trimethylsilyl-1-propyne) membranes synthesized with various catalysts.* Journal of Membrane Science, 1995. **105**(3): p. 261-272.
113. Bartos, J., Müller J., and Wendorff J.H., *Physical ageing of isotropic and anisotropic polycarbonate.* Polymer, 1990. **31**(9): p. 1678-1684.
114. Robertson, R.E., Simha R., and Curro J.G., *Free volume and the kinetics of aging of polymer glasses.* Macromolecules, 1984. **17**(4): p. 911-919.
115. Royal, J.S. and Torkelson J.M., *Physical aging effects on molecular-scale polymer relaxations monitored with mobility-sensitive fluorescent molecules.* Macromolecules, 1993. **26**(20): p. 5331-5335.
116. Hill, A.J., Heater K.J., and Agrawal C.M., *The effects of physical aging in polycarbonate.* Journal of Polymer Science Part B: Polymer Physics, 1990. **28**(3): p. 387-405.
117. Lin, W.-H. and Chung T.-S., *Gas permeability, diffusivity, solubility, and aging characteristics of 6FDA-durene polyimide membranes.* Journal of Membrane Science, 2001. **186**(2): p. 183-193.
118. Fu, Y.-J., Hsiao S.-W., Hu C.-C., Lee K.-R., and Lai J.-Y., *Prediction of long-term physical aging of poly(methyl methacrylate) membranes for gas separation.* Desalination, 2008. **234**(1): p. 51-57.
119. McCaig, M.S., Paul D.R., and Barlow J.W., *Effect of film thickness on the changes in gas permeability of a glassy polyarylate due to physical aging Part II. Mathematical model.* Polymer, 2000. **41**(2): p. 639-648.
120. Swaidan, R., Ghanem B., Litwiller E., and Pinnau I., *Physical Aging, Plasticization and Their Effects on Gas Permeation in "Rigid" Polymers of Intrinsic Microporosity.* Macromolecules, 2015. **48**(18): p. 6553-6561.
121. Huang, Y. and Paul D.R., *Effect of Film Thickness on the Gas-Permeation Characteristics of Glassy Polymer Membranes.* Industrial & Engineering Chemistry Research, 2007. **46**(8): p. 2342-2347.

122. Kim, J.H., Jang J., and Zin W.-C., *Estimation of the Thickness Dependence of the Glass Transition Temperature in Various Thin Polymer Films.* Langmuir, 2000. **16**(9): p. 4064-4067.
123. Rozenberg, B.A., Irzhak V.I., and Bogdanova L.M., *The role of diffusion of free volume at volume relaxation of amorphous polymers*, in *Relaxation in Polymers*, M. Pietralla and W. Pechhold, Editors. 1989, Steinkopff: Darmstadt. p. 187-197.
124. Shishatskii, A.M., Yampol'skii Y.P., and Peinemann K.V., *Effects of film thickness on density and gas permeation parameters of glassy polymers.* Journal of Membrane Science, 1996. **112**(2): p. 275-285.
125. Pfromm, P.H. and Koros W.J., *Accelerated physical ageing of thin glassy polymer films: evidence from gas transport measurements.* Polymer, 1995. **36**(12): p. 2379-2387.
126. Scholes, C.A., Chen G.Q., Stevens G.W., and Kentish S.E., *Plasticization of ultra-thin polysulfone membranes by carbon dioxide.* Journal of Membrane Science, 2010. **346**(1): p. 208-214.
127. Zhou, C., Chung T.-S., Wang R., Liu Y., and Goh S.H., *The accelerated CO2 plasticization of ultra-thin polyimide films and the effect of surface chemical cross-linking on plasticization and physical aging.* Journal of Membrane Science, 2003. **225**(1): p. 125-134.
128. Pfromm, P.H., Pinnau I., and Koros W.J., *Gas transport through integral-asymmetric membranes: A comparison to isotropic film transport properties.* Journal of Applied Polymer Science, 1993. **48**(12): p. 2161-2171.
129. Kesting, R.E., *The four tiers of structure in integrally skinned phase inversion membranes and their relevance to the various separation regimes.* Journal of Applied Polymer Science, 1990. **41**(11-12): p. 2739-2752.
130. Scholes, C.A., Stevens G.W., and Kentish S.E., *Membrane gas separation applications in natural gas processing.* Fuel, 2012. **96**: p. 15-28.
131. Rustemeyer, P. *1. History of CA and evolution of the markets*. in *Macromolecular Symposia*. 2004. Wiley Online Library.
132. Malm, C.J. and Clarke H.T., *The action of fatty acids on cellulose.* Journal of the American Chemical Society, 1929. **51**(1): p. 274-278.
133. De, W.G.G., *Chemical compound and process of making same*, U.P. Office, Editor. 1935, Du Pont.
134. Malm, C., Tanghe L., and Schmitt J., *Catalysts for acetylation of cellulose.* Industrial & Engineering Chemistry, 1961. **53**(5): p. 363-367.
135. Balser, K., Hoppe L., Eicher T., Wandel M., Astheimer H.-J., Steinmeier H., and Allen J.M., *Cellulose Esters*, in *Ullmann's Encyclopedia of Industrial Chemistry*. 2000, Wiley-VCH Verlag GmbH & Co. KGaA.
136. Maim, C., Barkey K., May D., and Lefferts E., *Treatment of cellulose prior to acetylation.* Industrial & Engineering Chemistry, 1952. **44**(12): p. 2904-2909.
137. Howsmon, J., *Recent progress in cellulose and cellulose acetate fibers.* Annals of the New York Academy of Sciences, 1957. **67**(1): p. 901-909.
138. Hosseini, S.S., Peng N., and Chung T.S., *Gas separation membranes developed through integration of polymer blending and dual-layer hollow fiber spinning process for hydrogen and natural gas enrichments.* Journal of Membrane Science, 2010. **349**(1): p. 156-166.
139. Sridhar, S., Smitha B., Mayor S., Prathab B., and Aminabhavi T.M., *Gas permeation properties of polyamide membrane prepared by interfacial polymerization.* Journal of Materials Science, 2007. **42**(22): p. 9392-9401.
140. Zhang, Y., Sunarso J., Liu S., and Wang R., *Current status and development of membranes for CO 2/CH 4 separation: a review.* International Journal of Greenhouse Gas Control, 2013. **12**: p. 84-107.
141. Mao, Z., Jie X., Cao Y., Wang L., Li M., and Yuan Q., *Preparation of dual-layer cellulose/polysulfone hollow fiber membrane and its performance for isopropanol*

*dehydration and CO2 separation.* Separation and Purification Technology, 2011. **77**(1): p. 179-184.
142. White, L.S., *Evolution of Natural Gas Treatment with Membrane Systems*, in *Membrane Gas Separation*. 2010, John Wiley & Sons, Ltd. p. 313-332.
143. Fouda, A.E., Matsuura T., and Lui A., *Permeation of Gas Mixtures in Cellulose Acetate Membranes Practical Approach to Predict the Permeation Rate Co2/Ch4 Mixture.* Separation Science and Technology, 1988. **23**(12-13): p. 2175-2190.
144. Rowley, M.E. and Slowig W.D., *Dry stabilized,rewettable semipermeable cellulose ester and ether membranes and their preparation*, U.S.P. Office, Editor. 1971, Eastman Kodak.
145. Minhas, B.S., Matsuura T., and Sourirajan S., *Formation of asymmetric cellulose acetate membranes for the separation of carbon dioxide-methane gas mixtures.* Industrial & Engineering Chemistry Research, 1987. **26**(11): p. 2344-2348.
146. Gantzel, P.K. and Merten U., *Gas Separations with High-Flux Cellulose Acetate Membranes.* Industrial & Engineering Chemistry Process Design and Development, 1970. **9**(2): p. 331-332.
147. Macdonald, W. and Pan C., *Method for drying water-wet membranes*, U.S. Patent, Editor. 1974, Helium A Ltd.: US.
148. Jie, X., Cao Y., Qin J.-J., Liu J., and Yuan Q., *Influence of drying method on morphology and properties of asymmetric cellulose hollow fiber membrane.* Journal of Membrane Science, 2005. **246**(2): p. 157-165.
149. Choi, H.-S., Kim H.-S., Park C.-S., Kim B.-Y., and Baik M.-Y., *Ultra high pressure (UHP)-assisted acetylation of corn starch.* Carbohydrate Polymers, 2009. **78**(4): p. 862-868.
150. Kim, H.-S., Choi H.-S., Kim B.-Y., and Baik M.-Y., *Characterization of Acetylated Corn Starch Prepared under Ultrahigh Pressure (UHP).* Journal of Agricultural and Food Chemistry, 2010. **58**(6): p. 3573-3579.
151. Malm, C.J., Genung L.B., and Williams Jr R.F., *Determination of Free Hydroxyl Content.* Industrial & Engineering Chemistry Analytical Edition, 1942. **14**(12): p. 935-940.
152. Fischer, S., Thümmler K., Volkert B., Hettrich K., Schmidt I., and Fischer K., *Properties and Applications of Cellulose Acetate.* Macromolecular Symposia, 2008. **262**(1): p. 89-96.
153. Kamide, K., Okajima K., and Saito M., *Nuclear Magnetic Resonance Study of Thermodynamic Interaction between Cellulose Acetate and Solvent.* Polym J, 1981. **13**(2): p. 115-125.
154. Mitchell, J.A., Bockman C.D., and Lee A.V., *Determination of Acetyl Content of Cellulose Acetate by Near Infrared Spectroscopy.* Analytical Chemistry, 1957. **29**(4): p. 499-502.
155. Kamide, K. and Saito M., *Cellulose and cellulose derivatives: Recent advances in physical chemistry*, in *Biopolymers*. 1987, Springer Berlin Heidelberg: Berlin, Heidelberg. p. 1-56.
156. Cao, S., Shi Y., and Chen G., *Influence of acetylation degree of cellulose acetate on pervaporation properties for MeOH/MTBE mixture.* Journal of Membrane Science, 2000. **165**(1): p. 89-97.
157. Weinkauf, D.H. and Paul D.R., *Effects of Structural Order on Barrier Properties*, in *Barrier Polymers and Structures*. 1990, American Chemical Society. p. 60-91.
158. Alvarez, V.A. and Vázquez A., *Thermal degradation of cellulose derivatives/starch blends and sisal fibre biocomposites.* Polymer Degradation and Stability, 2004. **84**(1): p. 13-21.
159. Youssef, M.A., Sefain M.Z., and El-Kalyoubi S.F., *Thermal behaviour of cellulose acetate.* Thermochimica Acta, 1989. **150**(1): p. 33-38.
160. Sada, E., Kumazawa H., Xu P., and Wang S.T., *Permeation of pure carbon dioxide and methane and binary mixtures through cellulose acetate membranes.* Journal of Polymer Science Part B: Polymer Physics, 1990. **28**(1): p. 113-125.
161. Sada, E., Kumazawa H., Wang J.S., and Koizumi M., *Separation of carbon dioxide by asymmetric hollow fiber membrane of cellulose triacetate.* Journal of Applied Polymer Science, 1992. **45**(12): p. 2181-2186.

162. Chiou, J.S. and Paul D.R., *Gas sorption and permeation in poly(ethyl methacrylate).* Journal of Membrane Science, 1989. **45**(1): p. 167-189.
163. Jordan, S.M., Koros W.J., and Fleming G.K., *The effects of CO2 exposure on pure and mixed gas permeation behavior: comparison of glassy polycarbonate and silicone rubber*. Journal of Membrane Science, 1987. **30**(2): p. 191-212.
164. Raymond, P.C. and Paul D.R., *Sorption and transport of pure gases in random styrene/methyl methacrylate copolymers.* Journal of Polymer Science Part B: Polymer Physics, 1990. **28**(11): p. 2079-2102.
165. Bos, A., Pünt I.G.M., Wessling M., and Strathmann H., *CO2-induced plasticization phenomena in glassy polymers.* Journal of Membrane Science, 1999. **155**(1): p. 67-78.
166. Houde, A.Y., Krishnakumar B., Charati S.G., and Stern S.A., *Permeability of dense (homogeneous) cellulose acetate membranes to methane, carbon dioxide, and their mixtures at elevated pressures.* Journal of Applied Polymer Science, 1996. **62**(13): p. 2181-2192.
167. Stern, S.A. and Kulkarni S.S., *Solubility of methane in cellulose acetate—conditioning effect of carbon dioxide.* Journal of Membrane Science, 1982. **10**(2-3): p. 235-251.
168. Sada, E., Kumazawa H., Yoshio Y., Wang S.T., and Xu P., *Permeation of carbon dioxide through homogeneous dense and asymmetric cellulose acetate membranes.* Journal of Polymer Science Part B: Polymer Physics, 1988. **26**(5): p. 1035-1048.
169. Costello, L.M. and Koros W.J., *Thermally stable polyimide isomers for membrane-based gas separations at elevated temperatures.* Journal of Polymer Science Part B: Polymer Physics, 1995. **33**(1): p. 135-146.
170. Stern, S.A. and De Meringo A.H., *Solubility of carbon dioxide in cellulose acetate at elevated pressures.* Journal of Polymer Science: Polymer Physics Edition, 1978. **16**(4): p. 735-751.
171. Yampolskii, Y., *2 - Fundamental science of gas and vapour separation in polymeric membranes*, in *Advanced Membrane Science and Technology for Sustainable Energy and Environmental Applications*, A. Basile and S.P. Nunes, Editors. 2011, Woodhead Publishing. p. 22-55.
172. Lee, S., Minhas B., and Donohue M. *Effect of gas composition and pressure on permeation through cellulose acetate membranes*. in *AIChE Symposium Series*. 1988.
173. Ellig, D.L., Althouse J.B., and McCandless F.P., *Concentration of methane from mixtures with carbon dioxide by permeation through polymeric films.* Journal of Membrane Science, 1980. **6**(0): p. 259-263.
174. Ettouney, H.M., Al-Enezi G., Hamam S.E.M., and Hughes R., *Characterization of the permeation properties of CO2/N2 gas mixtures in silicone rubber membranes.* Gas Separation & Purification, 1994. **8**(1): p. 31-36.
175. Jecht, U., *Flue Gas Analysis in Industry: practical guide for emission and process measurements*. 2004, New Jersey, USA: Testo USA.
176. Baker, R.W., *Membrane technology*. 2000: Wiley Online Library.
177. Hoover, S.R. and Mellon E.F., *Effect of Acetylation on Sorption of Water by Cellulose.* Textile Research Journal, 1947. **17**(12): p. 714-716.
178. Laatikainen, M. and Lindström M., *Measurement of sorption in polymer membranes with a quartz crystal microbalance.* Journal of membrane science, 1986. **29**(2): p. 127-141.
179. Kurokawa, Y., *Adsorption of water on cellulose acetate membrane.* Desalination, 1981. **36**(3): p. 285-290.
180. Toprak, C., Agar J.N., and Falk M., *State of water in cellulose acetate membranes.* Journal of the Chemical Society, Faraday Transactions 1: Physical Chemistry in Condensed Phases, 1979. **75**: p. 803-815.
181. Gocho, H., Shimizu H., Tanioka A., Chou T.-J., and Nakajima T., *Effect of acetyl content on the sorption isotherm of water by cellulose acetate: comparison with the thermal analysis results.* Carbohydrate polymers, 2000. **41**(1): p. 83-86.

182. Roussis, P.P., *Diffusion of water vapour in cellulose acetate: 1. Differential transient sorption kinetics and equilibria.* Polymer, 1981. **22**(6): p. 768-773.
183. Rosenbaum, S. and Cotton O., *Steady‐state distribution of water in cellulose acetate membrane.* Journal of Polymer Science Part A: Polymer Chemistry, 1969. **7**(1): p. 101-109.
184. Dias, C.R., Rosa M.J., and de Pinho M.N., *Structure of water in asymmetric cellulose ester membranes and ATR-FTIR study.* Journal of Membrane Science, 1998. **138**(2): p. 259-267.
185. Murphy, D. and de Pinho M.N., *An ATR-FTIR study of water in cellulose acetate membranes prepared by phase inversion.* Journal of membrane science, 1995. **106**(3): p. 245-257.
186. Rogers, C., *Permeation of gases and vapours in polymers.* Polymer permeability, 1985. **2**: p. 11-73.
187. Sanders, E., *Penetrant-induced plasticization and gas permeation in glassy polymers.* Journal of Membrane Science, 1988. **37**(1): p. 63-80.
188. Wessling, M., Schoeman S., Van der Boomgaard T., and Smolders C., *Plasticization of gas separation membranes.* Gas Separation & Purification, 1991. **5**(4): p. 222-228.
189. Satriana, M., *New developments in flue gas desulfurization technology*. 1981, Park Ridge, New Jersey, USA: Noyes Data Corporation.
190. Vienken, J., *Membranes in hemodialysis.* Membrane Technology, Volume 1: Membranes for Life Sciences, 2011: p. 1.2.
191. Vos, K.D., Burris F.O., and Riley R.L., *Kinetic study of the hydrolysis of cellulose acetate in the pH range of 2–10.* Journal of Applied Polymer Science, 1966. **10**(5): p. 825-832.
192. Thambimuthu, K., Soltanieh M., and Abanades J.C., *IPCC Special Report on Carbon Dioxide Capture and Storage*. 2005, Cambridge University: Cambridge.
193. Kuehne, D.L. and Friedlander S.K., *Selective Transport of Sulfur Dioxide through Polymer Membranes. 1. Polyacrylate and Cellulose Triacetate Single-Layer Membranes.* Industrial & Engineering Chemistry Process Design and Development, 1980. **19**(4): p. 609-616.
194. Seibel, D.R. and McCandless F., *Separation of sulfur dioxide and nitrogen by permeation through a sulfolane plasticized vinylidene fluoride film.* Industrial & Engineering Chemistry Process Design and Development, 1974. **13**(1): p. 76-78.
195. Moretti, A., Triscori R., and Ritzenthaler D., *A System Approach to SO.* 2006.
196. Zhang, L., Wang X., Yu R., Li J., Hu B., and Yang L., *Hollow fiber membrane separation process in the presence of gaseous and particle impurities for post-combustion CO2 capture.* International Journal of Green Energy, 2017. **14**(1): p. 15-23.
197. Faucett, H.L., Maxwell J.D., Burnett T.A., United States. Environmental Protection Agency. Office of Research and Development, Industrial Environmental Research Laboratory, and Electric Power Research Institute *Technical Assessment of NOx Removal Processes For Utility Application*. 1977, Springfield, Virginia: Environmental Protection Agency, Office of Research and Development, Industrial Environmental Research Laboratory.
198. Scholes, C.A., Chen G.Q., Stevens G.W., and Kentish S.E., *Nitric oxide and carbon monoxide permeation through glassy polymeric membranes for carbon dioxide separation.* Chemical Engineering Research & Design, 2011. **89**(9): p. 1730-1736.
199. Tsukahara, H., Ishida T., and Mayumi M., *Gas-Phase Oxidation of Nitric Oxide: Chemical Kinetics and Rate Constant.* Nitric Oxide, 1999. **3**(3): p. 191-198.
200. Yackel, E.C. and Kenyon W.O., *The Oxidation of Cellulose by Nitrogen Dioxide*.* Journal of the American Chemical Society, 1942. **64**(1): p. 121-127.
201. Rowen, J.W., Hunt C.M., and Plyler E.K., *Absorption spectra in the detection of chemical changes in cellulose and cellulose derivatives.* Textile Research Journal, 1947. **17**(9): p. 504-511.
202. Hao, J., Rice P.A., and Stern S.A., *Upgrading low-quality natural gas with H2S- and CO2-selective polymer membranes: Part I. Process design and economics of membrane stages without recycle streams.* Journal of Membrane Science, 2002. **209**(1): p. 177-206.

203. Kraftschik, B., Koros W.J., Johnson J.R., and Karvan O., *Dense film polyimide membranes for aggressive sour gas feed separations.* Journal of Membrane Science, 2013. **428**: p. 608-619.
204. Merkel, T. and Toy L., *Comparison of hydrogen sulfide transport properties in fluorinated and nonfluorinated polymers.* Macromolecules, 2006. **39**(22): p. 7591-7600.
205. Chatterjee, G., Houde A.A., and Stern S.A., *Poly(ether urethane) and poly(ether urethane urea) membranes with high H2S/CH4 selectivity.* Journal of Membrane Science, 1997. **135**(1): p. 99-106.
206. Harasimowicz, M., Orluk P., Zakrzewska-Trznadel G., and Chmielewski A., *Application of polyimide membranes for biogas purification and enrichment.* Journal of Hazardous Materials, 2007. **144**(3): p. 698-702.
207. Merkel, T., Gupta R., Turk B., and Freeman B., *Mixed-gas permeation of syngas components in poly (dimethylsiloxane) and poly (1-trimethylsilyl-1-propyne) at elevated temperatures.* Journal of Membrane Science, 2001. **191**(1): p. 85-94.
208. Orme, C.J., Klaehn J.R., and Stewart F.F., *Gas permeability and ideal selectivity of poly[bis-(phenoxy)phosphazene], poly[bis-(4-tert-butylphenoxy)phosphazene], and poly[bis-(3,5-di-tert-butylphenoxy)1.2(chloro)0.8phosphazene].* Journal of Membrane Science, 2004. **238**(1): p. 47-55.
209. Orme, C.J. and Stewart F.F., *Mixed gas hydrogen sulfide permeability and separation using supported polyphosphazene membranes.* Journal of membrane science, 2005. **253**(1): p. 243-249.
210. Li, N.N., Funk E.W., Chang Y.A., Kulkarni S.S., Swamikannu A.X., and White L.S., *Membrane separation processes in the petrochemicalindustry: Phase II*, in *Final Report for U.S. Department of Energy*. 1987, Allied-Signal: Des Plaines, IL.
211. Heilman, W., Tammela V., Meyer J.A., Stannett V., and Szwarc M., *Permeability of Polymer Films to Hydrogen Sulfide Gas.* Industrial & Engineering Chemistry, 1956. **48**(4): p. 821-824.
212. Løkken, T., Bersås A., Christensen K., Nygaard C., and Solbraa E. *Water content of high pressure natural gas: data, prediction and experience from field*. in *IGRC (International Gas Union Research Conference)*. 2008.
213. Gavlin, G. and Goltsin B., *Gas dehydration process*. 1998, Gas Research Institute. Chicago. Illinois.
214. Isa, M.A., Eldemerdash U., and Nasrifar K., *Evaluation of potassium formate as a potential modifier of TEG for high performance natural gas dehydration process.* Chemical Engineering Research and Design, 2013. **91**(9): p. 1731-1738.
215. Herskowitz, M. and Gottlieb M., *Vapor-liquid equilibrium in aqueous solutions of various glycols and polyethylene glycols. 1. Triethylene glycol.* Journal of Chemical and Engineering Data, 1984. **29**(2): p. 173-175.
216. Kidnay, A.J., Parrish W.R., and McCartney D.G., *Chapter 14 - Capital cost of gas processing facilities*, in *Fundamentals of natural gas processing*. 2011, CRC Press.
217. Kelland, M.A., *Production chemicals for the oil and gas industry*. 2009, Boca Raton: CRC Press. 437.
218. Sata, T., Mine K., and Matsusaki K., *Change in Transport Properties of Anion-Exchange Membranes in the Presence of Ethylene Glycols in Electrodialysis.* Journal of Colloid and Interface Science, 1998. **202**(2): p. 348-358.
219. Zafar, M., Ali M., Khan S.M., Jamil T., and Butt M.T.Z., *Effect of additives on the properties and performance of cellulose acetate derivative membranes in the separation of isopropanol/water mixtures.* Desalination, 2012. **285**: p. 359-365.
220. MEGlobal. *Ethylene Glycol - Product Guide*. 2008 [cited 2014 9-Oct]; Available from: http://www.meglobal.biz/media/product_guides/MEGlobal_MEG.pdf.

221. DOW. *Triethylene glycol*. 2017 [cited 2017 9-May]; Available from: http://www.meglobal.biz/media/product_guides/MEGlobal_MEG.pdf.
222. Merkel, T., *Novel polymer membrane process for pre-combustion $CO_2$ capture from coal-fired syngas*. 2011, Membrane Technology And Research, Incorporate: Menlo Park, CA (United States).
223. Woolcock, P.J. and Brown R.C., *A review of cleaning technologies for biomass-derived syngas.* Biomass and Bioenergy, 2013. **52**(Supplement C): p. 54-84.
224. Scholes, C.A., Bacus J., Chen G.Q., Tao W.X., Li G., Qader A., Stevens G.W., and Kentish S.E., *Pilot plant performance of rubbery polymeric membranes for carbon dioxide separation from syngas.* Journal of Membrane Science, 2012. **389**(Supplement C): p. 470-477.
225. Wind, J.D., Paul D.R., and Koros W.J., *Natural gas permeation in polyimide membranes.* Journal of Membrane Science, 2004. **228**(2): p. 227-236.
226. Omole, I.C., Bhandari D.A., Miller S.J., and Koros W.J., *Toluene impurity effects on $CO_2$ separation using a hollow fiber membrane for natural gas.* Journal of membrane science, 2011. **369**(1): p. 490-498.
227. Tanihara, N., Shimazaki H., Hirayama Y., Nakanishi S., Yoshinaga T., and Kusuki Y., *Gas permeation properties of asymmetric carbon hollow fiber membranes prepared from asymmetric polyimide hollow fiber.* Journal of membrane science, 1999. **160**(2): p. 179-186.
228. Al-Juaied, M. and Koros W., *Performance of natural gas membranes in the presence of heavy hydrocarbons.* Journal of Membrane Science, 2006. **274**(1): p. 227-243.
229. Scholes, C.A., Stevens G.W., and Kentish S.E., *Impact of Heavy Hydrocarbons on Natural Gas Sweetening Using Perfluorinated Polymeric Membranes.* Industrial & Engineering Chemistry Research, 2016. **55**(28): p. 7696-7703.
230. White, L.S., Blinka T.A., Kloczewski H.A., and Wang I.-f., *Properties of a polyimide gas separation membrane in natural gas streams.* Journal of Membrane Science, 1995. **103**(1-2): p. 73-82.
231. Wensley, C.G. and King W.M., *Effects of contaminant vapors on the separation of hydrogen from methane by CA membranes*, in *AlChE National Meeting*. 1986: New Orleans, Louisiana, USA.
232. Schnell, W. and Houston C.D., *Refinery hydrogen recovery with sepharex membrane systems*. 1985, Separex Corp., Anaheim, CA.
233. Daicel Corporation, *Cellulose acetate (Safety Data Sheet)*. 2009, Tokyo, Japan.
234. Albenze, E., *Mixed Matrix Membranes*, in *Carbon Capture Technology Meering*. 2013, U.S. Department of Energy - National Energy Technology Laboratory: Pittsburgh, Pennsylvania, U.S.
235. Ionita, M., Crica L.E., Voicu S.I., Pandele A.M., and Iovu H., *Fabrication of cellulose triacetate/graphene oxide porous membrane.* Polymers for Advanced Technologies, 2016. **27**(3): p. 350-357.
236. Das, A.M., Ali A.A., and Hazarika M.P., *Synthesis and characterization of cellulose acetate from rice husk: Eco-friendly condition.* Carbohydrate Polymers, 2014. **112**: p. 342-349.
237. Braun, J.L. and Kadla J.F., *CTA III: A Third Polymorph of Cellulose Triacetate.* Journal of Carbohydrate Chemistry, 2013. **32**(2): p. 120-138.
238. Yang, J., Kubota F., Baba Y., Kamiya N., and Goto M., *Application of cellulose acetate to the selective adsorption and recovery of Au(III).* Carbohydrate Polymers, 2014. **111**: p. 768-774.
239. Arous, O., Amara M., and Kerdjoudj H., *Synthesis and characterization of cellulose triacetate and poly(ethylene imine) membranes containing a polyether macrobicyclic: Their application to the separation of copper(II) and silver(I) ions.* Journal of Applied Polymer Science, 2004. **93**(3): p. 1401-1410.

240. Kulshreshtha, A.K. and Dweltz N.E., *A study on the further acetylation of SPA cotton.* Journal of Applied Polymer Science, 1979. **24**(4): p. 1139-1141.
241. Brandani, S., Mangano E., and Sarkisov L., *Net, excess and absolute adsorption and adsorption of helium.* Adsorption, 2016. **22**(2): p. 261-276.
242. Scholes, C.A., Tao W.X., Stevens G.W., and Kentish S.E., *Sorption of methane, nitrogen, carbon dioxide, and water in Matrimid 5218.* Journal of Applied Polymer Science, 2010. **117**(4): p. 2284-2289.
243. Lashof, D.A. and Ahuja D.R., *Relative contributions of greenhouse gas emissions to global warming.* Natural, 1990(344): p. 529-531.
244. Preston, B.L. and Jones R.N., *Climate change impacts on Australia and the benefits of early action to reduce global greenhouse gas emissions*. 2006, The Commonwealth Scientific and Industrial Research Organisation.
245. EPA, *Inventory of U.S. Greehouse gas emission and sinks (1990-2009)*. 2011, U.S. Environmental Protection Agency: Washington DC, U.S.
246. Cubasch, U., Wuebbles D., Chen D., Facchini M.C., Frame D., Mahowald N., and Winther J.-G., *Climate Change 2013: The Physical Science Basis. Fifth Assessment Report of the Intergovernmental Panel on Climate Change*. 2013, Cambridge, United Kingdom: Cambridge University Press.
247. Taajamaa, L., Rojas O.J., Laine J., and Kontturi E., *Phase-specific pore growth in ultrathin bicomponent films from cellulose-based polysaccharides.* Soft Matter, 2011. **7**(21): p. 10386-10394.
248. Niinivaara, E., Wilson B.P., King A.W.T., and Kontturi E., *Parameters affecting monolayer organisation of substituted polysaccharides on solid substrates upon Langmuir-Schaefer deposition.* React. Funct. Polym., 2016. **99**: p. 100-106.
249. Li, X.-G. and Huang M.-R., *Multilayer ultrathin-film composite membranes for oxygen enrichment.* J. Appl. Polym. Sci., 1997. **66**(11): p. 2139-2147.
250. Azher, H., Scholes C.A., Stevens G.W., and Kentish S.E., *Water permeation and sorption properties of Nafion 115 at elevated temperatures.* Journal of Membrane Science, 2014. **459**: p. 104-113.
251. Dias, C.R., Rosa M.J., and de Pinho M.N., *Structure of water in asymmetric cellulose ester membranes — and ATR-FTIR study.* Journal of Membrane Science, 1998. **138**(2): p. 259-267.
252. Dytnerskii, Y.I., Kagramanov G.G., Storozhuk I.P., and Kovalenko N.F., *SO2 Separation from gaseous mixtures by membranes.* Journal of Membrane Science, 1989. **41**: p. 49-54.
253. Zavaleta, R. and McCandless F., *Selective permeation through modified polyvinylidene fluoride membranes.* Journal of Membrane Science, 1976. **1**: p. 333-353.
254. Faucett, H.L., Maxwell. J.D., Burnett, T.A., *Technical Assessment Of NOx Removal Processes For Utility Application*, U.S.E.P. Agency, Editor. 1977: Washington D.C.
255. Scholes, C.A., Chen G.Q., Stevens G.W., and Kentish S.E., *Nitric oxide and carbon monoxide permeation through glassy polymeric membranes for carbon dioxide separation.* Chemical Engineering Research and Design, 2011. **89**(9): p. 1730-1736.
256. Potreck, J., Uyar F., Sijbesma H., Nijmeijer K., Stamatialis D., and Wessling M., *Sorption induced relaxations during water diffusion in S-PEEK.* Physical Chemistry Chemical Physics, 2009. **11**(2): p. 298-308.
257. Stec, A.A., Fardell P., Blomqvist P., Bustamante-Valencia L., Saragoza L., and Guillaume E., *Quantification of fire gases by FTIR: Experimental characterisation of calibration systems.* Fire Safety Journal, 2011. **46**(5): p. 225-233.
258. Guillaume, E., Saragoza L., Wakatsuki K., and Blomqvist P., *Effect of gas cell pressure in FTIR analysis of fire effluents.* Fire and Materials, 2014.
259. Isogai, A. and Atalla R.H., *Dissolution of Cellulose in Aqueous NaOH Solutions.* Cellulose, 1998. **5**(4): p. 309-319.

260. Glasser, W.G., *6. Prospects for future applications of cellulose acetate.* Macromolecular Symposia, 2004. **208**(1): p. 371-394.
261. Koros, W.J. and Paul D.R., *Design considerations for measurement of gas sorption in polymers by pressure decay.* Journal of Polymer Science: Polymer Physics Edition, 1976. **14**(10): p. 1903-1907.
262. Donohue, M.D., Minhas B.S., and Lee S.Y., *Permeation behavior of carbon dioxide-methane mixtures in cellulose acetate membranes.* Journal of Membrane Science, 1989. **42**(3): p. 197-214.
263. Dean, J.A., *Lange's Handbook of chemistry*. 11th Ed. ed. Knovel. 1973, Binghamton, N.Y.: McGraw-Hills.
264. Komatsuka, T. and Nagai K., *Temperature Dependence on Gas Permeability and Permselectivity of Poly(lactic acid) Blend Membranes.* Polym. J, 2009. **41**(5): p. 455-458.
265. Landry, C.J.T., Lum K.K., and O'Reilly J.M., *Physical aging of blends of cellulose acetate polymers with dyes and plasticizers.* Polymer, 2001. **42**(13): p. 5781-5792.
266. Cole, W.J., Medlock Iii K.B., and Jani A., *A view to the future of natural gas and electricity: An integrated modeling approach.* Energy Economics, 2016.
267. Lokhandwala, K., Jariwala A., and Malsam M. *High Performance Contaminant Resistant Membranes Minimize Pretreatment and Improve $CO_2$ Removal Economics*. in *The 57th Laurance Reid Gas Conditioning Conference*. 2007. Norman, OK.
268. Bhide, B.D. and Stern S.A., *Membrane processes for the removal of acid gases from natural gas. I. Process configurations and optimization of operating conditions.* Journal of Membrane Science, 1993. **81**(3): p. 209-237.
269. Lu, H.T., Kanehashi S., Scholes C.A., and Kentish S.E., *The potential for use of cellulose triacetate membranes in post combustion capture.* International Journal of Greenhouse Gas Control, 2016. **55**: p. 97-104.
270. Fox, T.G.B., *Influence of diluent and of copolymer composition on the glass temperature of a polymer system.* Am. Phys. Soc., 1956. **1**: p. 123-125.
271. Marcilla, A. and BeltrÁN M., *5 - Mechanisms of Plasticizers Action A2 - Wypych, George*, in *Handbook of Plasticizers (Second Edition)*. 2012, William Andrew Publishing: Boston. p. 119-133.
272. Angell, C.A., Sare J.M., and Sare E.J., *Glass transition temperatures for simple molecular liquids and their binary solutions.* The Journal of Physical Chemistry, 1978. **82**(24): p. 2622-2629.
273. Kesting, R.E. and Fritzsche A., *Membrane Polymers*, in *Polymeric gas separation membranes*. 1993, Wiley-Interscience: New York.
274. Archer, W.L., *Determination of Hansen solubility parameters for selected cellulose ether derivatives.* Industrial & Engineering Chemistry Research, 1991. **30**(10): p. 2292-2298.
275. Belmares, M., Blanco M., Goddard W.A., Ross R.B., Caldwell G., Chou S.H., Pham J., Olofson P.M., and Thomas C., *Hildebrand and Hansen solubility parameters from Molecular Dynamics with applications to electronic nose polymer sensors.* Journal of Computational Chemistry, 2004. **25**(15): p. 1814-1826.
276. Hansen, C.M., *Hansen solubility parameters: a user's handbook*. 2007, Florida, US: CRC press.
277. Klein, E., Eichelberger J., Eyer C., and Smith J., *Evaluation of semi permeable membranes for determination of organic contaminants in drinking water.* Water Research, 1975. **9**(9): p. 807-811.
278. Galvão, A.C. and Francesconi A.Z., *Solubility of methane and carbon dioxide in ethylene glycol at pressures up to 14 MPa and temperatures ranging from (303 to 423) K.* The Journal of Chemical Thermodynamics, 2010. **42**(5): p. 684-688.
279. Fernández-Prini, R., Crovetto R., and Gentili N., *Solubilities of inert gases in ethylene glycol.* The Journal of Chemical Thermodynamics, 1987. **19**(12): p. 1293-1298.

280. Jou, F.Y., Otto F., and Mather A., *Solubility of methane in glycols at elevated pressures.* The Canadian Journal of Chemical Engineering, 1994. **72**(1): p. 130-133.
281. Jou, F.Y., Deshmukh R.D., Otto F.D., and Mather A.E., *Vapor-liquid equilibria for acid gases and lower alkanes in triethylene glycol.* Fluid Phase Equilibria, 1987. **36**: p. 121-140.
282. Yang, J.S., Kim H.J., Jo W.H., and Kang Y.S., *Analysis of pervaporation of methanol-MTBE mixtures through cellulose acetate and cellulose triacetate membranes.* Polymer, 1998. **39**(6–7): p. 1381-1385.
283. Park, S., Baker J.O., Himmel M.E., Parilla P.A., and Johnson D.K., *Cellulose crystallinity index: measurement techniques and their impact on interpreting cellulase performance.* Biotechnology for biofuels, 2010. **3**(1): p. 10.
284. Cole, W.J., Medlock Iii K.B., and Jani A., *A view to the future of natural gas and electricity: An integrated modeling approach.* Energy Economics.
285. Bauer, N., Mouratiadou I., Luderer G., Baumstark L., Brecha R.J., Edenhofer O., and Kriegler E., *Global fossil energy markets and climate change mitigation – an analysis with REMIND.* Climatic Change, 2016. **136**(1): p. 69-82.
286. Liu, Q., Galizia M., Gleason K.L., Scholes C.A., Paul D.R., and Freeman B.D., *Influence of toluene on $CO_2$ and $CH_4$ gas transport properties in thermally rearranged (TR) polymers based on 3, 3′ -dihydroxy-4, 4′ -diamino-biphenyl (HAB) and 2, 2′ -bis-(3, 4-dicarboxyphenyl) hexafluoropropane dianhydride (6FDA).* Journal of Membrane Science, 2016. **514**: p. 282-293.
287. Schell, W. and Houston C.D., *Refinery hydrogen recovery with sepharex membrane systems*. 1985, Separex Corp., Anaheim, CA.
288. Lu, H.T., Kanehashi S., Scholes C.A., and Kentish S.E., *The impact of ethylene glycol and hydrogen sulphide on the performance of cellulose triacetate membranes in natural gas sweetening.* Journal of Membrane Science, 2017. **539**: p. 432-440.
289. Frisch, H.L., Wang T.T., and Kwei T.K., *Diffusion in glassy polymers. II.* Journal of Polymer Science Part A-2: Polymer Physics, 1969. **7**(5): p. 879-887.
290. Berens, A.R., *Sorption of organic liquids and vapors by rigid PVC.* Journal of Applied Polymer Science, 1989. **37**(4): p. 901-913.
291. Krüger, K.-M. and Sadowski G., *Fickian and Non-Fickian Sorption Kinetics of Toluene in Glassy Polystyrene.* Macromolecules, 2005. **38**(20): p. 8408-8417.
292. Windle, A., *Case II sorption*, in *Polymer Permeability*, C. J., Editor. 1985, Chapman & Hall: UK. p. 75-118.
293. Levy, C. and D'Arrigo G., *Relaxation processes in liquid and supercooled toluene by light scattering experiments.* Molecular Physics, 1983. **50**(5): p. 917-934.
294. Van Krevelen, D.W. and Te Nijenhuis K., *Properties of polymers: their correlation with chemical structure; their numerical estimation and prediction from additive group contributions*. Fourth ed. 2009, Amsterdam, The Netherlands: Elsevier.

# APPENDIX A: EXPERIMENTAL METHODS

## A.1 Membrane Density

The membrane density was determined by the standard buoyancy technique in which the membrane volume was assumed unchanged during the measurement. However, the sorption of solvent into the CTA could interfere the accuracy of the result. Therefore, the uptake (Eq. 3.1) of several common solvents in CTA membrane was studied (**Table A.1**) and n-hexane was the solvent selected for measuring the density of CTA membrane.

**Table A.1: Uptake of different solvents in CTA membranes**

| Solvent | n-hexane | n-heptane | Cyclohexane | Ethyl acetate | Ethanol |
|---|---|---|---|---|---|
| Solvent uptake (wt %) | 0.533 ± 0.3 | 0.816 ± 0.4 | 0.710 ± 0.3 | 110 | 16.5 ± 0.1 |